"This document is issued by The Boeing Company. The Boeing Company is not affiliated with Rockwell International Corporation."

ROCKETDYNE
A DIVISION OF NORTH AMERICAN ROCKWELL CORPORATION
6633 CANOGA AVENUE, CANOGA PARK, CALIFORNIA 91304

R-7450-2

J-2 ENGINE AS-502 (APOLLO 6)
FLIGHT REPORT
S-II AND S-IVB STAGES

VOLUME 3: S-IVB STAGE FAILURE ANALYSIS

Contract NAS8-19
Exhibit A,
Para. A.3.a

[redacted]

PREPARED BY

Rocketdyne Engineering
Canoga Park, California

APPROVED BY

P. D. Castenholz
J-2 Program Manager

NO. OF PAGES 182 & xii

REVISIONS

DATE 17 June 1968

DATE	REV. BY	PAGES AFFECTED	REMARKS

EXPORT CONTROLLED - This document contains technical data within the definition of the International Traffic in Arms Regulations, and is subject to the export control laws of the U.S. Government. Transfer of this data by any means to a foreign person, whether in the U.S. or abroad, without an export license or other approval from the U.S. Department of State, is prohibited.

FORM R18-G REV. 9-67

FOREWORD

Boeing document. No Rockwell affiliatic

This report was prepared by Rocketdyne, a division of North American Rockwell Corporation, under Contract NAS8-19.

ABSTRACT

This report is Volume 3 of a five-volume report on the operation of the J-2 engines during the flight of Apollo/Saturn AS-502. This volume presents the analysis of the J-2 engine J-2042 during first burn, orbital coast, and failure to restart.

The volumes of this report are:

- Volume 1: Flight Performance Analysis
- Volume 2: S-II Stage Failure Analysis
- ● Volume 3: S-IVB Stage Failure Analysis
- Volume 4: Flight Failure Verification Testing
- Volume 5: Post-Flight Design Modifications

[redacted] - This document contains technical data within the [illegible] International Traffic in Arms Regulations, and is subject to the export control laws of the U.S. Government. Transfer of this data by any means to a foreign person, whether in the U.S. or abroad, without an export license or other approval from the U.S. Department of State, is prohibited.

CONTENTS

Foreword iii

Abstract iii

Summary 1

Introduction to Flight Analysis and Verification Testing . . . 5

Externally Induced Vibration Effects on the J-2 Engine . . . 7

Event Description 7

Boost-Phase POGO Effect Testing 9

Abnormal J-2 Engine Gimbal Excursion at Engine Start and J-2 Engine Alignment During Operation 13

Event Description 13

Abnormal Gimbal Transients at Start 13

Shifts in Acturator Load and Position at 644 Seconds of Flight. 18

Gimbal Transients at 690 Seconds 19

Pitch Transient at Cutoff 23

Conclusion 25

J-2 Engine Area Temperature Anomalies 27

S-IVB First-Burn Thermal Environment 27

S-IVB Restart Thermal Environment 43

Gas Generator Valve Position Shifts 46

Oribital Thermal Environment 55

Engine Performance Analysis 67

Engine Performance Decay 67

Computer Model and Engine Performance Gain Factors 86

Gas Generator Temperature Surge at First-Burn Cutoff 99

Event Description: Fuel Turbine Inlet Temperature Overshoot After First-Burn Cutoff 99

Fuel Pump Discharge Pressure After First-Burn Cutoff 105

Event Description: Fuel Pressure Surge 105

Analysis 107

S-IVB Auxiliary Hydraulic Pump Failure During Orbital Coast . . 113

Event Description 113

Analysis 114A

Engine Failure to Restart 115

Description 115

Possible Failure Modes 122
Analysis 123
Conclusion 126
Overall Failure Analysis 127
Pressurization Systems 135
Oxidizer Pressurization System 135
Fuel Pressurization System 145
Engine Start Conditions 153
Event Description 153
Verification Testing at SSFL 165
Engine J016-4 Configuration 165
Test Objectives 167
Procedure 167
Test Results 171
Conclusions 182

ILLUSTRATIONS

1. AS-502 S-IVB Sequence of Events 6
2. Vehicle 502, S-1C Stage, 0 to 9 cps Low-Pass Filtered Data 8
3. J-2 Engine Boost-Phase Vibration Test, Longitudinal Axis . . 10
4. J-2 Engine Boost-Phase Vibration Test, Lateral Axis 11
5. Acoustic and Vibration Measurement Locations 12
6. AS-502 S-IVB, First Burn 14
7. AS-502 S-IVB, First Burn 15
8. AS-502 S-IVB, First Burn 16
9. Pitch Actuator Position and Thrust Chamber Pressure vs Time From Engine Start Signal, AS-502 S-IVB First Burn . . 17
10. Crossplot of Pitch Actuator Position vs Load, AS-502 S-IVB, First Burn 21
11. Crossplot of Yaw Actuator Position vs Load, AS-502 S-IVB, First Burn 22
12. Pitch Actuator Position and Thrust Chamber Pressure vs Time From Cutoff Signal, AS-502 S-IVB, First Burn . . . 24
13. First-Burn Thermal Environment 28
14. AS-502 S-IVB Temperature Measurements and Locations 29
15. First Burn MOV Closing Control Line Temperature, S-IVB Engine J2042 31
16. AS-502 S-IVB First Burn, MOV Actuator Temperature AS-501 and AS-502 Comparison 32
17. Gas Generator Fuel Inlet Wall Temperature, S-IVB Engine J2042 34
18. AS-502 S-IVB First Burn, Engine Compartment Heating Effects on Measurements on Fuel Pump Side of Engine 35
19. AS-502 S-IVB First Burn, Engine Compartment Heating Effects on Measurements on Oxidizer Pump Side of Engine . . 36
20. AS-502 S-IVB First Burn, Oxidizer Pump System Temperature . . 39
21. AS-502 S-IVB First Burn 40

[redacted]

22. J016-4 Posttest 313-041 Engine Side of Gimbal Bearing Showing Heating From ASI Hot Gas 42
23. S-IVB Engine J2042 Second-Burn MOV Closing Line Temperature Comparison 44
24. J-2 Engine System Leakage Paths Open Between Engine Start and STDV Signal 45
25. Gas Generator Valve Position Comparison 47
26. Gas Generator Valve Setup for LN_2 Spray 49
27. Gas Generator Valve Position and Valve Body Temperature vs Time 50
28. Gas Generator Valve Position and Valve Body Temperature vs Time 51
29. Gas Generator Valve Position and Valve Body Temperature vs Time 53
30. Gas Generator Control Valve 54
31. Thrust Chamber Temperatures 57
32. Turbine Temperatures During Orbital Coast 58
33. Hot-Gas System Temperatures 59
34. Start Tank and Helium Tank Pressures During Orbital Coast . . 60
35. MOV Control System Temperatures 61
36. Hydraulic System Temperatures 62
37. Gas Generator System Temperatures During Orbital Coast . . . 63
38. AS-502 S-IVB, First Burn 70
39. AS-502 S-IVB First Burn, Main Chamber Pressure Corrected to Constant Heat Exchanger Operation 71
40. AS-501 and AS-502 Comparison, Main Chamber Pressure at Engine Cutoff vs Time 72
41. Expected Leakage Flow for Various Break Points in the ASI Propellant Feed System 74
42. AS-502 S-IVB First Burn, Thrust Chamber Performance 77
43. AS-502 S-IVB First Burn, ASI Fuel Feed Flow Overboard . . . 79
44. AS-502 S-IVB First Burn, ASI Mixture Ratio 80
45. AS-502 S-IVB Failure Mode Simulation 82
46. AS-501 and AS-502 Comparison of Fuel Turbine in Temperature Characteristics at First-Burn Cutoff 100

47. AS-502 S-IVB First Burn, Engine Pump Purge Regulator Pressure vs Time 102
48. Gas Generator Oxidizer Purge System Schematic 104
49. AS-502 S-IVB First Burn, Fuel Pump Outlet Pressure Surge After Engine Cutoff 106
50. Fuel Feed and Recirculation System 108
51. Fuel Pump Speed 109
52. AS-502 S-IVB First Burn 110
53. AS-502 S-IVB First Burn, Fuel NPSH After Cutoff 111
54. S-IVB Hydraulic System Schematic 114
55. Comparison of AS-501 and AS-502 S-IVB Second Burn, Thrust Chamber Jacket Temperature and Fuel Injection Temperature vs Time 117
56. Comparison of AS-501 and AS-502 S-IVB Second Burn, Pump Discharge Pressures vs Time 118
57. Comparison of AS-501 and AS-502 S-IVB Second Burn, Gas Generator Chamber Pressure and Fuel Turbine Inlet Temperature vs Time 120
58. Comparison of AS-501 and AS-502 S-IVB Second Burn, Thrust Chamber Pressure vs Time 121
59. AS-502 S-IVB Second Burn, Pump Speeds vs Time 125
60. Oxidizer Tank Pressurization System 136
61. AS-502 S-IVB, First Burn 137
62. AS-502 S-IVB, Stage Acceptance, First Burn 138
63. AS-501 S-IVB, First Burn 139
64. AS-501 S-IVB, Stage Acceptance, First Burn 140
65. Helium Heat Exchanger Operating Band 142
66. Helium Heat Exchanger Operating Band 143
67. LH_2 Tank Pressurization System 146
68. AS-501 S-IVB First Burn, Fuel Tank Ullage Pressure and Fuel Tank Pressurization Flowrate vs Time 148
69. AS-502 S-IVB First Burn, Fuel Tank Ullage Pressure and Fuel Tank Pressurization Flowrate vs Time 149

[redacted]

70. AS-502 S-IVB First Burn, Hydrogen Tank Pressurization System Performance 150
71. AS-501 S-IVB First Burn, Hydrogen Tank Pressurization System Performance 151
72. AS-502 Engine Oxidizer Inlet Pressure vs Engine Oxidizer Inlet Temperature 157
73. AS-502 S-IVB Fuel Inlet Pressure vs Fuel Inlet Temperature at Start 158
74. AS-502 S-IVB Oxidizer Pump Discharge Pressure vs Oxidizer Pump Discharge Temperature at Start 159
75. AS-502 Start Tank Temperature vs Start Pressure at Start . . 160
76. AS-502 S-IVB Failure Simulation Test, Engine J016-4, Test 313-041 166
77. S-IVB Failure Simulation, Engine J016-4 170
78. ASI Injector Mixture Ratio 173
79. ASI Nozzle (Main Injector) Showing Erosion 174
80. Engine J016-4, Test 313-041, Posttest Injector Condition (Section at Element 1) 175
81. Engine J016-4, Test 313-041, Posttest Injector Condition (Section at Element 2) 176
82. Engine J016-4, Test 313-041, Posttest Injector Condition . . . 177
83. Engine J016-4 ASI Assembly Following Test 313-041 179
84. Engine J016-4 ASI Assembly and Oxidizer Dome Following Test 313-041 180
85. Engine J016-4, Test 313-041, Posttest Injector Condition Showing Oxidizer Dome Damage 181

[redacted]

TABLES

1. AS-502, S-IVB Engine J2042 Events Summary 4
2. AS-502 S-IVB Performance Shift Predictions 84
3. AS-502 S-IVB Performance Shift Predictions 85
4. J-2 Engine Gains for Fuel Tank Pressurization Line Failure 88
5. J-2 Engine Gains for ASI Oxidizer Line Failure 89
6. J-2 Engine Gains for ASI Fuel Line Failure 90
7. J-2 Engine Gains for ASI Fuel Line Failure 91
8. Comparison of Various Thrust Chamber Resistance Models . . 93
9. Comparison of Various Main Fuel Injector Resistance Models 94
10. Comparison of Various Main Oxidizer Injector Resistance Models 95
11. Effect of 3.5-lb/sec Fuel Leak 96
12. AS-502 S-IVB Failure Analysis 128
13. S-IVB Instrumentation Failures 133
14. Stage and Engine Propellant System Parameters 154
15. AS-502 S-IVB First-Burn and Restart Engine Sequence Data 161
16. Special Instrumentation for S-IVB Failure Simulation Test 168
17. Engine J016-4 Failure Simulation Test (313-041) 169

[redacted]

SUMMARY

J-2 engine J2042, installed on the S-IVB stage of the AS-502 vehicle, failed to achieve restart during flight on 4 April 1968. This report presents the results of the flight data analysis and the engine verification test program conducted to demonstrate the failure mode.

Analysis of flight data indicated that the augmented spark igniter fuel line had failed, allowing burnout of the igniter, thus preventing engine restart. Verification tests on an R&D J-2 engine demonstrated the predicted events. The analysis and verification tests, therefore, provide proof of the failure mode which prevented AS-502, S-IVB restart.

Prior to launch, engine J2042 had accumulated 704.6 seconds of mainstage operation in seven tests; five engine acceptance and two stage acceptance. All component modifications and replacements were accumulated in accordance with established procedures. Engine data do not indicate any significant areas of compromise or concern regarding the hardware quality. Engine J2042 was a 225K (225,000 pounds thrust) configuration engine (actual calibration point was approximately 229K), requiring restart after a 180-minute orbital coast.

No AS-502, S-IVB engine problems were noted during checkout, FRT, or CDDT operations, and prelaunch preparations were normal and satisfactory. Vehicle liftoff occurred on schedule at 0400 PST (range time = 0). A summary chronology of subsequent AS-502, S-IVB flight anomalies is shown in Table 1, and concludes with a failure to restart.

Flight data analysis indicates several anomalies during engine J2042 first-burn operation and attempted restart which enable definition of the primary mode of failure and subsequent damage:

1. The engine area external temperature environment data deviated significantly from data from AS-501, beginning at 645 seconds.

[redacted]

a. Between 645 and 696 seconds, chilling of the entire engine area was noted; the rate of chilling increased significantly at 684 seconds. Measurements indicate that the leakage was liquid hydrogen, and that the point of origin was near the MOV, fuel bleed valve, and gas generator valve, and gas generator oxidizer bootstrap line.

b. Between 696 and 703 seconds, substantial heating was noted. The first temperature increase was on the fuel pump side of the engine, while the second surge (peaking at 700 seconds) was more significant on the oxidizer pump side.

c. General chilling was re-established at 703 seconds, except that some low-level heating was noted in the oxidizer heatup across the turbopump.

d. No significant chilling was noted during coast. (The actuator hydraulic system apparently froze because of chilling residual in the lines from first-burn hydrogen leakage.)

e. Chilling began again at restart command when the MFV and ASI oxidizer valve were opened.

2. Engine performance, which had previously been normal and at the predicted level, decayed significantly beginning at 684 seconds.

a. A steady decay was noted between 684 and 692 seconds (3.6-psia loss in main chamber pressure).

b. Immediately thereafter, another steady decay was noted between 692 and 702 seconds (12.6-psia loss in main chamber pressure).

c. Between 702 seconds and cutoff at 747 seconds, no further performance loss occurred.

3. The engine failed to restart when the command was given. All start conditions were proper, pump speeds and accelerations from start bottle blowdown were as anticipated, all valve operations occurred as programmed, and gas generator ignition and subsequent

[redacted]

operation were satisfactory. Main chamber pressure failed to rise in a normal manner, and cutoff was initiated.

Examination of this evidence led to the formulation of the following failure mode hypothesis:

1. A small leak began at 645 seconds because of failure of the ASI fuel upper flex line. The initial failure was probably a fatigue crack in a bellows convolution. Leakage rate was less than 0.6 lb/sec.
2. Beginning at 684 seconds, the leakage rate increased because of continued and progressive failure of the ASI flex line. Fuel leakage increased to a level between 2.6 and 3.9 lb/sec (because of complete line failure, and depending on the location within the flex line), at which time backflow of propellant from the ASI began.
3. Backflow of propellant through the ASI caused rapid burnout of the ASI, allowing increased propellant leakage and performance decay during the erosion. The hot gas from ASI backflow caused a short-term heating to be recorded in the engine area, but cryogenic hydrogen leakage up to 3.9 lb/sec dominated the subsequent environment. Performance stabilized after ASI burnout.

To simulate the failure and attempt to duplicate the results, R&D engine J016-4 was configured and calibrated to simulate engine J2042. Special test equipment was added to allow control of ASI fuel flow (to simulate line leakage) and overboard dumping of fuel at the ASI (to simulate line failure), and a verification test performed. The test simulated the following:

1. 65 seconds of normal mainstage
2. 35 seconds of operation at simulated ASI fuel leakage of 0.6 lb/sec
3. Increasing leakage to complete line failure
4. Backflow of ASI combustion products for 29 seconds

[redacted]

Posttest evaluation indicated that all predicted events had occurred:

1. Operation at ASI mixture ratios over 2.4 produced substantial damage to the main injector ASI nozzle cavity.
2. The ASI burned out because of propellant backflow. The burnout completely destroyed the ASI fuel line and injection manifold, cut one spark cable in half and badly eroded both spark plugs, and eroded adjacent main injector and gimbal bearing surfaces.
3. A performance loss was noted, beginning at the time backflow was initiated and concluding shortly thereafter (when ASI erosion reached an equilibrium condition). This loss correlated well with the portion of engine J2042 losses hypothesized as a result of ASI failure.

In addition, adequate evidence existed during hot-fire testing to support the hypothesis model of the observed flight thermal environment.

The combination of flight analysis and test verification were deemed sufficient proof of AS-502, S-IVB events. Line testing and redesign were instituted.

A detailed discussion of all observed flight anomalies, failure analysis, and engine verification testing is presented in the following pages.

TABLE 1

AS-502, S-IVB ENGINE J2042 EVENTS SUMMARY

Range Time, seconds	Event
577.3	Engine Start (First Burn)
645	Start of Engine Compartment Temperature Decrease
684	Initial Performance Decay
692	Second Performance Decay
696	Start of Engine Compartment Heating
747	Engine Cutoff
11,614.7	Engine Start Signal (Second Burn)
11,617	Start of Engine Compartment Temperature Decrease
11,623	Thrust Chamber Fails to Ignite

[redacted]

INTRODUCTION TO FLIGHT ANALYSIS AND VERIFICATION TESTING

Several anomalies were observed during the S-IVB stage of flight AS-502. These are shown in Fig. 1 and described in detail in subsequent sections of this report. Each category event is described in turn, beginning with the first anomaly noted and continuing to the failure to restart, which was the final malfunction. Not all the unusual events discussed are relevant to the failure to restart; however, they all represent a deviation from previous experience, which made detailed examination mandatory.

Subsequent to the anomaly discussion, an overall failure analysis and evaluation of pressurization systems and engine start conditions is presented. From these data, a failure mode hypothesis is developed and an engine test verification plan is documented.

[redacted]

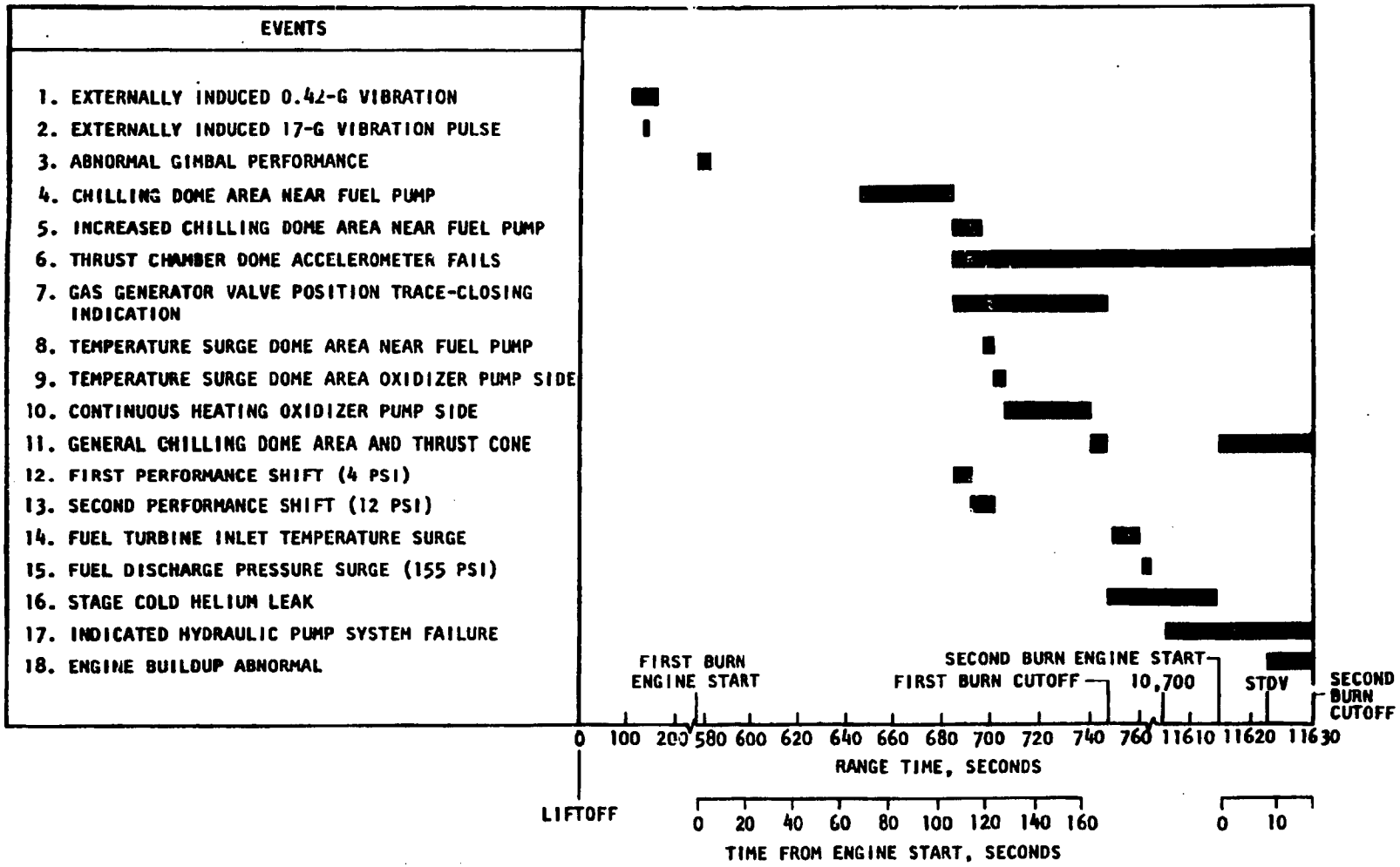

Figure 1. AS-502 S-IVB Sequence of Events

[redacted]

EXTERNALLY INDUCED VIBRATION EFFECTS ON THE J-2 ENGINE

EVENT DESCRIPTION

Descriptive Data

Approximately 105 seconds after liftoff, the S-IC stage exhibited abnormal longitudinal oscillations in the region of approximately 5.3 cps. The oscillations increased in amplitude between 110 and 128 seconds, at which time they began to decrease until S-1C cutoff which occurred at approximately 145 seconds. The phenomenon was analyzed and determined to be the POGO effect. The POGO phenomenon is a system closed-loop interaction of three vehicle systems: the vehicle structure, the vehicle suction propellant feed system, and the engine system. When the structural mode frequency approximates the vehicle suction resonant frequency, a tuning can occur which, with sufficient gain, can combine to produce flow disturbances that result in turbopump suction pressure oscillations. Resultant vibrations measured at the F-1 engine gimbal blocks reached peaks at 0.42 g. Figure 2 describes the POGO activity on AS-502 with plots of F-1 chamber pressure, fuel pump inlet pressure, and acceleration at the gimbal block. At approximately 133 seconds after liftoff, a sharp pulse (17 g peak to peak) was recorded on an accelerometer mounted on the S-IVB forward skirt. Various other instrumentation channels indicated disturbances at this time. J-2 engine acceleration instrumentation is not available in the low-frequency ranges (0 to 40 cps) because of response limitations of the single-side band telemetry channels. Also, the engine parameters were not being sampled during the 17 g pulse. Consequently, it is not possible to determine directly the vibration effects that the J-2 engines sustained during the POGO activity and the subsequent pulse anomaly.

Possible Failure Modes

None of the S-IVB anomalies can be linked directly with the POGO phenomenon. If any connection exists between the POGO vibration activities and the J-2

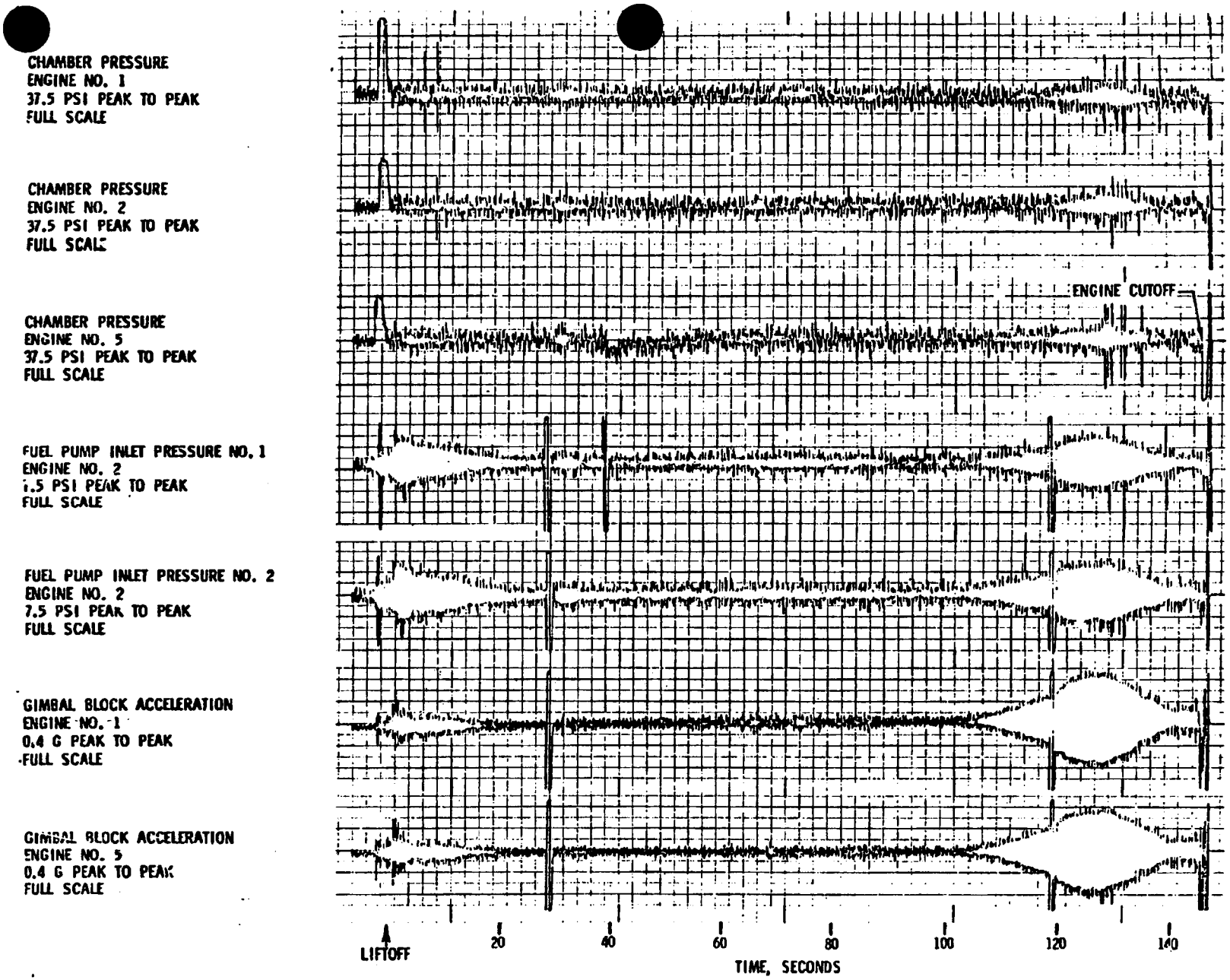

Figure 2. Vehicle 502, S-1C Stage, 0 to 9 cps Low-Pass Filtered Data

[redacted]

engine performance shift, it is indirect and indeterminate from available flight data. The only possible relationship would be a mode of failure in which minor damage could have been sustained by the ASI fuel line because of vibration (i.e., cracked bellows, broken or fatigued braid wires), which subsequently progressed to more serious failure with resultant fuel leakage after the engine was operating in the mainstage condition.

BOOST-PHASE POGO EFFECT TESTING

In an effort to simulate the vibration effects of the boost phase on the J-2 engine during the flight, engine J2C38 was instrumented and mounted on a vibration table to produce longitudinal and then lateral vibration inputs. Figures 3 and 4 show the levels of vibration up to 500 Hz encountered by engine J2042 during the boost phase of flight in both the longitudinal and lateral axes. The flight data points represent vibration levels measured during the boost phase at the S-IVB stage accelerometer mounting points, as noted on Fig. 3 and 4 and located on Fig. 5.

The vibration test program conducted on engine J2038 consisted of a standard vibration laboratory survey over all frequency ranges prevalent during the AS-502 flight. Acceleration levels known to have been encountered in flight were equalled or exceeded during the test program, as shown in Fig. 3 and 4 . The testing did not simulate flight environment with respect to vehicle spring rates (although stage actuators were used), altitude pressure, simultaneous three-axis vibration, or the acoustical environment. Liquid nitrogen was used to simulate the presence of cryogenic propellants in the engine. No relevant damage was incurred by the engine as a result of the test program; consequently, no evidence was produced to link the flight anomalies with a vibration problem.

Conclusion

In the absence of any substantiating data, it is not possible to infer any engine J2042 damage during boost-phase POGO.

[redacted]

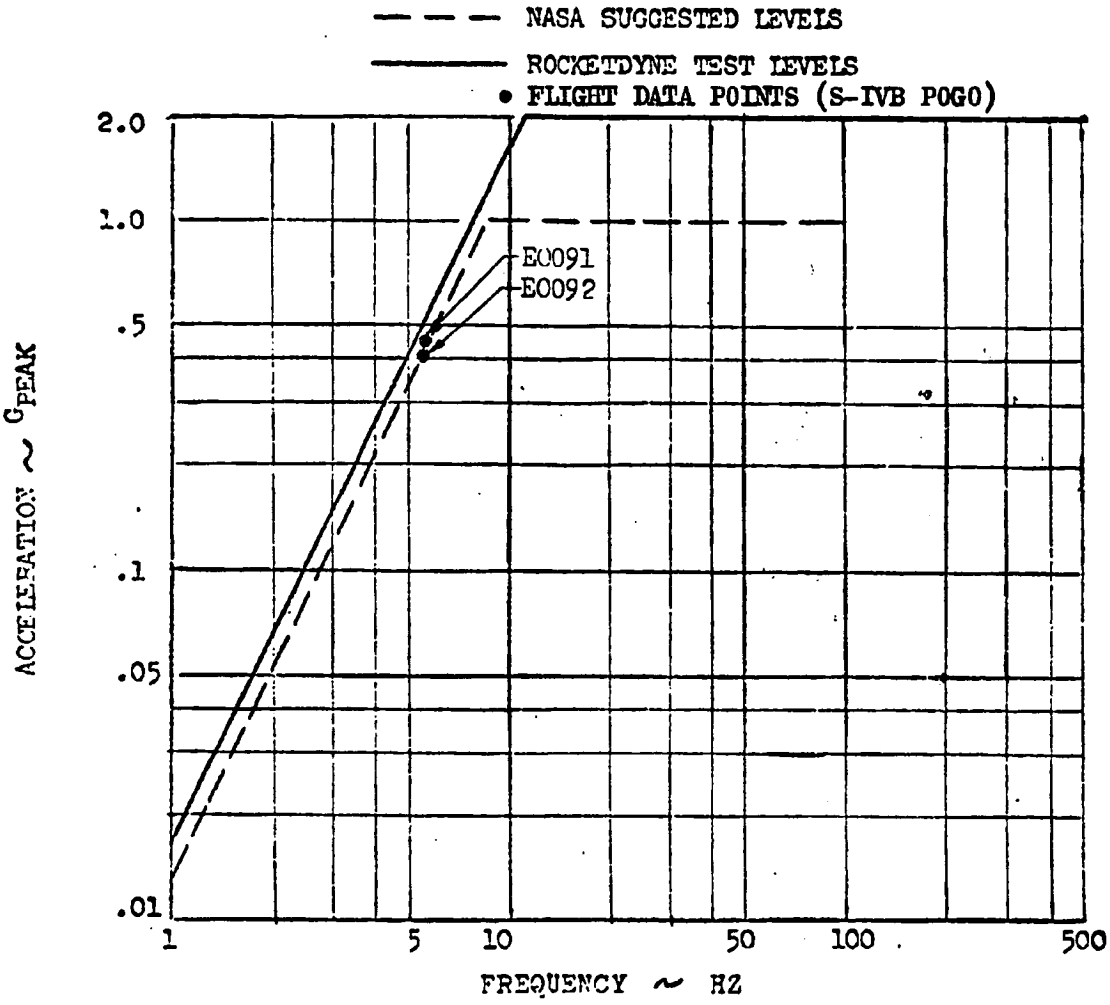

Figure 3. J-2 Engine Boost-Phase Vibration Test, Longitudinal Axis

[redacted]

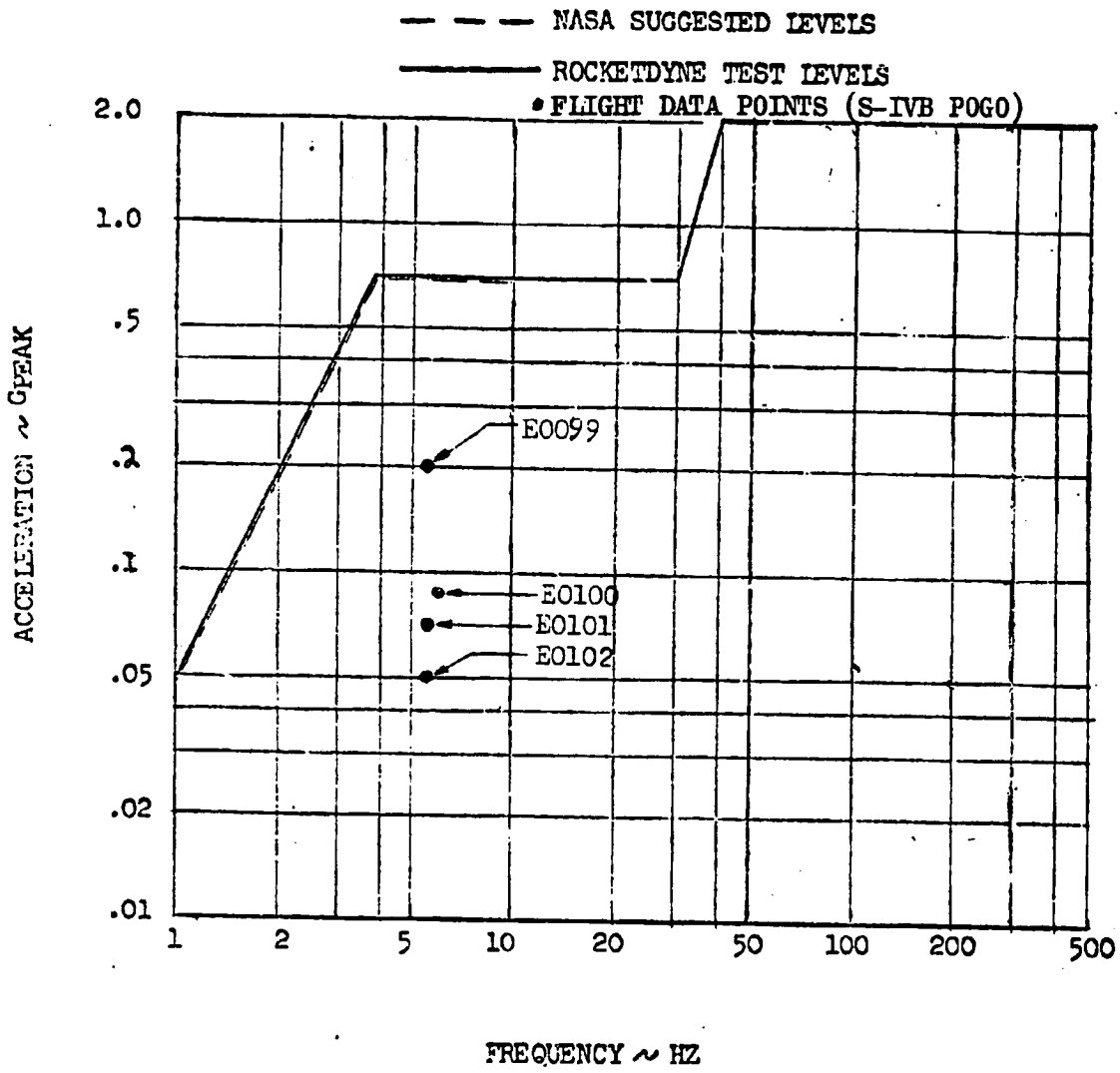

Figure 4. J-2 Engine Boost-Phase Vibration Test, Lateral Axis

[redacted]

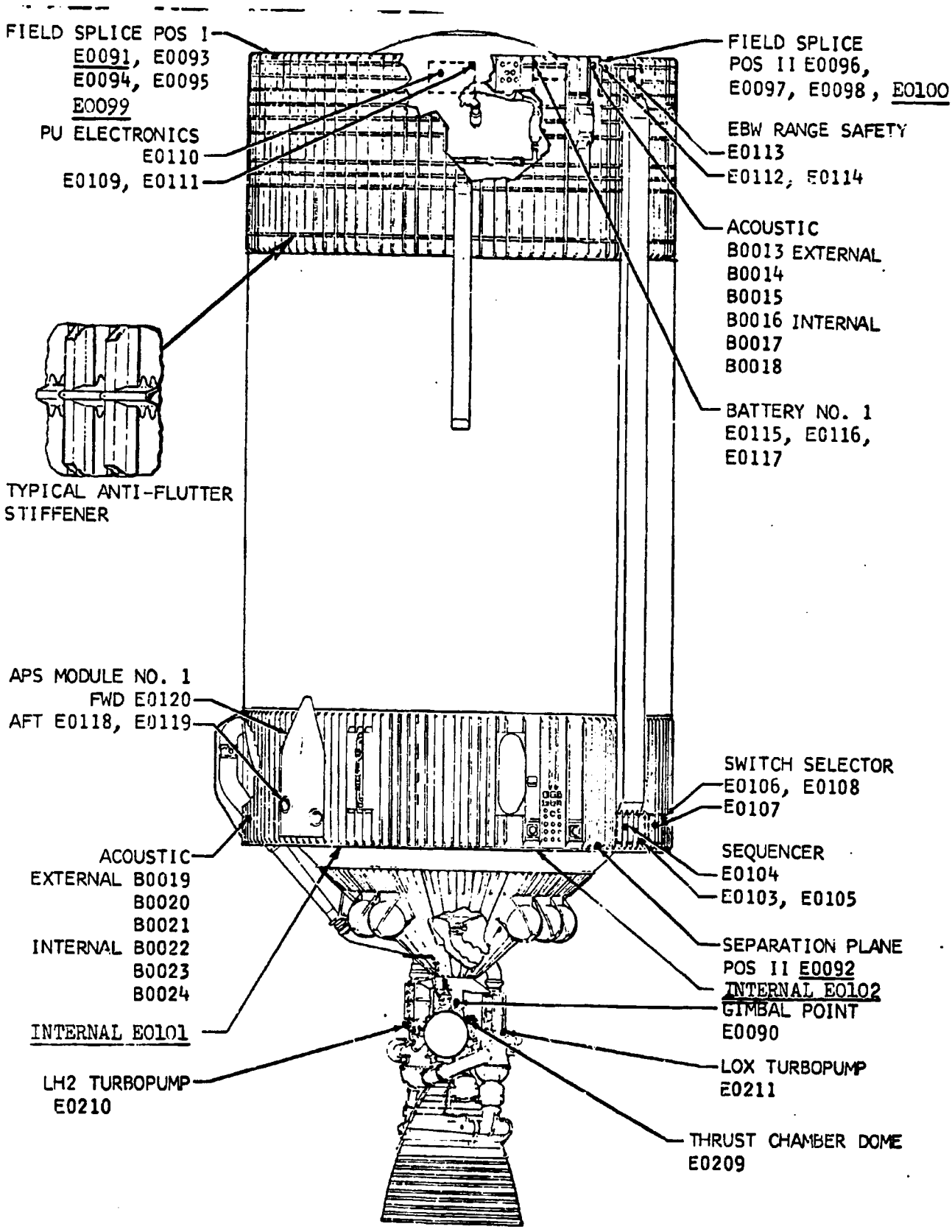

Figure 5. Acoustic and Vibration Measurement Locations

[redacted]

ABNORMAL J-2 ENGINE GIMBAL EXCURSION AT ENGINE START AND J-2 ENGINE ALIGNMENT DURING OPERATION

EVENT DESCRIPTION

Review of J-2 engine gimbal data from the S-IVB first burn of flight AS-502 revealed several unusual events that occurred during engine operation. A description of the events and results of the analysis made to determine whether or not the events were linked with the flight anomalies are presented. All times shown are from liftoff (range time).

ABNORMAL GIMBAL TRANSIENTS AT START

Defining Data

Engine gimbal transients were noted at the time of first-burn engine start signal (577.2 seconds). The pitch engine position went from 0 degree at 577.5 seconds to a peak of +6.7 degrees at 581.5 seconds, and then to a peak of -2.3 degrees at 585 seconds. The yaw engine position transient went from 0 degree to a peak of -1.37 degrees at 586 seconds. The transients gradually subsided to steady-state levels at 610 seconds. Maximum actuator forces noted during this activity were +5183 and -6774 pounds in pitch, and +3700 and -7657 pounds in yaw, respectively.

Figures 6, 7, and 8 are plots of pitch and yaw actuator position, differential pressure, and servovalve current and depict the gimbal transients at start, mainstage operation, and cutoff. Figure 9 is an expanded time plot of pitch actuator position and thrust chamber pressure and shows the chamber pressure buildup during the gimbal transients at start.

Cause of Event

Guidance commands and flight control system parameters revealed that the transients at start were commanded by the vehicle and resulted from several unexpected conditions existing at S-II/S-IVB separation. At separation

[redacted]

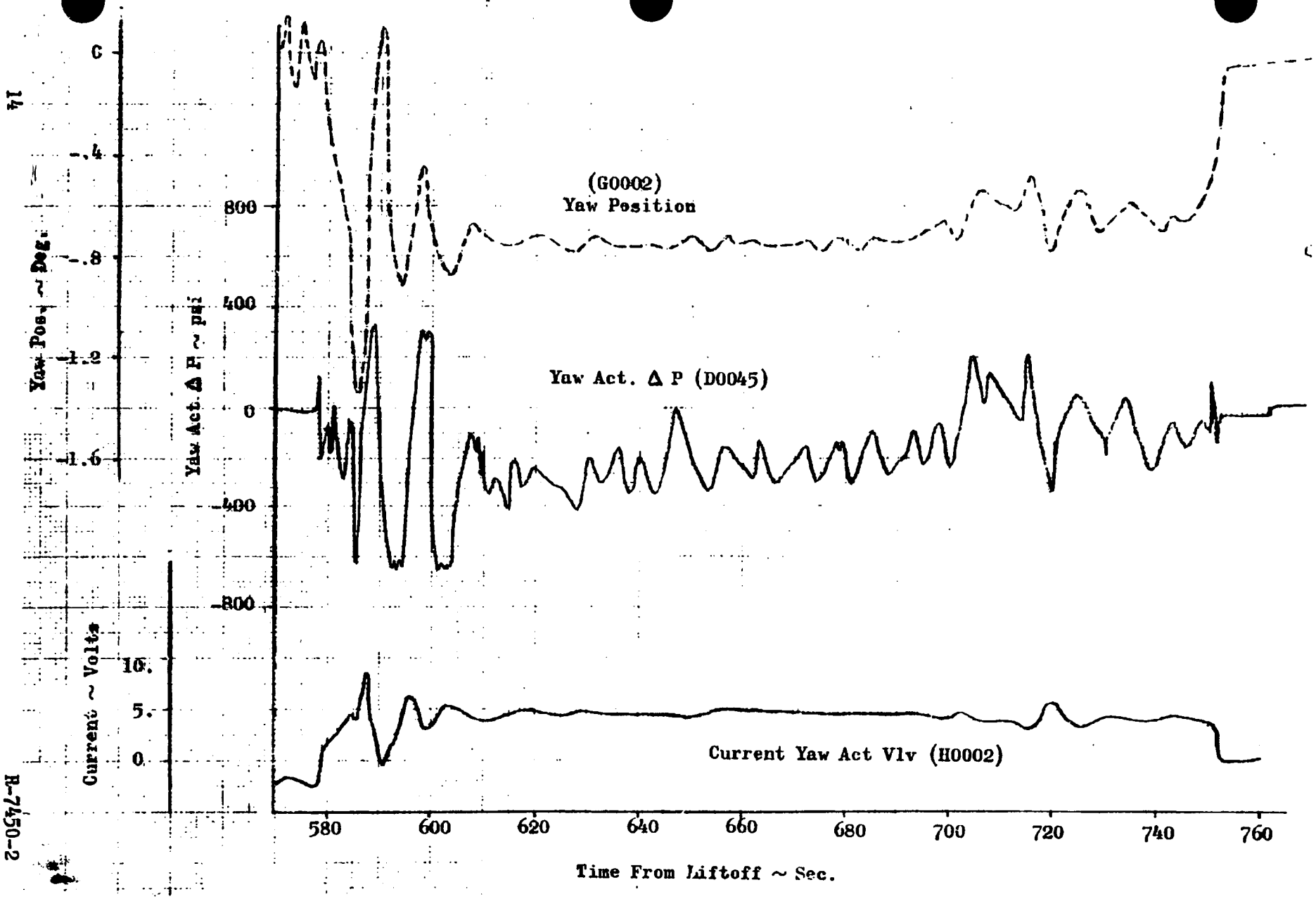

Figure 6. AS-502 S-IVB, First Burn

[redacted]

R-7450-2

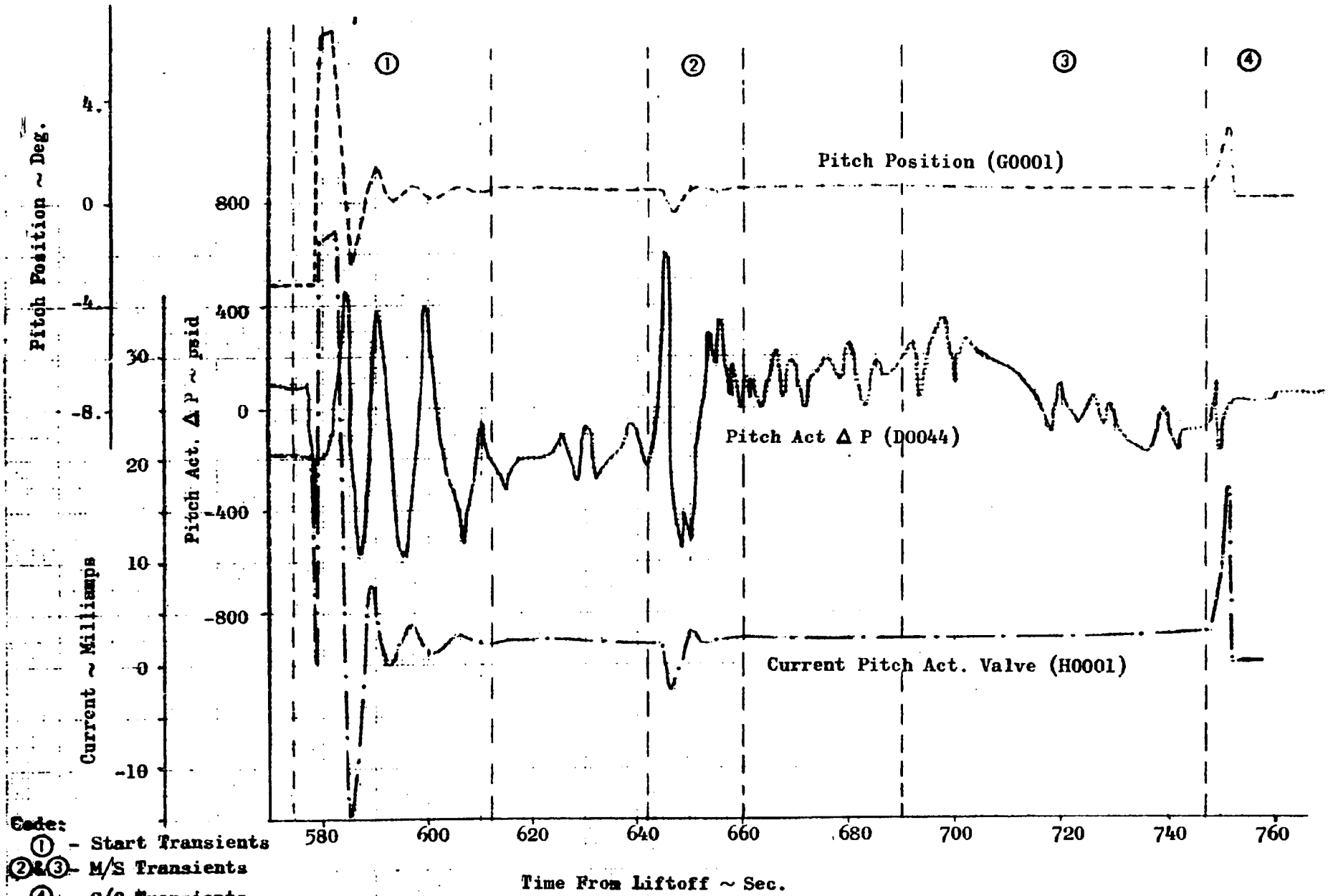

Figure 7. AS-502 S-IVB, First Burn

[redacted]

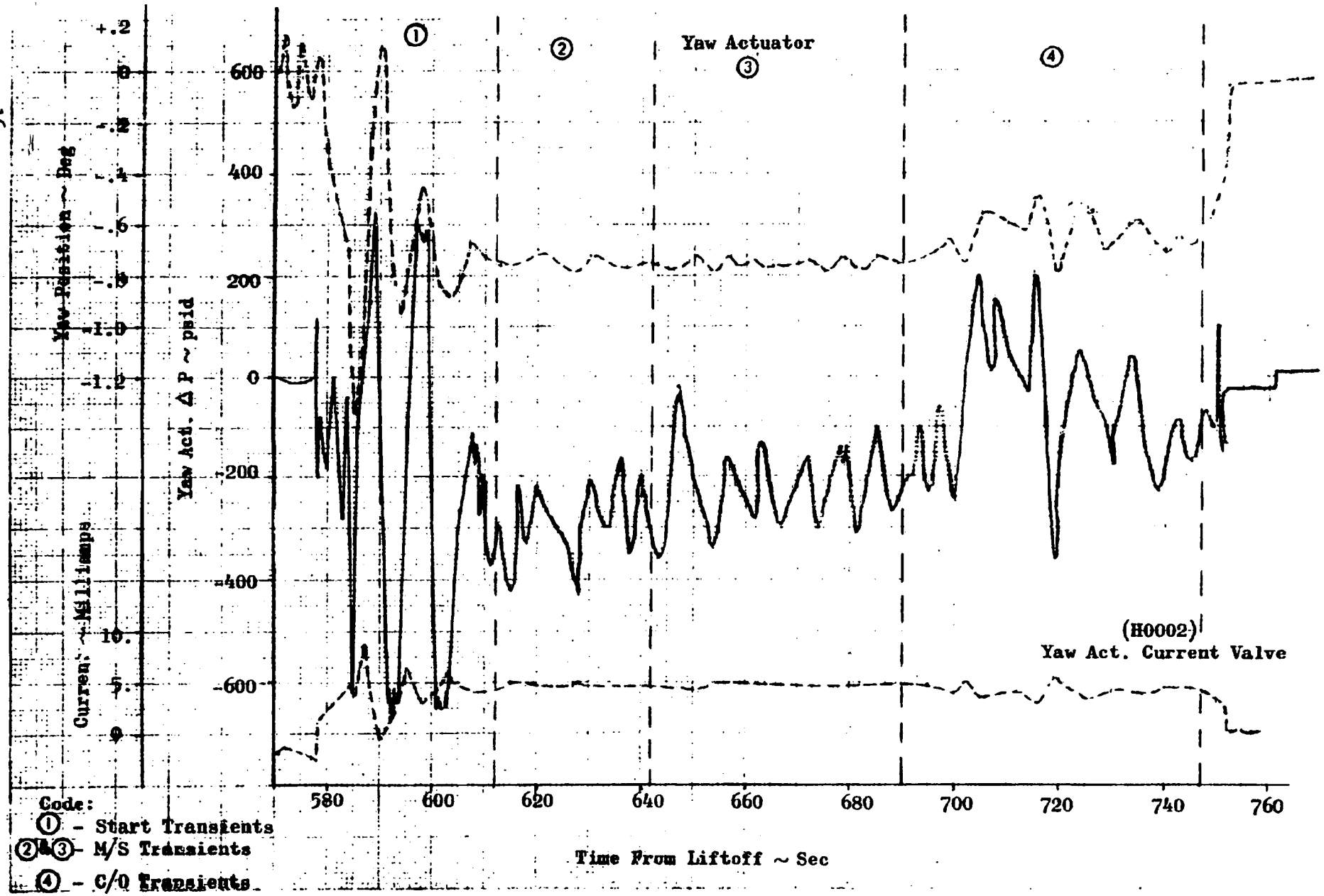

Figure 8. AS-502 S-IVB, First Burn

[redacted]

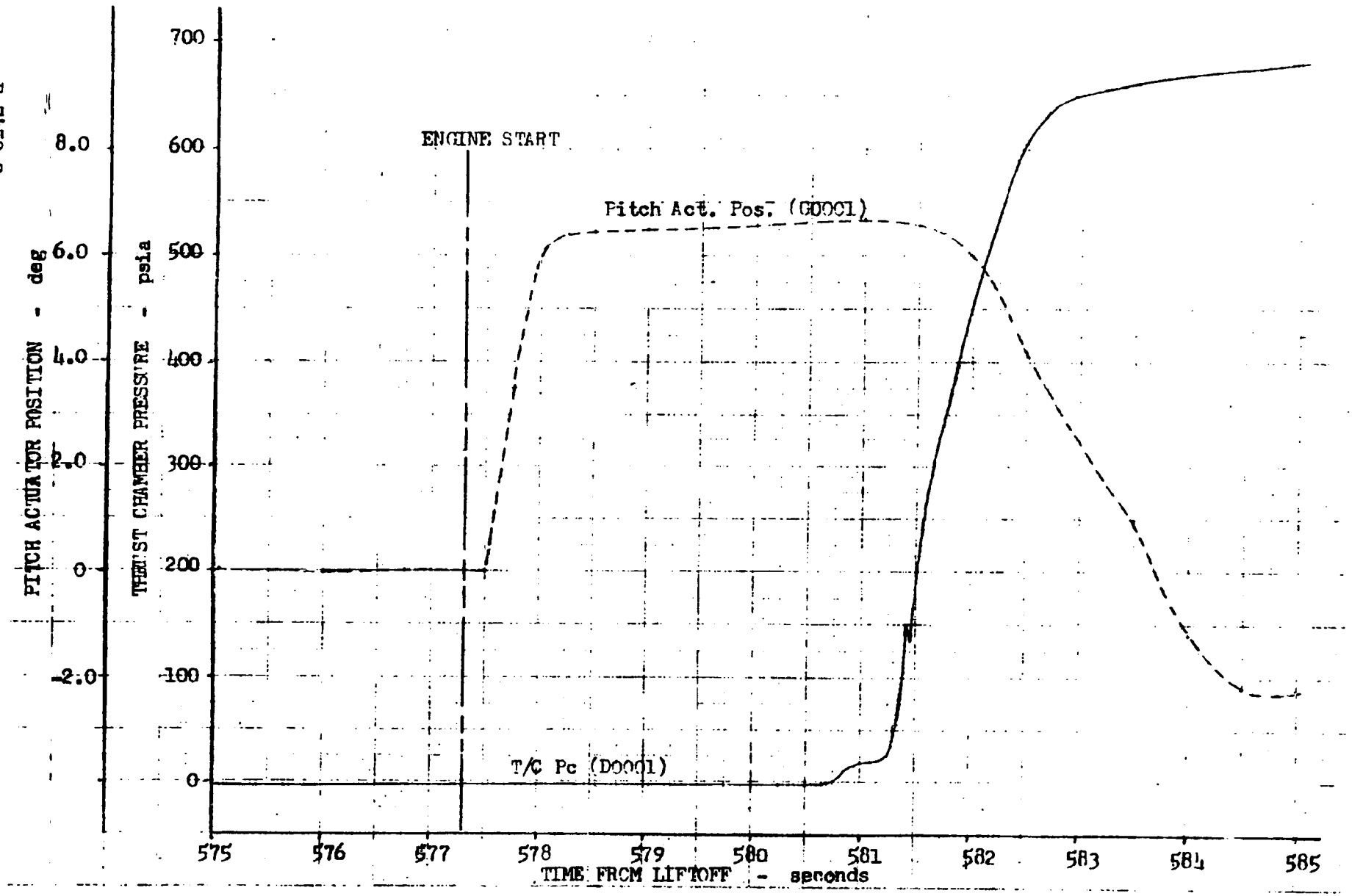

Figure 9. Pitch Actuator Position and Thrust Chamber Pressure vs Time From Engine Start Signal, AS-502 S-IVB First Burn

[redacted]

(575.6 seconds), the vehicle altitude errors and rates were +7.6 and 0.2 degree/sec in pitch, and -2.4 and 0.1 degree/sec in yaw, respectively. In addition, the vehicle altitude was 21,000 feet higher than desired. Vehicle attitude errors at S-II/S-IVB separation for a normal flight were expected to be within +2.5 degrees in the pitch and yaw axes.

Conclusion

No apparent adverse effects were incurred by the engine as a result of the gimbal transients at start, as evidenced by normal engine starting through to mainstage levels. Gimbal acceleration, velocity, and loads during the transients were well below engine model specifications and structural design limits.

SHIFTS IN ACTUATOR LOAD AND POSITION AT 644 SECONDS OF FLIGHT

Defining Data

At 644 seconds of flight, a gimbal maneuver in pitch was commanded by guidance to correct for a vehicle overspeed condition. The pitch engine position went from -0.43 degree peak at 645 seconds to a peak of +0.6 degree at 650 seconds (Fig. 6 and 7), and then settled down to a steady-state level of +0.25 degree. Yaw transients were negligible. Following the maneuver, a change in steady-state levels was noted in pitch actuator differential pressure (Δ P) and position. The Δ P changed from -175 to +100 psid (Δ +275 psi), and the position changed from +0.37 to +0.25 degree (Δ -0.12 degree).

Possible Causes of Event

The possible causes were:

1. A change in the vehicle's center of gravity and/or effects of thrust structure compliance following the maneuver
2. An external load induced by the engine system

[redacted]

Conclusions

The shift in actuator load and position was not caused by an external applied load. The phenomenon was probably allied with item 1 (above). The fact that the vehicle had just completed a gimbal maneuver tends to support this conclusions.

Analysis

The effect of gimbal bearing friction was determined by crossplotting actuator position and pressure data (Fig. 10 and 11). A 5500-pound actuator force and a 0.2-degree indicated actuator motion was required to break static gimbal friction about each axis. The magnitude of the shifts observed in actuator load and position was well within the gimbal bearing friction envelope. An externally applied force would be manifested by a load outside of the friction envelope with the absence of a command signal. Because none of these conditions were evident, it was concluded that item 2 (above) was not the cause of the phenomenon.

GIMBAL TRANSIENTS AT 690 SECONDS

Defining Data

Starting at 692 seconds, and continuing for the remainder of the first burn, small perturbations in pitch and yaw actuator positions and loads were noted. During this event, a shift in engine performance was in progress (684 to 702 seconds).

Possible Causes of Event

The possible causes were:

1. An external load induced by the engine system
2. Guidance commands

Conclusions

The gimbal transients between 690 seconds and cutoff were induced by guidance commands. There was no indication of external applied forces.

No significant shifts in thrust alignment were noted during engine operation.

Analysis

Actuator position data during the noted transients were compared with the guidance command data. All actuator motions were accompanied by command signals. This indicates that no motions were caused by suddenly applied external forces.

For the given command signals and actuator motions, corresponding actuator differential pressure (load) characteristics appeared normal and reasonable.

Engine thrust alignment, as determined from the gimbal actuator crossplots, did not agree well with engine acceptance test data, as shown in the table below; however, no significant shifts in thrust alignment occurred during engine operation. This alignment difference is not considered to be an anomaly in engine performance; it is probably the result of thrust structure compliance and/or vehicle installation tolerance. It was not possible to obtain useful thrust misalignment data for stage acceptance testing because of the lack of adequate pretest information of actuator and side-load restrainer load cell preloaders.

	Engine Acceptance	AS-502
Lateral Displacement Along X Axis, inch	-0.0610	-0.044
Lateral Displacement Along Z Axis, inch	+0.0487	-0.159

[redacted]

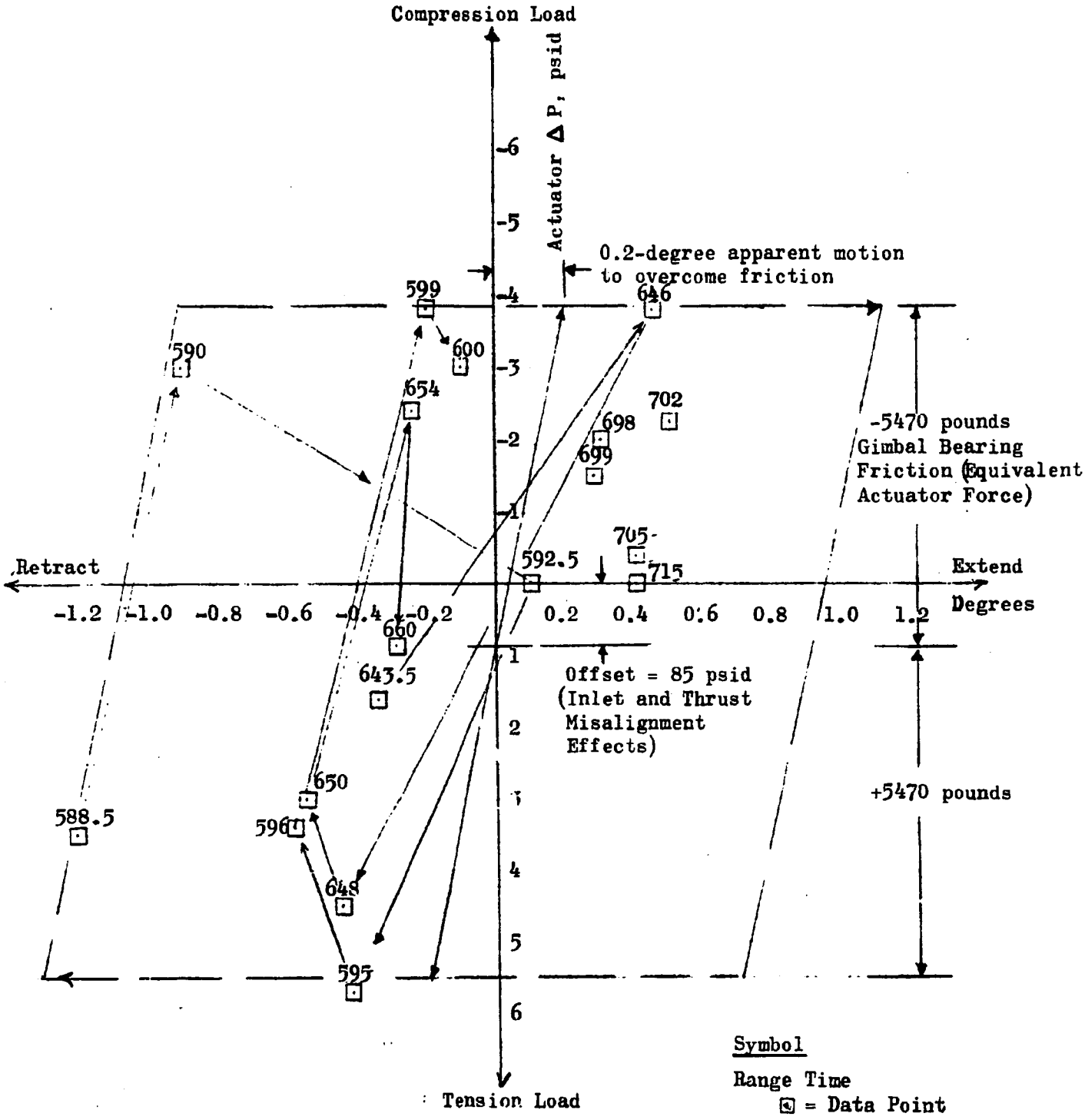

NOTE: Data points at 698, 699, 702, 705, and 715 seconds (Range Time) are plotted to show the pitch actuator transients that occurred between 690 seconds and cutoff

Figure 10. Crossplot of Pitch Actuator Position vs Load, AS-502 S-IVB, First Burn

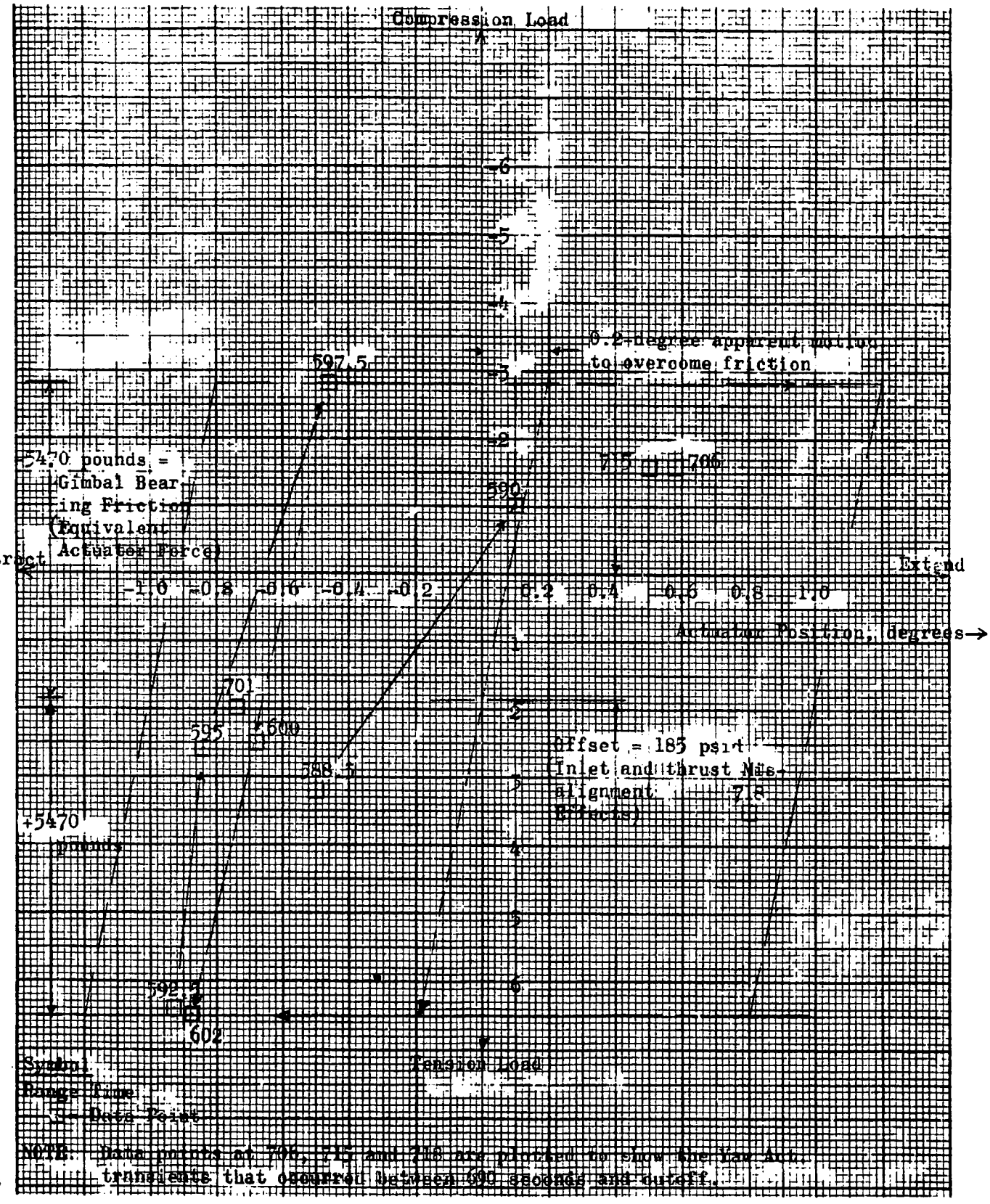

Figure 11. Crossplot of Yaw Actuator Position vs Load, AS-502 S-IVB, First Burn

[redacted]

PITCH TRANSIENT AT CUTOFF

Defining Data

At 747.2 seconds (approximately 0.17 second after engine cutoff signal), the engine was moved by the flight control system to +2.7 degrees pitch engine position (Fig. 12), and then returned to null position at 750.8 seconds.

Possible Causes of Event

The possible causes were:

1. Transients were induced by an abnormal engine shutdown
2. Transients were induced by the vehicle

Conclusion

The pitch transient at cutoff was induced by the vehicle and was a normal system behavior.

No engine hardware damage resulted from the noted pitch transient.

Analysis

Telemetered data of main engine chamber pressure and actuator differential pressure and position were analyzed. Engine chamber pressure decay was normal, and both pitch and yaw actuator loads (differential pressure) during chamber pressure decay were reasonable (approximately 1000 pounds maximum). No evidence was found that linked the gimbal transients to the engine system.

[redacted]

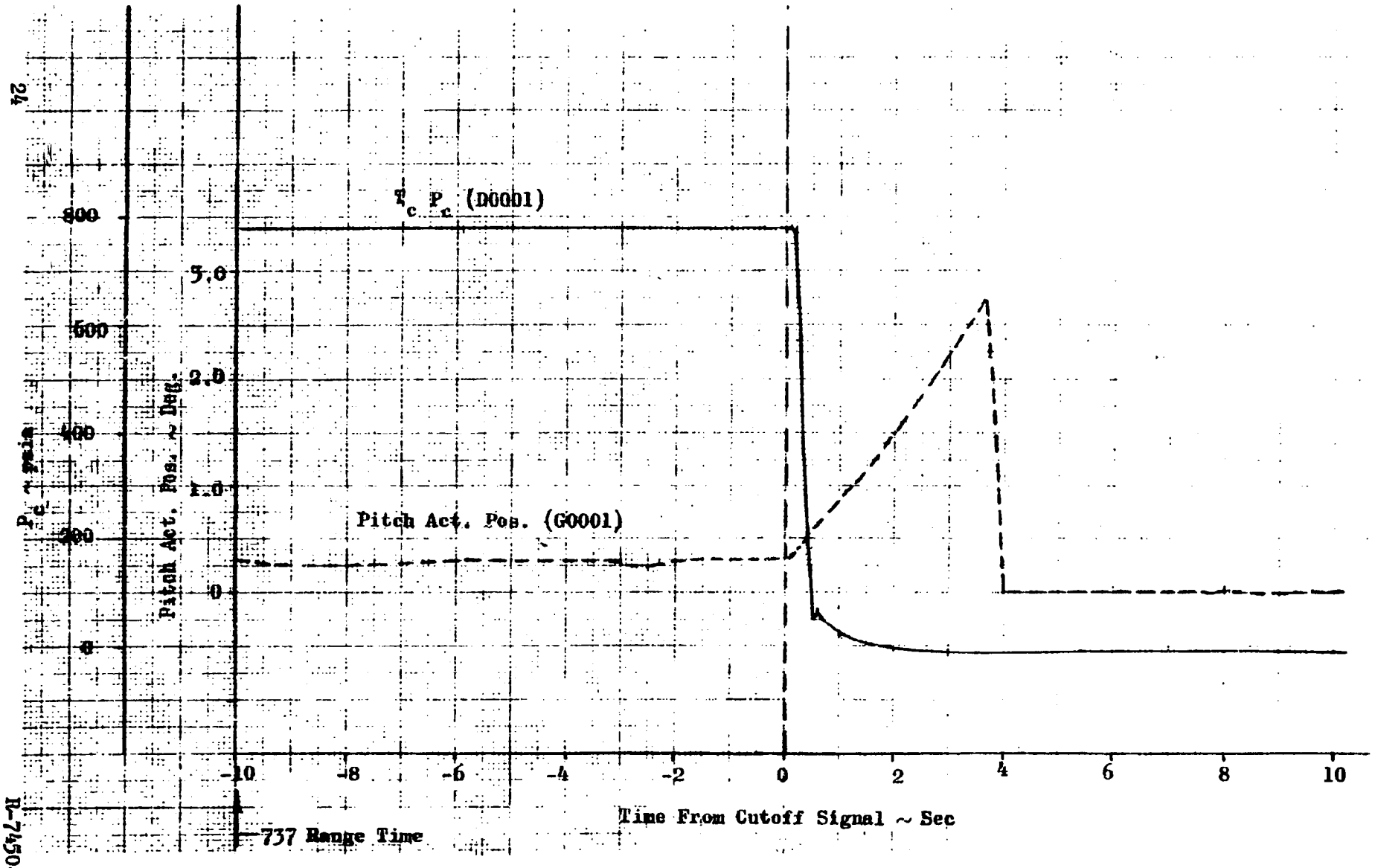

Figure 12. Pitch Actuator Position and Thrust Chamber Pressure vs Time From Cutoff Signal, AS-502 S-IVB, First Burn

[redacted]

The pitch transient at cutoff was induced by the vehicle and was a normal system behavior. Chi (χ) freeze guidance mode began 8 seconds prior to S-IVB stage engine cutoff, as intended. This mode locks out guidance and helps reduce the transients going from burn to coast. When this occurred, a substantial error signal was still being impressed by guidance to the flight control servosystem. The abrupt removal of the command signal produced a momentary imbalance in the servosystem, together with the thrust tailoff, resulted in the displacement of the pitch actuator. "S-IVB Burn Mode Off" at 750.8 seconds subsequently returned the pitch actuator to the null position, as intended.

No hardware damage resulted from the gimbal transient at cutoff, as evidenced by the normal engine start operation during subsequent restart.

CONCLUSION

Engine gimbal operation was satisfactory throughout the S-IVB stage first burn. There were no problems evident in the engine gimbal data.

[redacted]

J-2 ENGINE AREA TEMPERATURE ANOMALIES

The significant events of the thermal environment during the first burn are presented in Fig. 13. Each of these events is discussed in detail, as well as the results during restart. Figure 14 defines the temperature measurement locations.

Conclusions based on first- and second-burn thermal environment data are as follows:

1. A small cryogenic hydrogen leak started at 645 seconds and substantially increased in magnitude at 684 seconds.
2. The leak was downstream of the main fuel valve. (This includes the ASI fuel line.)
3. The location of greatest chilling was in the area of the upper ASI fuel line.
4. Two heating surges were seen; one at 696 seconds and the other at 700 seconds.
5. A low level of heating continued on the oxidizer pump side of the engine (until nearly cutoff) as a result of hot-gas leakage from the ASI; chilling resumed on the fuel pump side of the engine because of the liquid hydrogen leakage from the ASI fuel line.

The first heating surge was most likely associated with the rupture of the J-2 engine ASI fuel line at the break interface and the second heating surge with the resulting ASI failure caused by back flow from the ASI.

S-IVB FIRST-BURN THERMAL ENVIRONMENT

Event Description

Engine compartment temperatures started abnormally chilling at 645 seconds. This chilling increased in magnitude at 684 seconds.

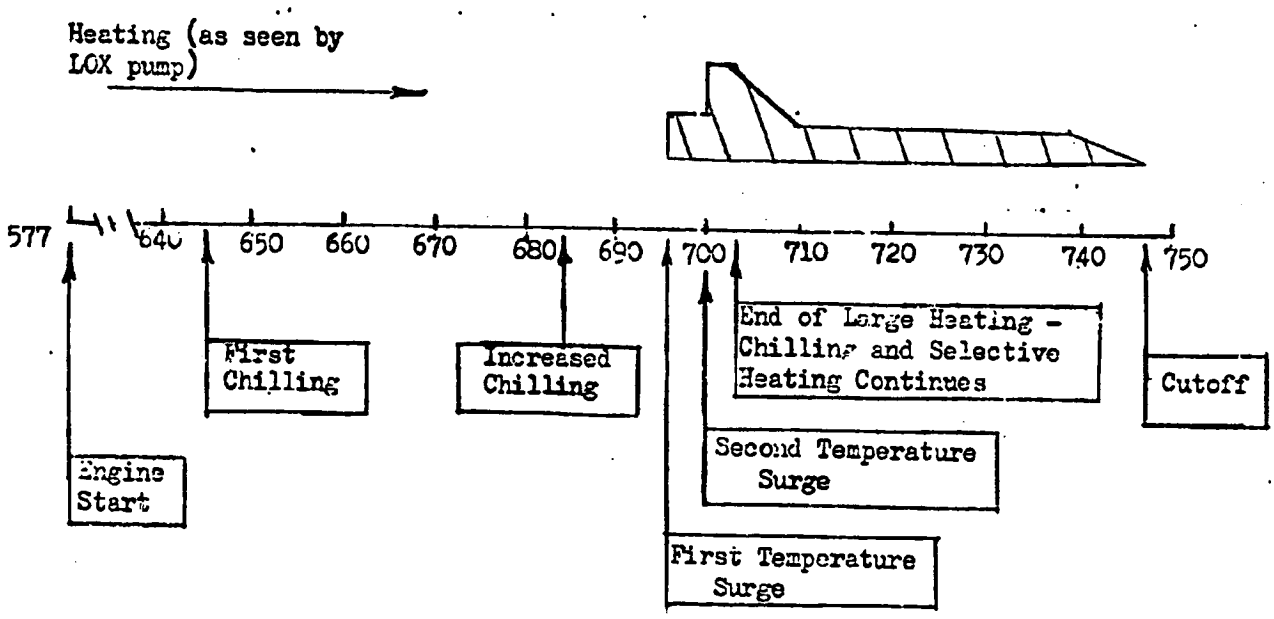

Significant Events

1. Engine compartment temperature decrease starting at 645 seconds and increasing in magnitude at 684 seconds.
2. Engine compartment heating at 696 and 700 seconds.
3. Chilling and selective heating following 703 seconds.

Figure 13. First-Burn Thermal Environment

[redacted]

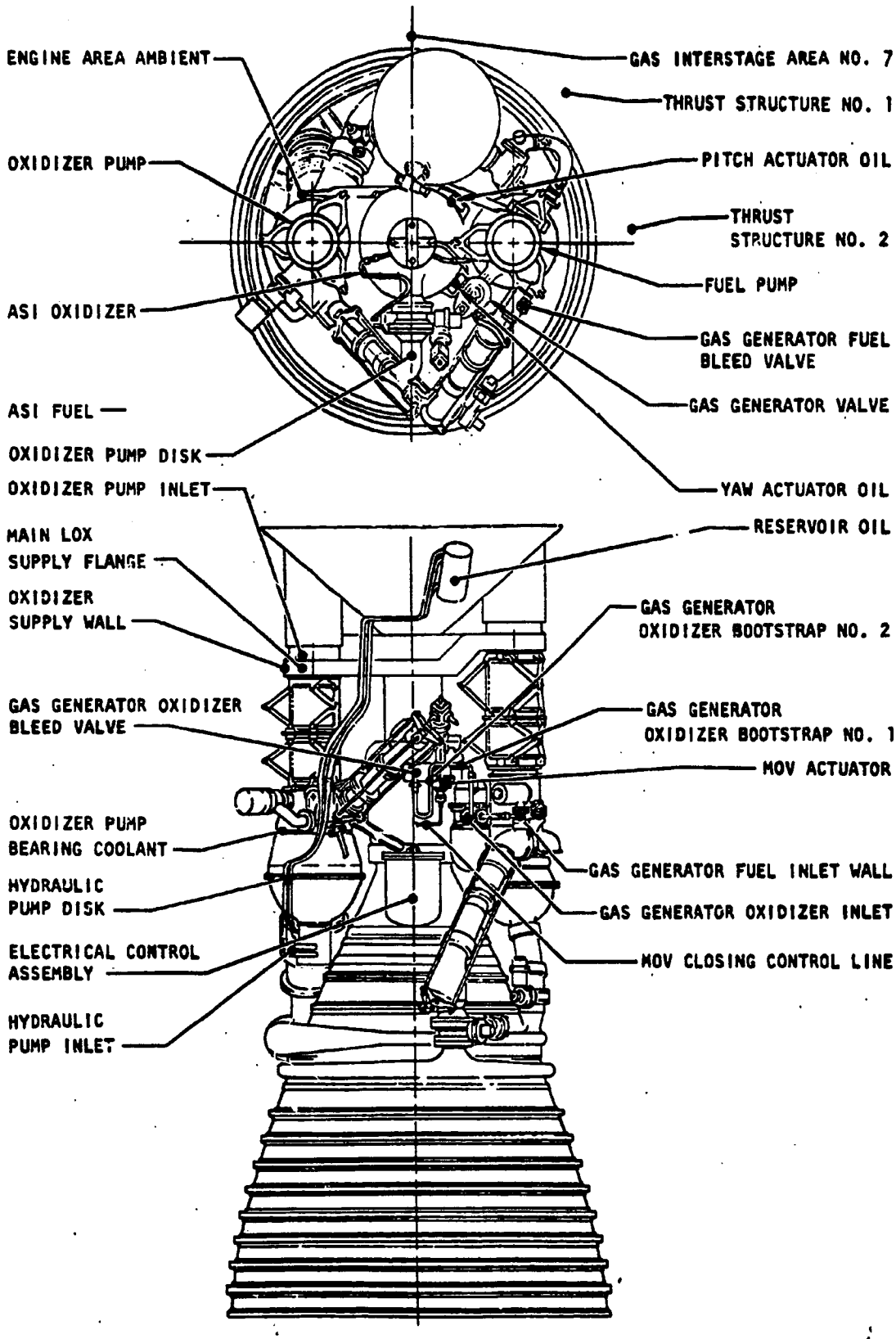

Figure 14. AS-502 S-IVB Temperature Measurements and Locations

Data. MOV closing control line temperature (Fig. 15) is representative of the engine compartment chilling that started at 645 seconds and was noted on at least six other low thermal mass parameters. At 684 seconds, the chilling rate substantially increased and was noted on at least five additional measurements.

Failure Modes. The failure mode was leak from a stage or vehicle propellant or pressurization system.

Best Hypothesis. The best hypothesis is that a small cryogenic hydrogen leak in the area of the upper ASI fuel line started at 645 seconds and substantially increased in magnitude at 684 seconds.

Analysis. A comparison of the AS-501 and AS-502 MOV closing control line temperature (Fig. 15) demonstrates that, on AS-502, a chilling of the measurement began at 645 seconds. At least six other low thermal mass measurements also showed chilling at this time. This is indicative of a small cryogenic leak. The leak rate increased substantially at 684 seconds, as indicated by the increased chilling rate on the smaller thermal mass components and the beginning of chilling of larger thermal mass components. Some of these parameters are the MOV actuator (Fig. 16), gas generator valve position indicator (gas generator valve position shifts), and gas generator fuel inlet wall (Fig. 17). These parameters are located on the fuel pump side of the engine (Fig. 14).

From the temperature decrease observed (to less than -260 F on the MOV closing control line), it is known that the leak is cryogenic in nature. Both engine helium usage and the hydrogen and helium pressurization flows from the engine were normal during the first burn and, therefore, it is known these systems are not responsible for the leakage.

An analysis based on the properties of a liquid expanding into a high vacuum was accomplished to determine the chilling effect on engine components. It was found that some components were chilled more than is

[redacted]

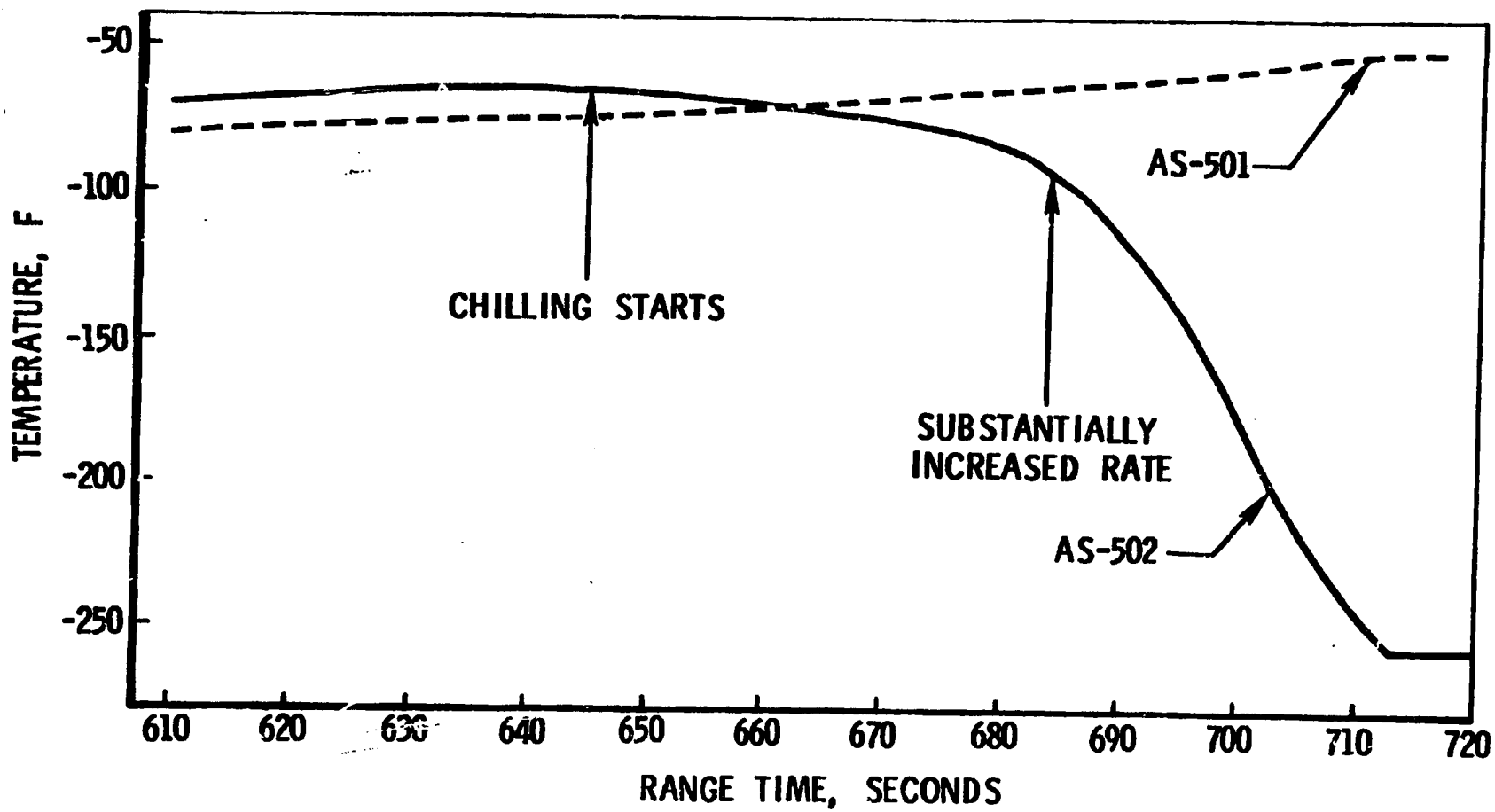

Figure 15. First-Burn MOV Closing Control Line Temperature, S-IVB Engine J2042

[redacted]

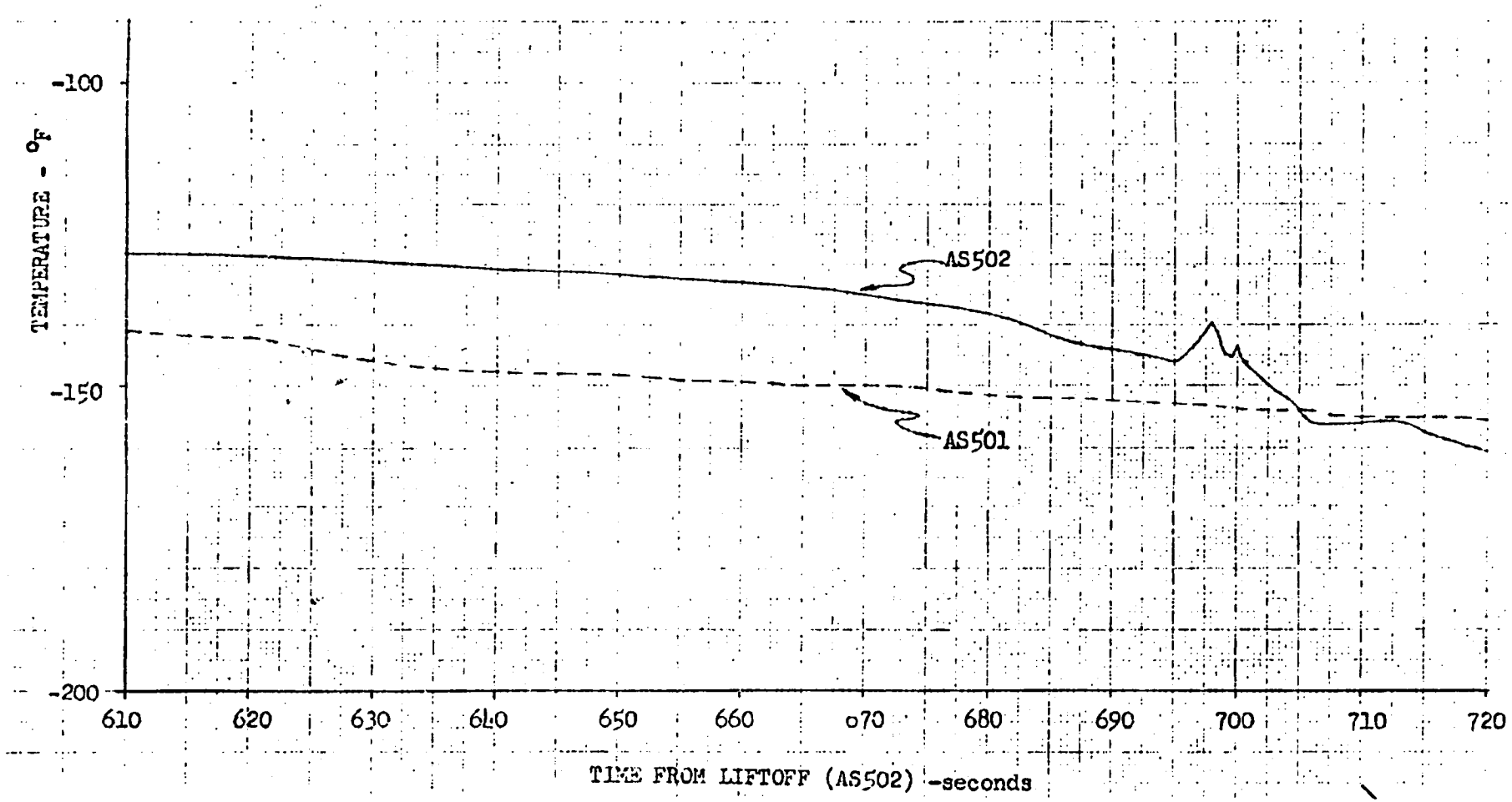

Figure 16. AS-502 S-IVB First Burn, MOV Actuator Temperature AS-501 and AS-502 Comparison

[redacted]

possible with oxygen expansion (-380 F is the minimum temperature for the vacuum environment encountered). The gas generator fuel inlet wall temperature (Fig. 17) attained -409 F, and from this it was concluded the leak source was hydrogen rather than oxygen. By knowing the properties as a function of distance of the expanding liquid in a vacuum, and the rate of chill of different components, it was possible to locate the general area of the leak source as the upper section of the ASI fuel line.

Event Description

Engine compartment heating at 696 and 700 seconds.

Data. Figure 18 is a comparison of the gas generator oxidizer bootstrap line No. 1 and the MOV actuator temperature measurements during the period of initial engine compartment heating. Figure 19 is a similar comparison for the main oxidizer supply line flange and the oxidizer pump discharge temperature. These parameters demonstrate the two general types of heating seen. Temperature parameters on the fuel pump side of the engine (Fig. 18) had an initial temperature surge at 696 seconds of greater magnitude than the surge at 700 seconds. Parameters on the oxidizer pump side of the engine (Fig. 19) showed the opposite effect.

Causes

A hot-gas source of leakage is required for heating in the vacuum environment of the flight because combustion cannot be sustained below a pressure of about 0.2 psia. The available sources of hot gas are:

1. Gas generator and exhaust system
2. Thrust chamber
3. ASI

To explain the two temperature surges seen, it is necessary that there be either: (1) a single source of hot-gas leakage increasing in magnitude,

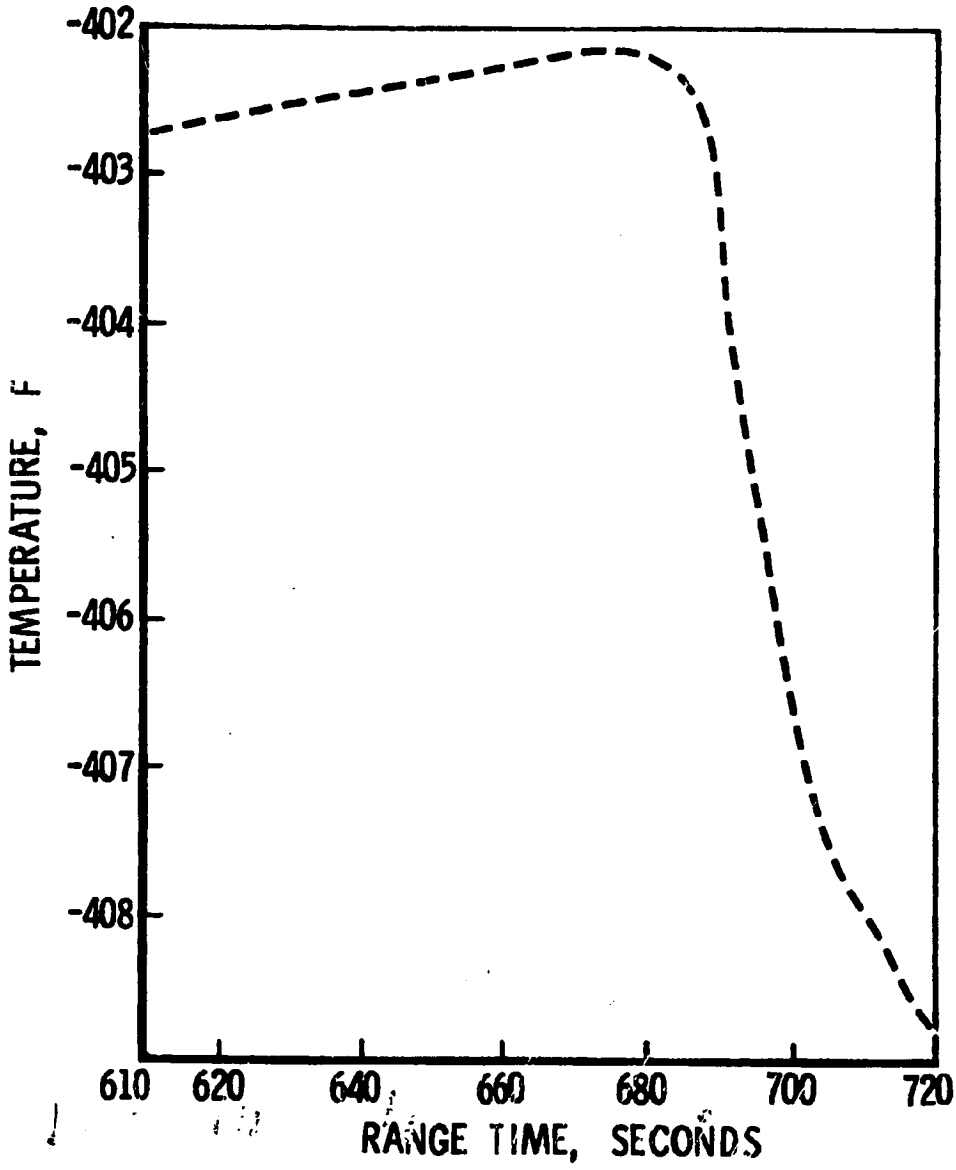

Figure 17. Gas Generator Fuel Inlet Wall Temperature, S-IVB Engine J2042

[redacted]

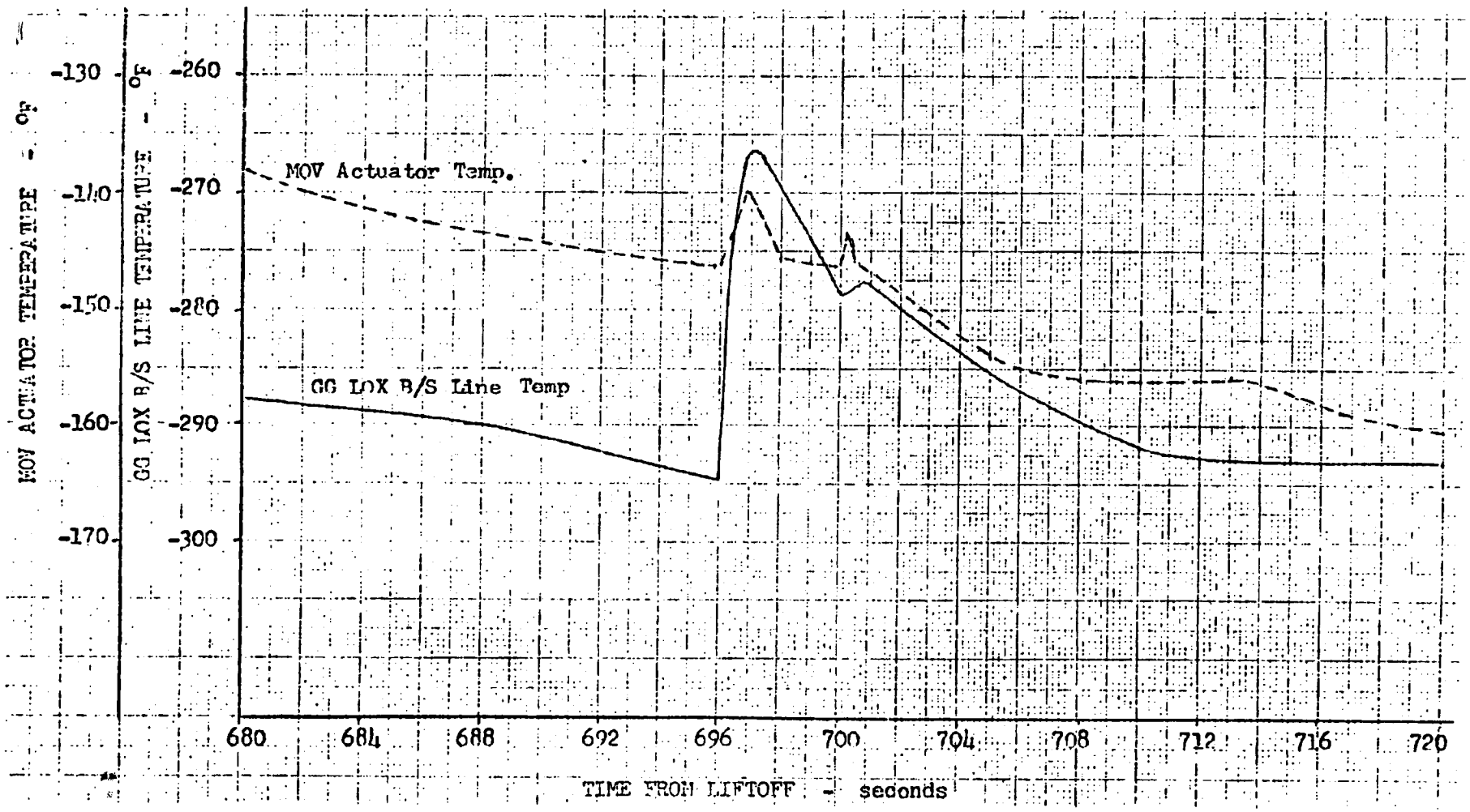

Figure 18. AS-502 S-IVB First Burn, Engine Compartment Heating Effects on Measurements on Fuel Pump Side of Engine

[redacted]

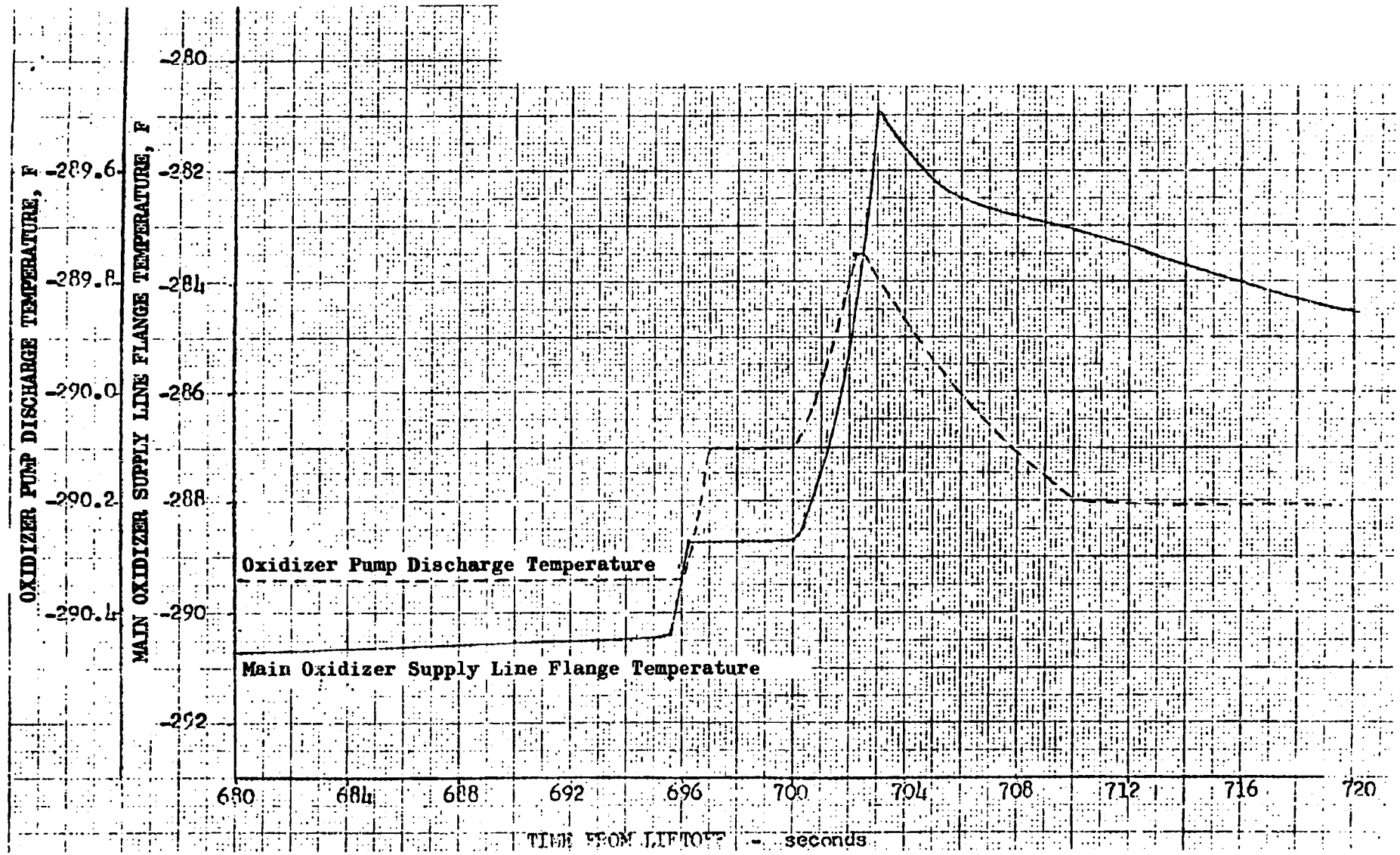

Figure 19. AS-502 S-IVB First Burn, Engine Compartment Heating Effects on Measurements on Oxidizer Pump Side of Engine

[redacted]

or (2) a hot-gas leak that is redirected or changed in character by increasing cryogenic leakage and/or component erosion.

Best Hypothesis. The first heating was associated with the destruction of the ASI fuel line at the break interface with resulting backflow from the engine; the second is associated with the redirection of the hot gas from the ASI when the upper fuel flex line ASI were destroyed by the backflow.

Analysis. The temperature surges seen in Fig. 18 and 19 show two distinct characteristics. On the fuel pump side of the engine (Fig. 18), the initial surge is of greater magnitude than the surge at 700 seconds. For the oxidizer pump-side parameters (Fig. 19), the opposite situation is present, i.e., the second surge is of greater magnitude than the first. From this it is concluded that the hot-gas leak is either redirected or changed in character by increasing cryogenic leakage, not just an increase in magnitude of heating as this would have been reflected in an equal manner to the first surge in all parameters.

A hydrogen leak from the thrust chamber jacket that eventually results in hot-gas leakage from the combustion chamber fails to satisfy sufficient criteria. A leak in the jacket could be hypothesized to cause erosion through the jacket walls, but this would have to occur between the leak source and fuel manifold on the same set of tubes. The temperature data do not support this hypothesis; they neither explain the two temperature surges nor the chilling of components after the hot-gas leakage below the fuel manifold in the area of initial leakage while heating exists on the opposite side of the engine (gas generator valve position shifts). Also, it fails to explain the failure to restart.

A gas generator or exhaust system leak also fails to explain the temperature data seen. A hot-gas leakage from this source would not account for the chilling, the second temperature surge, the lack of external heating on restart, nor the failure to restart.

From the simulated ASI fuel line failure test on engine J014-6, it was found that hot-gas leakage from the ASI would destroy the upper flex line at the ASI shortly after backflow developed. The initial temperature surge is, therefore, believed to be associated with backflow leakage from the ASI at the break interface, and the second surge with the destruction of the ASI fuel line at the ASI. This source of hot gas (about 1 lb/sec) was redirected because of its new location and the effects of the fuel leak from the broken ASI fuel line (about 4 lb/sec), thus accounting for the larger heating effects on the oxidizer pump side of the engine.

Event Description

General chilling of the vehicle with selective heating of components on the oxidizer pump followed the second temperature surge at 700 seconds.

Data. Figure 20 shows the increases in temperature of the oxidizer pump inlet and the change in temperature across the pump, and between the pump and the discharge measurements. Figure 21 demonstrates the resumption of the chilling trend in vehicle parameter on the fuel pump side of the engine.

Possible Cause. Hot gases heating part of the engine area combined with chilling from a cryogenic leak to produce selective heating and general chilling.

Best Hypothesis. Following destruction of the upper fuel flex line and ASI, chilling of vehicle parameters on the fuel pump side resumed because a flow from the liquid side of the fuel line, and heating of the oxidizer pump side of the engine continued at a reduced level because of leakage of hot gas from the ASI past the gimbal bearing.

Analysis. The temperature surge starting at 700 seconds increased in intensity until 703 seconds and then decreased. Heating continued on the oxidizer pump side of the engine until nearly cutoff. To isolate the area of heating, the change in temperature between measurements on the

[redacted]

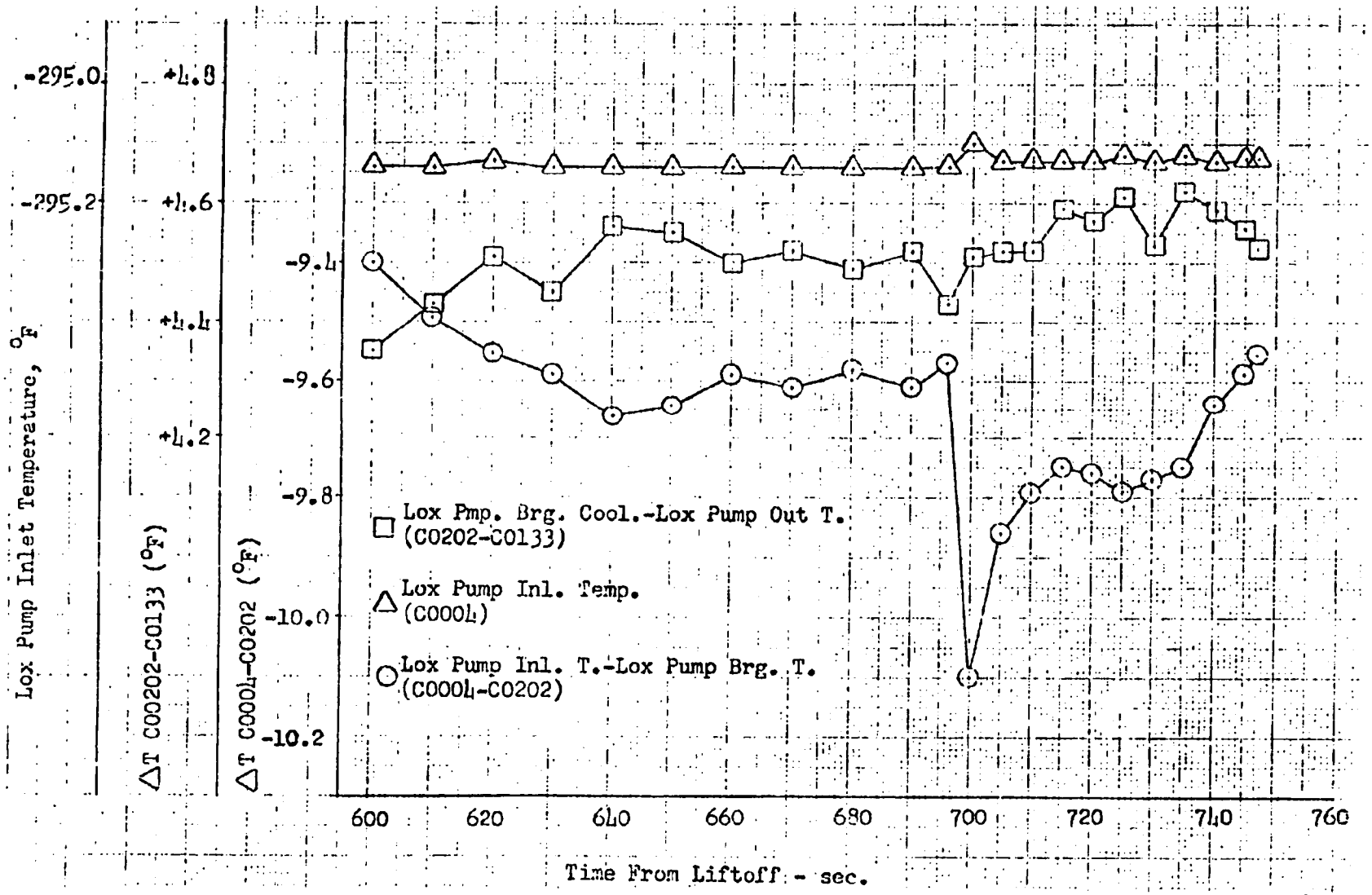

Figure 20. AS-502 S-IVB First Burn, Oxidizer Pump System Temperatures

[redacted]

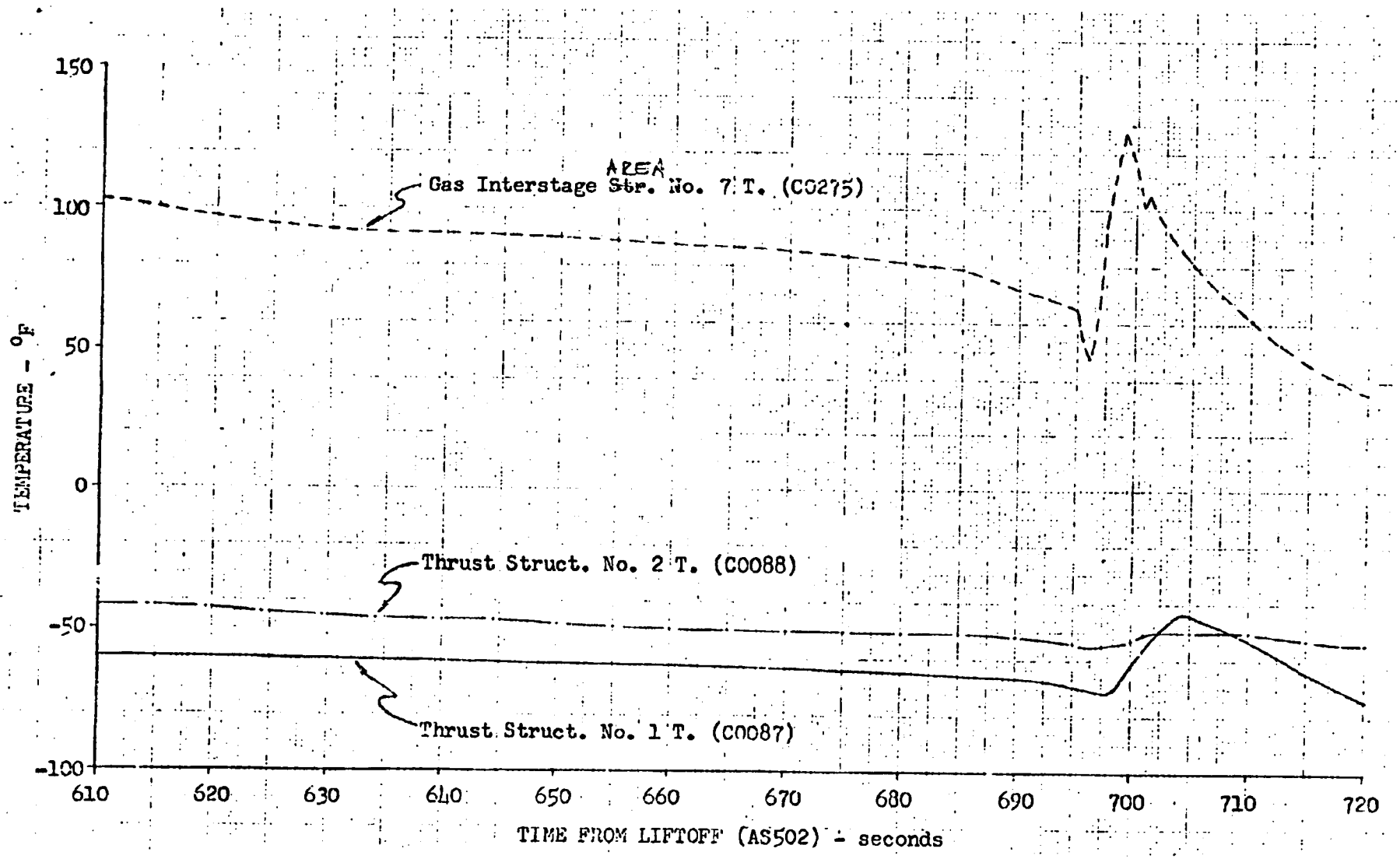

Figure 21. AS-502 S-IVB First Burn

[redacted]

oxidizer system was found (Fig. 20). The pump inlet-to-bearing coolant change in temperature yields the heating across the pump, whereas any heating to the pump discharge ducting would be reflected in the bearing coolant-to-pump discharge measurement. A small temperature increase was seen at the oxidizer pump inlet (0.04 F maximum with a sustained level of 0.01 F), but the largest temperature increase was seen between this measurement and the oxidizer pump bearing coolant (0.5 maximum with a sustained level of 0.15). No heating was seen on the discharge ducting. Therefore, some small heating persisted after the initial temperature surge to the oxidizer pump inlet ducting until nearly cutoff.

Test 313-041 on engine J016-4 was accomplished to simulate the flight failure of the ASI fuel line. Although the engine test did not exactly simulate the thermal environment to be seen on the flight, it did produce some useful supporting data in this regard. In several important aspects, there would be a difference between this test and a flight. In the vacuum environment of a flight, external combustion will not take place once the pressure becomes less than about 0.2 psia, nor would oxygen be present to support combustion for any unburned hydrogen from the ASI. Also, fuel from the destroyed upper flex section would be present on the flight to chill at least the fuel pump side of the engine.

Heating of the oxidizer pump side of the engine was experienced on engine J014-6 partially because of hot-gas leakage past the gimbal bearing (Fig. 22). This would account for the similar condition that was present during flight. The difference between the oxidizer pump inlet and oxidizer pump bearing temperature for the test on engine J016-4 was 0.5 F during the time of sustained heating. This substantiates the fact that heating to the oxidizer side of the engine can occur from ASI fuel-side hot-gas leakage. (The magnitude of heating cannot be compared because the conditions encountered on flight were not present.)

The parameters on the fuel pump side of the engine continued their temperature decrease following 703 seconds. Some temperature parameters on

[redacted]

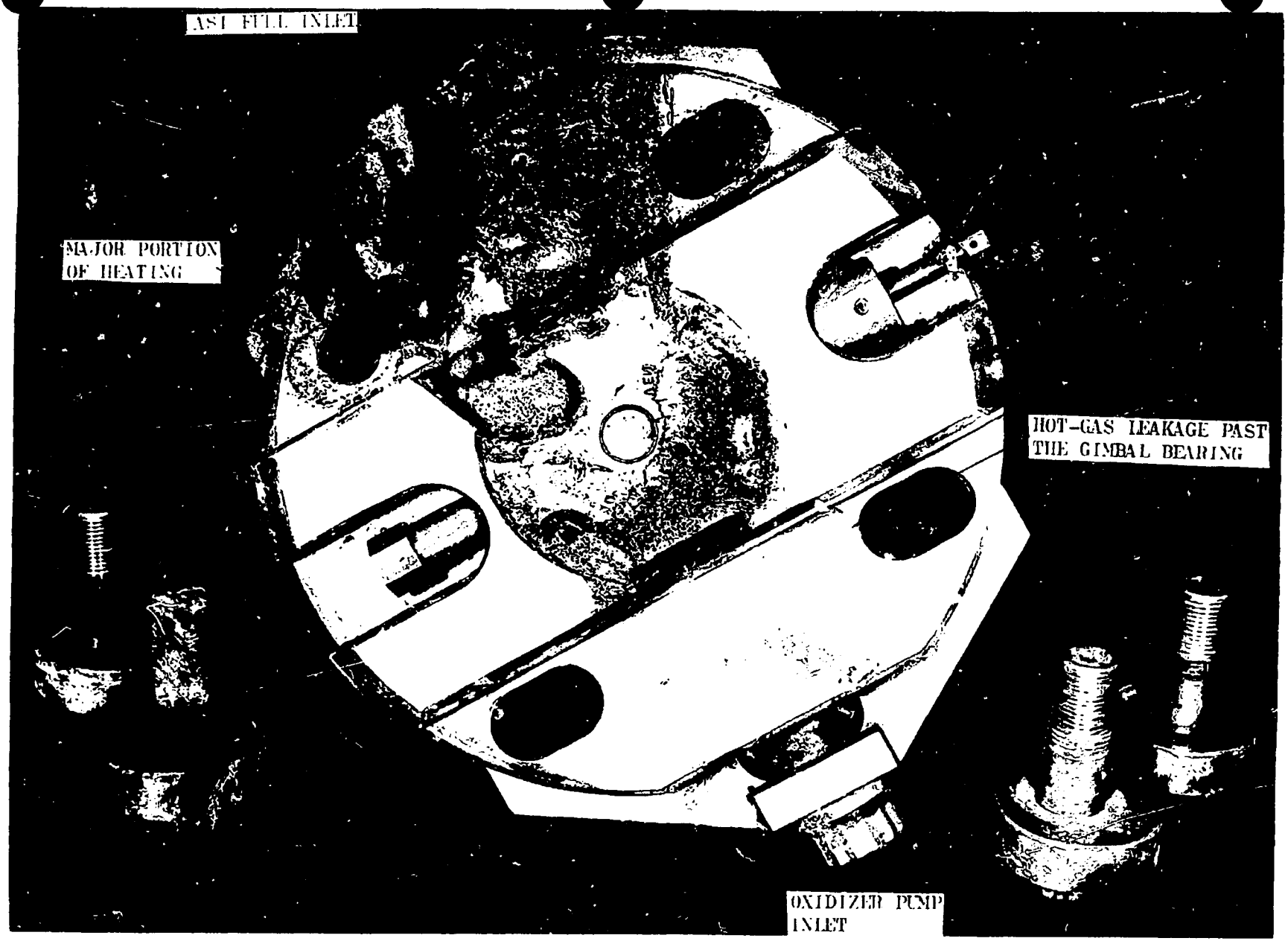

1CT25-5/7/68-S1F*

Figure 22. J016-4 Posttest 313-041 Engine Side of Gimbal Bearing Showing Heating From ASI Hot Gas

the fuel pump side of the engine showed heating until 703 seconds but, after this time, chilling was observed to be the predominant thermal effect (Fig. 21). Hot gas undoubtedly was present on the fuel side of the engine, but the chilling effect of the hydrogen was dominant. This would be expected with failure of the ASI fuel line because of the large liquid hydrogen leak flow.

S-IVB RESTART THERMAL ENVIRONMENT

Event Description

Upon engine start command at restart, chilling was again noted in the engine area.

Data. Figure 23 is a comparison plot of AS-501 and AS-502 MOV line temperature at restart. Chilling is noted on the measurement 2 seconds after engine start command, 11,617 seconds range time.

Possible Causes. The possible cause was leakage of a cryogenic propellant.

Best Hypothesis. Leakage occurred from somewhere downstream of either the main fuel valve, including the ASI fuel line, or the ASI oxidizer line.

Analysis

Figure 23 shows the MOV line temperature measurement is not chilled until after engine start command. Because propellants are down to all engine valves prior to engine start, it must be concluded that the source of leakage is in the areas shown in Fig. 24. either downstream of the MFV, including the ASI fuel line, or downstream of the ASI oxidizer valve. Other engine parameters showed chilling after mainstage signal when the pumps have developed sufficient pressure to produce the flows required to chill these parameters. No parameters showed heating, thus eliminating the gas generator and exhaust system as the source of hot gas. These data support the earlier hypothesis of failure of the ASI fuel line.

[redacted]

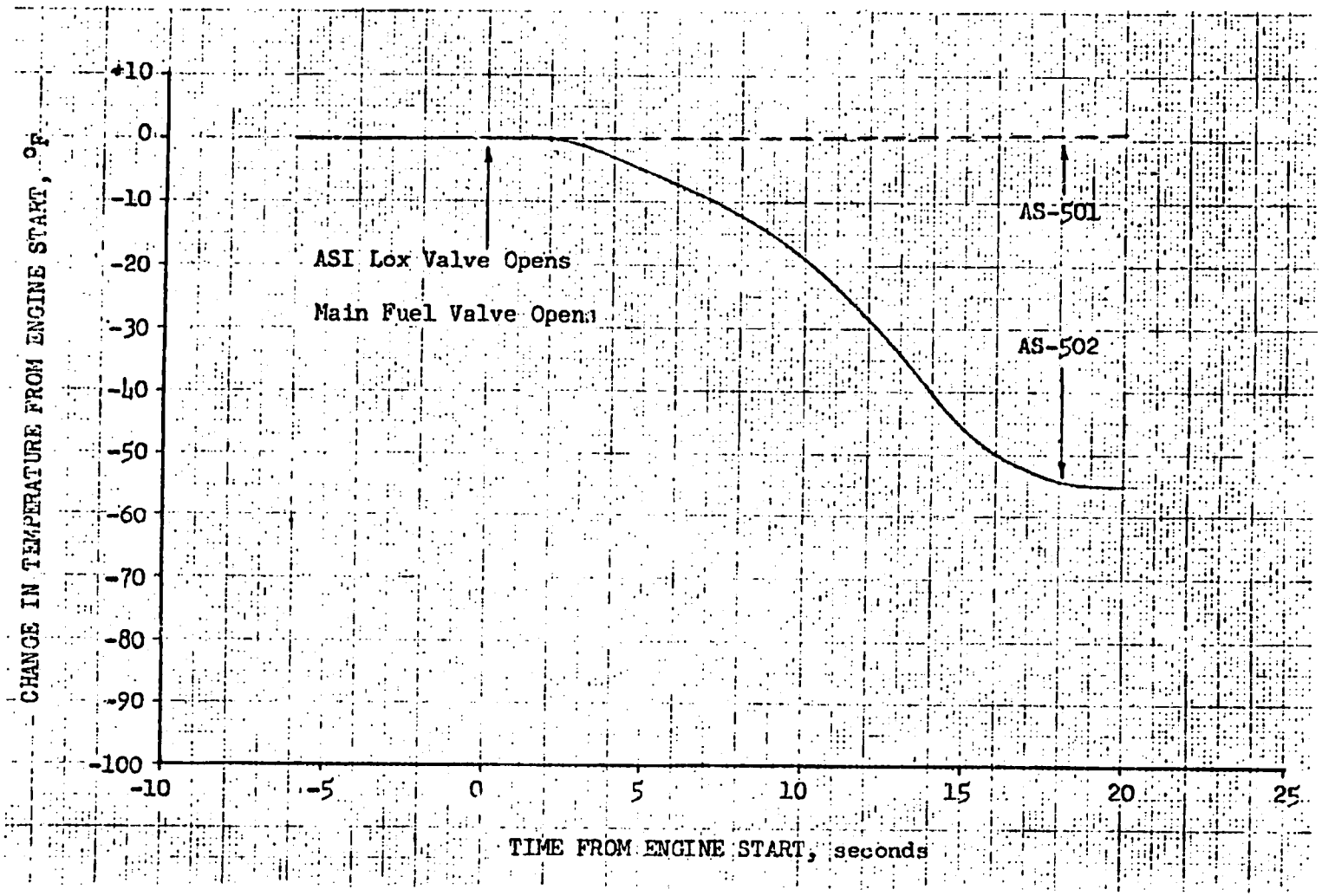

Figure 23. S-IVB Engine J2042 Second-Burn MOV Closing Line Temperature Comparison

[redacted]

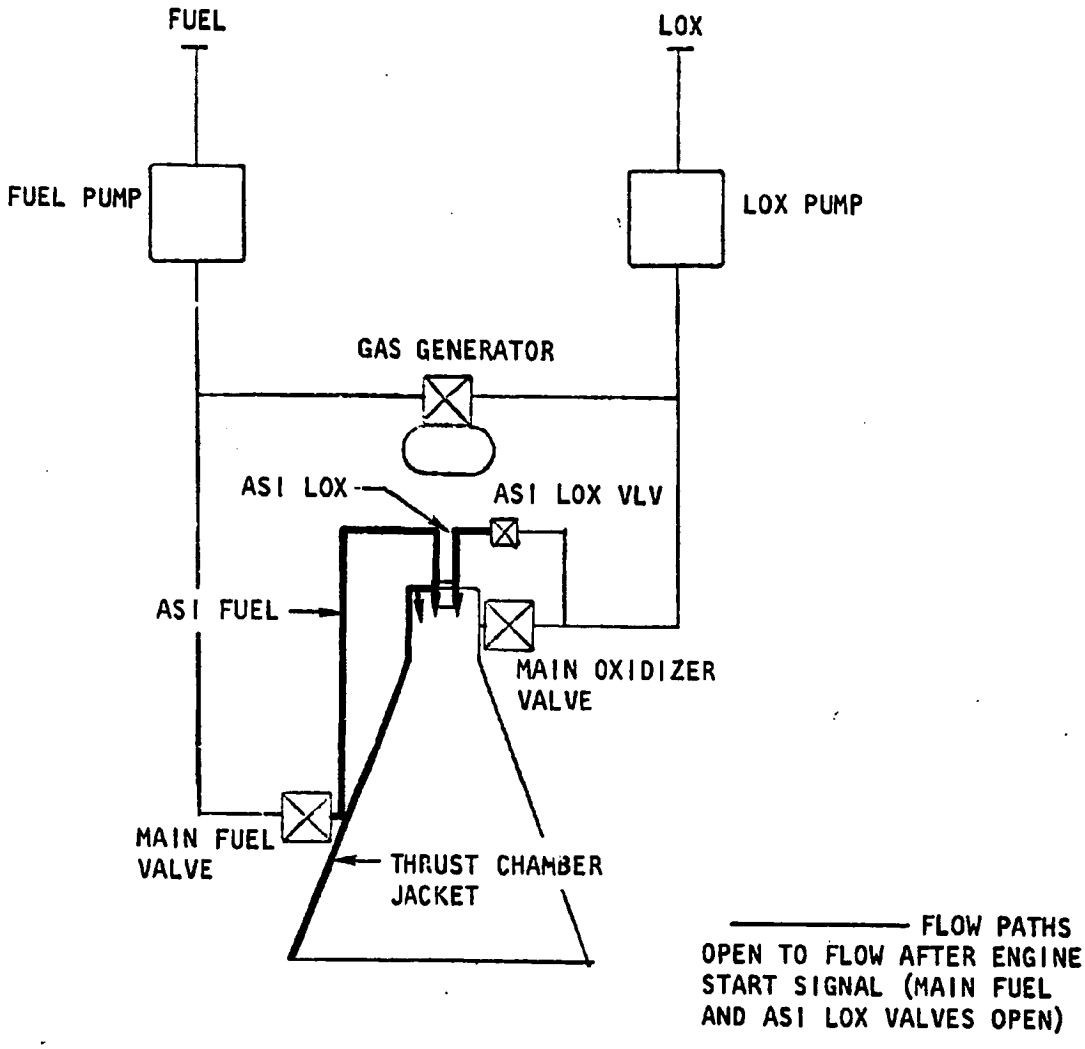

Figure 24. J-2 Engine System Leakage Paths Open Between Engine Start and STDV Signal

[redacted]

GAS GENERATOR VALVE POSITION SHIFTS

Event Description

In the time span between 680 and 745 seconds from liftoff, the gas generator valve position trace indicated an abnormal drift of 3.2 percent toward closed (Fig. 25). Because the drift was coincident with the engine performance changes and the other anomalies, a study was conducted to determine its cause, and to establish if it could have contributed to gas generator and engine performance decay.

Supporting Data

A plot of gas generator valve position and chamber pressure versus time from liftoff for S-IVB first and second burn is shown in Fig. 25. On the first burn, the valve position exhibited the typical overshoot at start, held at 92 percent until 685 seconds, and then drifted toward closed. At engine cutoff (747 seconds), the valve had drifted to 89-percent open and the position versus time trace still was trending closed. A plot of valve position versus time for a typical firing also is plotted in Fig. 25.

Possible Cause

It was postulated that the position shift was the result of the engine compartment cryogenic leak, which caused contraction of the housing by chilling. A laboratory test program was conducted to attempt duplication of valve closing by chilling the potentiometer or actuator housing.

The test program and study were performed as planned, and the conclusions are as follows.

[redacted]

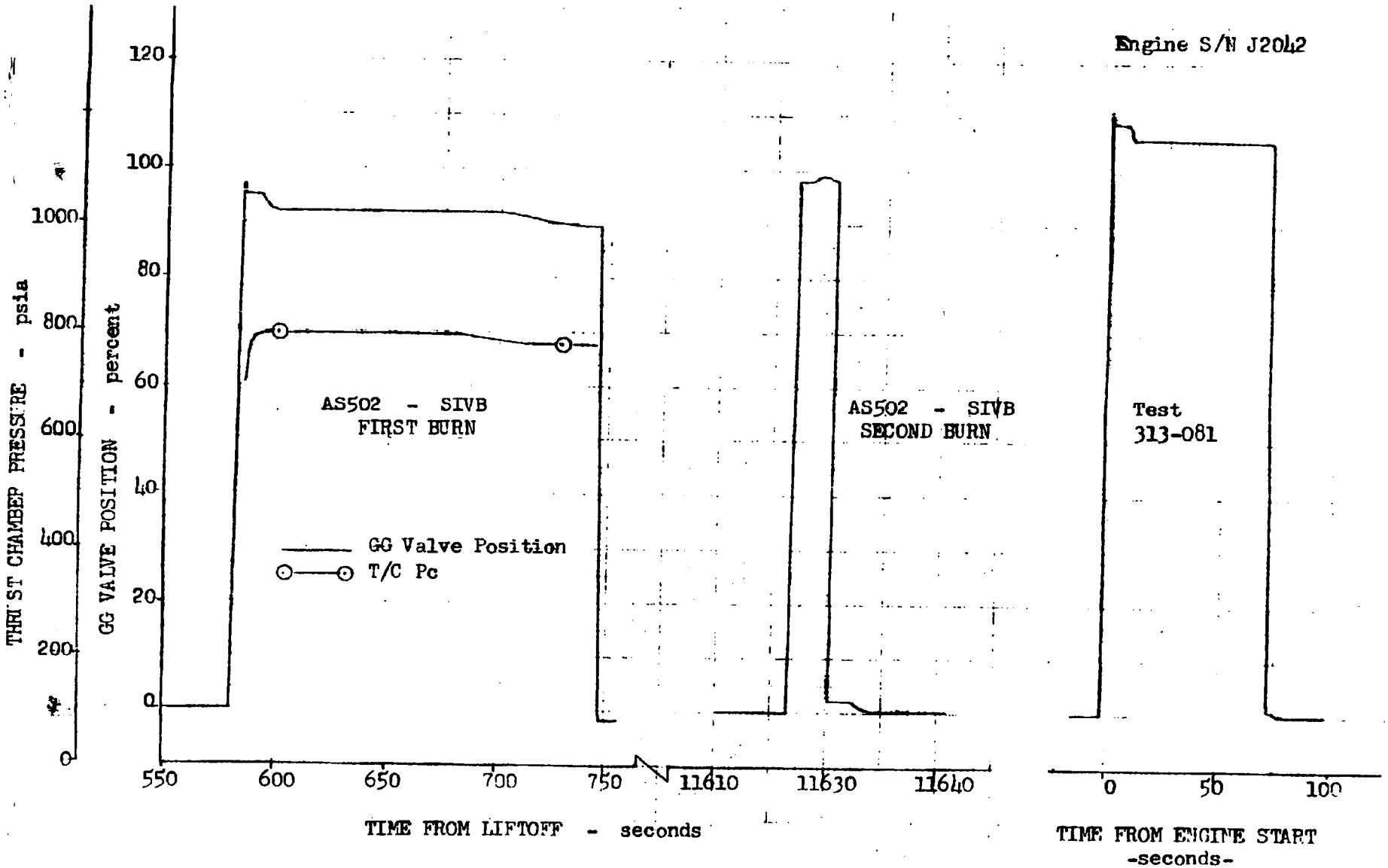

Figure 25. Gas Generator Valve Position Comparison

[redacted]

Conclusions

1. The gas generator valve motion between 685 and 747 seconds was the result of a cryogenic fluid spraying the valve body, resulting in differential contraction between the body and its internal components.

2. The motion was insufficient to cause an increase in gas generator valve resistance and did not cause the engine performance shift.

3. The fluid leakage was from some source other than the gas generator system.

4. No gas generator system anomalies occurred on the subject flight.

Test Program

The test program was conducted in the Rocketdyne environmental laboratory. The test apparatus consisted of a gas generator control valve with a 400-psi helium source for valve opening (Fig. 26). Skin temperature thermocouples were attached to the actuator body and to the potentiometer. For chilling, 0.8 lb/sec of LN_2 was sprayed onto the actuator housing. Continuous recordings of valve position and body temperatures were taken.

Two tests were run with LN_2 impinging on the exterior of the actuated gas generator valve. On the first test (No. 10), the LN_2 was directed to impinge on the side of the actuator housing, as shown in Fig. 26. On the second test (No. 11), the LN_2 was directed to impinge on the potentiometer housing. On both tests, approximately half the actuator housing was bathed in LN_2.

Plots of valve position, gas generator valve body temperature, and potentiometer body temperature versus time from start of LN_2 flow for tests No. 10 and 11 are given in Fig. 27 and 28. The differences between the chilldown rates for the body and potentiometer are explained by location of the LN_2 spray. On test No. 10, the flow was directed to the body near

[redacted]

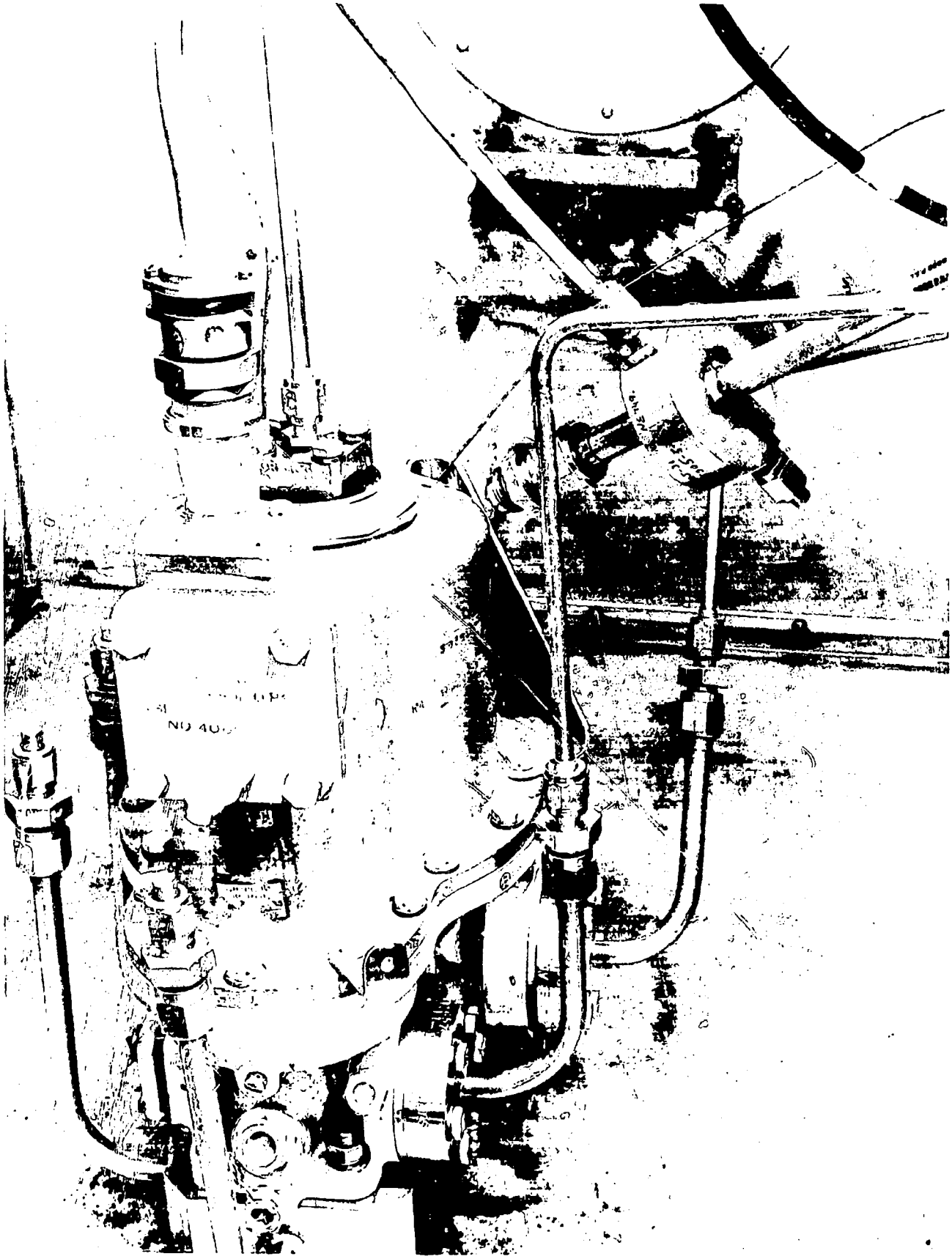

1CT64-4/18/68-C1A

Figure 26. Gas Generator Valve Setup for LN_2 Spray

[redacted]

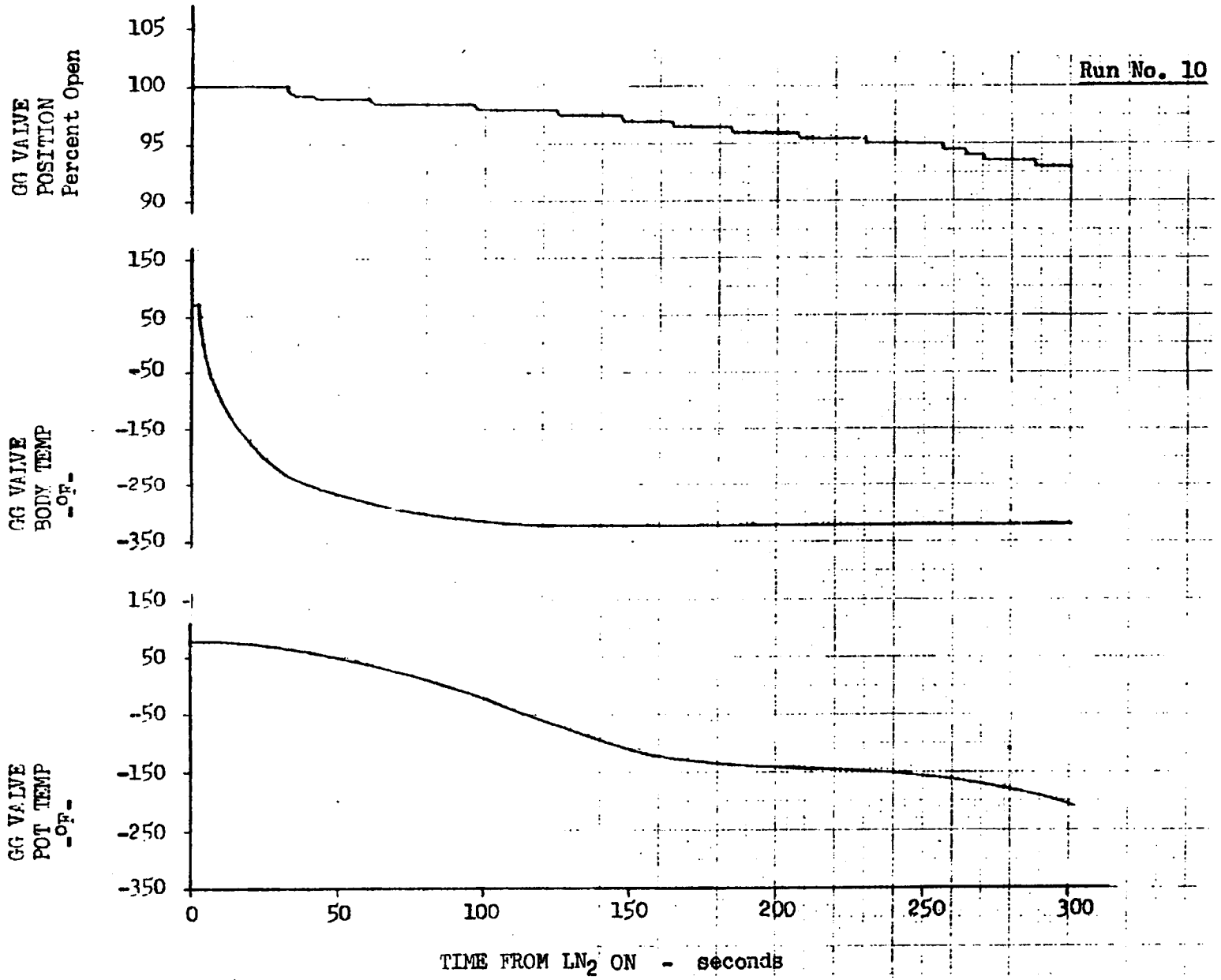

Figure 27. Gas Generator Valve Position and Valve Body Temperature vs Time

[redacted]

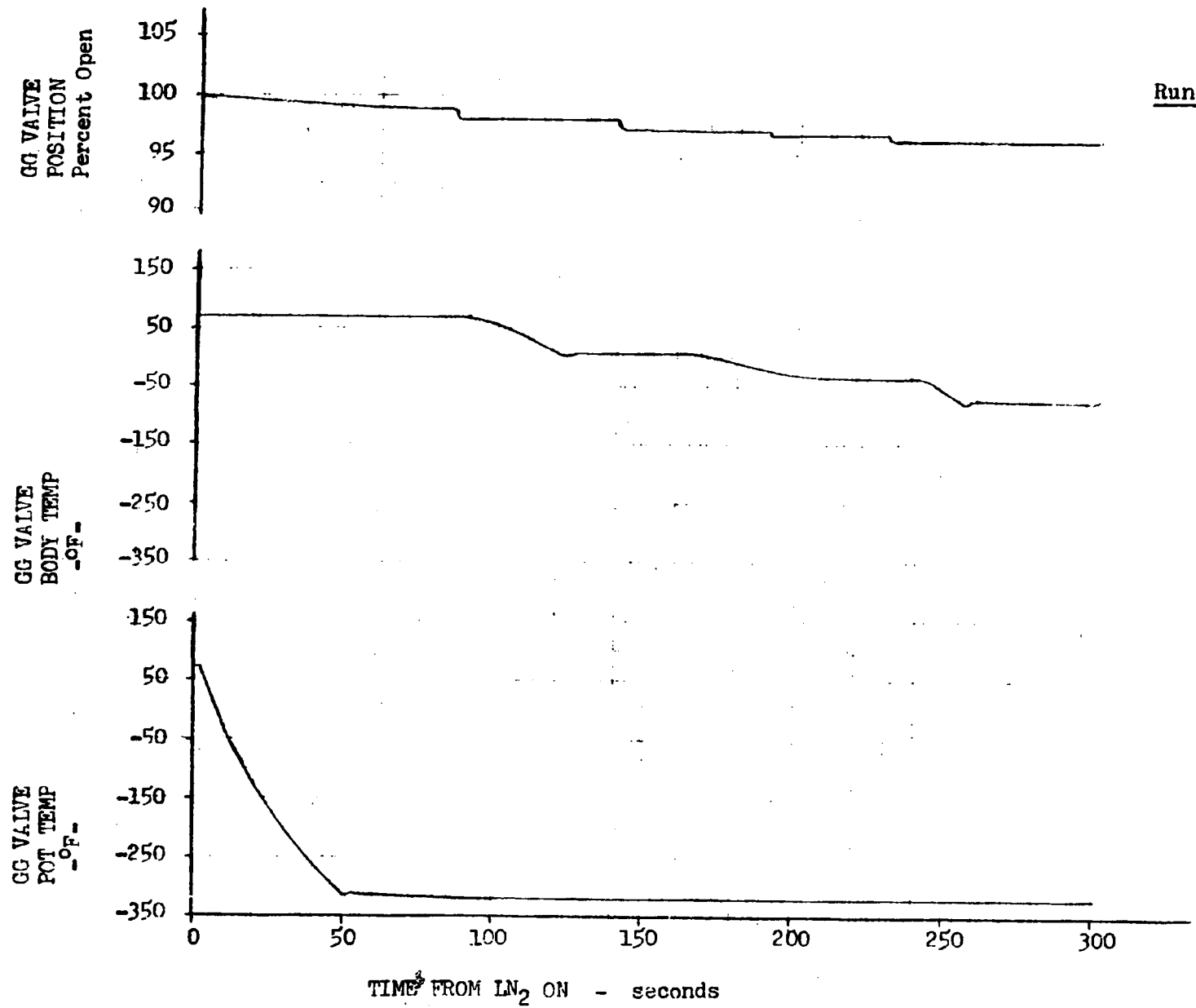

Figure 28. Gas Generator Valve Position and Valve Body Temperature vs Time

the body thermocouple location whereas, on test No. 11, the flow was directed onto the potentiometer.

Although body and potentiometer apparent chill rates were quite different for the two tests, the valve closing rates were similar. The slow chilling of the body on test No. 11 was because the spray was directed on the side away from the thermocouple and the actual body chill rate was similar for the two tests. The time for the valve to move 3.3-percent closed was 165 seconds on test No. 10 and 185 seconds on test No. 11. This indicates the motion is caused by chilling the valve body while the internal components remain warm. Both tests were for approximately 2500 seconds. Each time, the valve moved toward closed for approximately 350 seconds, then began to move toward open. By 2000 seconds, it was back to 100-percent open. An extended time plot for test No. 10 is shown in Fig. 29.

Analysis

The apparent valve motion is the result of differential contraction between the housing and internal components, caused by chilling from the external cryogenic leak. As illustrated on test No. 11, very rapid chilling of the potentiometer alone will not cause the motion. It is caused by temperature difference between the body and internal components. As chilling continues, the internal components finally chill and the motion reverses itself as shown in Fig. 29.

The apparent valve motion can be understood by referring to a valve section view (Fig. 30). Chilling of the housing will cause housing shrinkage while internal components remain initially warm. With the potentiometer mounted to the housing and measuring differential motion between the housing and yoke, relative shrinkage appears as valve motion.

Chilling the valve will cause changes in the length of the fuel and oxidizer poppet stroke, the maximum difference being approximately 0.007 inch. Previous tests have shown that gas generator valve resistance does

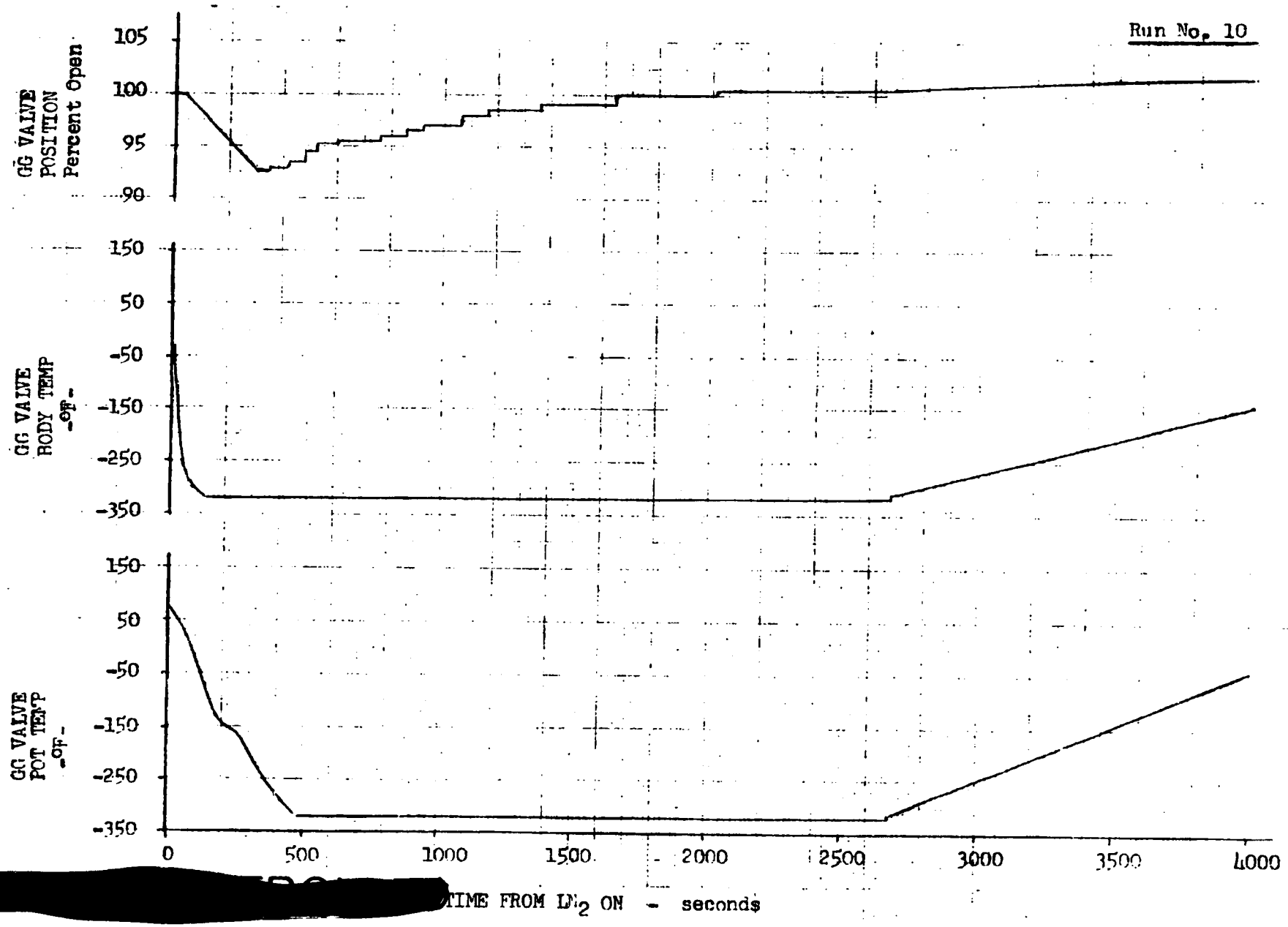

Figure 29. Gas Generator Valve Position and Valve Body Temperature vs Time

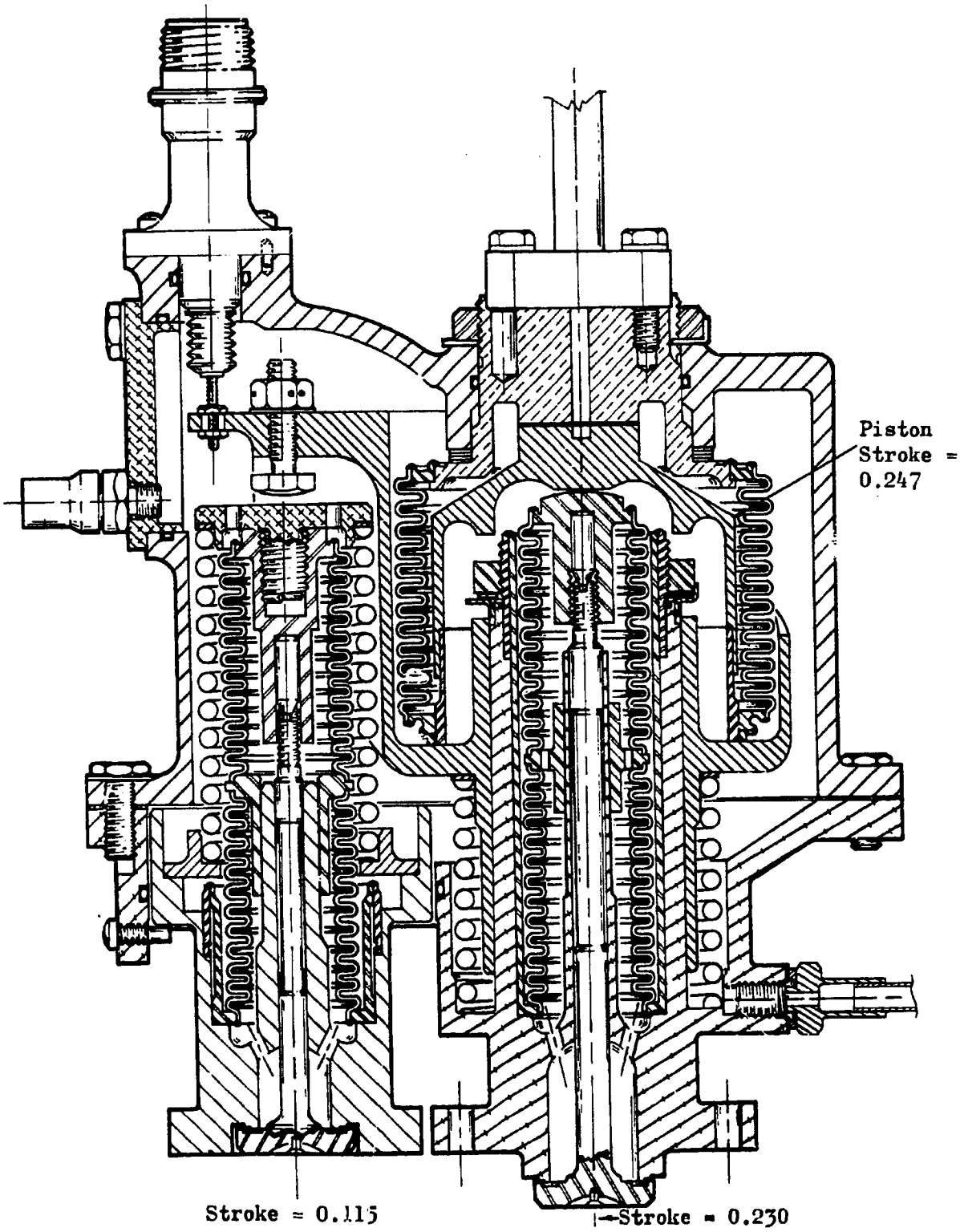

Figure 30. Gas Generator Control Valve

[redacted]

not change until poppet stroke has been decreased by at least 0.0[illegible] inch. Chilling the valve in any manner will not cause poppet stroke changes approaching that magnitude. It is, therefore, concluded that the apparent valve motion did not affect gas generator operation.

On test No. 10, 165 seconds were required for the valve to move 3.2-percent closed. Based upon a weighted average of the two temperature measurements, it is estimated that the average body temperature at the end of 165 seconds was approximately -250 F. On test No. 11, the corresponding time was 185 seconds and the estimated average body temperature was -200 F. Averaging the two and taking an initial body temperature of 70 F, this means that, to achieve 3.3-percent potentiometer motion, the body temperature must be decreased approximately 290 degrees.

Assuming that one-half the body mass of 21.5 pounds gets chilled, the sensible heat extracted from the body is approximately 650 Btu or, over 175 seconds, the body average heat flux was -3.6 Btu/sec.

On the flight, the time for 3.3-percent motion was 52 seconds. If the same temperature change occurred as on the tests, the average body heat flux on the flight was -12 Btu/sec over the 52 seconds, or three times greater than on the test.

An attempt was made to estimate the probable distance of the leak source from the valve body to cause the observed chilling. The analysis was based on the limited knowledge of characteristics of cryogenic fluids leaking to a vacuum, and on the estimated leak from the ASI fuel line. That distance was calculated between 1 and 2 feet, which provides reasonable correlation with the assumed leak location.

ORBITAL THERMAL ENVIRONMENT

Orbital Coast

The coast period on the S-IVB was slightly longer than two orbits. The orbit, which was planned to be nearly circular, was elliptical with a

195-mile apogee and a 95-mile perigee due to S-II propulsion problems. The vehicle orientation was fin No. 3 in the down position until 5780 seconds when a roll maneuver oriented the vehicle to the fin No. 1 down position. The start tank is on the fin No. 1 side of the vehicle. At first burn cutoff, the vehicle axis was 45 degrees above the local horizontal. At 837 seconds, a pitch down maneuver oriented and maintained the axis parallel to the local horizontal. Between 3207 and 5427 seconds, the axis was in a pitch down position 20 degrees below the local horizontal. From 5494 seconds till engine restart at 11,614 seconds, the axis was maintained parallel to the local horizontal. The roll maneuvers were at the rate of 0.5 deg/sec, and the pitch maneuvers were at the rate of 0.3 deg/sec.

The vehicle was in the sun from liftoff to 3100 seconds, from 5700 to 8800 seconds, and from 11,200 seconds until restart. The vehicle was in the earth's shadow from 3000 to 5000 seconds and from 8700 to 11,200 seconds.

In an inclined equatorial orbit such as on AS-502 flight, the greatest total radiant heat input per orbit is to the "down" side of the vehicle or engine, i.e., the side facing the earth. This occurs from a combination of solar radiation, earth emission, and earth albido. The greatest instantaneous radiant heat input occurs to the side directly facing the sun.

Orbital Data

Plots of significant engine temperatures and pressures are presented in Fig. 31 through 37. The thrust chamber jacket and nozzle temperatures are presented in Fig. 31. The two nozzle temperatures (C0385 and C0396), located approximately 90 degrees apart on the bell, were stabilized within 3000 seconds at approximately -100 F. Their temperatures cycled thereafter as the vehicle orbited from shadow to sunshine. The fuel injection manifold temperature (C0200) was probably measuring the average temperature of the injector body and forward manifold. After the initial warmup, this temperature increased at a much slower rate and was -175 F at restart.

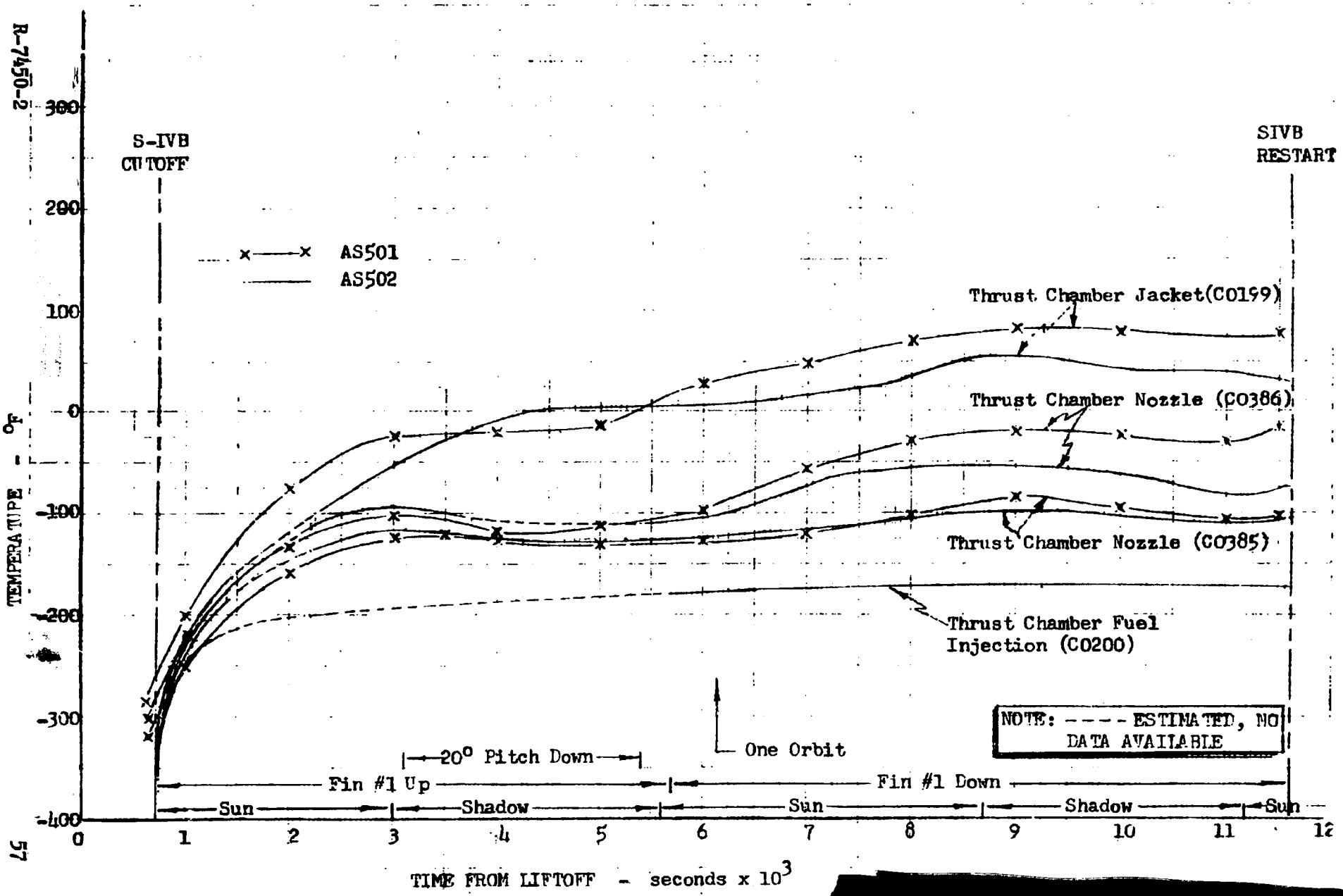

[redacted]

Figure 31. Thrust Chamber Temperatures

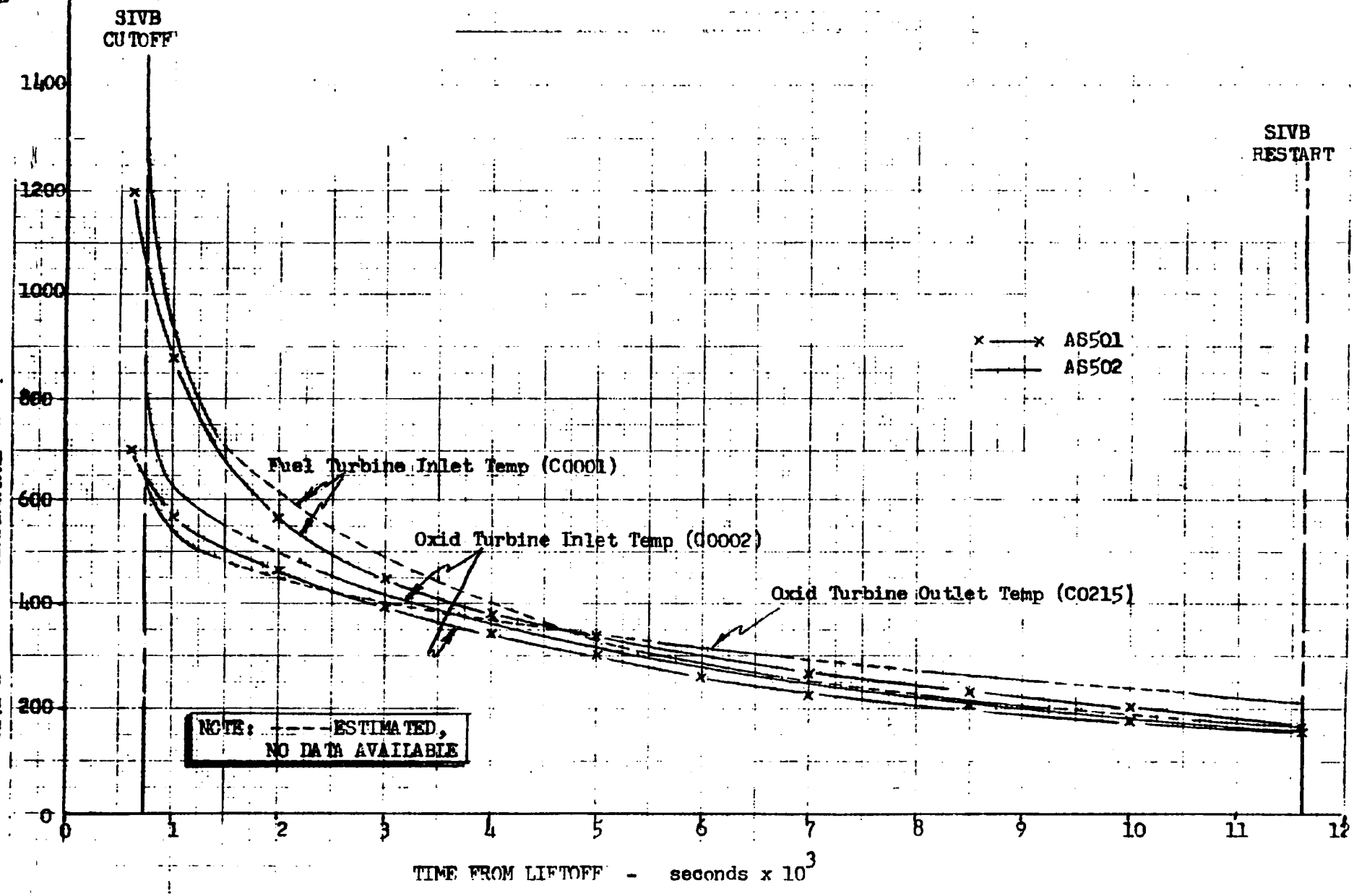

Figure 32. Turbine Temperatures During Orbital Coast

[redacted]

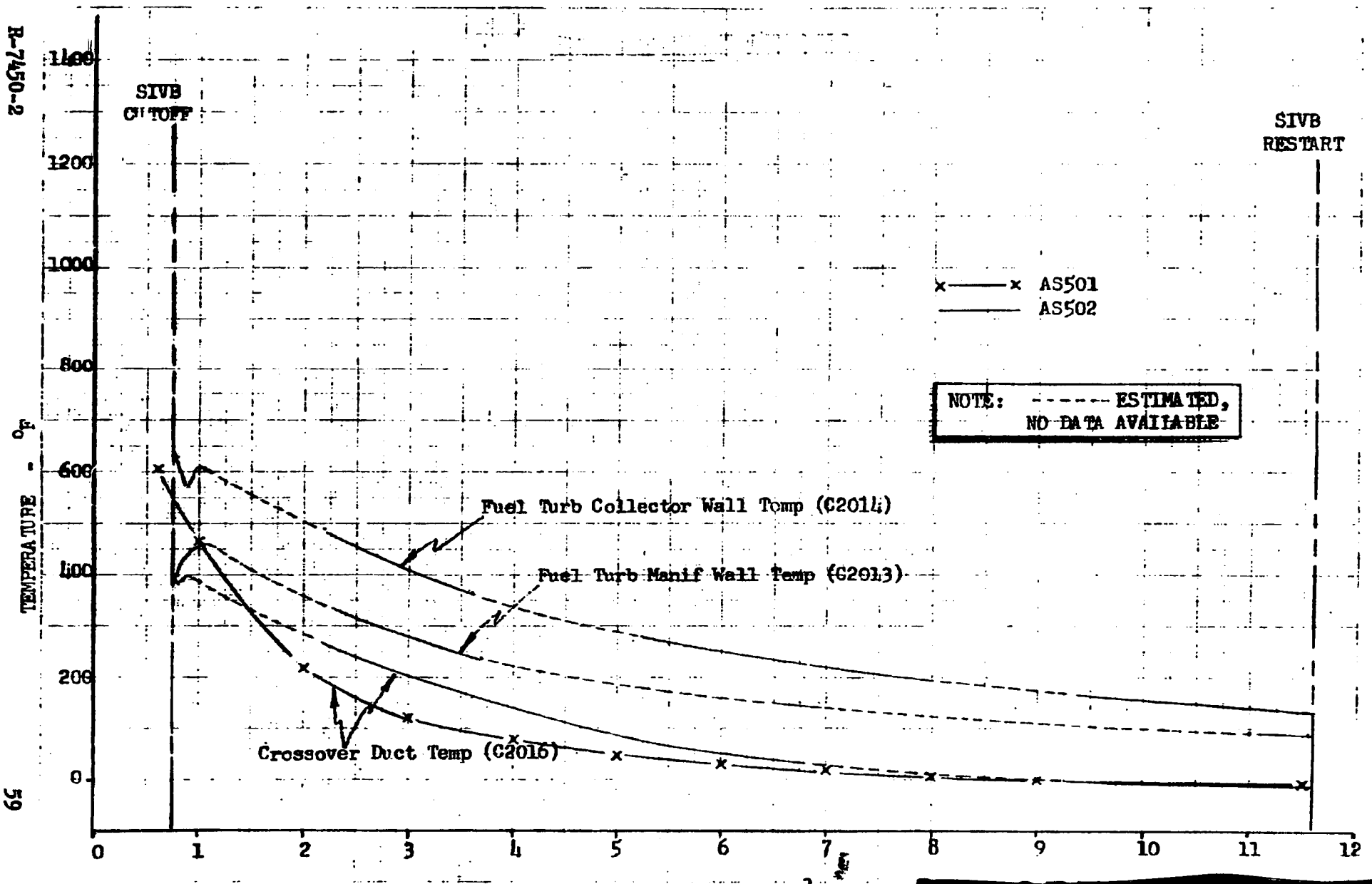

[redacted]

Figure 33. Hot-Gas System Temperatures

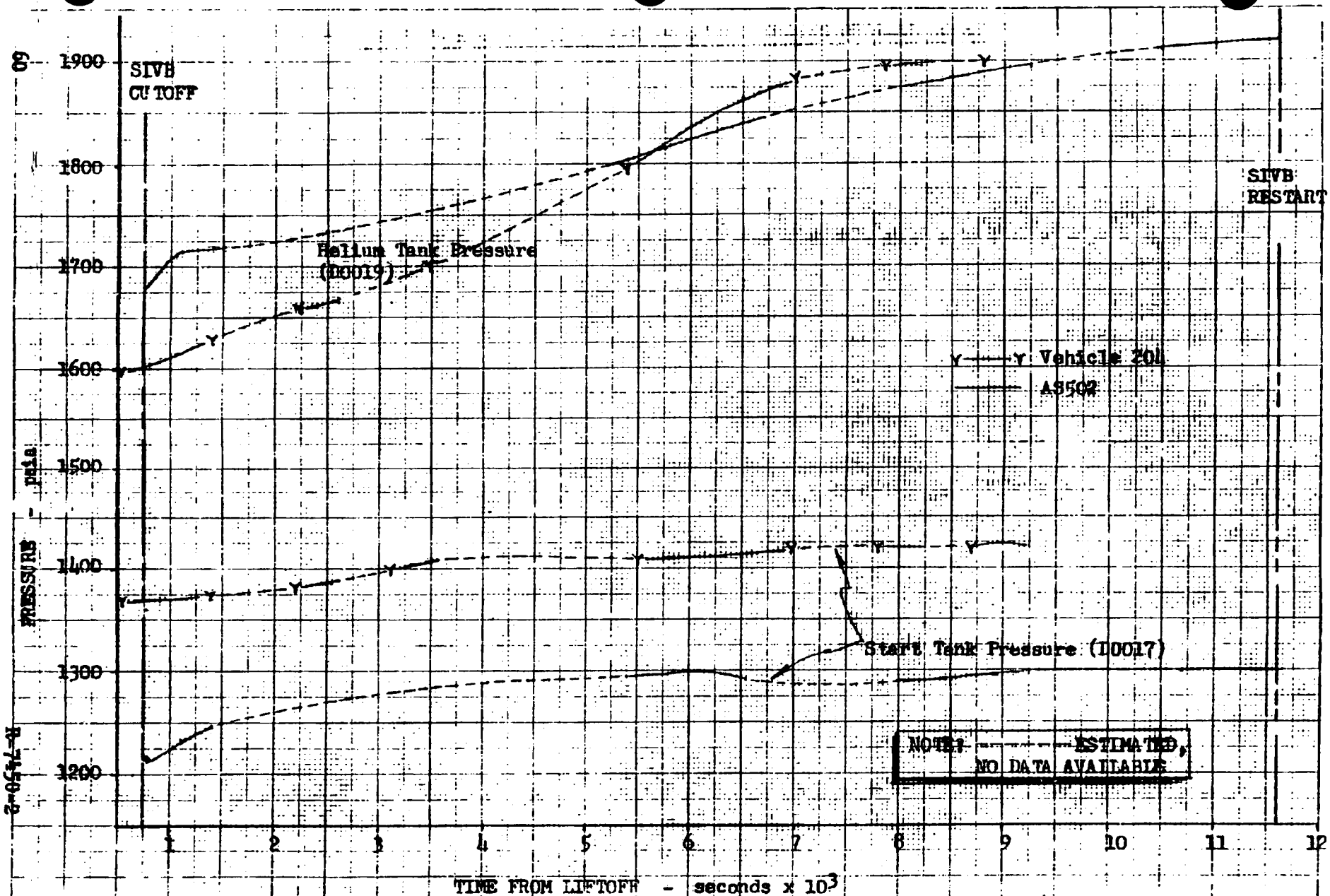

Figure 34. Start Tank and Helium Tank Pressures During Orbital Coast

[redacted]

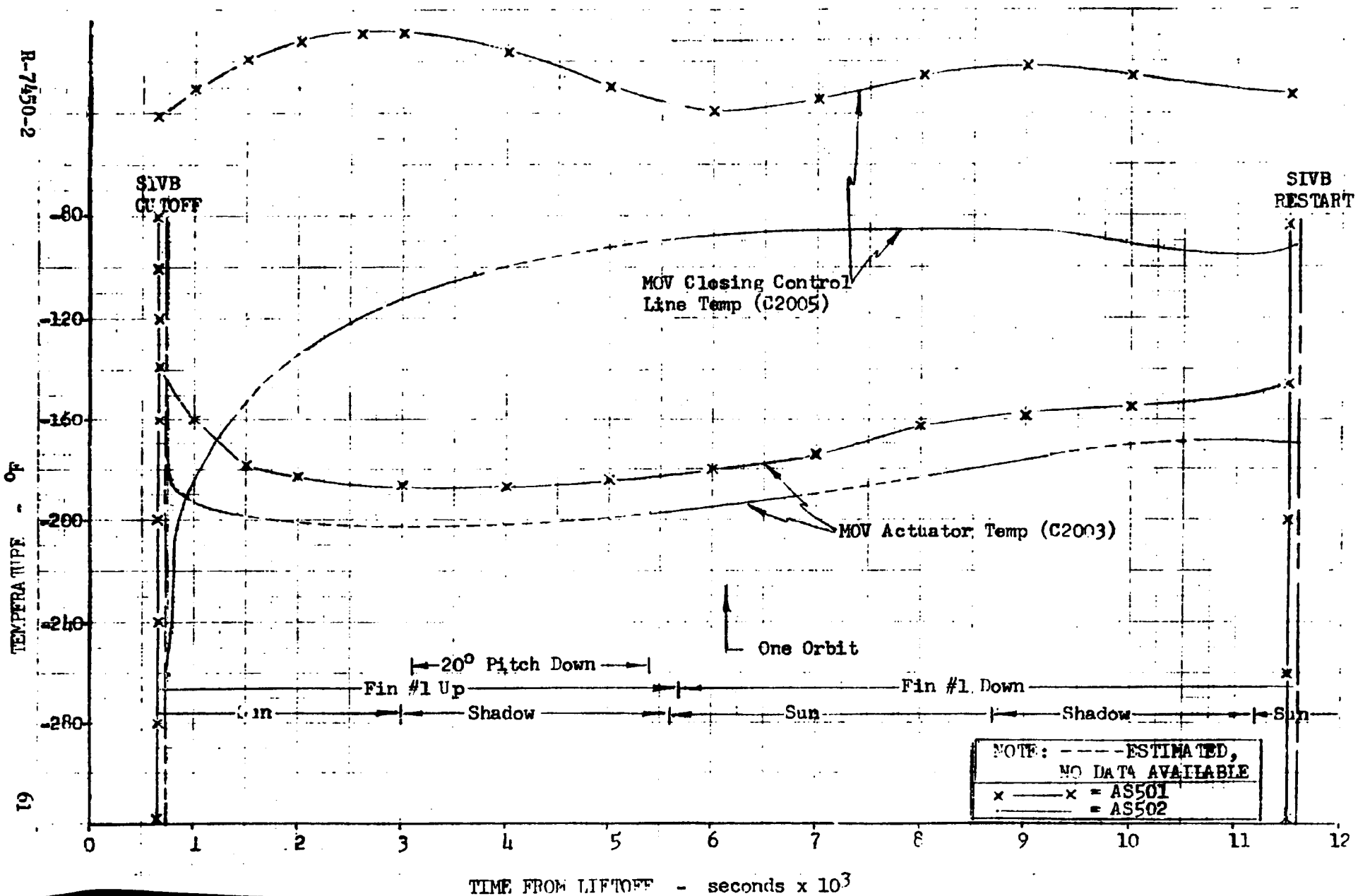

[redacted] Figure 35. MOV Control System Temperatures

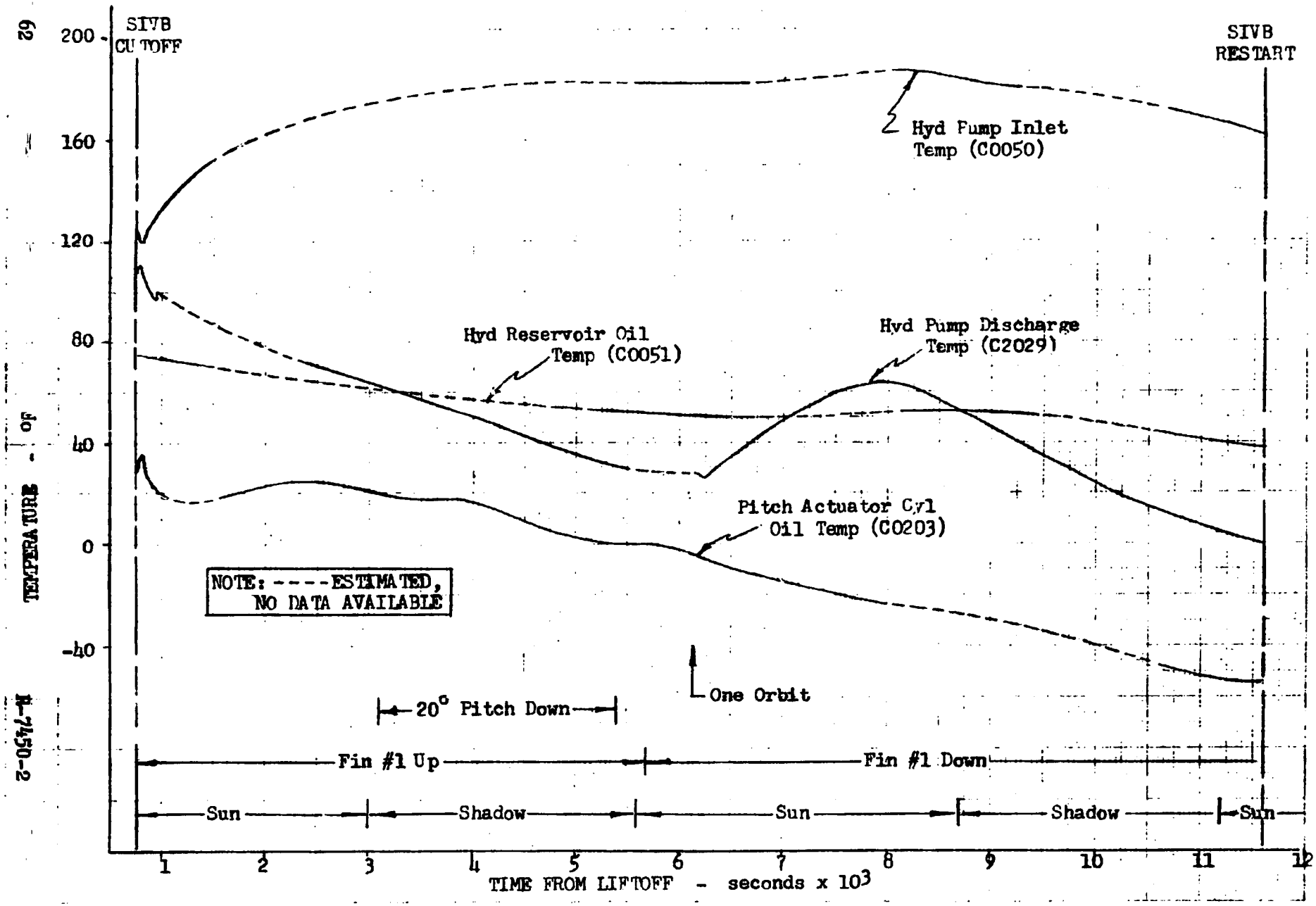

Figure 36. Hydraulic System Temperatures

[redacted]

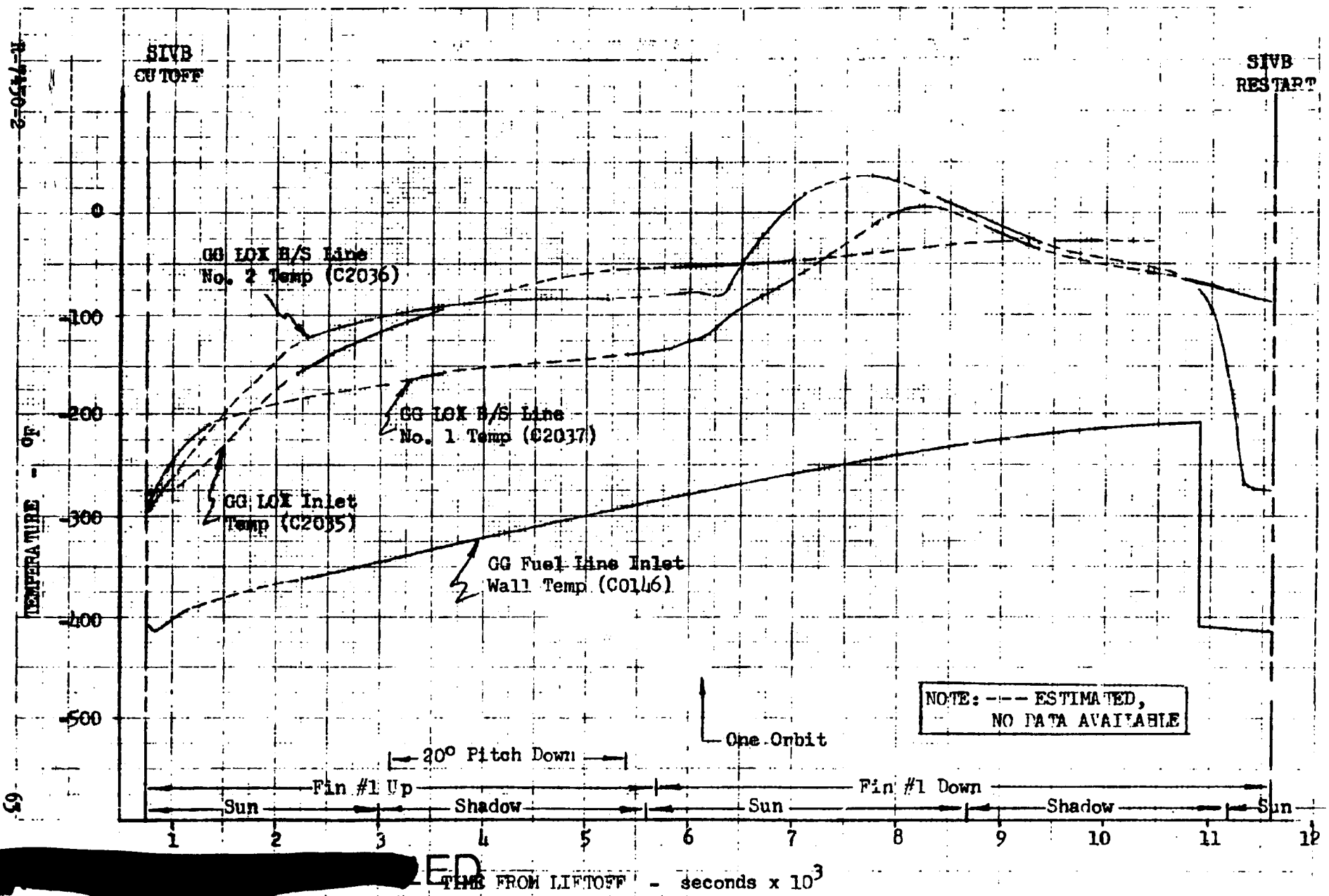

[redacted]ED

Figure 37. Gas Generator System Temperatures During Orbital Coast

Included in Fig. 31 are plots of thrust chamber jacket temperature and the two nozzle temperatures (C0385 and C0386) from vehicle AS-501 orbital coast. As seen, there was very close correlation between these parameters on the two flights. The temperature profiles were nearly identical throughout the coast period.

The turbine temperatures (Fig. 32) exhibited normal decays following engine cutoff. At the end of two orbits, these temperatures had decayed exponentially to 200 F, and were not yet stabilized. Fuel and oxidizer turbine inlet temperature from AS-501 are also included in Fig. 32 . These temperature decays were nearly identical for the two flights.

Figure 33 presents plots of fuel turbine inlet manifold wall temperature (C2013) fuel turbine exhaust manifold wall temperature (C2014), crossover duct skin temperature (C2016), and the crossover duct skin temperature from AS-501 flight. All parameters exhibited the normal exponential temperature decay. As expected, the thin-walled crossover duct cooled at a much faster rate than the others, and by 9000 seconds was approaching a stabilized -20 F. The crossover duct temperature decay for the two flights was nearly identical throughout the two-orbit coast period.

Start tank pressure and helium tank pressure are presented in Fig. 34 as well as the corresponding measurements from vehicle AS-204. The stabilized start tank pressure on the two flights differed because of start tank vent relief valve settings, which was 1400 psia on AS-204 and 1300 psia on AS-502. The start tank temperature was -260 F at first-burn cutoff, and had warmed up to -195 F by 10,000 seconds. At engine cutoff, helium tank temperature was -240 F. Assuming helium tank and start tank temperatures were the same after two orbits, and assuming no helium leak, the helium tank pressure, based upon the temperature change, was predicted to be 1970 psia at 11,000 seconds. This agreed reasonably well with the 1940 psia measured, and indicates that no significant helium leak occurred.

MOV actuator temperature (C2003) and MOV closing control line temperature (C2005) from AS-501 and AS-502 are presented in Fig. 35. These temperatures

exhibited similar trends on both flights. The temperatures responded more on AS-501 than on AS-502 to the variations in radiant heat input from shadow to sunshine. This apparent lack of response on AS-502 is unexplained. The longer-term temperature trends for the two flights are similar, however; the temperatures on AS-502 are considered normal. The closing control line temperature is measuring a smaller mass temperature and will warm up at a faster rate than the actuator temperature as shown in Fig. 35.

The hydraulic system temperatures (Fig. 36) exhibited temperature variations during orbit. Hydraulic pump inlet temperature rose from 120 degrees at cutoff to a maximum of 190 degrees. This is apparently due to soakback from the oxidizer turbine exhaust manifold. At 9000 seconds, the hydraulic pump inlet temperature and oxidizer turbine discharge temperature were both approximately 200 F, and both temperatures decayed from that time at approximately the same rate.

Hydraulic pump discharge temperature (C2029) and reservoir oil temperature (C0051) cycled normally during the periods of high- or low-radiation-heat input. The sharp rise in hydraulic pump discharge temperature at 6000 seconds was coincident with the roll maneuver at 5780 seconds, which oriented the hydraulic pump toward the sun. The other parameters of Fig. 36 exhibit a similar increasing tendency, apparently for the same reason.

The pitch actuator oil temperature (C0203) decayed from +20 to -40 F at a near steady rate throughout coast. That actuator is situated behind many components and received comparatively little radiation. The decay was likely the result of soakback from the cold components in the vicinity without compensating radiant heat input.

There are no data from the AS-501 hydraulic system during orbit to make comparisons of those temperatures.

Gas generator oxidizer and fuel bootstrap line temperatures are presented in Fig. 37. The one measurement on the fuel line (C0146) exhibited a steady increasing trend throughout coast, and at restart the slope of the curve indicates the line would have eventually stabilized at a temperature much high than -200 F. The three oxidizer bootstrap line temperatures all began warmup immediately at engine shutdown. The rapid warmup beginning at 5700 seconds coincided with the vehicle leaving the earth's shadow and the No. 1 down roll maneuver, which oriented the gas generator side toward the sun for maximum solar radiation. The chilling at 7700 seconds apparently occurred because the bootstrap line was shadowed by some engine or vehicle component. It is inferred from these data that a stable bootstrap line temperature, when not receiving direct solar radiation, is approximately -50 F.

[redacted]

ENGINE PERFORMANCE DECAY

Event Description

Decreasing performance in two distinct phases was observed during AS-502, S-IVB first burn. The first decay began at 684 seconds range time (approximately 107 seconds after engine start), and was a 4-psi decrease in main chamber pressure over 8 seconds. The second decay began at 692 seconds range time, with a 12-psi decrease in main chamber pressure occurring over 10 seconds. A loss in engine c* efficiency, denoting a propellant leak overboard and/or main injector damage, also was noted. No additional shifts in performance following 702 seconds range time were detected, and the engine proceeded into a normal shutdown. The performance decrease at 684 seconds correlates with increased engine chilling attributable to hydrogen leakage near the dome area (Thermal Environment section) but the less rapid chilling of the engine over some 40 prior seconds was not detected in performance.

Failure Mode Possibilities. The following general areas were defined as potential sources for the AS-502, S-IVB performance shifts:

1. External propellant leakage upstream of the main engine valves including stage ducting and prevalves
2. Mechanical failure of either turbopump
3. Gas generator propellant feed system leak
4. Start system leak
5. Hydrogen pressurization system leak
6. Main thrust chamber jacket leak
7. Main injector degradation or instability
8. ASI propellant feed system failure

[redacted]

Hypothesis. Consideration of the above failure modes and correlation with the observed performance decay, as well as other pertinent S-IVB anomalies, was approached from the standpoint that the failure mode should propagate or be a source of the engine area temperature variation phenomenon and a potential source of restart failure. As such, the following hypothesis was formulated and ultimately demonstrated (Verification Testing section) as an explanation of the first-burn performance shift, thermal variations, and a direct source for engine restart failure. The performance decay is initially caused by progressive fuel leakage from the upper flex section of the ASI fuel propellant feed line which, after leaking overboard for 40 seconds at flows of 0.6 lb/sec or less, increased between 684 and 692 seconds range time to approximately 1.5 lb/sec fuel overboard, causing the first observed decay in performance. At 692 seconds range time, the overboard fuel leakage rate again increased, so that performance began to decay at an increased rate, and high ASI mixture ratio operation resulted.

Continually increasing flow overboard eventually led to ASI reverse flow, consisting primarily of oxidizer entering through the oxidizer inlet into the ASI cavity and flowing back out through the ASI fuel orifices. ASI oxidizer flow for AS-502, S-IVB was restricted by the 0.125-inch-diameter ASI oxidizer orifice and high oxidizer injector pressure drop at constant mass flowrate which, in conjunction with some flow of fuel from the main chamber, was sufficient to produce high-temperature backflow. The backflow caused burnout of the ASI fuel line at 696 seconds (first sign of heating) and, subsequently, eroded into the ASI fuel orifices and body, essentially burning out the ASI with additional loss of ASI oxidizer feed flow overboard. By 702 seconds range time, the ASI body erosion was essentially complete, with the maximum oxidizer flow through the burned out ASI, chamber backflow, and failed ASI fuel line flow (approximately 4.5 lb/sec total fuel and 1.0 lb/sec total oxidizer) being damped overboard and the performance stabilized.

[redacted]

Analysis

Figure 38 depicts the observed main chamber pressure from 650 to 750 seconds range time. The oxidizer tank stage-supplied helium pressurization flow-rate through the engine heat exchanger also is shown because changes in heat transfer to the oxidizer turbine exhaust gases between low and high flow heat exchanger operation (Vehicle Analysis section) significantly affect turbine backpressure and engine performance. The chamber pressure, normalized to constant heat exchanger flowrate (Fig. 39), illustrates the performance shift occurring in two decaying phases rather than abrupt performance shifts. Following 702 seconds range time, the performance is essentially stabilized with normal cutoff occurring at 747.0 seconds range time. Figure 40 compares the cutoff AS-502 of S-IVB first burn with AS-501, S-IVB cutoff. The cutoff impulse values at standard conditions are within approximately 3000 lb-sec, or well within the expected engine-to-engine variation in cutoff impulse for normal engine shutdown.

All projected failure hypotheses explaining the phenomenon represented by Fig. 40 were judged with regard to their correlation with a single-source point failure mode, and satisfy the following criteria:

1. The suspected failure mode must be consistent with the observed thermal chilling and heating conditions as stated in the Stage Hydraulic Failure During Orbital Coast section.
2. The suspected failure mode must be a reasonable match with respect to predicted changes in engine performance resulting from the failure mode.
3. The suspected failure mode must be a potential source for failure of the engine to restart (Engine Failure to Restart section).
4. The suspected failure mode must be verified or reasonably duplicated by an engine or component test program (Verification Testing section).

[redacted]

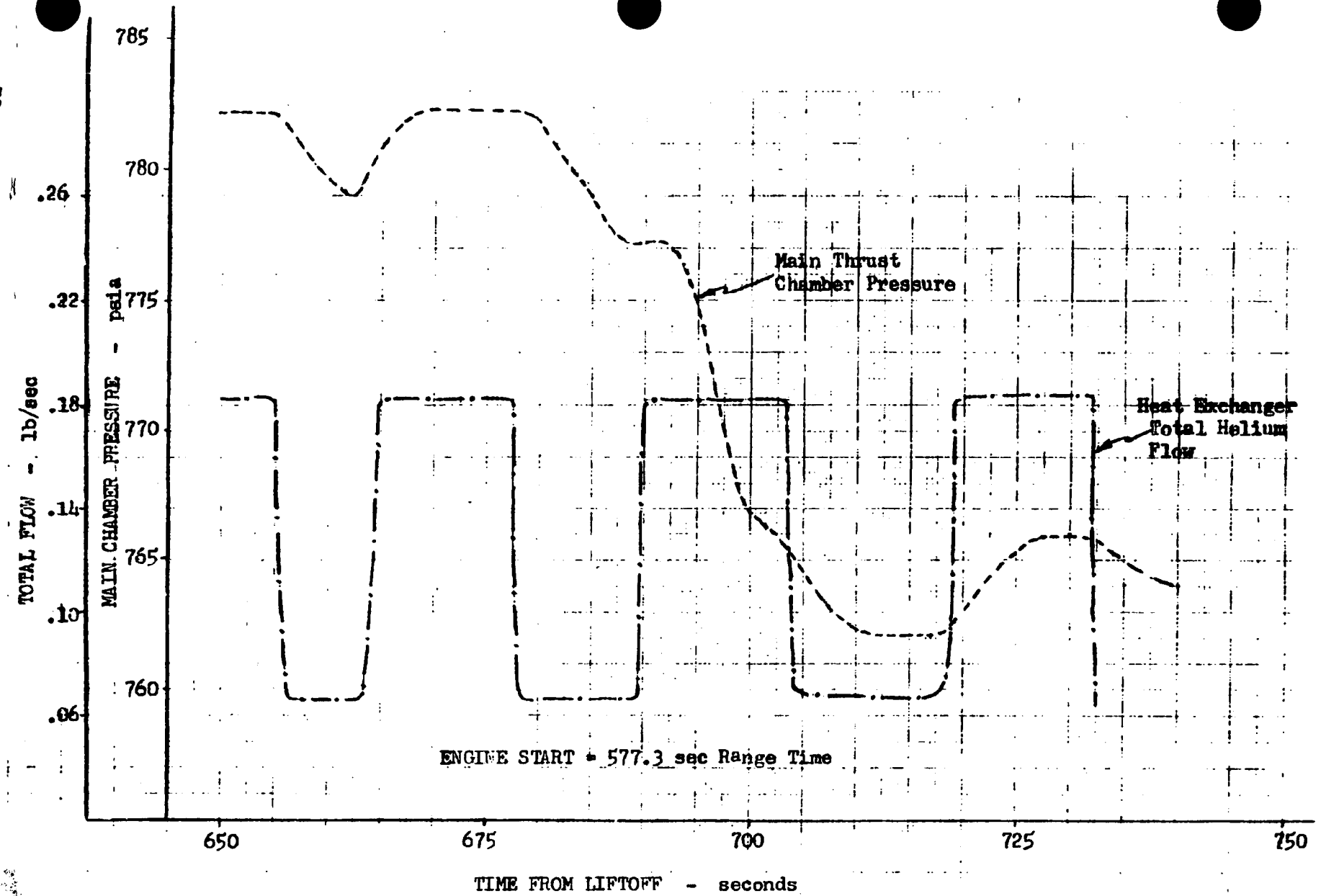

Figure 38. AS-502 S-IVB, First Burn [redacted]

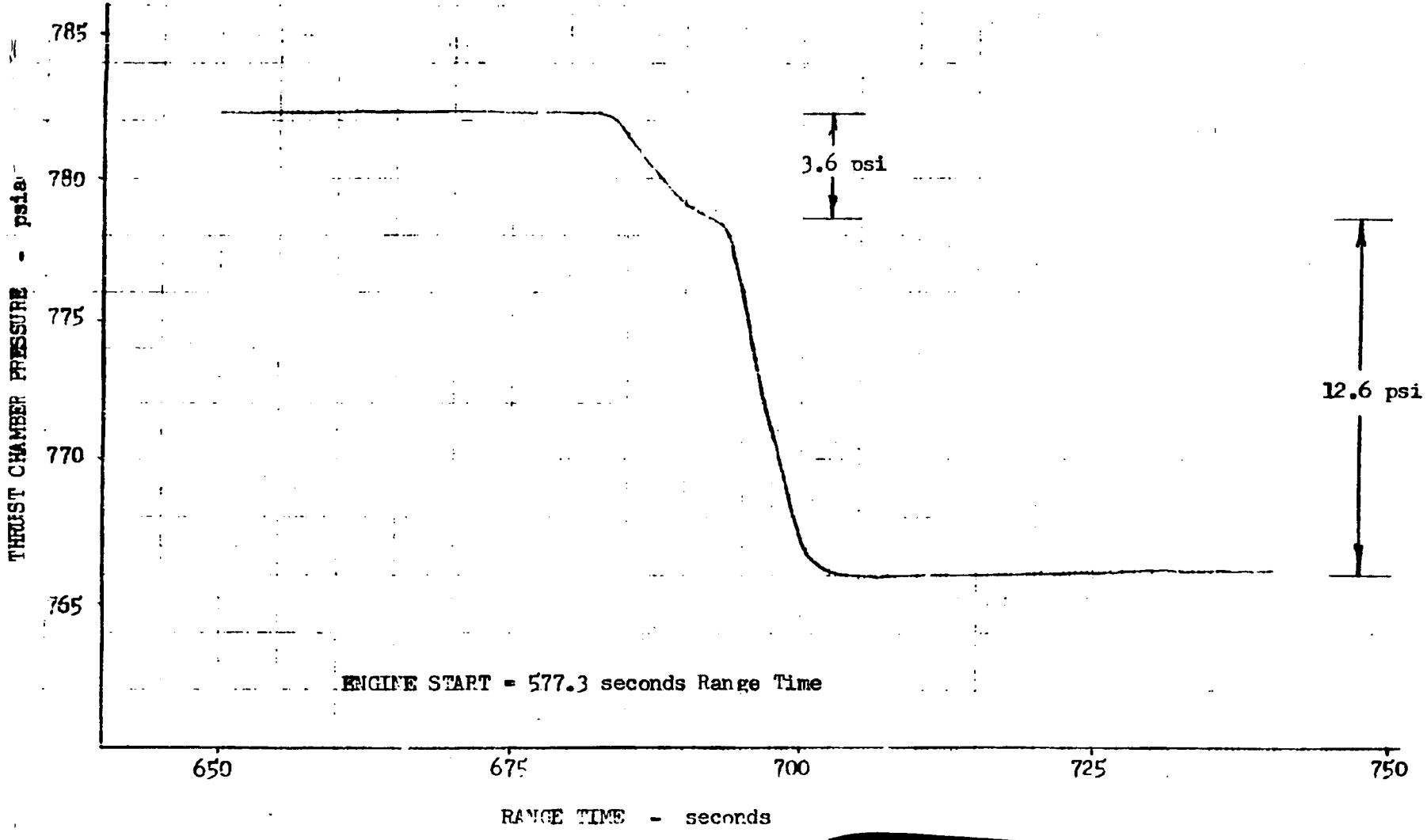

[redacted]

Figure 39. AS-502 S-IVB First Burn, Main Chamber Pressure Corrected to Constant Heat Exchanger Operation

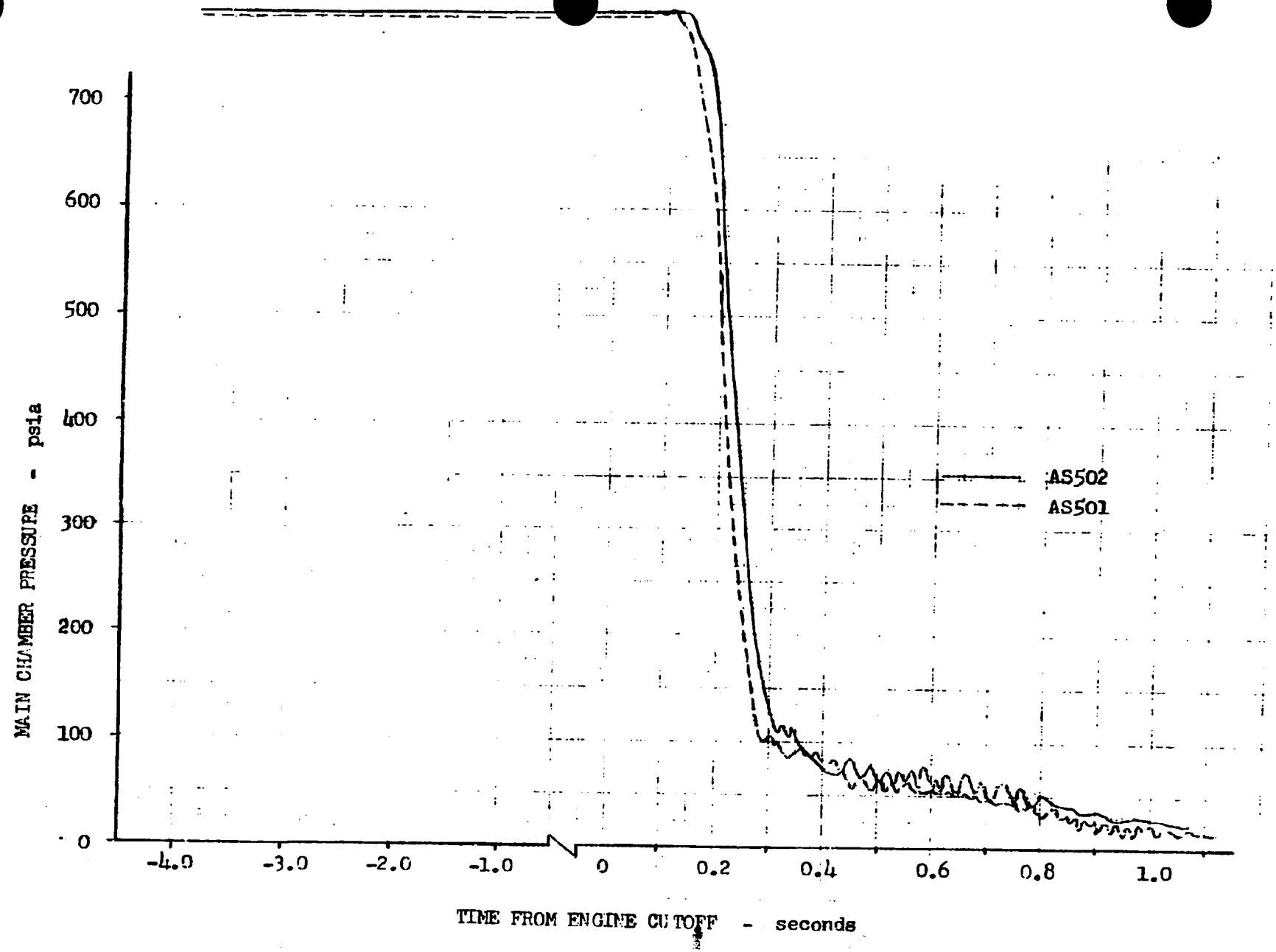

Figure 40. AS-501 and AS-502 Comparison, Main Chamber Pressure [redacted] Engine Cutoff vs Time

All potential failure modes, including the general areas listed in the failure mode possibilities for the 684 to 702 seconds range time, two-level performance decay (summarized in Overall Failure Analysis section) were eliminated either by direct verification from data of normal operation integrity or failure to correlate as a single-source point failure mode with the above outlined conditions, with the exception of a failure localized to the ASI propellant feed system. As such, the stated failure mode hypothesis was developed in the sequence shown below.

Progressive ASI Fuel Leakage. The performance decay began with progressive overboard leakage of fuel from the ASI fuel feed line beginning at a low level (less than 0.6 lb/sec) at 645 seconds range time. As a gross indication, the fuel system pressure loss at constant flowrate, the fuel pump flow coefficient (volumetric flow divided by pump speed), as well as the increase in main fuel injection temperature (indicating an increase in main chamber mixture ratio), all support a loss of propellant from the fuel system downstream of the engine flowmeter beginning at 645 seconds, increasing at 684 seconds, and again at 692 seconds.

Fuel Leak Located Near Dome Area Section of the ASI Fuel Line. Analysis of engine area temperature data (Thermal Environment section) conclusively supports hydrogen leakage (i.e., chilling to cryogenic hydrogen temperature) localized to the engine dome area on the fuel pump side of the engine or the general area of the ASI fuel line between the instrumentation block and the ASI fuel inlet. Figure 41, summarizing the ASI system flows based on best estimates of nominal line resistance for various break points in either line, indicates the total ASI fuel feed system leakage between the instrumentation block and the ASI inlet is between 2.6 and 3.9 lb/sec with the line totally failed. Such overboard leakage is sufficient to explain a significant portion of the observed performance shift.

[redacted]

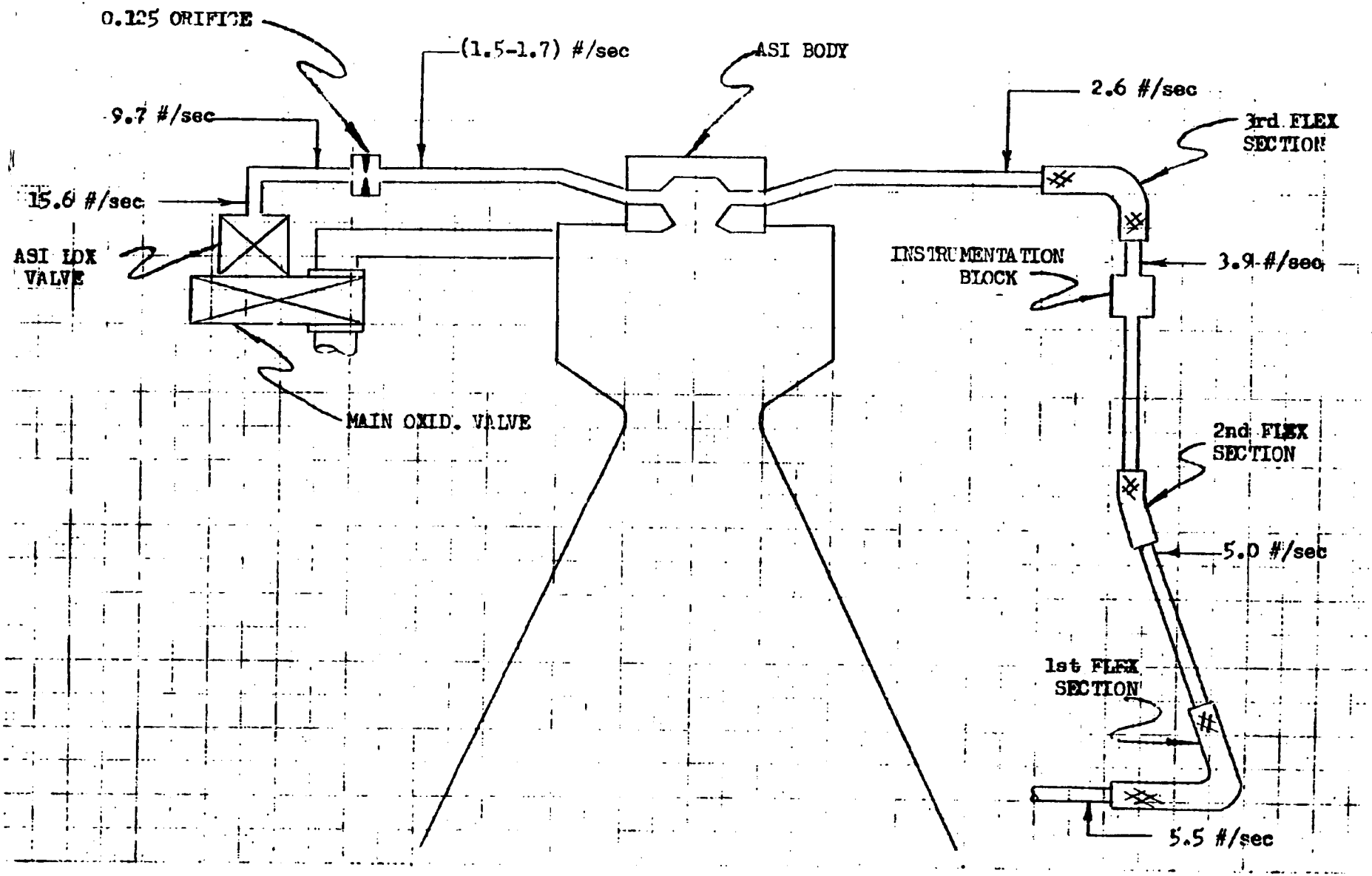

Figure 41. Expected Leakage Flow for Various Break Points in the ASI Propellant Feed System

[redacted]

Fuel Leak Progresses to ASI Backflow. For the above-described propellant levels to be lost overboard to explain performance, the ASI fuel line leakage must ultimately progress to total line failure, which is also a minimal condition to allow heating of the engine area in terms of elevated temperature gas emerging from the ASI through the ASI end of the line. As a function of the line resistance, a backflow condition would be reached between 1.4 and 2.1 lb/sec overboard, depending on the leak location in the upper section. As leakage increases with time, causing the performance to decay, the total pressure at the leak point decreases to ASI chamber pressure, causing oxidizer entering the ASI cavity to flow back through the ASI fuel injector orifices. This causes ASI chamber pressure to approach main chamber pressure, which may then allow positive fuel flow to the ASI to resume.

Therefore, until the overboard leakage becomes large enough to drop the total pressure at the leak point below main chamber pressure, an unstable oscillatory flow condition exists.

The leakage rate overboard also establishes the ASI operating mixture ratio, which will increase as leakage flow increases. A high-temperature mixture ratio in the ASI will, therefore, exist over a finite period of time prior to and after the backflow condition is approached.

Backflow Causes ASI Burnout. Analyses further predicted that the performance shift and the extended general heating on the oxidizer and fuel side of the dome required substantial ASI erosion from high-temperature backflow to the extent oxidizer feed flow would be in part or totally dumped overboard, either by severence of the oxidizer line caused by heating or erosion through the ASI fuel manifold, essentially opening a direct passage for oxidizer and thrust chamber backflow overboard.

[redacted]

Figure 42 depicts the indicated thrust chamber c* versus thrust chamber mixture ratio before and after the total shift of 684 to 702 seconds range time, as determined by the PAST 641 ALTITUDE REDUCTION program. The c* after the shift can deviate from the theoretical frozen equilibrium slope (known to be an adequate description of engine operation over the range in question) because of loss of flow overboard downstream of the engine flowmeters, which can be represented by a total fuel, oxidizer, or combination of leakage varying the mixture ratio, or by a real c* loss because of physical degradation of the injector. As noted in the figure, an oxidizer-only leak of 15 lb/sec or 5.5 lb/sec fuel-only leak is required to match the theoretical slope. From Fig. 41 (which charts the flows for a total break at various points in the ASI propellant feed system) such leakages would require, in the oxidizer case, a leak at the ASI oxidizer valve or, in the fuel case, a leak upstream of the second ASI line flex section. As previously discussed, an oxidizer leak only does not correlate with the indicated temperature phenomenon, i.e., the increase in main injection temperature, and the leak magnitude is not supported by oxidizer system pressure drops at constant mass flowrate. A fuel-only leak does not correlate with the indicated temperature phenomenon because the required source of leakage is well below the dome area and would predict a greater than observed increase in fuel injection temperature. A combination leakage of primarily fuel and some oxidizer flow overboard was, therefore, the most legitimate match both for the c* slope and expected fuel injection temperature rise.

Evaluation of system capacity showed that, with an intact ASI, a maximum flow of 3.9 lb/sec hydrogen from a total break in the fuel ASI line upstream of the third flex section and 0.6 lb/sec oxidizer flow overboard through the fuel injector orifices would require a significant loss of c* because of unexpected degradation of the main injector for the amount of dwell time at high mixture ratio prior to backflow, and probably would not provide sufficient gas temperature leaving the ASI to explain the engine area heating. A flow, however, of 5 lb/sec hydrogen and 1.5 lb/sec

[redacted]

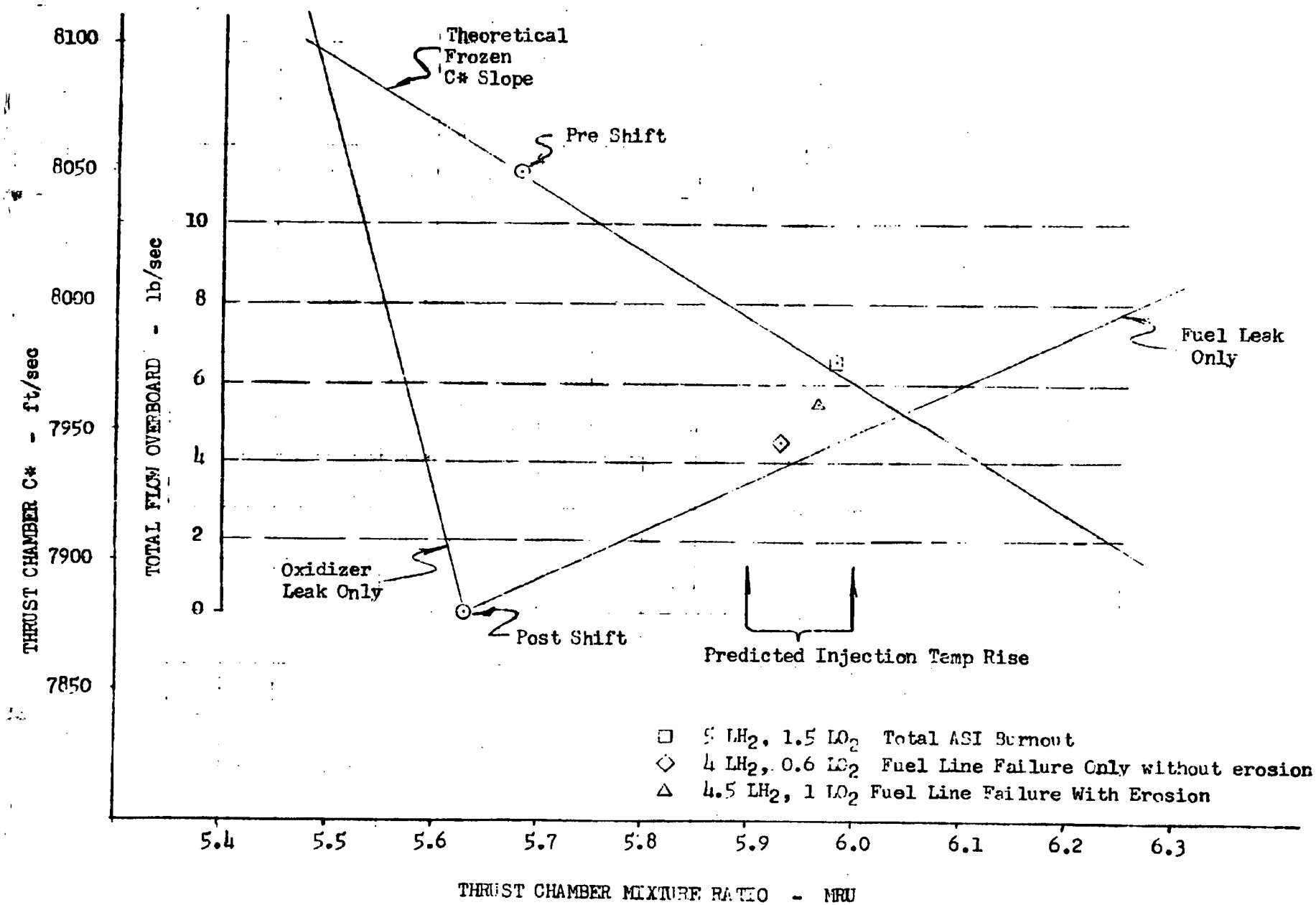

Figure 42. AS-502 S-IVB First Burn, Thrust Chamber Perf[redacted]

oxidizer overboard, associated with total ASI burnout, represents the other extreme of no loss of c* because of main injector degradation, but would provide gas temperatures explaining the engine area heating. The best estimate, as discussed below, of 4.5 lb/sec hydrogen and 1.0 lb/sec oxidizer overboard during the flight also is shown in Fig. 42.

Test Verification of Hypothesis. Figure 43 depicts the predicted range of fuel feed flow overboard versus time for AS-502 S-IVB in which minimum to maximum limits were picked by matching the following sequence of events:

1. Between 645 and 684 seconds range time, a constant or gradually increasing hydrogen leakage flow overboard between 0.4 and 0.6 lb/sec would be sufficient to cause chilling of the engine area without detectably affecting performance.
2. Between 684 and 692 seconds range time, a flowrate between 1.1 and 1.5 lb/sec would be sufficient to match performance as well as the increased chilling.
3. After 696 seconds range time, the first sign of heating indicating total line failure allows overboard flow between 2.6 and 3.9 lb/sec.

These limits resulted in the predicted mixture ratio limits shown in Fig. 44 for the AS-502 flight which were utilized to program a simulated test at SSFL on engine J016-4 (Verification Testing section). The most important factors of the failure hypothesis to be verified or disproved by the test were the following:

1. How much potential main injector damage would result because of the high ASI mixture ratio operation predicted between approximately 690 and 696 seconds range time before total fuel line failure?

[redacted]

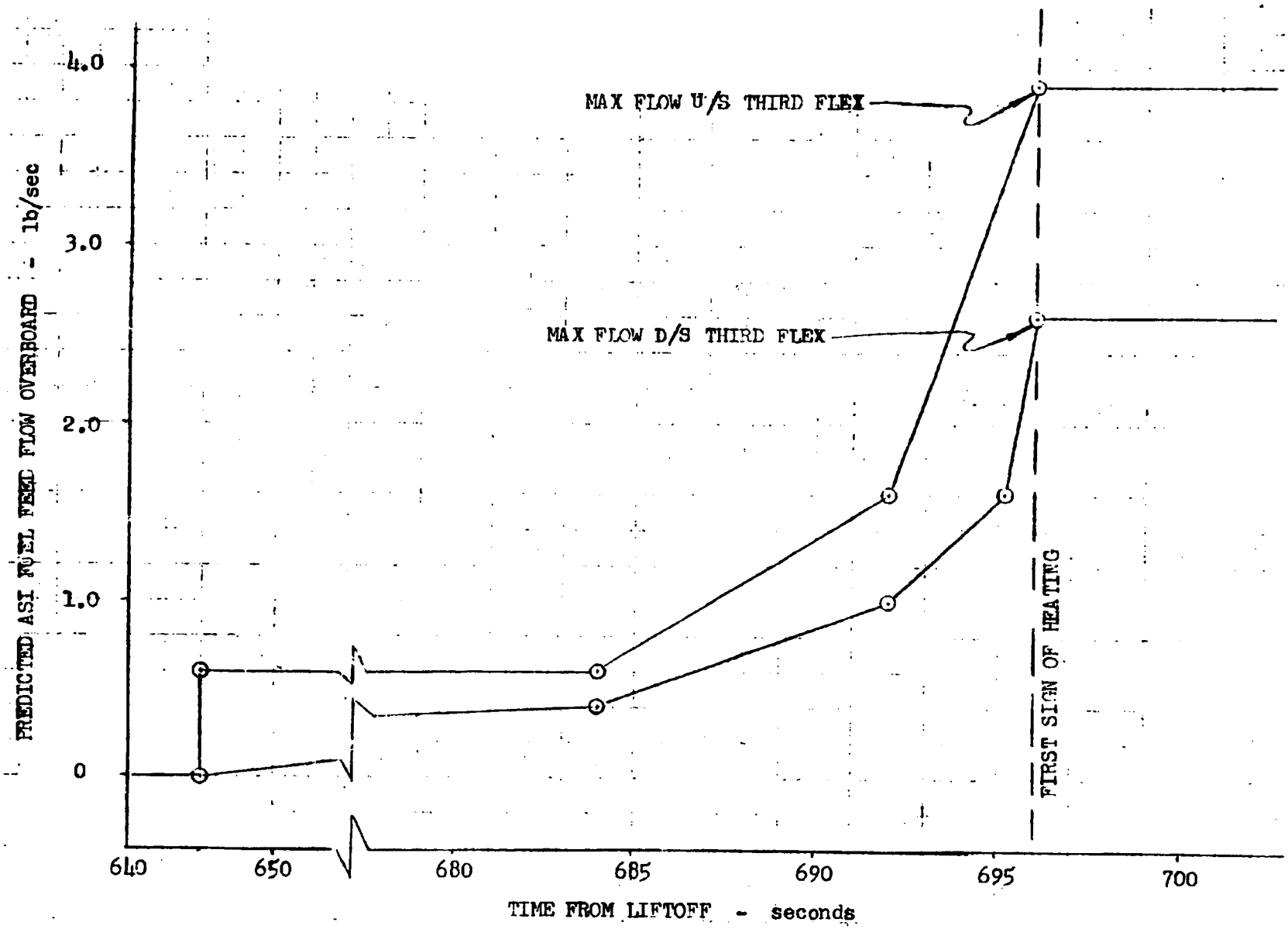

Figure 43. AS-502 S-IVB First Burn, ASI Fuel Feed Flow Overboard

[redacted]

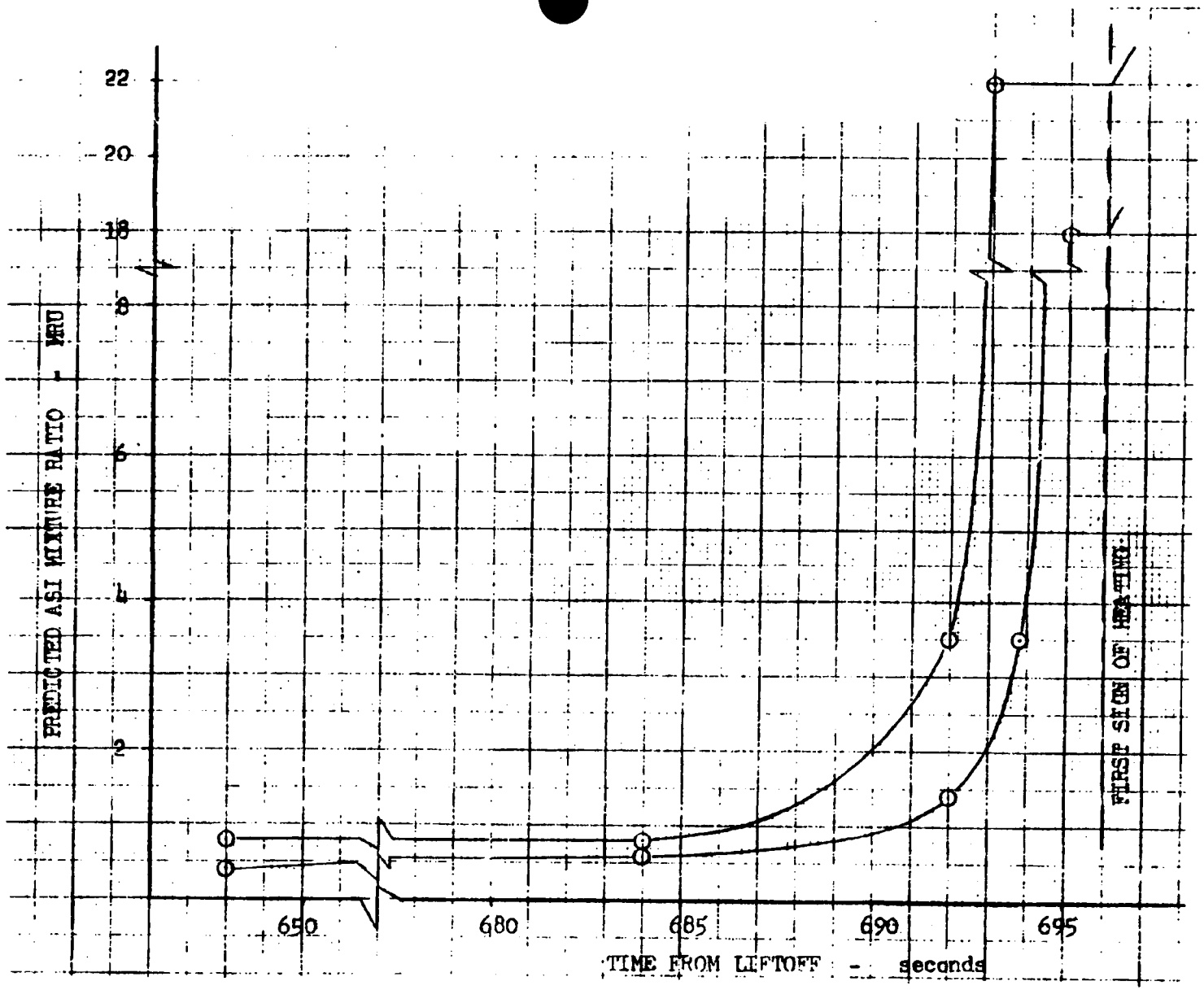

Figure 44. AS-502 S-IVB First Burn, ASI Mixture Ratio

[redacted]

2. Would the mixture ratio of the backflow gases be sufficient to continue ASI erosion to the point of burnout, allowing loss of oxidizer overboard? This was the most critical aspect of the hypothesis to be verified because previous tests simulating S-II conditions (i.e., ASI oxidizer orificing and ASI oxidizer injector pressure drop) tended to show the oxidizer supply flow dominated the flow back out of the ASI fuel injector orifices, with the ASI fuel supply totally removed so that mixture ratio was so high that the gas flow was below eroding temperature.

As summarized in the Verification Testing section, the physical sequence of events hypothesized for AS-502 S-IVB were verified. Figure 45 summarizes the performance during the high mixture ratio operation of the R&D test engine (J016-4). Main injector erosion prior to backflow simulation produced no detectable effect on performance. Following hot-gas dump valve opening (simulated line failure), the continued erosion of the injector and ASI assembly caused a total loss in performance over 12 seconds of 8 psi in main chamber pressure. Although heating of the engine flight instrumentation packages because of the subsequent fire tends to reduce the quality of the data, calculation of the maximum backflow from the burned out ASI is sufficient to explain only part of the performance loss. The additional loss is attributed to a c* efficiency degradation of the main injector of approximately 0.5 percent because of the damage (described in the Verification Testing section), which was incurred during the test.

Based on the engine J016-4 test results, it is expected that the total fuel flow overboard for AS-502 S-IVB was approximately 4.5 lb/sec. This includes approximately 4 lb/sec from the failed fuel feed line which, based on SSFL results, would have been burned off upstream of the third flex section once complete backflow is established, and 0.5 lb/sec thrust chamber fuel backflow. Although the oxidizer feed line was not severed, the ASI fuel manifold burnout would have permitted approximately 1.0 lb/sec oxidizer overboard. It is expected that some real c* efficiency loss in the main injector also was incurred, as indicated in Fig. 42.

[redacted]

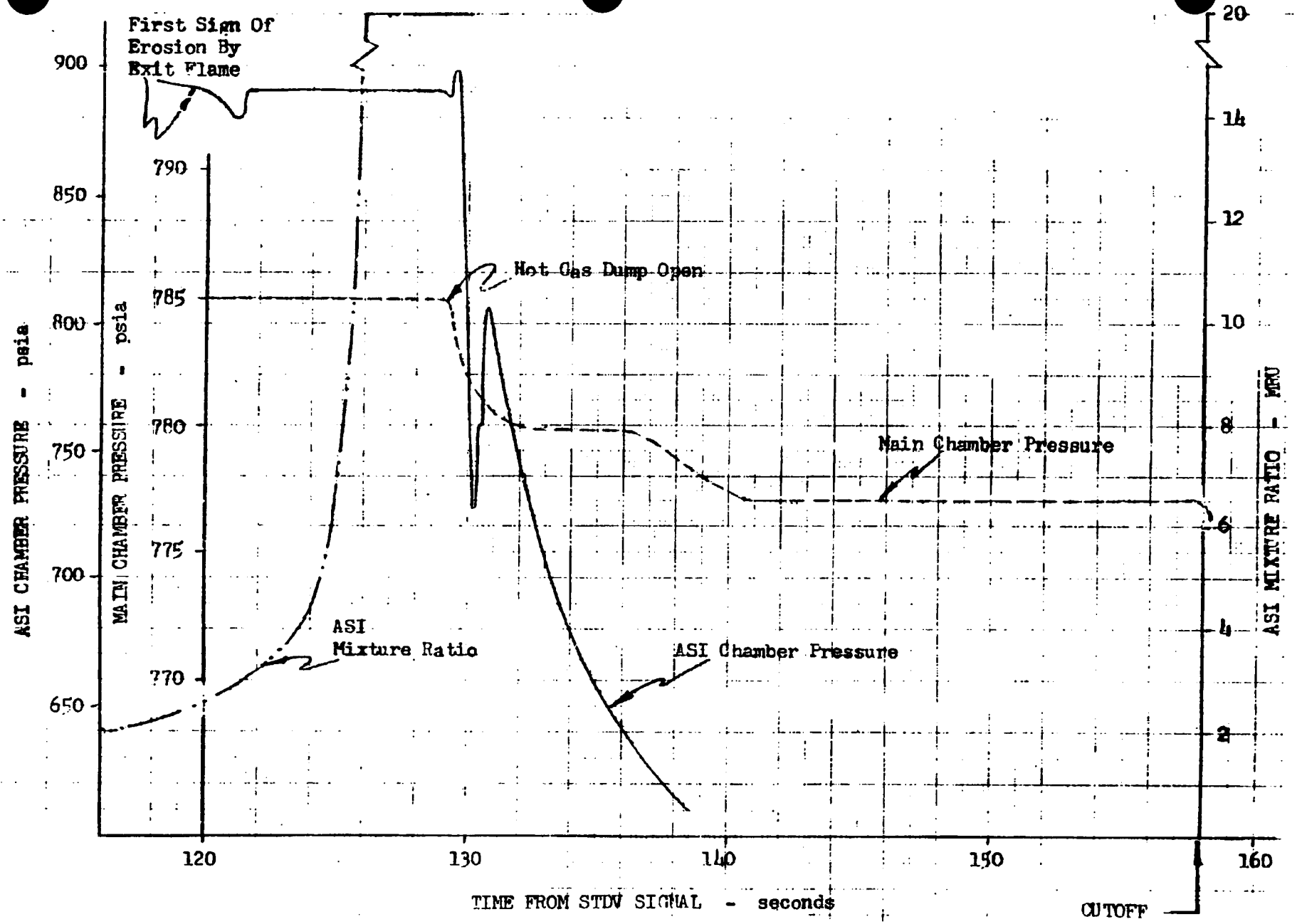

Figure 45. AS-502 S-IVB Failure Mode Simulation (Engine J016-4, Test 313-041)

[redacted]

Performance

An integral part of the development of the AS-502 S-IVB hypothesis was consideration of the observed shifts and correlation with the various failure modes projected to expected performance parameter changes (i.e., changes in flows, speeds, pressure, and temperatures). A good deal of effort (Computer Model Gains section) was directed toward refinement of this technique in terms of analytical model development based on empirical data from engine test. Utilizing the appropriate gain factors from the Computer Model Gains section, Table 2 compares the actual changes in performance between 684 and 702 seconds range time and predicted values for 4.5 lb/sec hydrogen and 1.0 lb/sec oxidizer flow overboard from the ASI system. The predicted values for an oxidizer line failure just upstream of the restrictor orifice (9.5 lb/sec) was included for comparison. The observed flight data for fuel flow and speed were corrected for the observed in-run performance trend typically present on all engines. The table shows the projected overboard flows for the hypothesized failure mode are a reasonable approximation of the shift and a total oxidizer failure is again a poor correlation. Table 3 compares the J016-4 shift performance with the AS-502 S-IVB data corrected for zero ASI fuel feed flow overboard using the performance gains. A close agreement is shown in the table, indicating the likelihood of injector degradation similar to engine J016-4 present during flight.

Therefore, it is concluded from the data presented in the two tables that the sequence of events leading to the above total propellant loss overboard, with some c* loss because of injector damage predicted for the AS-502 S-IVB flight failure mode, is a totally adequate explanation of the observed performance phenomenon.

[redacted]

TABLE 2

AS-502 S-IVB PERFORMANCE SHIFT PREDICTIONS

Parameter	Observed J2042 Engine Decay (first-burn 684-702)	ASI Fuel Line Failure and ASI Burnout (4.5 lb/sec LH_2 1.0 lb/sec LO_2 overboard)	ASI Oxidizer Line Failure Only (15 lb/sec LO_2 overboard)
Fuel Pump Discharge Discharge Pressure, psia	-24.7	-20.2	-25.5
Oxidizer Pump Discharge Pressure, psia	-21.5	-17.9	-37.5
Gas Generator Chamber Pressure, psia	-10.0	-8.8	-16.5
Main Chamber Pressure, psia	-16.2	-13.5	-19.5
Main Fuel Injector Temperature, F	+6.4	+6.0	-4.5
Fuel Flow*, gpm	+15.7	+28.3	-60.0
Oxidizer Flow, gpm	-6.9	-8.1	0
Fuel Speed*, rpm	-126	-94	-150
Oxidizer Speed, rpm	-71.2	-56.0	-90.0
Fuel Turbine Inlet Temperature, F	-1.2	-5.5	-31.5
Oxidizer Turbine Inlet Temperature, F	-5.5	-5.2	-30.9

*Corrected for in-test trend prior to and after shift

[redacted]

TABLE 3

AS-502 S-IVB PERFORMANCE SHIFT PREDICTIONS

Parameter	S-IVB 684-702 Shift Corrected to Zero ASI Fuel Feed Flow Overboard	Engine J016-4 (SSFL 313-041) Shift With Zero ASI Fuel Feed Flow Overboard
Fuel Pump Discharge Pressure, psia	-8	-12
Oxidizer Pump Discharge Pressure, psia	-8	-11
Gas Generator Chamber Pressure, psia	-3	-6
Main Chamber Pressure, psia	-5	-8
Main Fuel Injection Temperature, F	0	-1
Fuel Flow, gpm	-10	-10
Oxidizer Flow, gpm	-3	-5
Fuel Speed, rpm	-50	-30
Oxidizer Speed, rpm	-20	-18
Fuel Turbine Inlet Temperature, F	-1	-7
Oxidizer Turbine Inlet Temperature, F	-3	-3

[redacted]

COMPUTER MODEL AND ENGINE PERFORMANCE GAIN FACTORS

Summary of SSFL Tests

Objectives. Tests 313-031, -032, and -033 were accomplished on 18 and 19 April 1968. The primary objective of these tests was to assess the influence of a high and abrupt fuel repressurizing flow change on engine performance.

Test 313-034 was accomplished on 19 April 1968. The object of the test was to simulate a break in the ASI oxidizer line downstream of the orifice, and to determine its effect on engine operation.

Test 313-035 was run on 21 April 1968. The primary test objective was to simulate a partial failure and then a complete failure of the ASI fuel line and its effect on engine operation and hardware.

Results. The engine was calibrated to a level corresponding to engine J2044.

Test 313-031 was accomplished as planned. At 75 seconds, fuel repressurizing valve signalled open. Engine performance shifted with no hardware damage. Fuel repressurizing flowrate was 5.1 lb/sec.

Test 313-032 did not accomplish test objectives because the facility fuel repressurizing overboard dump valve failed to respond to its opening signal. The test was terminated to conserve engine time.

Test 313-033 was accomplished as planned. At 75 seconds, fuel repressurizing valve signalled open. Engine performance shifted with no hardware damage. Fuel repressurizing flowrate was 8.5 lb/sec.

Test 313-034 simulated ASI oxidizer line failure. As oxidizer leak was observed in the facility hot-gas dump system at 27.07 seconds. The oxidizer leak in the hot-gas dump system increased so that oxidizer flow to

ASI apparently stopped at 53.72 seconds; at 122 seconds, ASI oxidizer flow reversal resulted in combustion in ASI hot-gas dump. Performance gain data from the test was not usable because of the indeterminate gradual leak. Data from an MTF test on engine J2014, which had an ASI oxidizer line failure, was used for comparison.

Test 313-035 was accomplished as planned. The test simulated a partial failure and then a complete failure of the ASI fuel line. The engine operated for 95 seconds with the ASI fuel system in the failed "mode." In addition to 313-035, test 624-062 on engine J018 (31 August 1965) was used. During the test, the ASI fuel line partially failed. The leak on 624-062 was estimated to be 0.5 lb/sec.

Comparison of SSFL Gains to Existing Model

The J-2 data reduction program and influence coefficient model were used to simulate performance shifts encountered during SSFL tests. The performance shifts predicted by the J-2 model did not agree with performance shifts obtained during SSFL tests. Tables 4 through 6 compare the model with the SSFL, MTF, and engine J018 gains at constant flowrates. Table shows the engine gains for an ASI fuel leak. Table 5 shows the engine gains for an ASI oxidizer leak (MTF test used instead of SSFL test). Table 6 shows the engine gains for a fuel pressurization leak. In all fuel leakage cases, the J-2 model did not agree closely with the hot-fire gains; oxidizer leakage gains were close to model predictions. Table 7 shows the effect on performance of fuel leakages less than 0.5 lb/sec. It should be noted that the magnitude of change is within signal noise level for flight data.

[redacted]

TABLE 4

J-2 ENGINE GAINS FOR FUEL TANK PRESSURIZATION LINE FAILURE

Engine Parameter	Model	Engine J004-5	
		Test 313-031	Test 313-033
Fuel Tapoff Flow, lb/sec	1	1	1
Main Chamber Pressure, psi	-3.1	-2.5	-2.9
Oxidizer Pump Discharge Pressure, psi	-2.9	-2.9	-2.9
Oxidizer Injection Pressure, psi	-3.0	-2.9	-2.6
Fuel Pump Discharge Pressure, psi	-4.1	-1.7	-2.0
Fuel Manifold Pressure, psi	-4.3	-1.7	-2.0
Fuel Injection Pressure, psi	-5.1	-3.1	-3.4
Fuel Injection Temperature, F	--	0.5	0.5
Main Fuel Flow, gpm	8.1	-1.9	-2.9
Main Oxidizer Flow, gpm	0.7	1.9	2.3
Fuel Pump Speed, rpm	-16.6	-9.8	-16.5
Oxidizer Pump Speed, rpm	-9.2	-9.8	-8.8
Gas Generator Chamber Pressure, psi	-1.4	-1.3	-1.1
Fuel Turbine Inlet Temperature, F	0.6	-1.3	-2.0
Fuel Turbine Inlet Pressure, psi	--	--	--
Oxidizer Turbine Inlet Temperature, F	--	-0.9	-1.1
Oxidizer Turbine Inlet Pressure, psi	-0.1	-0.1	-0.1

[redacted]

TABLE 5

J-2 ENGINE GAINS FOR ASI OXIDIZER LINE FAILURE

Engine Parameter	ASI Oxidizer Line Failure	
	Model	Engine J2014
ASI Oxidizer Leak Flow, lb/sec	1	1
Main Chamber Pressure, psi	-1.1	-1.3
Oxidizer Pump Discharge Pressure, psi	-2.3	-2.5
Oxidizer Injection Pressure, psi	-1.9	-1.5
Fuel Pump Discharge Pressure, psi	-1.7	-1.7
Fuel Manifold Pressure, psi	-1.6	--
Fuel Injection Pressure, psi	-1.2	-1.5
Fuel Injection Temperature, F	—	-0.3
Main Fuel Flow, gpm	-4.5	-4.0
Main Oxidizer Flow, gpm	0.5	0
Fuel Pump Speed, rpm	-17.2	-10.0
Oxidizer Pump Speed, rpm	-7.3	-6.0
Gas Generator Chamber Pressure, psi	-0.9	-1.1
Fuel Turbine Inlet Temperature, F	-1.7	-2.1
Fuel Turbine Inlet Pressure, psi	-0.9	—
Oxidizer Turbine Inlet Temperature, F	-1.2	—
Oxidizer Turbine Inlet Pressure, psi	-0.1	—

[redacted]

TABLE 6

J-2 ENGINE GAINS FOR ASI FUEL LINE FAILURE

Engine Parameter	Model	Engine J018, Test 624-062	Engine J004-5 Test 313-035	
ASI Fuel Leak Flow, lb/sec	1.0	1.0	1.0	1.0
Main Chamber Pressure, psi	-1.888	-3.0	-2.5	-2.7
Oxidizer Pump Discharge Pressure, psi	-1.85	-4.0	-4.3	-3.5
Oxidizer Injection Pressure, psi	-1.85	—	-3.6	-2.8
Fuel Pump Discharge Pressure, psi	-7.8	-4.0	-2.2	-4.1
Fuel Manifold Pressure, psi	-8.45	-4.0	-4.3	-4.8
Fuel Injection Pressure, psi	-3.175	-4.0	-4.3	-3.3
Fuel Injection Temperature, F	—	4.0	0	1.4
Main Fuel Flow, gpm	42.85	-20.0	34.0	7.1
Main Oxidizer Flow, gpm	0.175	0	0	-1.1
Fuel Pump Speed, rpm	7.625	-40.0	34.0	-17.1
Oxidizer Pump Speed, rpm	-5.95	-10.0	-15.9	-12.4
Gas Generator Chamber Pressure, psi	-1.3	—	0	-1.7
Fuel Turbine Inlet Temperature, F	8.175	-12.0	-11.3	-0.5
Fuel Turbine Inlet Pressure, psi	—	—	—	—
Oxidizer Turbine Inlet Temperature, F	6.625	—	-5.9	-0.4
Oxidizer Turbine Inlet Pressure, psi	-0.15	—	-0.4	-0.2

[redacted]

TABLE 7

J-2 ENGINE GAINS FOR ASI FUEL LINE FAILURE

Engine Parameter	Engine J018, Test 624-062	Engine J004-5, Test 313-035
ASI Fuel Leak Flow, lb/sec	0.5 (estimated)	0.44
Main Chamber Pressure, psi	-1.5	-1.1
Oxidizer Pump Discharge Pressure, psi	-2.0	-1.9
Oxidizer Injection Pressure, psi	—	-1.6
Fuel Pump Discharge Pressure, psi	-2.0	-1.0
Fuel Manifold Pressure, psi	-2.0	-1.9
Fuel Injection Pressure, psi	-2.0	-1.9
Fuel Injection Temperature, F	2.0	0
Main Fuel Flow, gpm	-10.0	15.0
Main Oxidizer Flow, gpm	0	0
Fuel Pump Speed, rpm	-20.0	15.0
Oxidizer Pump Speed, rpm	-5.0	-7.0
Gas Generator Chamber Pressure, psi	—	0
Fuel Turbine Inlet Temperature, F	-6.0	-5.0
Fuel Turbine Inlet Pressure, psi	—	—
Oxidizer Turbine Inlet Temperature, F	—	-2.6
Oxidizer Turbine Inlet Pressure, psi	—	-0.2

[redacted]

J-2 Model Evaluation

A study was made to determine the validity of the J-2 models. To determine possible problem areas with the J-2 model, engine hardware characteristics were compared over a PU excursion. The differences in hardware characteristics over the PU range were averaged to determine if a bias existed. The thrust chamber jacket ΔP, the oxidizer injector ΔP, and the fuel injector ΔP showed to be areas of significant bias.

Table 8 shows the results of the thrust chamber jacket ΔP study. Data for a fuel pressurization change, ASI fuel leak, PU excursion, and large engine recalibrations were tabulated. The influence coefficient program and data reduction program were used to predict the thrust chamber pressure drop at the higher flowrate from the tabulated data. Tabulated is the error that resulted in predicting the jacket pressure drop for the various models. The influence coefficient program was as good as any of the methods studied. Apparently, a parameter not used by any of the models is responsible for the errors observed.

Tables 9 and 10 show the results of a similar study for the fuel and oxidizer injector study. The influence coefficient program appears to be best for prediction of the fuel injector pressure drop. A modification of the influence coefficient model using flow raised to the 1.66 power best predicts the oxidizer injector pressure drop.

Table 8 indicates that the influence coefficient model is in error by 23.7 psi for an ASI fuel leak of 3.5 pounds. This 23.7-psi error is approximately 6 percent of the total thrust chamber jacket pressure drop. The change in the influence coefficient gains were calculated for a ±6-percent error in thrust chamber resistance, and are presented in Table 11. The +6-percent gains for a 3.5-lb/sec fuel leak are in better agreement with the gains from engine J004-5. This shows that Tables 8 through 10 can be used to help predict reasonable gains by modifying the J-2 model gains by the error indicated.

[redacted]

TABLE 8

COMPARISON OF VARIOUS THRUST CHAMBER RESISTANCE MODELS*

Cause of Performance Variation	Engine No.	Test No.	Influence Coefficient Program	Data Reduction Program	Data Reduction Using Flow Squared	Flow Squared Considering Density	Data Reduction Considering Density
Fuel Pressurization (0 → 8.59)	J004-5	313-033	-12.0	-12.0	-12.0	1.3	1.2
ASI Fuel Leak (3.5 → 0)	J004-5	313-035	23.7	8.3	20.7	15.2	3.0
PU Excursion (minimum → maximum)	J2133	313-025	-12.5	-41.5	-24.2	-4.9	-21.5
PU Excursion (minimum → maximum)	J2090	313-095	1.1	-40.6	-13.5	-9.6	-33.2
PU Excursion (minimum → maximum)	J2110	624-019	-17.2	-49.6	-29.0	3.3	-19.8
Recalibration at Maximum PU	J2119	624-050, 624-051	7.0	-3.0	4.8	-4.5	-12.6
Recalibration at Maximum PU	J2133	313-026, 313-025	11.9	2.1	9.7	27.2	19.3
Recalibration at Minimum PU	J2133	313-026, 313-025	8.5	0.5	5.5	12.0	6.9
No Change			2.4	0.4	2.1	2.1	0.4

*Tabulated is the error in the thrust chamber pressure drop, when the pressure drop is corrected from the lower thrust chamber flow to the higher flowrate.

[redacted]

TABLE 9

COMPARISON OF VARIOUS MAIN FUEL INJECTOR RESISTANCE MODELS*

Cause of Performance Variation	Engine No.	Test No.	Influence Coefficient Program	Data Reduction Program	Influence Coefficient Program Considering Density	Data Reduction Program Considering Density
Fuel Pressurization (0 → 8.59)	J004-5	313-033	+3.2	+18.8	+8.6	+23.8
ASI Fuel Leak (3.5 → 0)	J004-5	313-035	+0.2	+4.4	+2.0	+6.2
PU Excursion (minimum → maximum)	J2133	313-025	-1.4	+5.4	-8.1	-1.7
PU Excursion (minimum → maximum)	J2090	313-095	-11.4	-2.0	-9.9	-0.6
PU Excursion (minimum → maximum)	J2110	624-019	+1.6	+9.5	-8.8	-1.3
Recalibration at Maximum PU	J2119	624-050, 624-051	-5.2	-2.9	-2.2	+0.2
Recalibration at Maximum PU	J2133	313-026, 313-025	+4.0	+6.4	-1.0	+1.0
Recalibration at Maximum PU	J2133	313-026, 313-025	-1.8	-1.0	-3.9	-2.3
No Change			+0.2	+0.7	+0.3	+0.8

*Tabulated is the error in the fuel injector pressure drop, when the pressure drop is corrected from the lower injector flow to the higher flowrate.

[redacted]

[redacted]

TABLE 10

COMPARISON OF VARIOUS MAIN OXIDIZER INJECTOR RESISTANCE MODELS*

Cause of Performance Variation	Engine No.	Test No.	Influence Coefficient Program	Data Reduction Program	Influence Coefficient and Data Reduction Program Using Flow to 1.66 Power
Fuel Pressurization (0 → 8.59)	J004-5	313-033	-1.0	-1.0	-1.0
ASI Fuel Leak (3.5 → 0)	J004-5	313-035	+0.2	+0.2	-0.6
PU Excursion (minimum → maximum)	J2133	313-025	+20.2	+20.2	-1.8
PU Excursion (minimum → maximum)	J2090	313-095	+26.2	+26.2	+0.9
PU Excursion (minimum → maximum)	J2110	624-019	+24.0	+24.0	+0.9
Recalibration at Maximum PU	J2119	624-050, 624-051	+3.2	+3.2	-0.6
Recalibration at Maximum PU	J2133	313-026, 313-025	+2.5	+2.5	+1.0
Recalibration at Minimum PU	J2133	313-026, 313-025	+0.5	+0.5	-0.2
No Change			-0.3	-0.3	-0.3

*Tabulated is the error in the oxidizer injector pressure drop, when the pressure drop is corrected from the lower injecto[redacted]

TABLE 11

EFFECT OF 3.5-LB/SEC FUEL LEAK

	Influence Coefficient Error Thrust Chamber Resistance			Engine J004-5, Test 313-035
	-6 percent	0	+6 percent	
Chamber Pressure, psi	-4.56	-6.6	-8.64	-10
Oxidizer Pump Discharge Pressure, psi	-4.34	-6.5	-8.66	-13
Oxidizer Injection Pressure, psi	-4.34	-6.5	-8.66	-10
Fuel Pump Discharge Pressure, psi	-35.0	-27.5	-20.1	-15
Fuel Manifold Pressure, psi	-38.2	-29.7	-21.2	-17
Fuel Injection Pressure, psi	-7.3	-11.1	-14.9	-12
Main Fuel Flow, gpm	+216.4	+150.0	+83.6	+25
Main Oxidizer Flow, gpm	+0.3	+0.6	+0.9	-4
Oxidizer Pump Speed, rpm	-13.8	-20.8	-27.8	-44
Fuel Pump Speed, rpm	+62.1	+26.7	-8.7	-60
Gas Generator Chamber Pressure, psi	-4.46	-4.6	-4.74	-6
Fuel Turbine Inlet Pressure, psi	-4.25	-4.4	-4.55	-5
Fuel Turbine Inlet Temperature, F	+43.7	+28.6	+13.5	-2
Oxidizer Turbine Inlet Pressure, psi	-0.48	-0.5	-0.52	-0.9
Oxidizer Turbine Inlet Temperature, F	+35.3	+23.2	+11.1	-2

[redacted]

Tests at SSFL have shown that the J-2 model cannot precisely predict all performance changes due to propellant leakage. Tables 8 through 10 indicate the precision of the various models for some types of engine changes. The problem areas have been defined and action initiated toward improving the model. In the interim, computer model programs should be considered as general indicators only of failure modes; actual engine tests are required for confirmation.

[redacted]

GAS GENERATOR TEMPERATURE SURGE AT FIRST-BURN CUTOFF

EVENT DESCRIPTION: FUEL TURBINE INLET TEMPERATURE OVERSHOOT AFTER FIRST-BURN CUTOFF

Defining Data

A 100 F temperature overshoot (Fig. 46), as measured by the fuel turbine inlet temperature bulb, occurred 2 seconds after cutoff (749 seconds range time).

Possible Failure Modes or Causes of Event

Possible causes were:

1. Improper closing of the GG valve
2. Residual oxygen in purge system due to a leaking GG oxidizer purge or oxidizer dome purge check valve
3. Improper sequencing of stage-supplied GG fuel purge
4. A density change of the oxygen entrapped in the GG oxidizer purge and GG oxidizer injection pressure lines due to chilling of the lines

Conclusions

The most probable cause of the temperature overshoot was a quality and density change of the oxygen entrapped in the GG oxidizer purge system (brought about by chilling of the purge and GG oxidizer injection pressure lines during engine operation and subsequent injection of the more-dense oxygen into the GG following engine cutoff).

Improper sequencing of the stage-supplied GG fuel purge may have had a contributory effect to the temperature overshoot. However, another

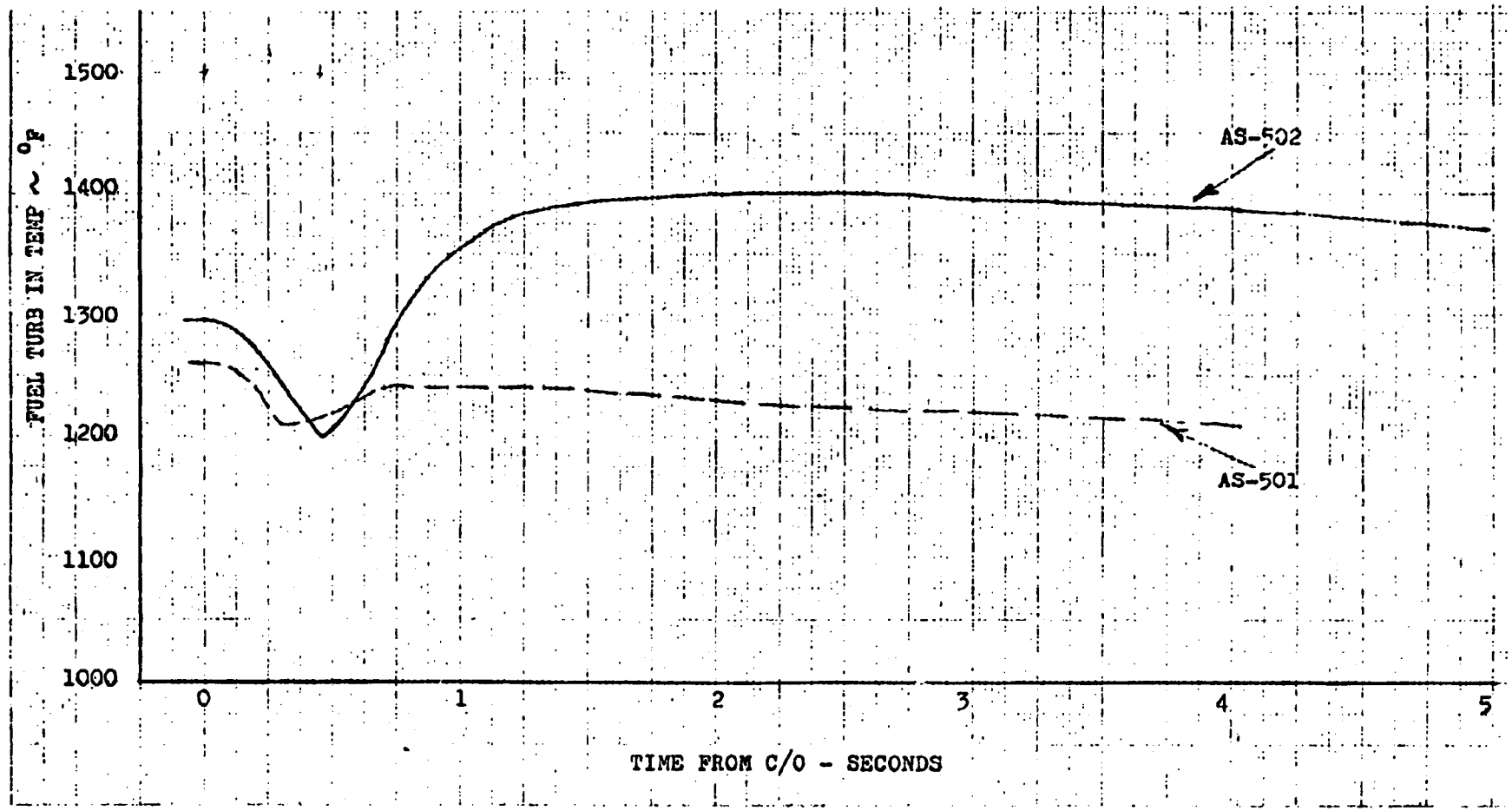

Figure 46. AS-501 and AS-502 Comparison of Fuel Turbine in Temperature Characteristics at First-Burn Cutoff

[redacted]

serious consequence of the improper purge sequence could have been the degradation of the GG fuel injection system due to icing. This problem could prevent a successful restart (although GG operation at restart was proper). Corrective action must be taken on future S-IVB flights to prevent recurrence of the stage purge sequencing problem.

The inadequacy of the GG fuel purge did not contribute to the failure of the engine to restart.

No hardware damage was sustained by the fuel turbine as a result of the temperature overshoot.

Analysis

The analysis indicates that:

1. The high temperature occurred when GG chamber pressure (and mass flowrate) was low, thus minimizing the heat input to the turbine.
2. No apparent damage was sustained by the fuel turbine as a result of the temperature overshoot. Normal spinup of the pumps was noted during subsequent restart attempt.
3. Gas generator valve operation was normal at cutoff.
4. Stage sequencing of the turbopump and GG fuel purge occurred 7 seconds later than programmed (0.1 second prior to cutoff), such that purge pressure was not up to the required level at cutoff. This purge is required to be at operating pressure (82 to 130 psia) at the customer connect panel withon 0.2 second of engine cutoff.

   Figure 47 depicts the engine pump purge regulator pressure buildup at cutoff. The data revealed that the highest pressure level attained during the purge was below the minimum required limit (6 psi low). This has been brought to the attention of the S-IVB stage contractor (Huntington Beach Facility).

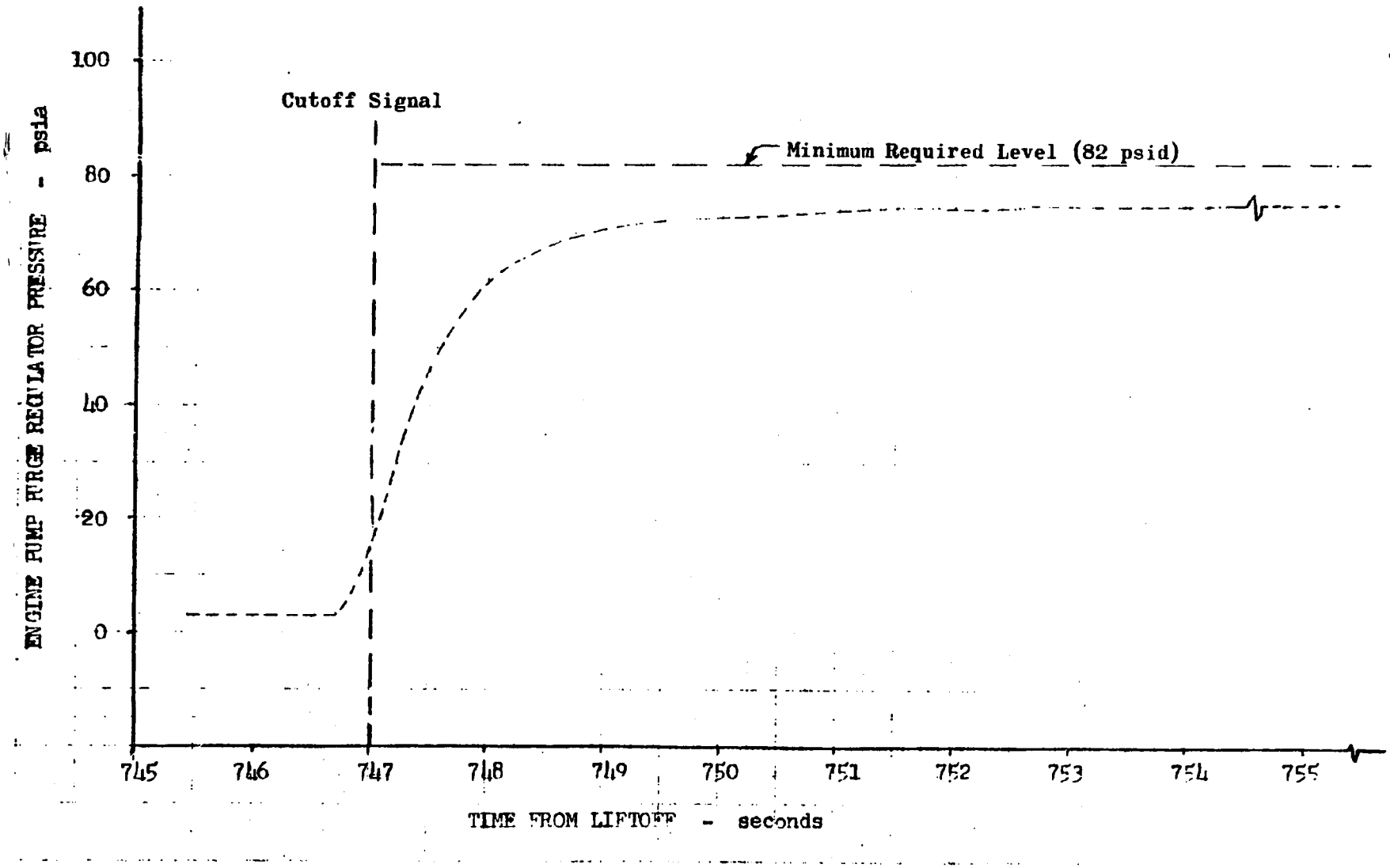

Figure 47. AS-502 S-IVB First Burn, Engine Pump Purge Regulator Pressure vs Time

[redacted]

The inadequacy of the GG fuel purge did not contribute to the failure of the engine to restart.

5. Pressure profiles of GG oxidizer injection pressure at cutoff for AS-502 S-IVB flight and stage acceptance were compared. The data did not indicate any significant deviations that would relate the temperature overshoot to a leaking check valve in the GG oxidizer purge system. However, severe chilling in the vicinity of the GG throughout much of the first burn suggested the following explanation for the temperature overshoot:

   a. The GG oxidizer purge and instrumentation lines (shown by dash marks in Fig. 48) chilled down to liquid oxygen temperatures. This assumption is reasonable on the basis of the MOV closing control line temperature measurement—located within inches of the purge lines--which indicated a temperature below -260 F for better than 30 seconds prior to engine cutoff.

   b. Gaseous oxygen entrapped in the lines became more dense and probably reached liquid state. The volume of the GG purge and GG oxidizer injection pressure lines is approximately 3.3 times greater than the volume of the GG oxidizer manifold. Calculated results showed that it is possible to trap approximately 0.115 pound of oxygen if the entire line volumes in Fig. 48 were filled with liquid.

   c. When cutoff occurred, the engine supplied helium purge injected the more-dense oxygen into the GG combustor. With the GG valve closed and burning of residual oxygen and fuel from the GG injector manifolds taking place, the additional oxygen supplied via the purge lines momentarily raised the mixture ratio in the GG sufficiently to produce the temperature overshoot.

6. No further problems of this nature are expected on future S-IVB flights since corrective actions are being implemented to eliminate the cause of the abnormal engine chilldown experienced AS-502 S-IVB.

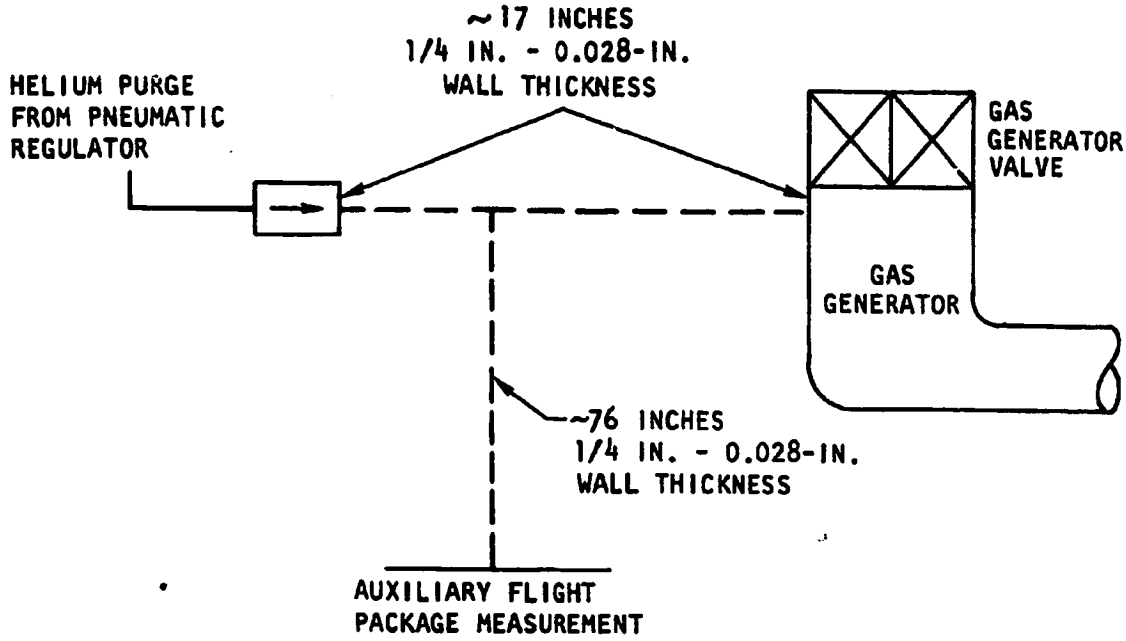

TOTAL VOLUME OF PURGE SYSTEM SHOWN:

$V_T = V_{LINES} + V_{OXIDIZER}$ WHERE $L = \sim 93$ INCHES

$$A_c = \frac{\pi(0.194)^2}{4} = 0.735\ (0.038) = 0.03\ \text{IN.}^2$$

$V_{LINE} = 93 \times 0.03 = 2.79\ \text{IN.}^3$

$V_{OXIDIZER\ MANIFOLD} = 0.9\ \text{IN.}^3$

$V_T = 3.88\ \text{IN.}^3$

VOLUME RELATIONSHIP:

GAS GENERATOR FUEL MANIFOLD TO GAS GENERATOR OXIDIZER MANIFOLD = 25:1

GAS GENERATOR OXIDIZER PURGE AND GAS GENERATOR OXIDIZER INJECTION PRESSURE LINES TO GAS GENERATOR OXIDIZER MANIFOLD 3.3:1

Figure 48. Gas Generator Oxidizer Purge System Schematic

FUEL PUMP DISCHARGE PRESSURE SURGE AFTER FIRST-BURN CUTOFF

EVENT DESCRIPTION: FUEL PRESSURE SURGE

Supporting Data

Fourteen seconds after the engine cutoff of the S-IVB first burn, a surge occurred in fuel pump discharge pressure. The magnitude of the spike exceeded 150 psia and conceivably could cause damage to the fuel recirculation return system. Figure 49 is a plot of fuel pump discharge pressure during the period following engine cutoff showing the anomaly as it appeared in the flight data. Also, similar fuel pump discharge pressure data from simulated altitude tests at AEDC are superimposed to illustrate similarity of pressure surges observed in ground test data.

Possible Cause of Events

Because the J-2 fuel turbopump normally continues to coast at a relatively high rate of speed for up to 3 minutes after cutoff, a substantial quantity of kinetic energy remains available in the turbopump during this period. If liquid hydrogen of adequate quality is permitted to enter the pump while it is still spinning, a discharge pressure surge of considerable magnitude will be produced until the pump stalls. The phenomenon appears as a spike in fuel pump discharge pressure.

Conclusion

A pressure spike produced in this manner could possibly jeopardize the integrity of the recirculation return system of the S-IVB stage because it occurs after the engine bleed valves have reopened. The possibility of a serious pressure spike is minimized if the stage prevalve and recirculation discharge valve are closed during the cutoff sequence, as was done during the flight of AS-501. No relationship was established between this pressure spike anomaly and the major AS-502 flight malfunctions.

[redacted]

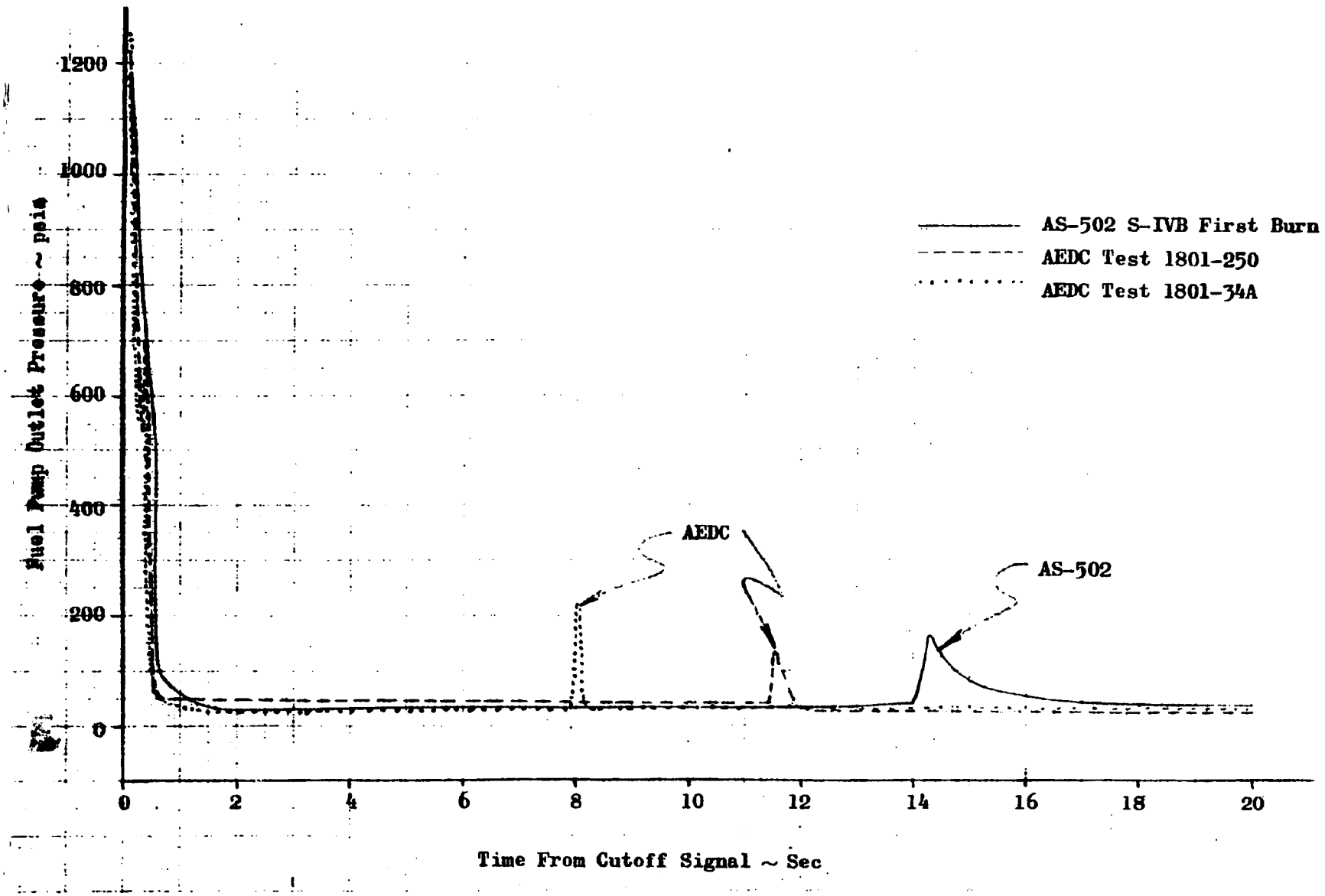

Figure 49. AS-502 S-IVB First Burn, Fuel Pump Outlet Pressure Surge After Engine Cutoff

[redacted]

Although the McDonnell-Douglas Corporation has been advised to return to the prevalve sequencing utilized on AS-501, rather than leaving these valves open as was done on the AS-502 vehicle, AEDC data indicate that closing the prevalve and recirculation discharge valve at cutoff does not guarantee that a surge will not be produced. Figure 49 shows two AEDC tests which had a surge even though the prevalve and recirculation discharge valve were closed immediately after cutoff.

ANALYSIS

Figure 50 is a schematic of the fuel feed and recirculation system. At AS-502 cutoff, the fuel prevalve and recirculation discharge (chilldown) valve remained open. The engine bleed valve opens about 4 seconds after cutoff.

After cutoff, the fuel pump continues to turn for 15 seconds (Fig. 51). With cutoff signal, the fuel pump inlet temperature increases (as gaseous conditions are reached), while the fuel tank outlet temperature remains cold (liquid), as shown in Fig. 52 . When liquid re-enters the engine, a pressure surge results.

The NPSH at the fuel pump inlet after cutoff is shown in Fig. 53 . This is an indicator of fuel quality (a positive value is subcooled liquid).

At the time of the surge, the NPSH at the pump inlet becomes sufficient for the pump to develop head again with its remaining speed. Therefore, it is thought that a gas bubble forms at the pump inlet after cutoff and, when this bubble collapses, liquid again is introduced to the pump.

The problem is associated with the fuel feed and recirculation systems and it has been seen on the S-IVB battleship stand at AEDC (Fig. 49).

[redacted]

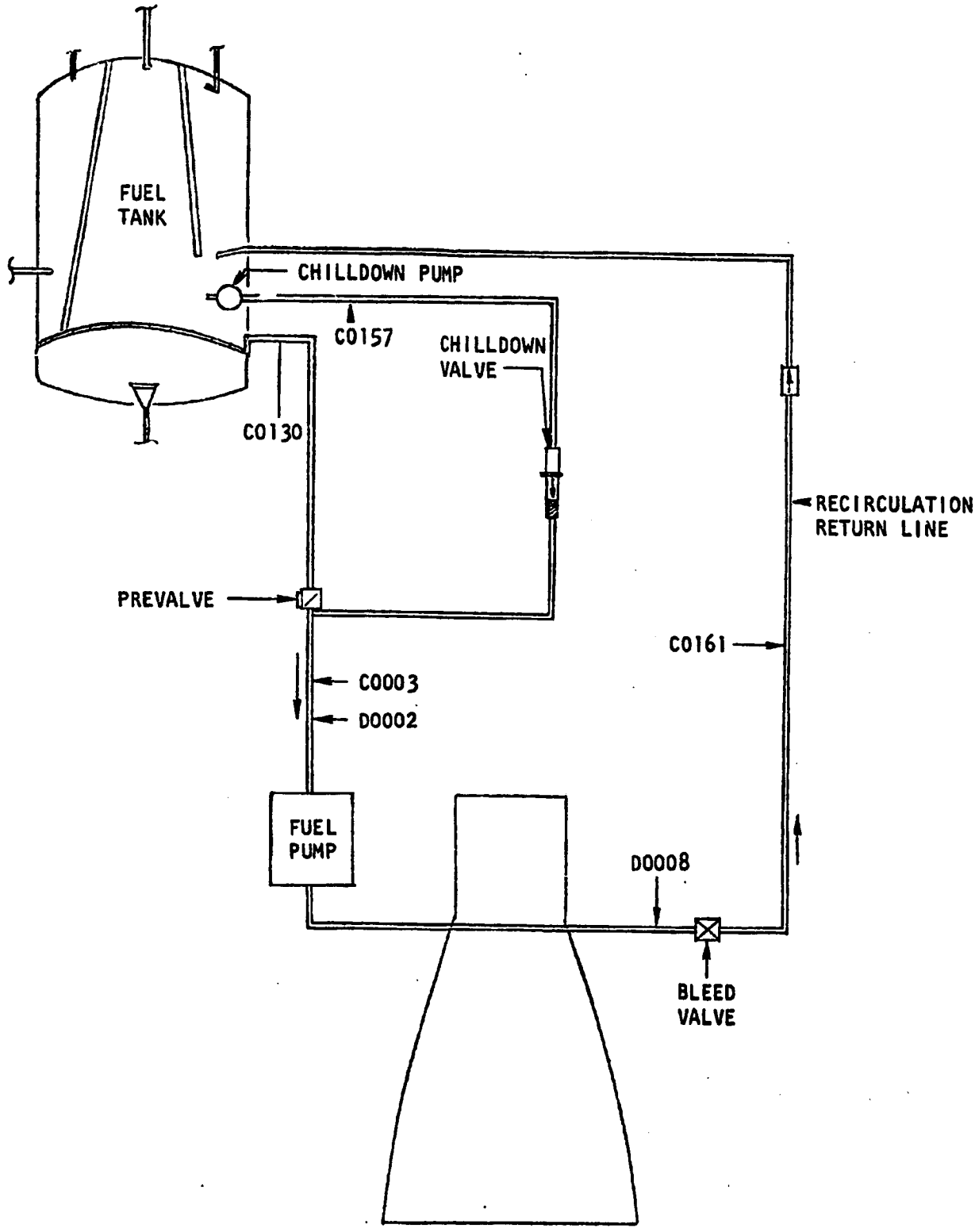

Figure 50. Fuel Feed and Recirculation System

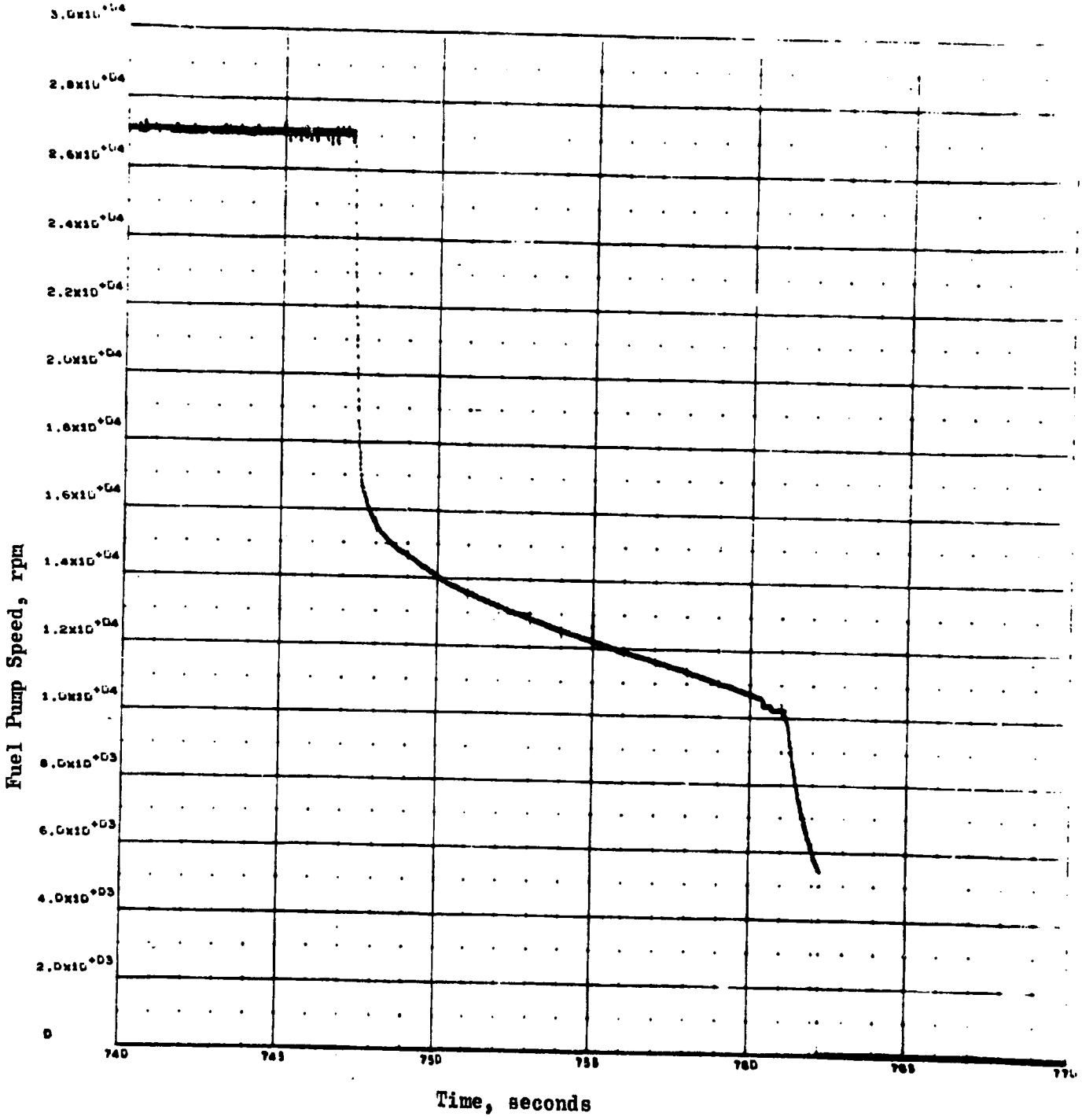

Figure 51. Fuel Pump Speed

[redacted]

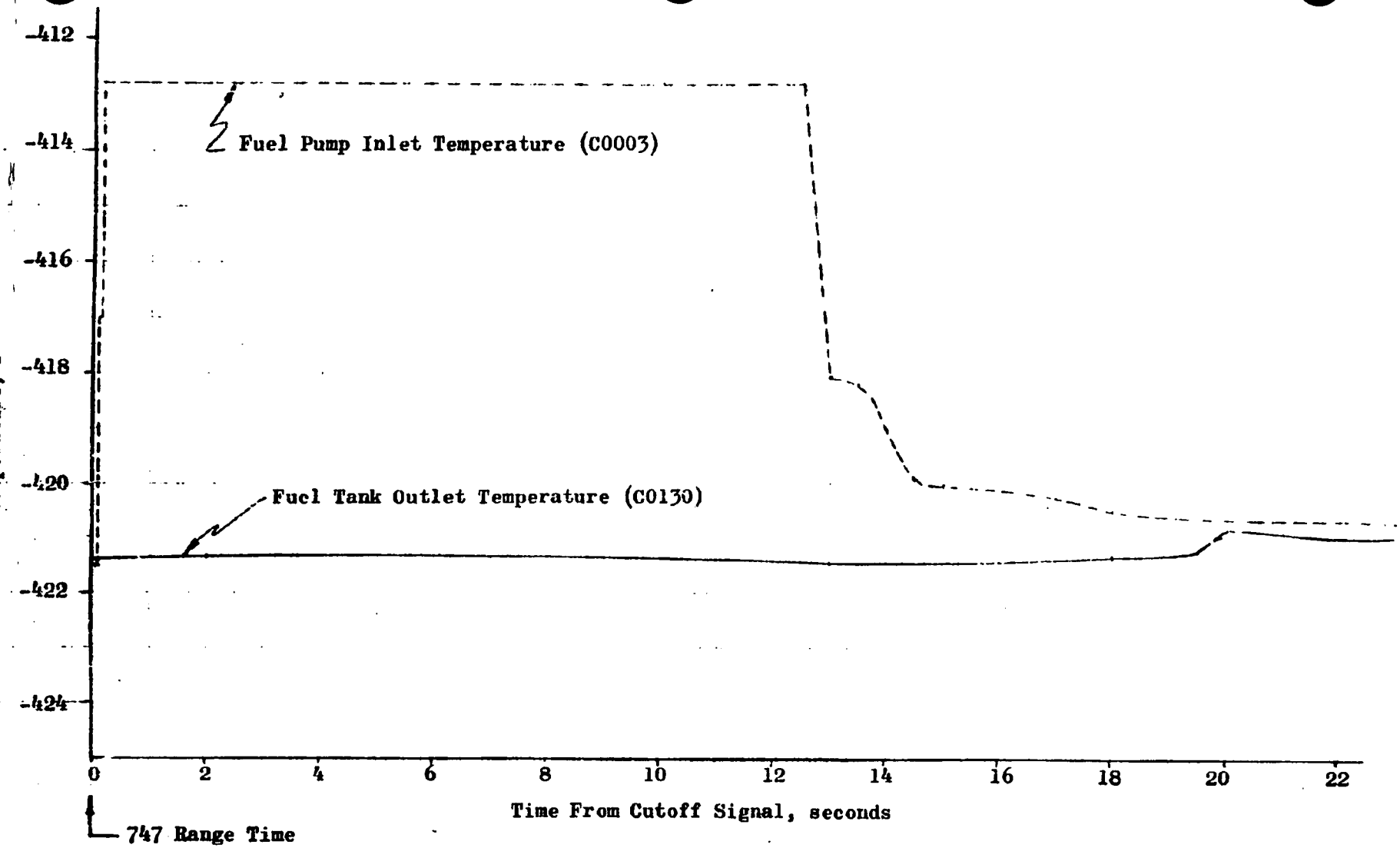

Figure 52. AS-502 S-IVB First Burn

[redacted]

[redacted]

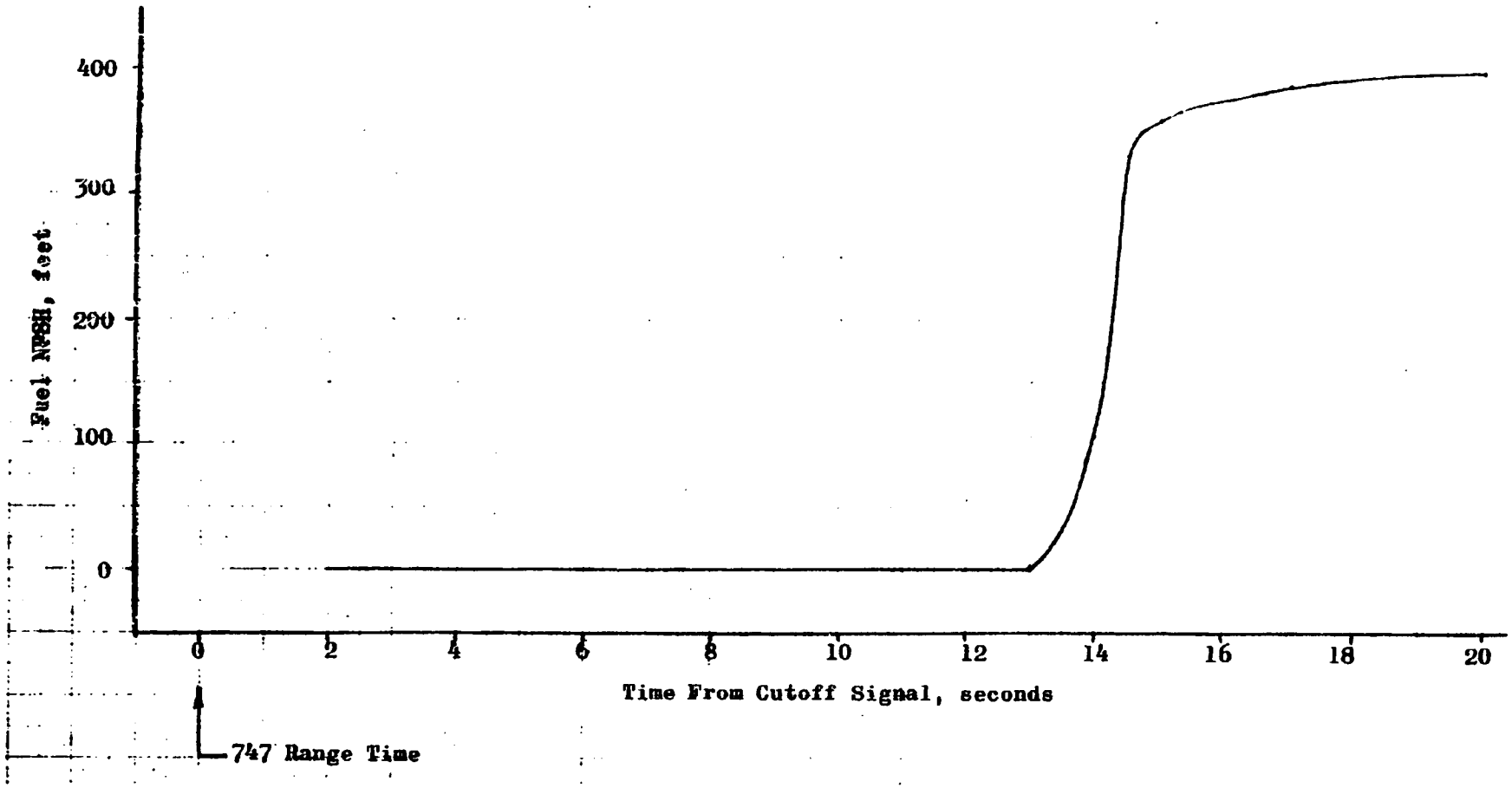

Figure 53. AS-502 S-IVB First Burn, Fuel NPSH After Cutoff

[redacted]

Conclusions and Recommendations

A potential problem exists if this pressure surge should exceed structural limitations in the recirculation return system. Following are the existing proof pressure levels for the various sections of the engine and stage fuel recirculation return system:

Engine Bleed Valve Discharge Flange, psig	110
Engine Fuel Bleed Line, psig	225
Stage Recirculation Return Line, psig	200

Existing engine hardware is capable of considerably higher pressure rating without redesign. To ensure safe operation in the future it is recommended that one of the following actions be taken:

1. Resequence the engine bleed valves to prevent opening for 30 seconds after cutoff. This would require a change in the pneumatic system bleed orifice.
2. Uprate and re-identify the engine bleed valve and bleed line by raising proof pressure to 600 psig. No hardware redesign would be required on the engine. However, the stage recirculation return line might require redesign.

S-IVB AUXILIARY HYDRAULIC PUMP FAILURE DURING ORBITAL COAST

EVENT DESCRIPTION

Supporting Data

During the S-IVB restart preparations sequence, when the auxiliary hydraulic pump was commanded on, the pump failed to produce the normal discharge pressure and flow. Proper current and voltage drops indicated normal pump rotation. Figure 54 is a schematic of the S-IVB hydraulic system.

Possible Failure Modes

In the process of analyzing this anomaly, the following potential failure modes were considered:

1. Hydraulic pump failure
2. Hydraulic system line breakage
3. Hydraulic fluid freezing in the low- and/or high-pressure system lines

Conclusion

In view of the low-temperature environment that occurred during the first burn of the J-2 engines as a result of cryogenic leakage, the most logical cause of the hydraulic pump failure appears to be freezing of hydraulic fluid because of impingement of cryogenics on hydraulic system lines and/or hoses. Laboratory test data support this hypothesis, and the flight anomaly was reproduced by the S-IVB stage contractor, McDonnell-Douglas Corporation, during their special test program. The hydraulic pump anomaly was a result rather than a cause, of the J-2 engine anomalies.

[redacted]

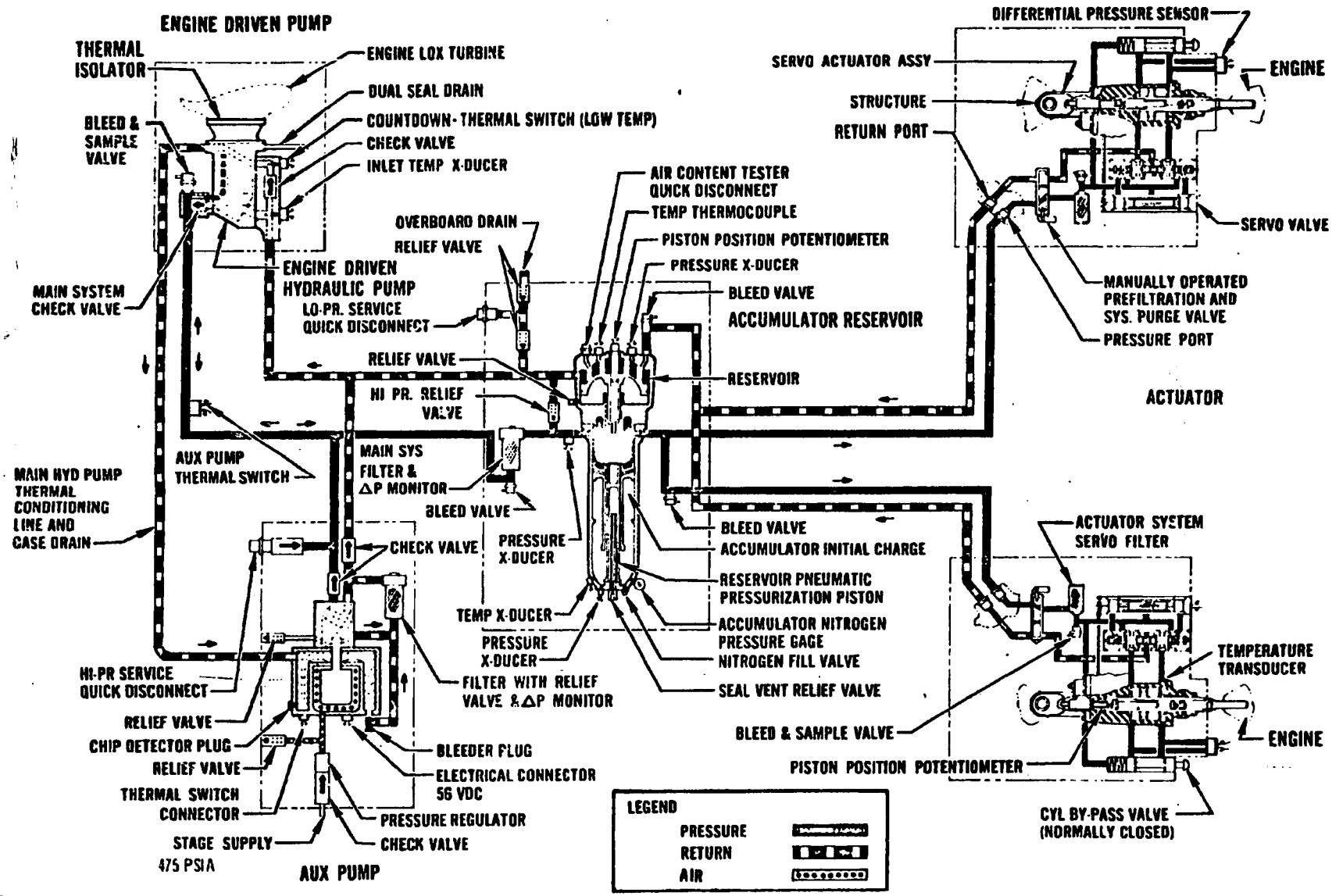

Figure 54. S-IVB Hydraulic System Schematic

ANALYSIS

When flight data analysis indicated that cryogenic chilling was a likely cause of the auxiliary hydraulic pump anomaly, the stage contractor conducted a series of laboratory tests to simulate the effects of cryogenic chilling on their hydraulic system. They were able to reproduce the anomaly quite conclusively by chilling (with liquid nitrogen) sections of hydraulic system tubing and hosing externally with LN_2 while pumping hydraulic oil through at the operating system flowrate (0.2 gpm).

The pumping continued normally under the environment with only a relatively small drop in hydraulic fluid temperature (approximately 35 F) after 5 minutes of operation. When the liquid nitrogen flow and hydraulic fluid flow were terminated, the flight anomaly was reproduced. The hydraulic fluid remaining in the test specimen dropped rapidly in temperature and froze. In the case of the tubing, the temperature of the fluid dropped below -180 F after a 4-minute period. The test of the hydraulic system hosing produced a fluid temperature of -155 F after a 4-1/2-minute period.

Removal of latent heat from hydraulic system hardware accounts for the blockage incurred during the flight of AS-502, as evidenced by lack of pump discharge pressure from the auxiliary hydraulic pump when it was turned on during second-burn preparations, as well as lack of discharge pressure from the main hydraulic pump during the attempted engine start transient. Although temperature measurements are not available to pinpoint the exact location of the freezing, it is most likely to have occurred in any or all three of the hydraulic system lines (Fig. 54) that cross the gimbal plane, running from the main hydraulic pump (mounted on the J-2 engine oxidizer pump) to the accumulator reservoir and auxiliary hydraulic pump (both mounted on the S-IVB thrust cone). The two low-pressure lines would be most sensitive to low temperature because approximately -90 F would cause sufficient slushiness of fluid to result in pump cavitation.

[redacted]

ENGINE FAILURE TO RESTART

DESCRIPTION

During the flight of AS-502, the S-IVB engine (J2042) failed to restart after a two-orbit coast. The primary events are listed below:

	Event	Range Time, seconds
1.	Engine restart command	11,614.671
2.	MOV closing control line temperature begins to indicate abnormal chilling	11,617
3.	STDV control signal	11,622.678
4.	Main chamber pressure fails to rise normally	11,623.2
5.	Engine cutoff command	11,630.397

The engine conditions prior to restart were within the allowable limits on all parameters. These conditions are listed in the Vehicle Analysis, Test Conditions section.

Specific data on the external chilling, beginning 2 seconds after engine restart command, are presented and discussed in the Thermal Environment section. It was evident that the chilling did not occur prior to engine start signal and did occur prior to STDV signal.

The thrust chamber and fuel injection temperatures indicate that the 8-second fuel lead was normal. Figure 55 shows these temperatures on AS-502 and fuel injection temperature on AS-501.

Start tank discharge valve position, start tank pressure, pump speeds, main flows, and pump discharge pressures all indicated that the start tank blowdown and turbopump acceleration were normal. The pump discharge pressures from AS-502 are compared with those of AS-501 in Fig. 56.

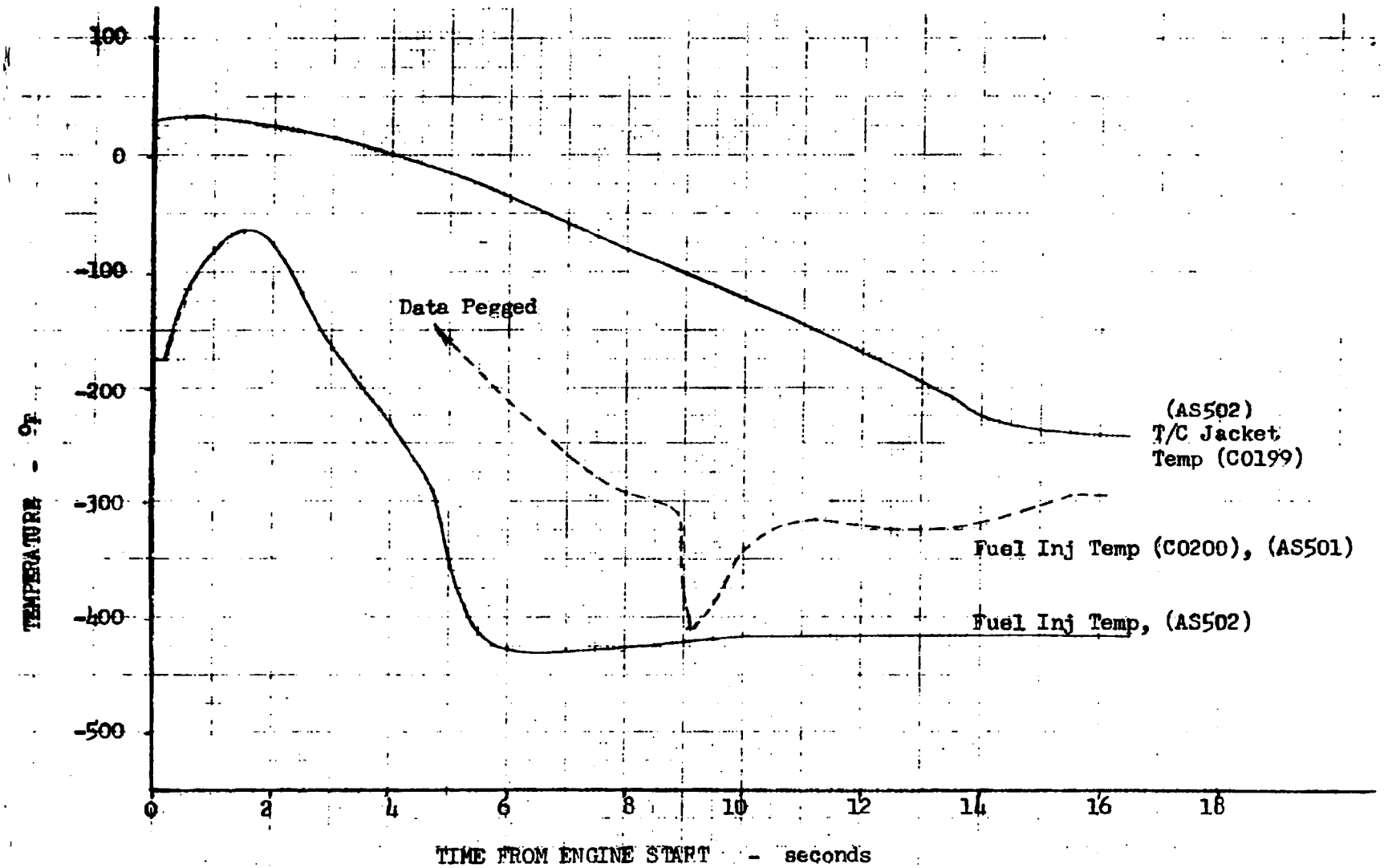

Figure 55. Comparison of AS-501 and AS-502 S-IVB Second Burn, Thrust Chamber Jacket Temperature and Fuel Injection Temperature vs Time

[redacted]

[redacted]

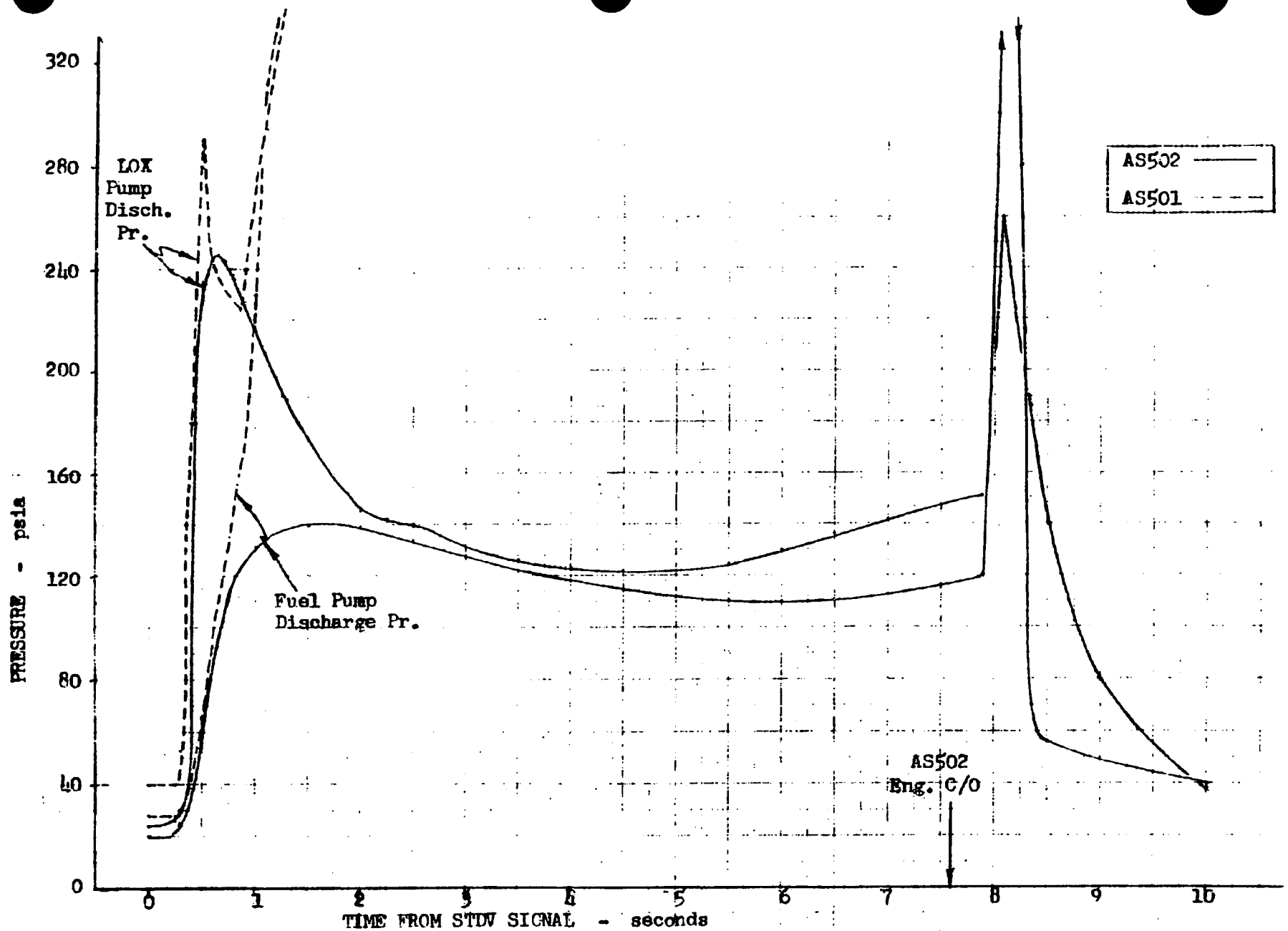

Figure 56. Comparison of AS-501 and AS-502 S-IVB Second Burn, Pump Discharge Pressures vs Time

[redacted]

Gas generator chamber pressure and fuel turbine inlet temperature both indicated normal gas generator ignition took place. These parameters are compared with AS-501 in Fig. 57.

The main oxidizer position indicated proper valve actuation, but main chamber pressure did not respond normally when the main oxidizer valve moved to the first position. Main chamber pressure normally rises from 6 or 7 psia, which it attains during the fuel lead, to approximately 30 psia when the main oxidizer valve moves to the first position (14 degrees). On AS-502 restart, main chamber pressure was only 10 psia. Main chamber pressure continued to increase gradually, reaching 38 psia 2 seconds after STDV. Figure 58 illustrates a normal chamber pressure transient (AS-501) and the abnormal one experienced on AS-502.

Normally, after the main oxidizer valve opens and main propellant ignition has occurred, the main fuel injection temperature increases from liquid hydrogen temperatures to the mainstage operating temperature (approximately-280 F), as it did on AS-501 (see Fig. 55). On AS-502, the fuel injection temperature remained below -415 F from STDV until cutoff.

Fuel turbine inlet temperature normally approaches 1050 F at nominal PU and 1200 F at maximum thrust (full-closed PU valve), as it does for AS-501 in Fig. 57 . On AS-502, the fuel turbine inlet temperature initially rose to 1460 F quite rapidly, showing quicker response than this resistance bulb normally does. This may have been caused by the excessive gas generator temperature that resulted from the abnormal start. Fuel turbine inlet temperature remained excessive for the duration of the second burn, pegging upscale at 1800 F 300 milliseconds prior to cutoff. Comparing Fig. 55 and 56, it can be seen that fuel turbine inlet temperature follows the same trend as the differential between oxidizer pump discharge pressure and fuel pump discharge pressure.

[redacted]

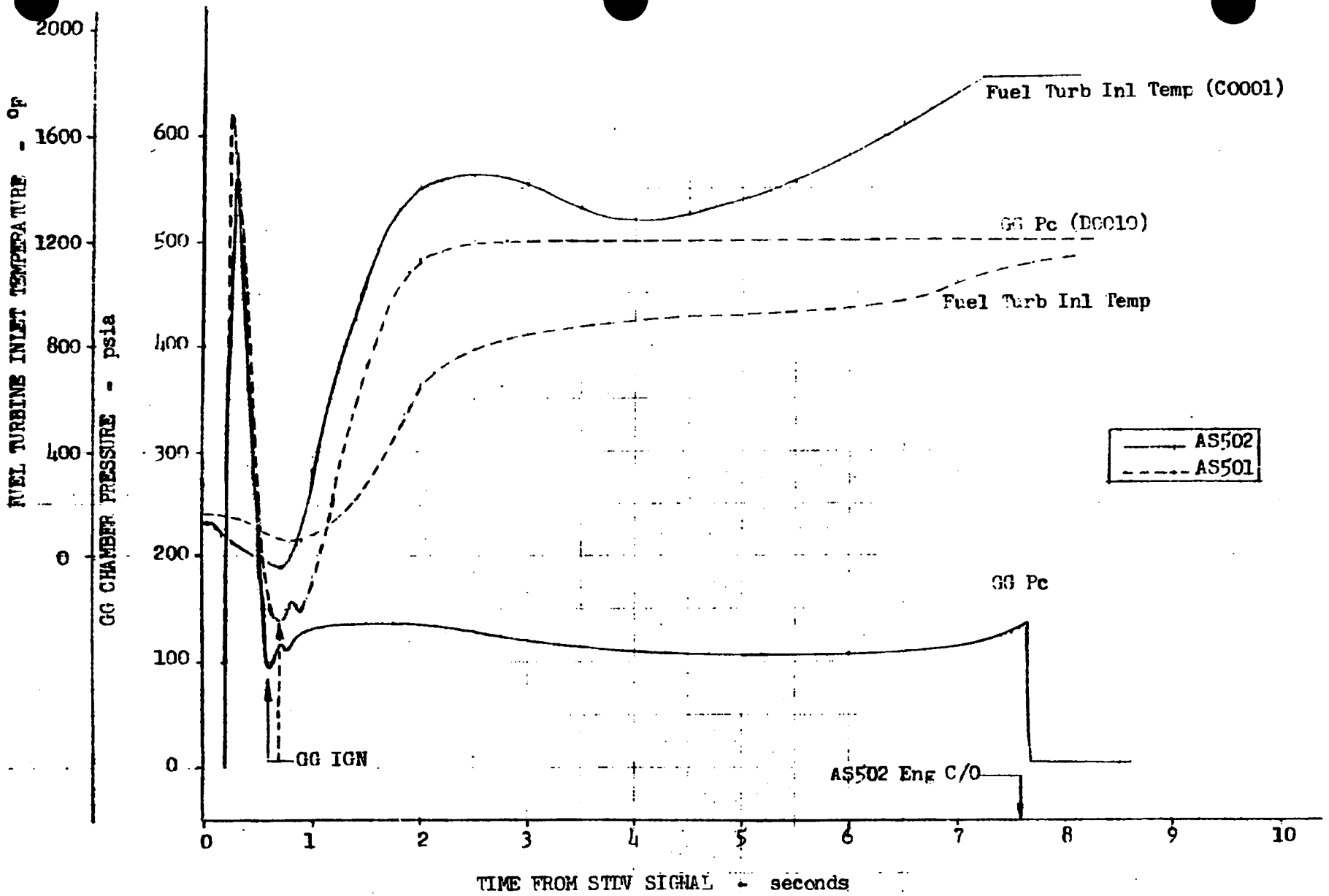

Figure 57. Comparison of AS-501 and AS-502 S-IVB Second Burn, Gas Generator Chamber Pressure and Fuel Turbine Inlet Temperature vs Time

[redacted]

[redacted]

[redacted]

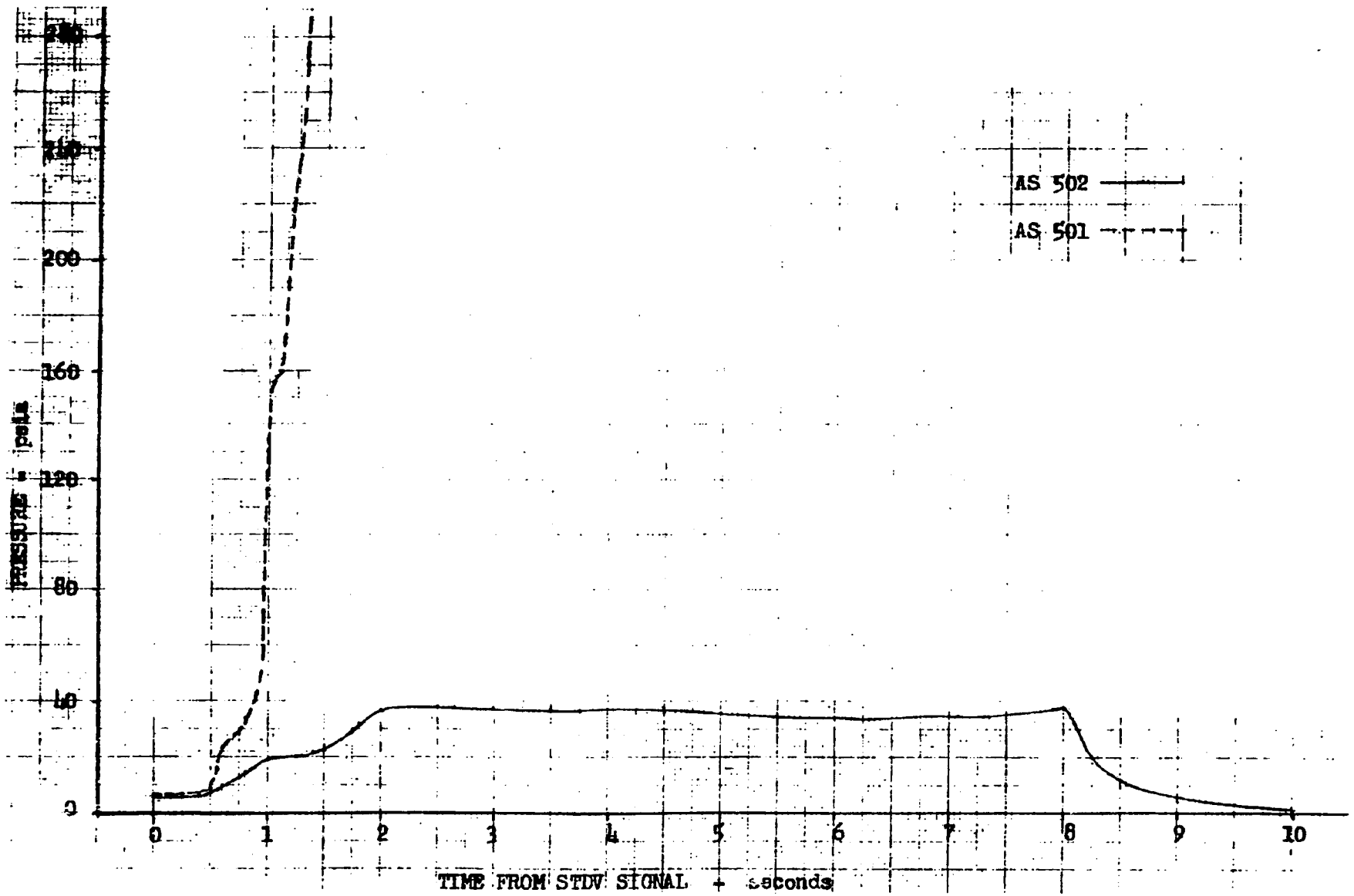

Figure 58. Comparison of AS-501 and AS-502 S-IVB Second Burn, Thrust Chamber Pressure vs Time

[redacted]

From 2 to 5 seconds after STDV, all engine pressures gradually decreased to the point where main chamber pressure was 35 psia, oxidizer pump discharge pressure was 122 psia, and fuel pump discharge pressure was 110 psia. During this period, oxidizer flow was 250 lb/sec and fuel flow was 60 lb/sec.

At 5 seconds after STDV, the PU valve was signalled closed and oxidizer flow began to increase. Engine pressures increased until chamber pressure was 38 psia, oxidizer pump discharge pressure was 150 psia, and fuel pump discharge pressure was 120 psia at 7.6 seconds after STDV, at which time the engine received a cutoff signal.

When a timer in the instrumentation unit expired (set for engine start plus approximately 15 seconds), the instrumentation unit checked on the status of the engine "mainstage OK" pressure switches and the vehicle acceleration, found that neither indicated positive thrust, and signalled the engine to shut down.

POSSIBLE FAILURE MODES

The following is a list of the most suspect failure modes that could have caused a failure to restart:

1. Fuel pump stall
2. Fuel pump cavitation
3. Oxidizer pump cavitation
4. Failure to bootstrap
    a. Gas generator ignition failure
    b. Insufficient power from start tank blowdown
5. Non-ignition of thrust chamber
    a. ASI ignited
    b. ASI not ignited

ANALYSIS

Fuel Pump Stall

Fuel pump discharge pressure (head) and flow indicated normal fuel pump operation; therefore, the possibility of fuel pump stall was eliminated as a suspect.

Fuel Pump Cavitation

Fuel pump inlet pressure and temperature were within the allowable limits, indicating propellant quality was satisfactory. Fuel pump discharge pressure did not indicate cavitation was occurring; therefore, the possibility of fuel pump cavitation was eliminated.

Oxidizer Pump Cavitation

Oxidizer pump inlet pressure and temperature were within the allowable limits, indicating propellant quality was satisfactory. Oxidizer pump discharge pressure indicated cavitation was not occurring, thereby eliminating oxidizer pump cavitation as a possibility.

Failure to Bootstrap

Gas Generator Ignition Failure. Gas generator chamber pressure and fuel turbine inlet temperature both indicated normal gas generator ignition (Fig. 57). Consequently, gas generator ignition failure was eliminated as a suspect.

Insufficient Spin Power. Prior to restart, start tank pressure was 1325 psia and start tank temperature indicated -207 F. It is believed that the actual start tank temperature was considerably colder, but self heating of the resistance bulb raised the indicated temperature to -207 F. These measurements show that start tank energy was adequate. Oxidizer and fuel pump speeds reached values of 3650 and 14,400 rpm, respectively, from the start tank energy, which is more than adequate for a satisfactory

start. Pump speeds are shown in Fig. 59. Insufficient power from the start tank was ruled out as a possible failure mode.

Non-Ignition of Thrust Chamber

ASI Ignited. The possibility of the ASI being properly ignited but failing to ignite the main chamber was eliminated for two reasons. First, this failure has never occurred during J-2 engine tests. Second, a failure of this type does not explain the first-burn abnormalities discussed in earlier sections.

ASI Did Not Ignite. The possibility of the thrust chamber failure to ignite because the ASI failed to ignite remains the prime suspect. It has been shown earlier that an ASI fuel line failure best explains the external temperature phenomena and the performance shifts.

A failed ASI fuel line would prevent fuel from entering the ASI injector, thereby preventing ASI ignition. This failure mode would explain the chilling of the MOV control line, beginning after engine start and prior to STDV on the restart, because the ASI fuel supply (main fuel valve) opens at engine start.

Several other failures that could have resulted in failure of the ASI to ignite are: failure of the spark exciters, failure of the spark plugs because of icing, failure of the ASI oxidizer line, blockage of either ASI propellant line, and the ASI oxidizer valve failing to open. All five of these were eliminated as possible single-point failure modes because they could not explain the external chilling or the performance shift.

The ASI oxidizer valve open switch picked up properly, indicating satisfactory valve operation. Although spark exciter performance could not be definitely verified, it is presumed to have been satisfactory by the following reasoning. The No. 1 ASI spark current driver and spark exciter are supplied from the same power source as the No. 1 gas generator spark current driver and spark exciter. Similarly, the No. 2 systems are supplied

[redacted]

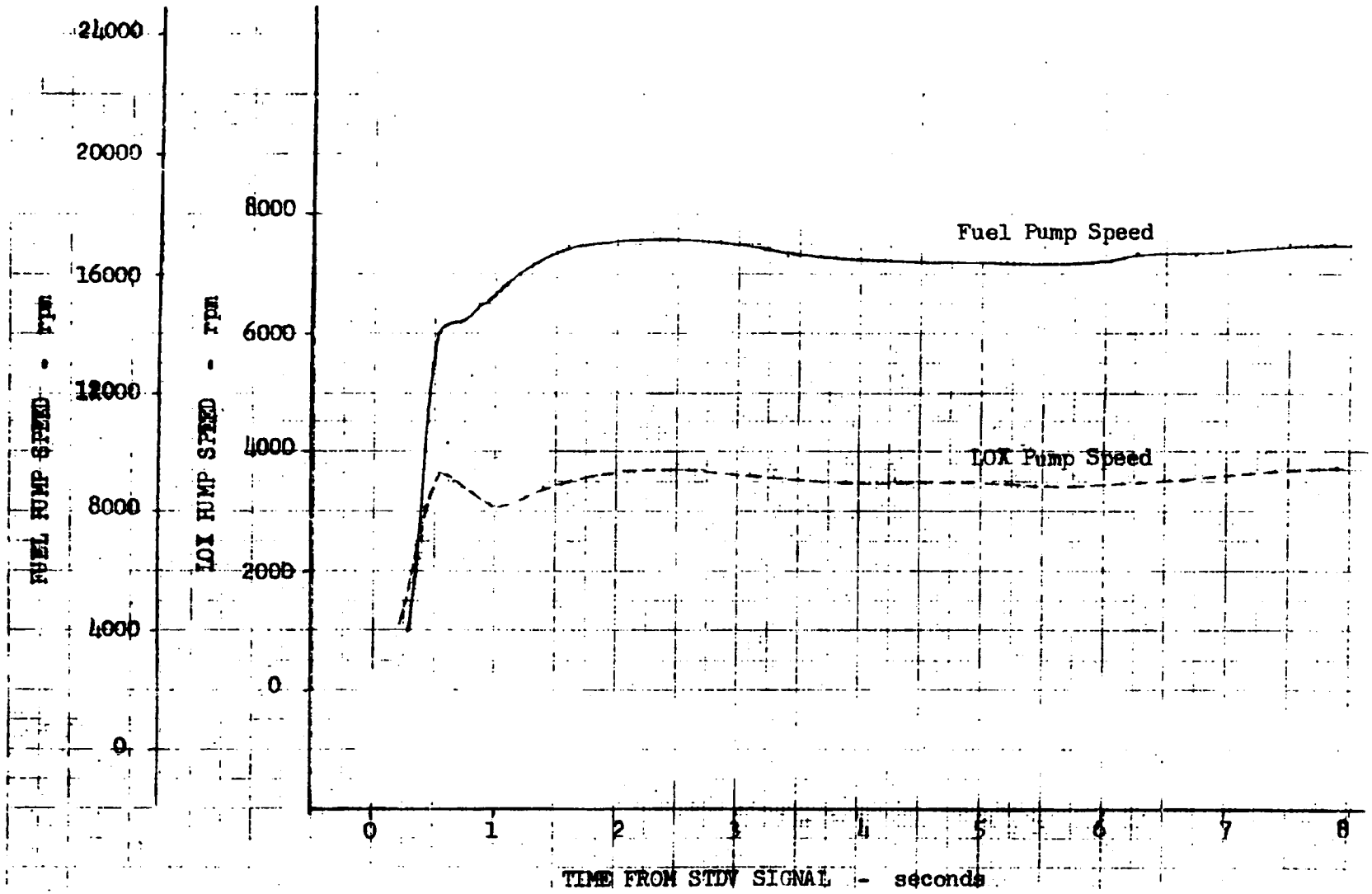

Figure 59. AS-502 S-IVB Second Burn, Pump Speeds vs Time

[redacted]

from the same source. Because the gas generator ignited properly, it is evident that at least one of the ASI spark current drivers had a power input. In any event, it would take a complex multiple failure to obtain gas generator sparks without obtaining power to the ASI spark exciters.

Results of the S-IVB failure simulation test (Verification Testing section) indicated the spark plug electrodes can be severly damaged as a result of ASI erosion occurring during and after an ASI fuel line failure. It is conceivable that ASI oxidizer and main injector fuel could mix in the ASI, but not ignite because of spark plug electrode damage preventing adequate spark.

Shutdown

Even though the ASI and main chamber did not ignite, a safe engine shutdown occurred without the main propellants igniting from the hot turbine exhaust gas.

CONCLUSION

Engine restart was not achieved because of non-ignition of the ASI, which is necessary to ignite the main chamber. The ASI failed to ignite because the ASI fuel line had failed during the first burn.

OVERALL FAILURE ANALYSIS

To ensure that all possible failure modes were investigated, each of the major components in each engine subsystem was evaluated with respect to the flight data and the possible failure modes. Table 12 lists the engine systems and components, the potential failure modes associated with each component, and the five major abnormalities of the flight: first-burn external chilling, external heating, restart external chilling, performanceance shifts, and the failure to restart. In these columns, an X is placed if the flight data and analysis indicate the failure mode in column 2, on the component in column 1, does <u>not</u> explain the column heading in columns 3 through 7. The last column contains an X if the data verified normal operation. This column is used only for components that can be related to a specific performance parameter, i.e., valve operations, turbine efficiencies, pump efficiencies, and injector efficiencies. From this table, it is possible to locate the prime suspect by finding the component and failure mode for which no X could be supplied. The ASI fuel line external leak is the only one in this category.

Table 13 lists the instrumentation parameters that failed during the flight.

TABLE 12

AS-502 S-IVB FAILURE ANALYSIS

AREA OR COMPONENT	PROJECTED FAILURE MODE	DOES NOT EXPLAIN OBSERVED EXTERNAL TEMP. TRANSIENTS			DOES NOT EXPLAIN PERFORMANCE SHIFTS	DOES NOT EXPLAIN RESTART FAILURE	NORMAL OPERATION VERIFIED FROM DATA
		DURING FIRST CHILL	DURING HEATING	DURING RESTART			
I. Fuel Feed System							
A. Stage Ducting and Prevalves	1. External Leak		X	X	X	X	
	2. Restriction	X	X	X	X	X	
B. Engine Inlet Duct	1. External Leak		X	X	X	X	
	2. Restriction	X	X	X	X	X	
C. Fuel Pump	1. External Leak		X	X	X	X	
	2. Cavitation; Stall	X	X	X	X	X	X
	3. Mechanical Failure	X	X	X	X	X	X
D. High Pressure Duct	1. External Leak		X	X		X	
	2. Restriction	X	X	X	X	X	
E. Main Fuel Valve	1. External Leak		X			X	
	2. Restriction	X	X	X	X	X	
	3. Mechanical Failure	X	X	X	X	X	X
F. Main Thrust Chamber	1. External Leak		X			X	
	2. Restriction	X	X	X	X	X	
G. Injector	1. Seal Leak		X			X	
	2. Mechanical Failure	X	X	X		X	X
	3. Instability	X	X	X		X	
II. Oxidizer Feed System							
A. Stage Ducting Prevalves	1. External Leak		X	X	X	X	
	2. Restriction	X	X	X	X	X	
B. Engine Inlet Duct	1. External Leak		X	X	X	X	
	2. Restriction	X	X	X	X	X	
C. Oxdizer Pump	1. External Leak		X	X	X	X	
	2. Cavitation	X	X	X	X	X	X
	3. Mechanical Failure	X	X	X	X	X	X

[redacted]

TABLE 12

(Continued)

AREA OR COMPONENT	PROJECTED FAILURE MODE	DOES NOT EXPLAIN OBSERVED EXTERNAL TEMP. TRANSIENTS			DOES NOT EXPLAIN PERFORMANCE SHIFTS	DOES NOT EXPLAIN RESTART FAILURE	NORMAL OPERATION VERIFIED FROM DATA
		DURING FIRST CHILL	DURING HEATING	DURING RESTART			
D. P.U. Valve & Duct	1. External Leak		X	X		X	
	2. Mechanical Failure	X	X	X	X	X	X
	3. Restriction	X	X	X	X	X	
E. High Pressure Duct	1. External Leak		X	X		X	
	2. Restriction	X	X	X	X	X	
F. Main Oxidizer Valve	1. External Leak		X	X			
	2. Restriction	X	X	X	X	X	
	3. Mechanical Failure	X	X	X	X	X	X
G. Oxidizer Dome & Injector	1. External Leak		X	X		X	
	2. Restriction	X	X	X	X	X	
	3. Mechanical Failure	X	X	X		X	X
III. GG & Exhaust System							
A. Oxid. Bleed Valve	1. External Leak		X	X		X	
	2. Mechanical Failure	X	X	X		X	X
B. Fuel Bleed Valve	1. External Leak		X	X	X	X	
	2. Mechanical Failure	X	X	X	X	X	X
C. Oxid. Bootstrap Line	1. External Leak		X	X		X	
	2. Restriction	X	X	X	X	X	
D. Fuel Bootstrap Line	1. External Leak		X	X	X	X	
	2. Restriction	X	X	X	X	X	
E. GG Control Valve	1. External Leak		X	X		X	
	2. Restriction	X	X	X	X	X	
	3. Mechanical Failure	X	X	X	X	X	X
F. GG Injector	1. Restriction	X	X	X		X	
	2. Mechanical Failure	X	X	X		X	
G. GG Combustor	1. External Leak	X		X		X	

TABLE 12

(Continued)

AREA OR COMPONENT	PROJECTED FAILURE MODE	DOES NOT EXPLAIN OBSERVED EXTERNAL TEMP. TRANSIENTS			DOES NOT EXPLAIN PERFORMANCE SHIFTS	DOES NOT EXPLAIN RESTART FAILURE	NORMAL OPERATION VERIFIED FROM DATE
		DURING FIRST CHILL	DURING FIRING	DURING RESTART			
H. Fuel Turbine	1. External Leak	X		X		X	
	2. Restriction	X	X	X		X	
	3. Mechanical Failure	X	X	X		X	X
I. Crossover Duct	1. External Leak	X		X		X	
J. Oxid. Turb. By-pass Duct	1. External Leak	X		X		X	
K. Oxid. Turb. By-pass Valve	1. External Leak	X		X		X	
	2. Restriction	X	X	X		X	
	3. Mechanical Failure	X	X	X		X	X
L. Oxidizer Tur-bine	1. External Leak	X		X		X	
	2. Restriction	X	X	X		X	
	3. Mechanical Failure	X	X	X		X	X
M. Heat Exchanger	1. External Leak	X		X		X	
IV. Start System							
A. Start Tank	1. External Leakage		X	X	X	X	X
B. Start Tank Disch. Valve	1. External Leakage		X	X	X	X	
	2. Internal Leakage	X	X	X	X	X	
	3. Mechanical Failure	X	X	X	X	X	X
C. Spin Line	1. External Leak		X	X	X	X	
	2. Restriction	X	X	X	X	X	
D. Start Tank Liquid Refill Line (Upstream of Check Valve)	1. External Leak		X			X	
	2. Restriction	X	X	X	X	X	
E. Start Tank Liquid Refill Line (Down-stream of check valve)	1. External Leak		X	X		X	X
	2. Restriction	X	X	X	X	X	

TABLE 12

(Continued)

AREA OR COMPONENT	PROJECTED FAILURE MODE	DOES NOT EXPLAIN OBSERVED EXTERNAL TEMP. TRANSIENTS			DOES NOT EXPLAIN PERFORMANCE SHIFTS	DOES NOT EXPLAIN RESTART FAILURE	NORMAL OPERATION VERIFIED FROM DATA
		DURING FIRST CHILL	DURING HEATING	DURING RESTART			
F. Start Tank Gas Refill Line	1. External Leak		X			X	
	2. Restriction	X	X	X		X	
G. St. Tk. Fill & Refill Pkg.	1. Leak		X		X	X	X
H. St. Tk. Vent & Relief Valve	1. Leak		X		X	X	
V. Ignition System							
A. ASI Oxidizer Valve	1. External Leakage		X				
	2. Restriction	X	X	X	X		
	3. Mechanical Failure	X	X	X	X		X
B. ASI Fuel Line	1. Leakage						
	2. Restriction	X	X	X	X		
C. ASI Lox Line	1. Leakage	X			X		
	2. Restriction	X	X	X	X		
D. ASI Spark Plug	1. Leakage	X		X	X		
	2. Failure to Spark	X	X	X	X		
E. ASI Ign. Det. Probe	1. Leakage	X		X	X		
F. Spark Exciter	1. Mechanical Failure	X	X	X	X		X
G. Power Supply	1. Mechanical Failure	X	X	X	X		X
VI. Tank Pressurization System							
A. H_2 Repressurization Line	1. External Leak		X			X	X
B. Helium Inlet Line	1. External Leak		X		X	X	X

[redacted]

TABLE 12

(Concluded)

AREA OR COMPONENT	PROJECTED FAILURE MODE	DOES NOT EXPLAIN OBSERVED EXTERNAL TEMP. TRANSIENTS			DOES NOT EXPLAIN PERFORMANCE SHIFTS	DOES NOT EXPLAIN RESTART FAILURE	NORMAL OPERATION VERIFIED FROM DATA
		DURING FIRST CHILL	DURING HEATING	DURING RESTART			
C. Heat Exchanger	1. Internal Leak	X	X	X	X	X	X
D. Helium Return Line	1. External Leak	X		X	X	X	X
VII. Helium Control Sys.							
A. Helium Tank	1. External Leak	X	X	X	X	X	X
B. Pneumatic Regulator	1. External Leak		X		X	X	X
C. Pneumatic Lines	1. External Leak		X		X	X	X
D. Purge Control Valve	1. Internal Leak		X		X	X	
VIII. Instrumentation System							
A. All Cryogenic Instr. Ports Downstream of Main Propellant Valves	1. External Leakage		X			X	X
B. Pressure Switches	1. External Leakage		X	X		X	
IX. Misc. Systems							
A. Lox Purge Check Valves	1. Reverse Leakage	X	X	X		X	
B. Thrust Chamber Purge Check Valve	1. Reverse Leakage	X	X	X		X	

[redacted]

[redacted]

TABLE 13

S-IVB INSTRUMENTATION FAILURES

MEASUREMENT NUMBER	TITLE	COMMENTS
00008	Heat Exchanger Helium Inlet Temp.	Recorder Failed
00010	Engine Area Ambient Temp.	Pegged Throughout Coast, Burned Out at Tr = 700 Sec.
00012	GG Fuel Bleed Valve Temp.	Pegged Throughout Coast, Wrong Range for Coast Data
00123	Aft Interstage Temp.	Data Not Valid During Coast
00050	Fuel Pump Wall Temp.	Data Not Valid During Coast
00151	Oxid. Pump Wall Temp.	Data Not Valid During Coast
00202	Lox Pump Bearing Colant Temp.	Pegged During Coast, Wrong Range for Coast Data
00231	Fuel Tank Pressurization Module Inlet Tamp.	Pegged During Coast
02036	GG Bootstrap Line Temp.	Signal Invalid During Coast and Second Burn
00003	Lox Pump In Pr	Pegged From 6380 Seconds on
00013	H_2 Tapoff Orifice Outlet Pr	Recording Lost Throughout Flight
00058	PU Valve Inlet Pr	Pegged Throughout First Burn
00224	Fuel Pump Interstage Pr	Recording Lost at Restart
E0209	Lox Dome Accelerometer	Signal Lost at 686 Seconds from Liftoff
E0210	Fuel Pump Lateral Accelerometer	Signal Lost at Engine Restart

PRESSURIZATION SYSTEMS

OXIDIZER PRESSURIZATION SYSTEM

Description

A study was made of the S-IVB oxidizer tank pressurization system operation to determine if the system performed satisfactorily and to determine if the system may have contributed to the engine failure. A leak in the stage cold helium system resulted in a loss of between 130 and 200 pounds of helium during the 180-minute orbital coast period. Part of this study was to determine if that leak was associated with the engine failure.

System Operation

A schematic of the oxidizer tank pressurization system is shown in Fig. 60. For S-IVB use, the J-2 heat exchanger operates with two open coils. Cold helium is supplied from a stage regulator at 385 ±25 psia. Downstream of the heat exchanger, the vehicle pressurization module contains two parallel flow paths. One path contains a fixed orifice and is always open. The other contains an open-closed overpressurization valve controlled from a pressure switch sensing tank ullage pressure. The switch opens the valve at 38 psia and closes it at 40-psia tank pressure. Downstream of the pressurization module, the hot gas from the heat exchanger mixes with 0.5-lb/sec cold bypass helium prior to injection into the tank. The temperature of the pressurant varies between 300 and 500 R.

Plots of heat exchanger weight flow, outlet pressure, outlet temperature, and oxidizer tank pressure for first burn on AS-502 flight, AS-502 stage acceptance, AS-501 flight, and AS-501 stage acceptance are presented in Fig. 61 through 64, respectively. The step changes to helium flow and heat exchanger outlet pressure occur with opening and closing the overpressurization valve.

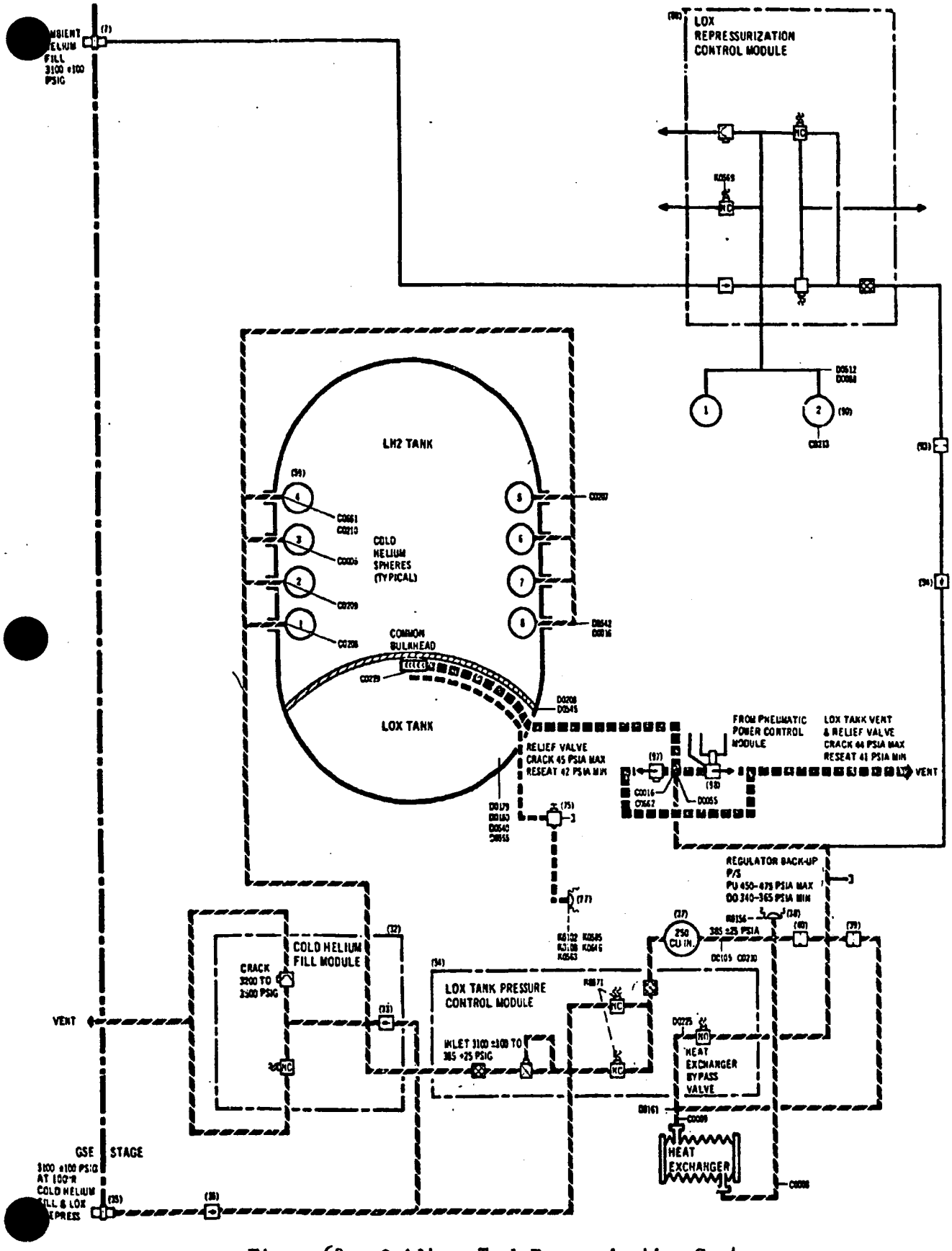

Figure 60. Oxidizer Tank Pressurization System

[redacted]

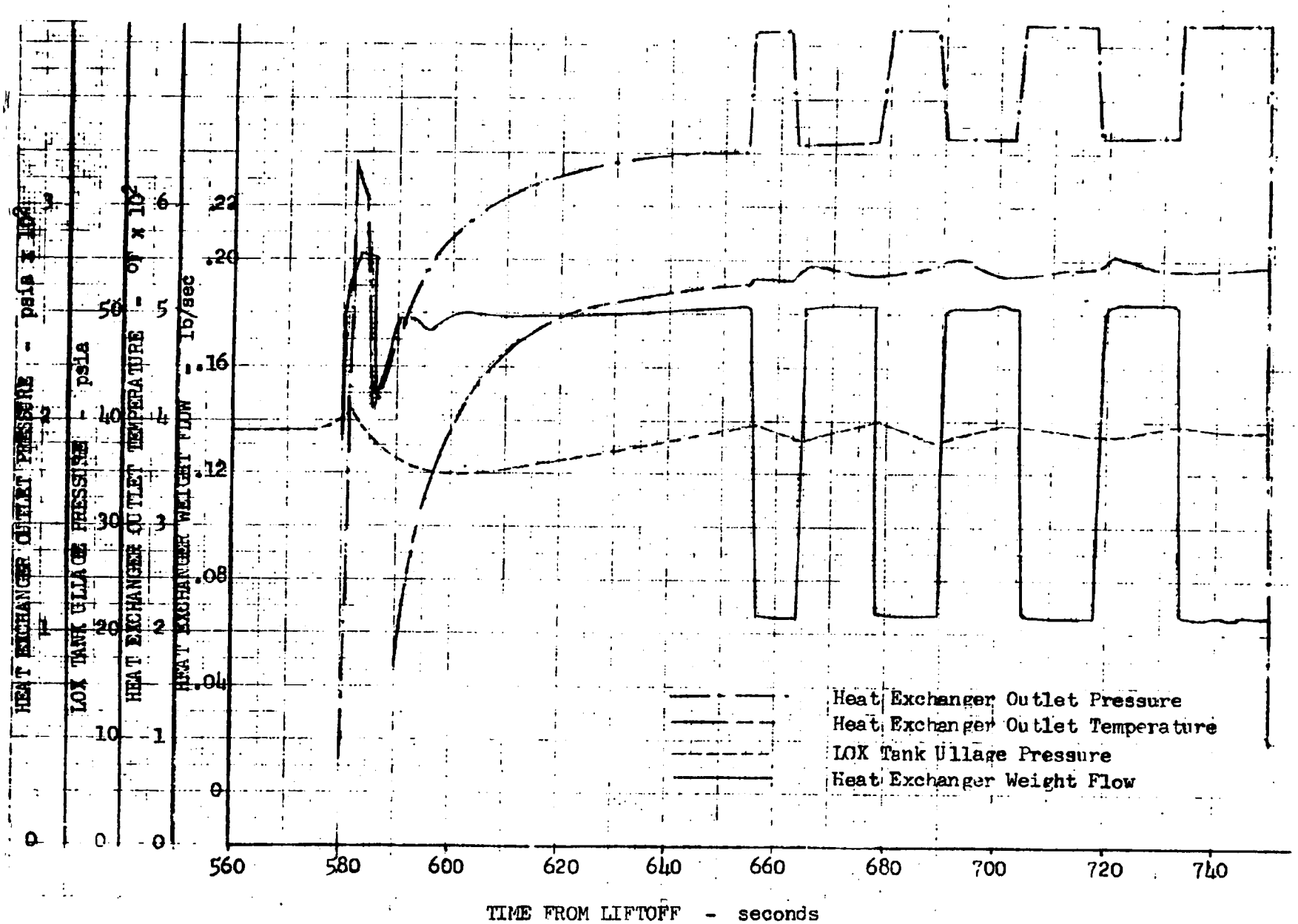

Figure 61. AS-502 S-IVB, First Burn

[redacted]

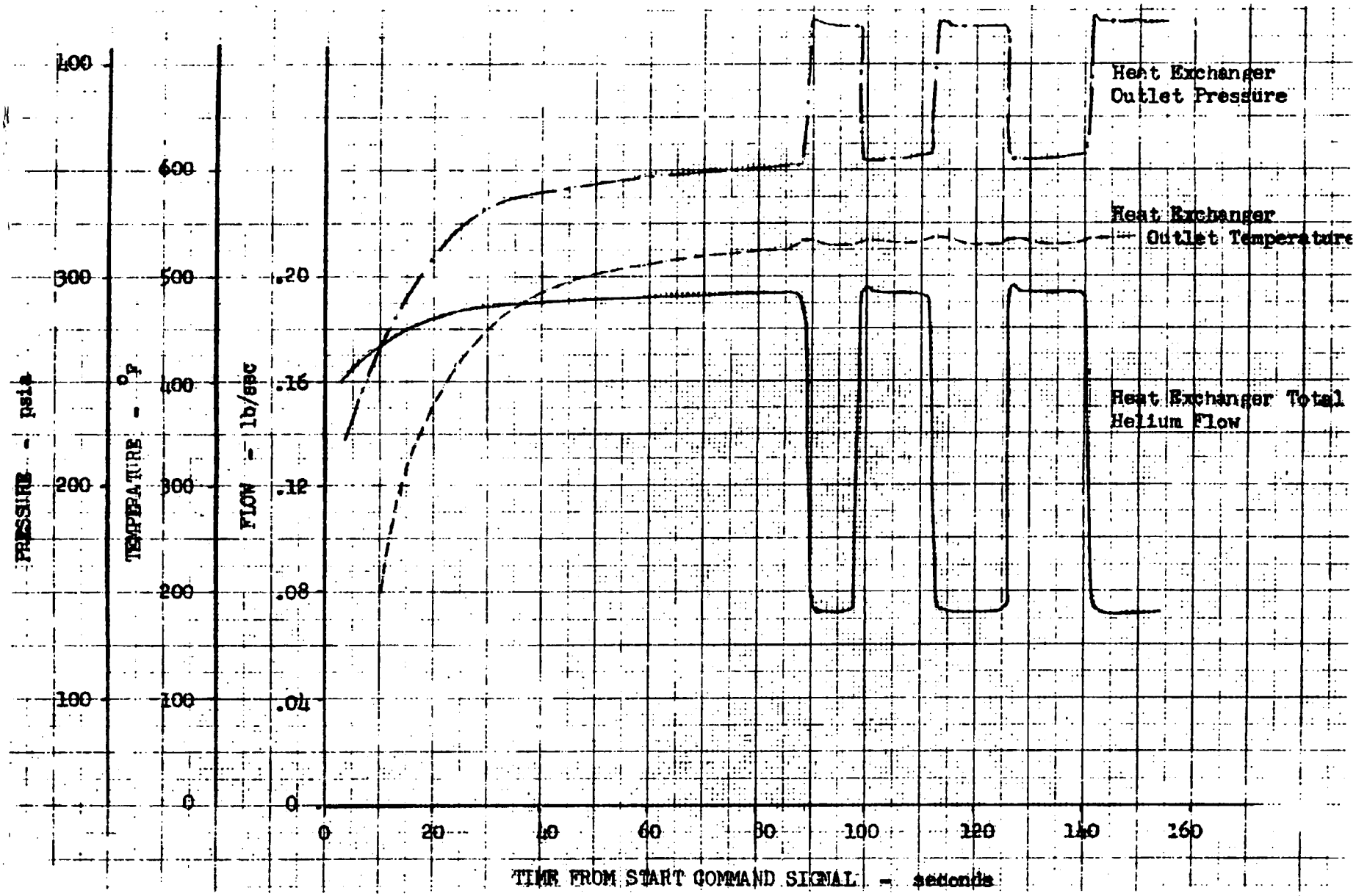

Figure 62. AS-502 S-IVB, Stage Acceptance First Burn

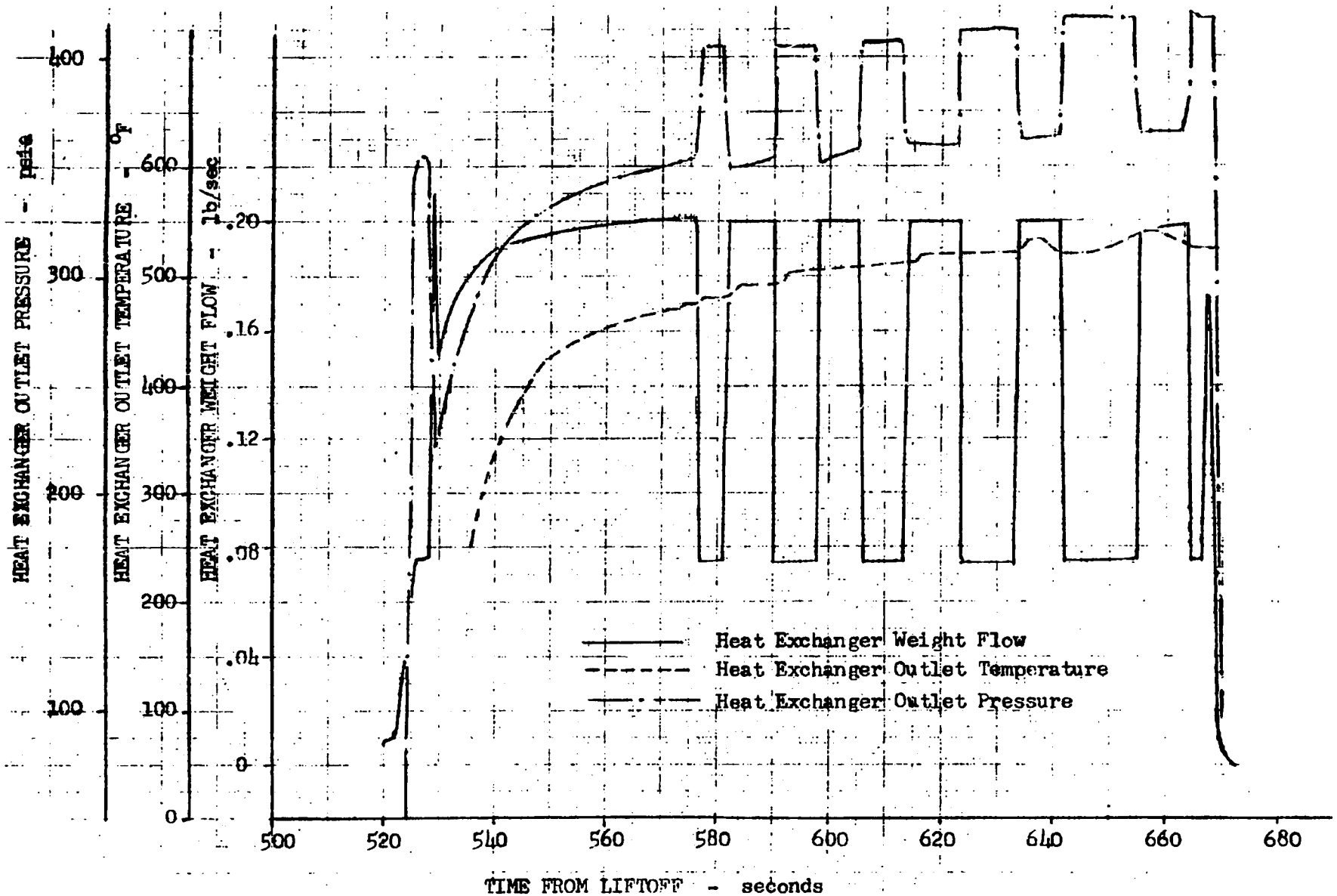

Figure 63. AS-501 S-IVB, First Burn

[redacted]

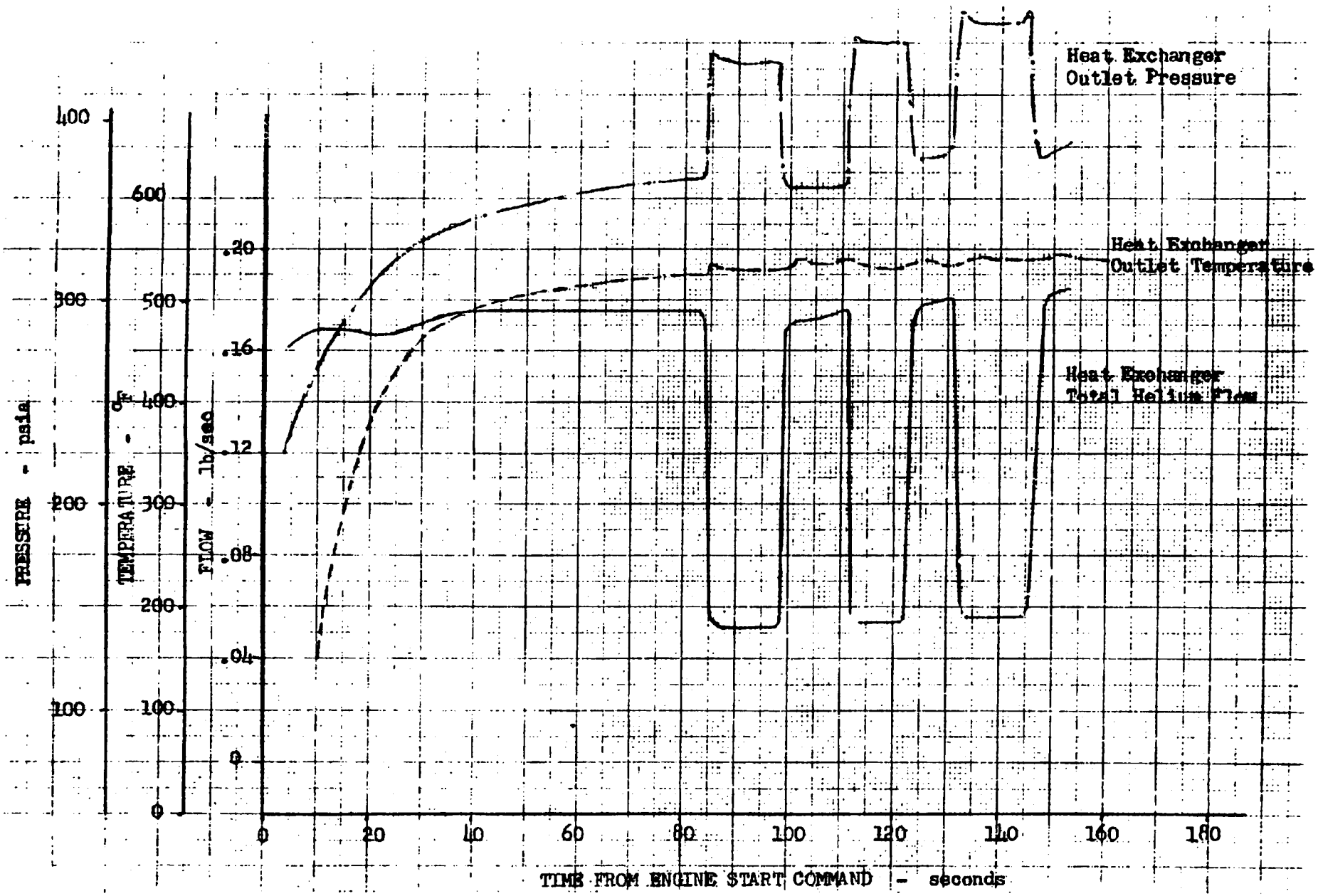

Figure 64. AS-501 S-IVB, Stage Acceptance, First Burn

Conclusions

It was concluded that:

1. The heat exchanger and oxidizer tank pressurization system operated within model specification limits of flow, pressure, and temperature throughout the first burn.
2. Heat exchanger flow and discharge pressure were approximately 10 percent lower on AS-502 flight than on stage acceptance or on AS-501 flight.
3. Some of the flight data suggest a leak in the tank pressurization system throughout first burn, but this evidence is inconclusive. If a helium leak was present, the leak rate was between 0.02 and 0.06 lb/sec.
4. No connection has been established between the oxidizer tank pressurization system and the engine failure.
5. No direct connection has been established between the helium leak during orbital coast and the engine failure.

Analysis

Operation of the tank pressurization system for AS-501 and AS-502 first-burn stage acceptance and flight are presented in Fig. 61 through 64. Included in the figures are plots versus time of heat exchanger outlet pressure, outlet temperature, weight flowrate, and oxidizer tank ullage pressure.

On AS-502 flight, the heat exchanger operated within model specification limits of flow, discharge pressure, and discharge temperature throughout first burn. The heat exchanger operating envelopes are shown in Fig. 65 and 66 with the flight operating points marked. As shown, the outlet pressure was on the low side of the envelope.

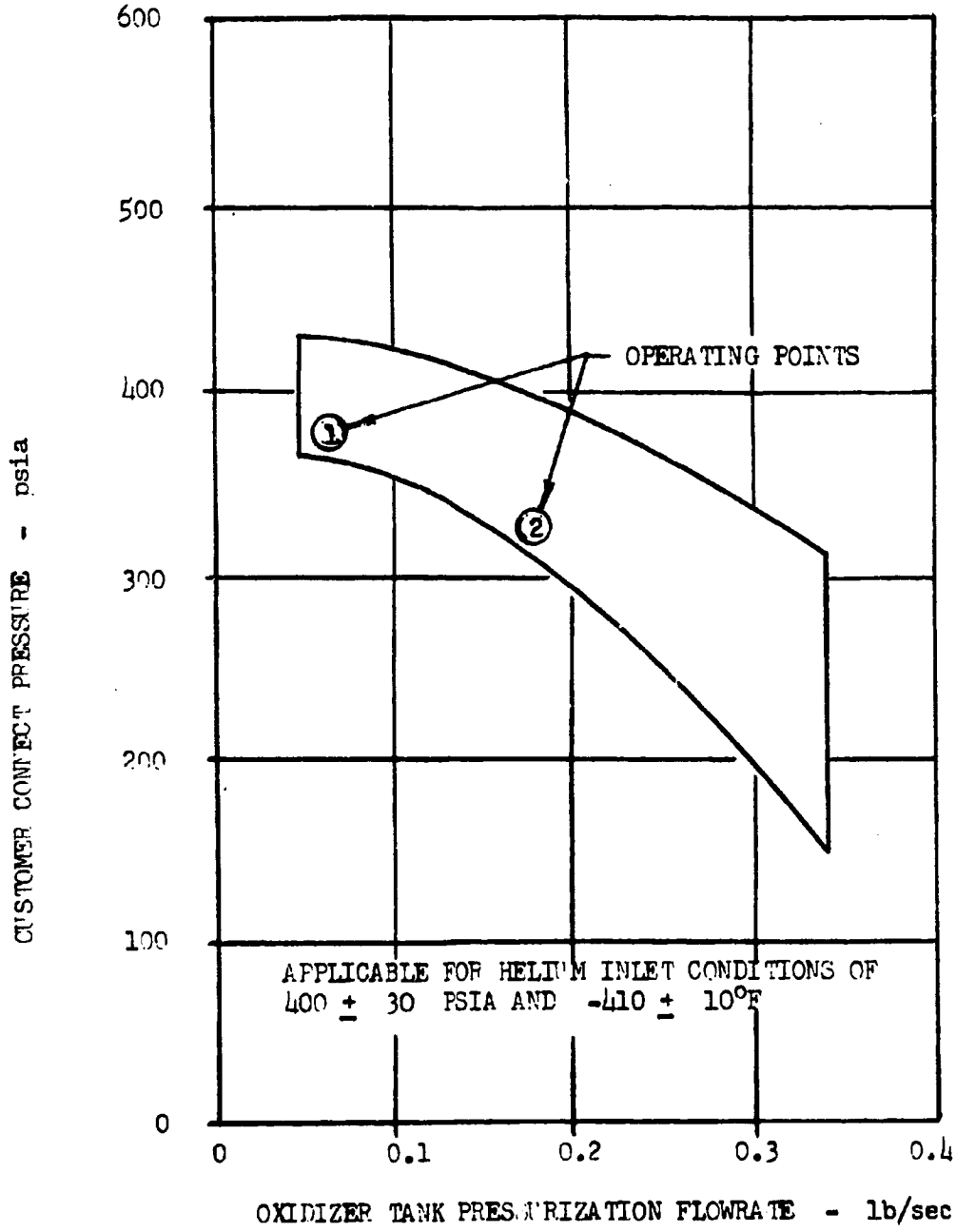

OVER-PRESSURIZATION VALVE: CLOSED (1)
OPEN (2)

Figure 65. Helium Heat Exchanger Operating Band

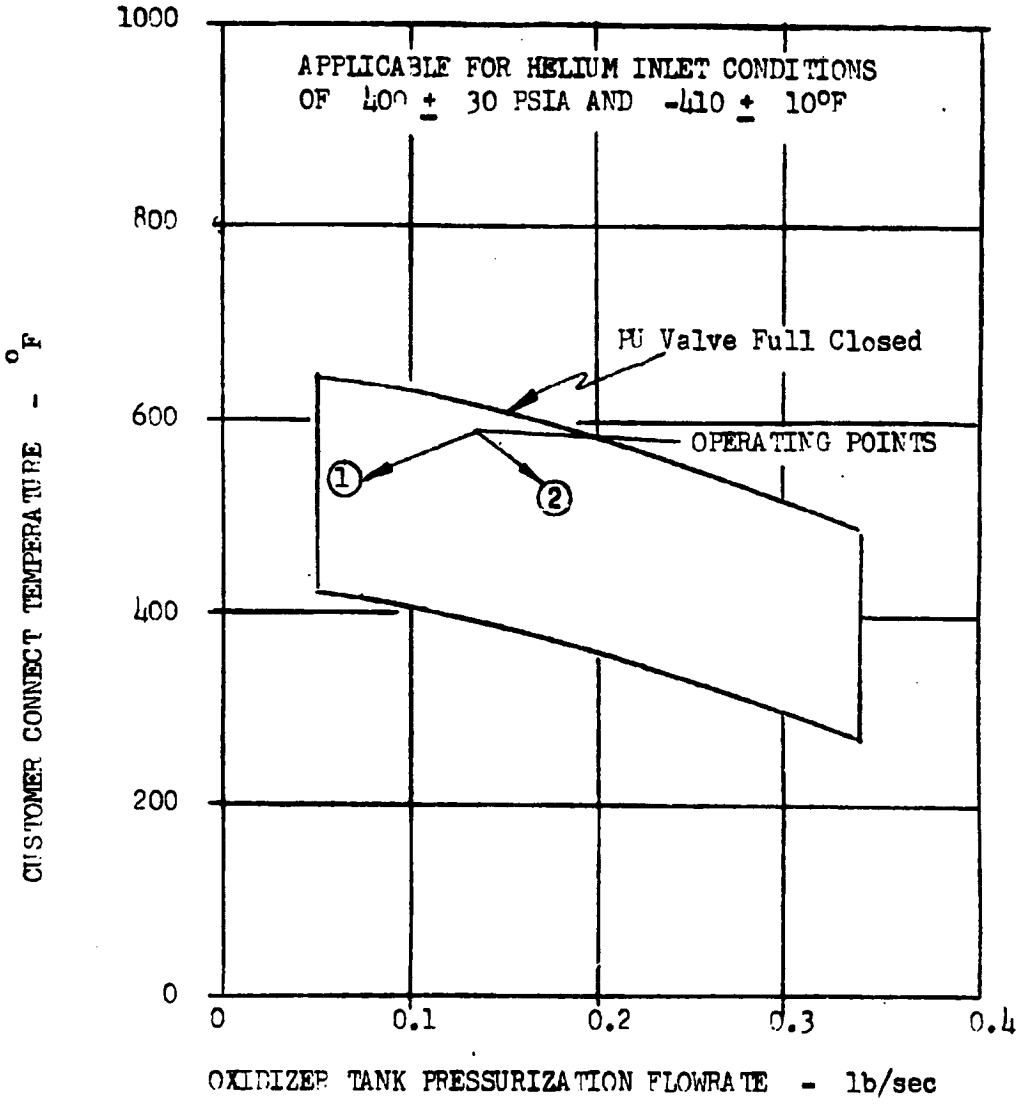

OVER-PRESSURIZATION VALVE: CLOSED (1)

OPEN (2)

Figure 66. Helium Heat Exchanger Operating Band

Flow and pressure were lower by approximately 10 percent than on stage acceptance or on AS-501 flight or stage acceptance. In the three latter cases, system operation was quite consistent. On flight AS-502, the two pressure measurements (DO 161 and DO 225) in the discharge line confirmed the lower level. Heat exchanger inlet pressure (DO 105) malfunctioned on the flight, so this pressure was unknown.

The lower pressure and flow could be explained by a lower regulator discharge pressure or by a leak in the engine or stage helium line downstream of the regulator. Following the stage acceptance firing, the regulator was replaced, so no data are available on operation of that specific regulator in the stage. The specification limits on regulator discharge pressure are 385 ±25 psia. If regulator pressure was lower on the flight, it still operated within specification limits. If no leak occurred on AS-502, the estimated regulator discharge pressure was 380 psia. On AS-501, the estimated regulator discharge pressure was 415 psia. If the lower pressure resulted from helium leakage, the leak occurred between the regulator and the pressurization module downstream of the heat exchanger. Assuming regulator discharge pressure was the same as on stage acceptance firing, the calculated leakage was between 0.02 and 0.06 lb/sec, depending on the leak location. The lower flow assumes a leak at the pressurization module downstream of the heat exchanger. The higher flow assumes a leak in the heat exchanger inlet line at the engine interface. The available leakage evidence is inconclusive and no positive statement can be made without regulator discharge pressure data.

Stage Helium Leak

There was a leak in the stage helium system during orbital coast. Between 130 and 200 pounds of helium were lost during the 180-minute coast, for an average leakage between 0.012 and 0.018 lb/sec. One of the objects of this study was to determine if the helium leak was associated with the engine problems or if it could have caused chilling of any engine components.

The stage helium system contains shutoff valves that close at engine cutoff. Because it occurred with those valves closed, the leak had to be in the stage system either through or upstream of the valves. The valves and other components of the pressurization system are mounted to the thrust cone several feet from the engine. The leakage rate was so low, 0.012 to 0.018 lb/sec, that it is doubtful if this could have caused significant chilling of any component away from the immediate vicinity of the leak. In venting to a vacuum, the gas diffuses so rapidly that a component several feet away would not see significant mass flux from a leak of this magnitude.

The fire or propellant leaks from the engine may have been the cause of the helium leak, but it is doubtful if the leak had any adverse effect upon the engine.

FUEL PRESSURIZATION SYSTEM

The S-IVB fuel mainstage pressurization system consists of the line from the thrust chamber fuel injection manifold to the engine interface, a stage line from the interface to the pressurization module, the module, and the ducting from the module to the tank. A study was made of the system to determine if its operation was satisfactory, if the system was associated with the engine failure, and if system leakage occurred.

System Operation

A schematic of the S-IVB fuel pressurization system is shown in Fig. 67. Gaseous fuel from the thrust chamber injection manifold is used for pressurization during engine firing. The flowrate is controlled by the stage pressurization module. The module contains three parallel flow paths. The primary flow path contains a fixed orifice and is always open. The two secondary paths contain fixed orifices and an on-off valve in each leg. No. 1 secondary is active during first burn. The valve is controlled

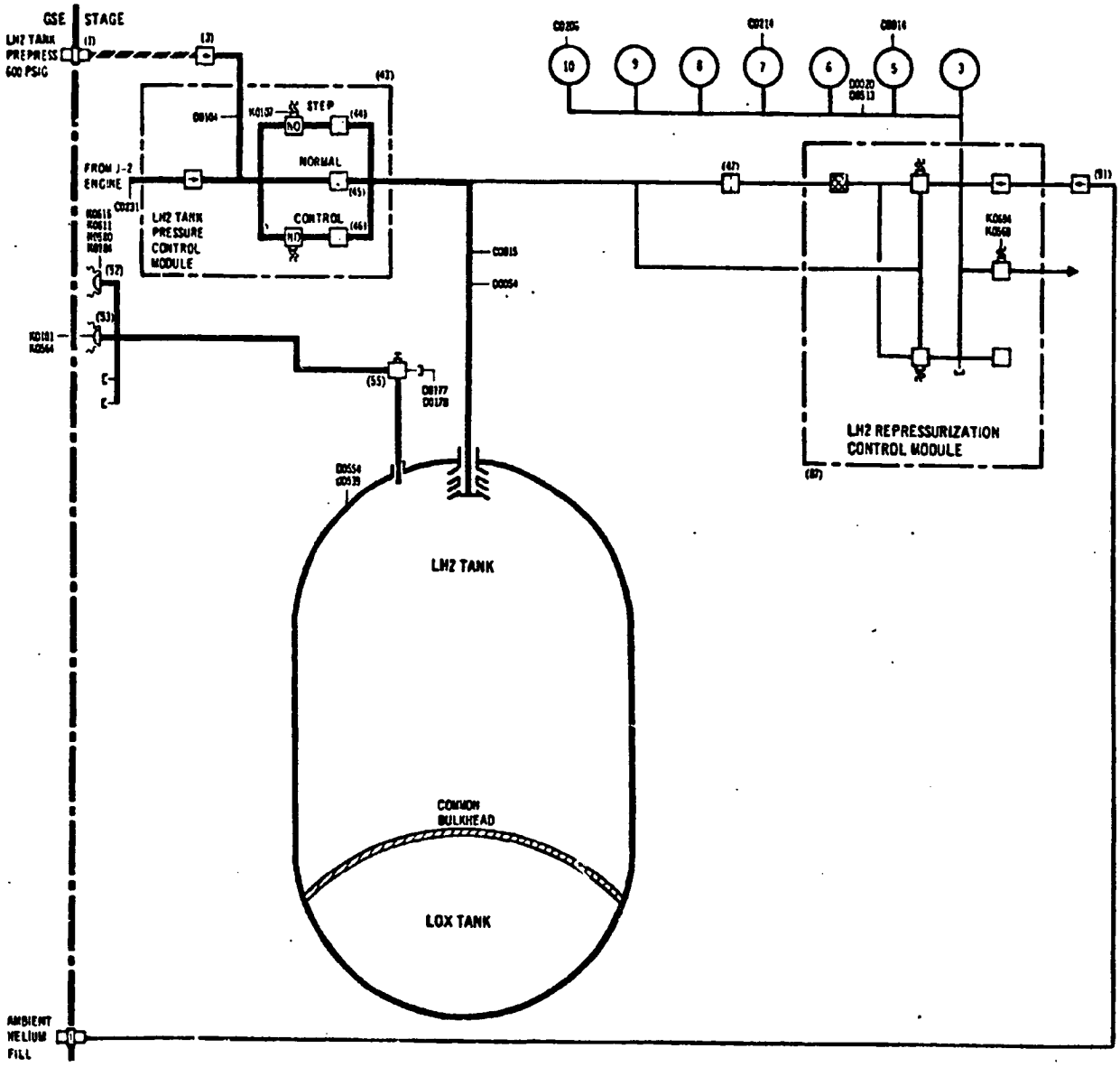

Figure 67. LH_2 Tank Pressurization System

[redacted]

by a pressure switch sensing tank ullage pressure, is opened when the pressure drops to 28 psia, and closed when the pressure increases to 31 psia. No. 2 secondary is active during second burn. Its actuation pressures are 31 psia pickup and 34 psia dropout. Both secondary flow paths are open at engine start and signalled closed at engine start command plus 5 seconds. The pressure switch then takes over operation of the secondary system.

Conclusions

It is concluded that:

1. Fuel pressurization system operation was satisfactory throughout the flight.
2. No leakage was found in the fuel pressurization system.

Analysis

On AS-502 flight, the fuel tank pressure was 36 psia at first-burn engine start and steadily decayed to 32.6 psia by engine cutoff. The secondary valves were closed at 5 seconds and tank pressure never dropped low enough to signal reopen. The same events occurred on AS-501 flight first burn, on AS-501 stage acceptance, and on AS-502 stage acceptance firing. Plots of fuel tank pressure for AS-501 and AS-502 flight first burn are given in Fig. 68 and 69.

Plots of pressurization system operation are presented in Fig. 68 through 71. If leakage occurred in the system down to the fuel pressurization module, this would appear as an increase in the pressure drop between engine fuel injection manifold (D0004) and pressurization module inlet pressure (D0104). No such pressure drop increase occurred. Comparing those pressure differences on AS-502 (Fig. 70) with AS-501 (Fig. 71), the pressure drops are essentially the same on both. On AS-502, the pressurization flowrate decreased beginning at 680 seconds (Fig. 69), coincident with the engine performance decay and the increased fuel injection temperature, but the line pressure drop remained essentially the same.

[redacted]

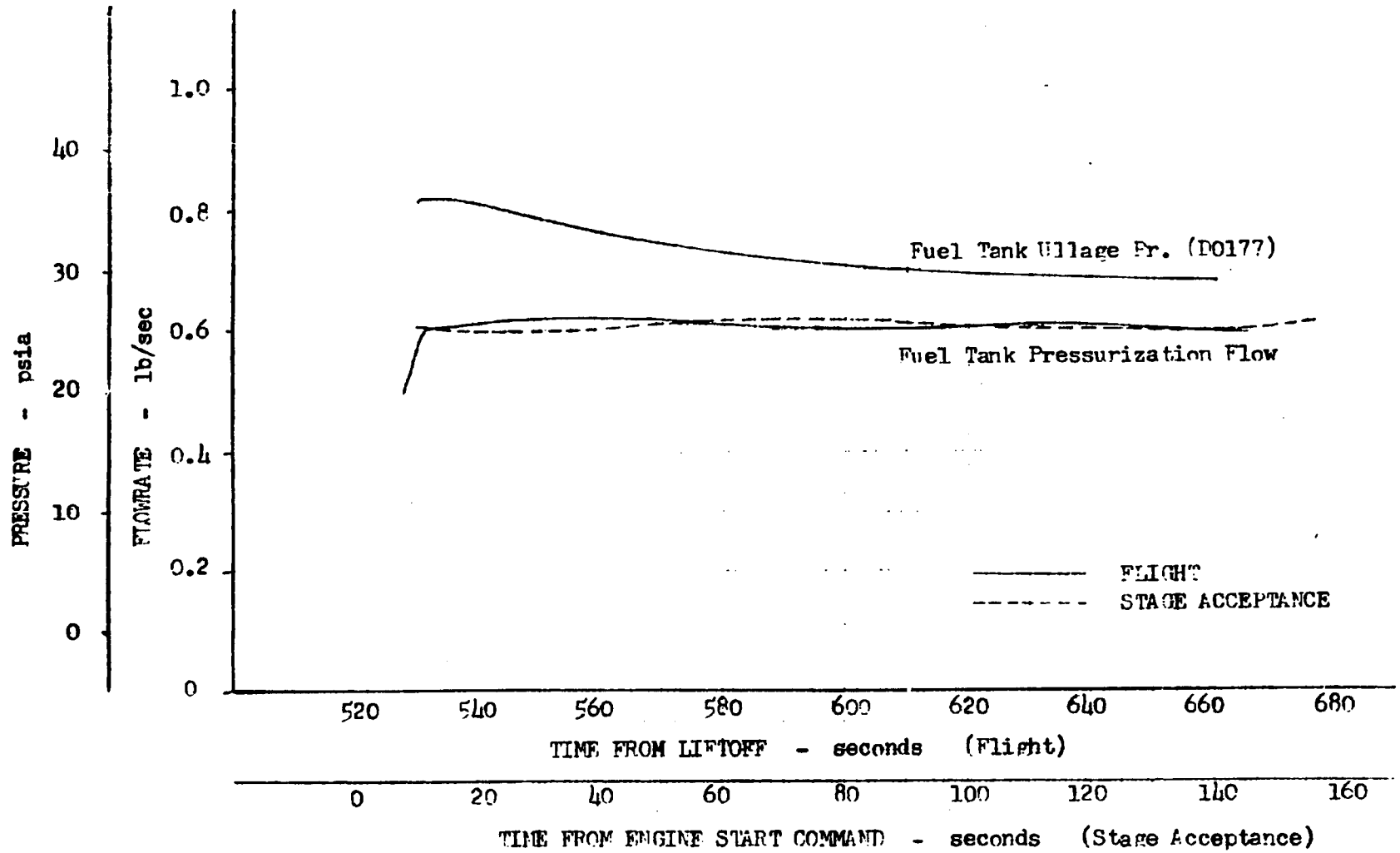

Figure 68. AS-501 S-IVB First Burn, Fuel Tank Ullage Pressure and Fuel Tank Pressurization Flowrate vs Time

[redacted]

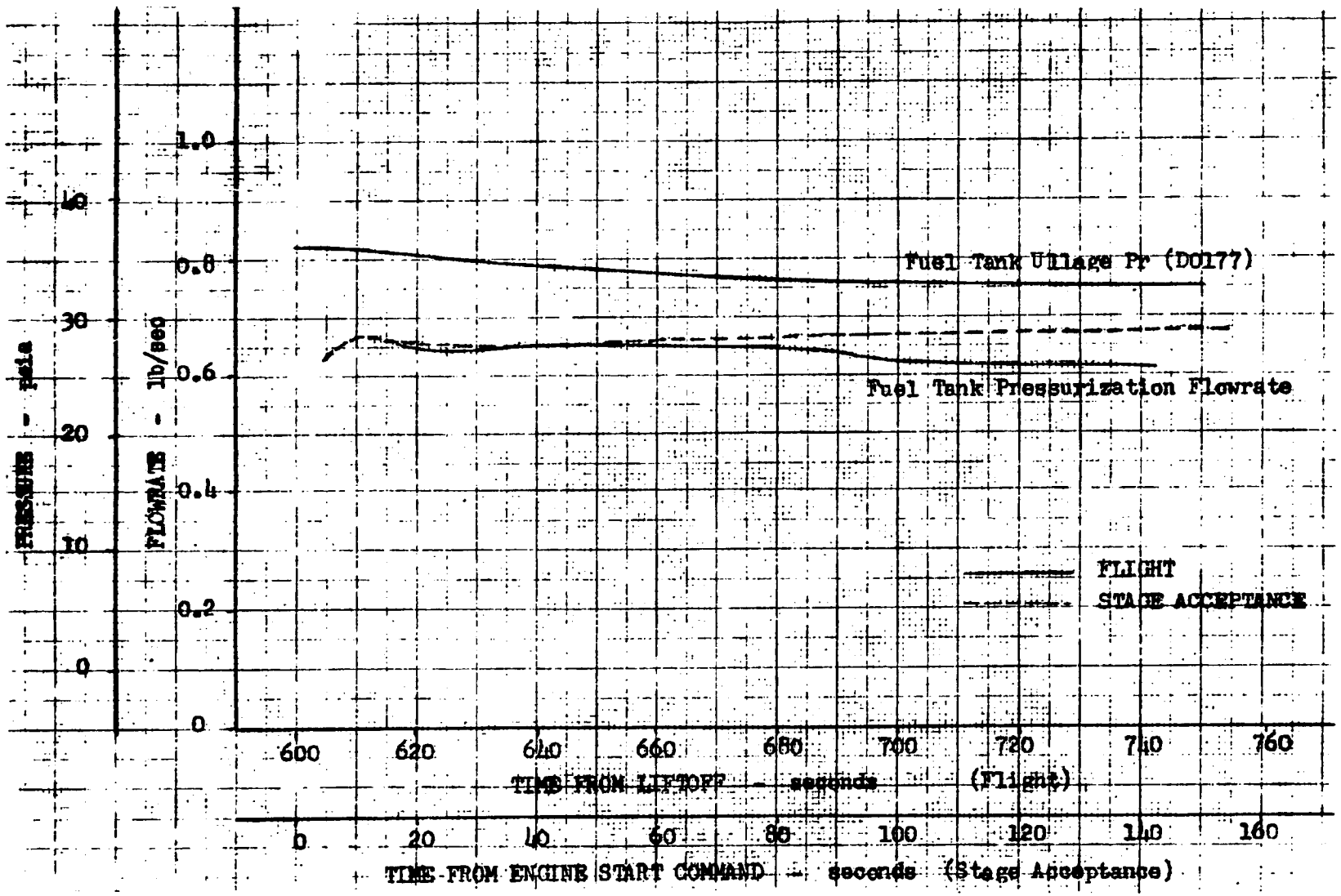

Figure 69. AS-502 S-IVB First Burn, Fuel Tank Ullage Pressure and Fuel Tank Pressurization Flowrate vs Time

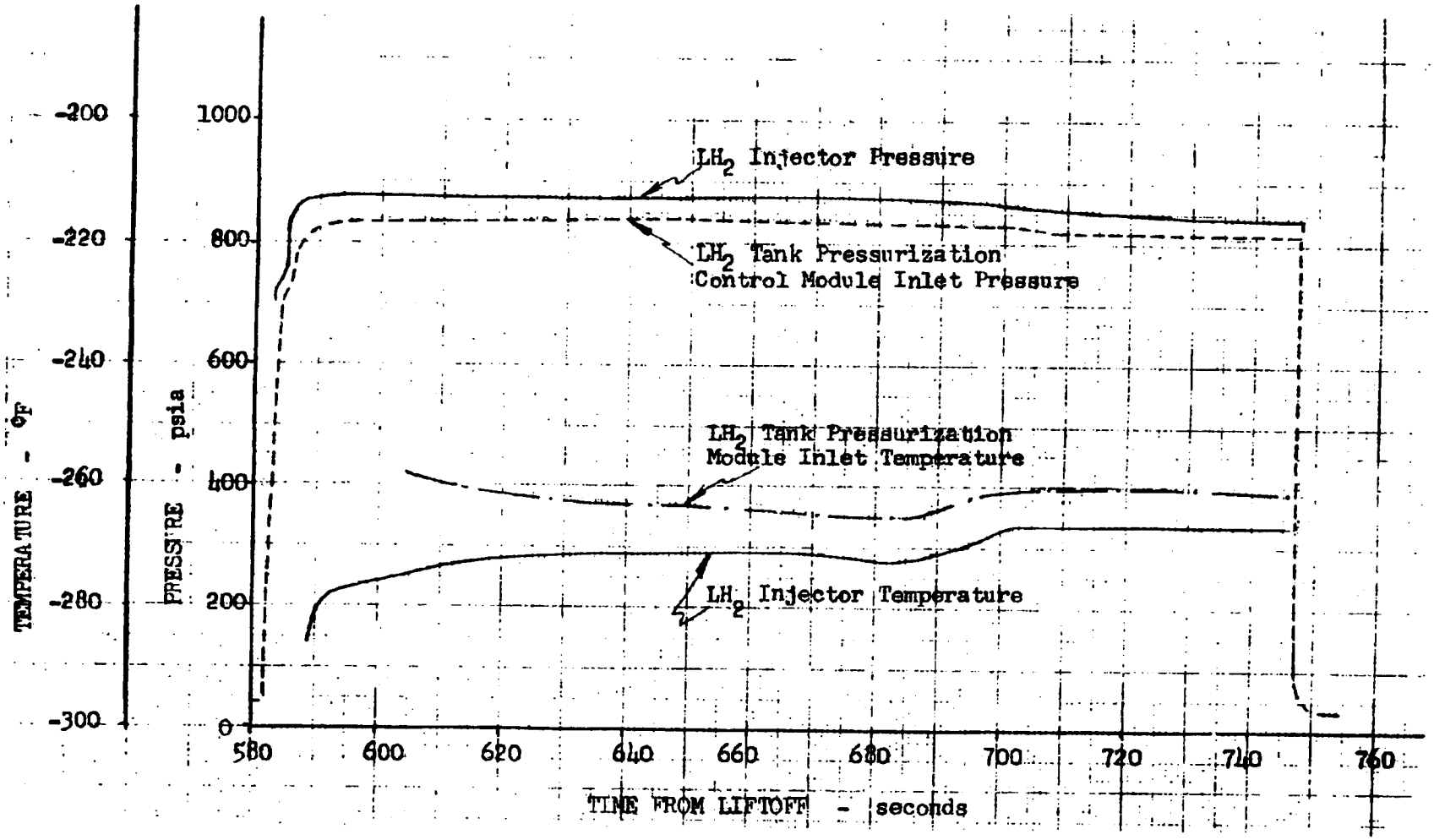

Figure 70. AS-502 S-IVB First Burn, Hydrogen Tank Pressurization System Performance

[redacted]

[redacted]

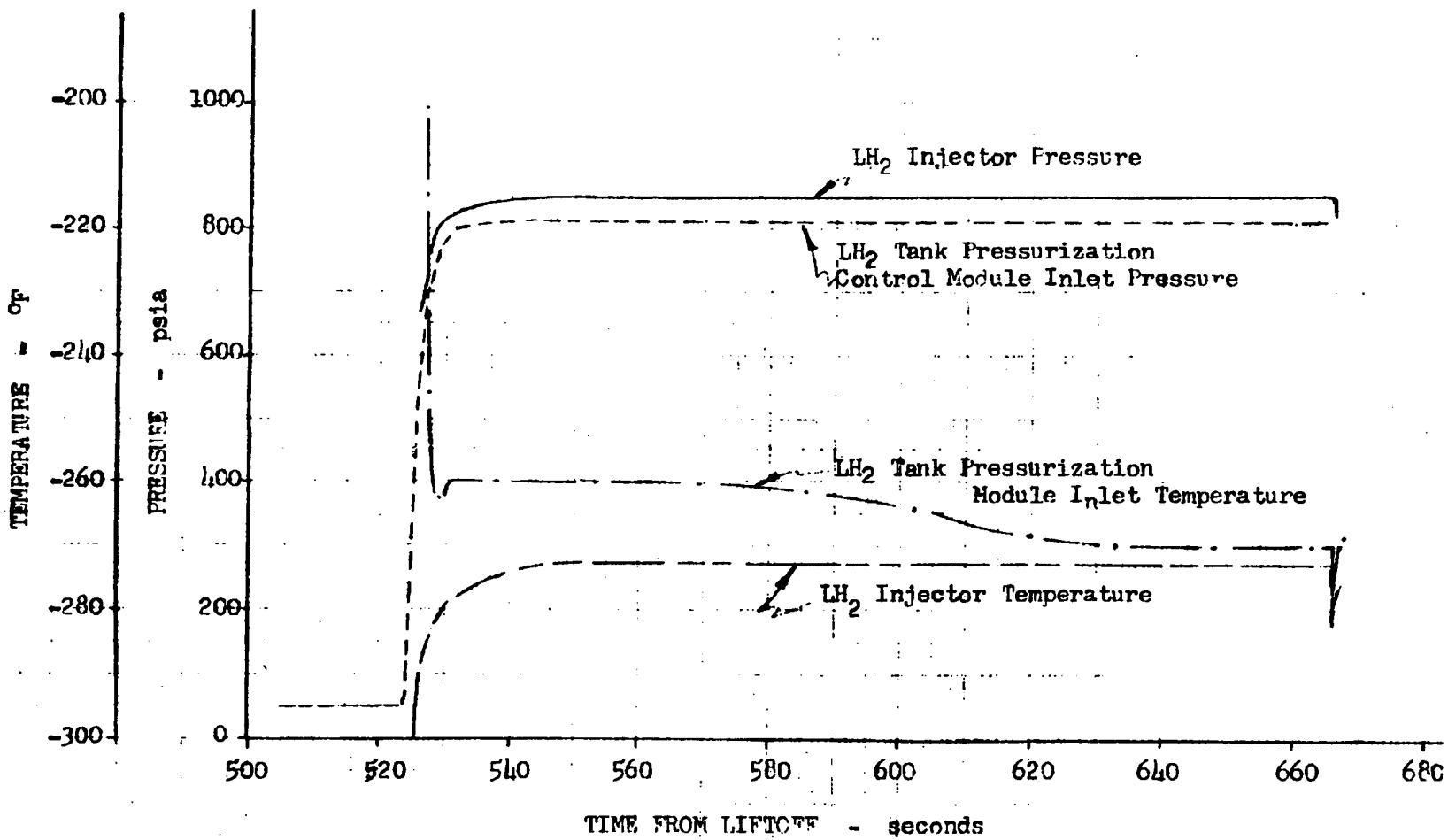

Figure 71. AS-501 S-IVB First Burn, Hydrogen Tank Pressurization System Performance

Pressurization flow on stage acceptance and flight for AS-502 and AS-501 are presented in Fig. 68 and 69. Prior to the engine performance decay at 685 seconds, the flow during flight was the same as during stage acceptance. The flow decrease correlated with the thrust decay and fuel injection temperature increase, and the shifts are explained by the engine performance changes.

On both vehicles, the pressure drop from fuel injection manifold to module inlet was steady at approximately 35 psi throughout first burn. Based on instrumentation accuracy, etc., it is believed that a detectable increase in that pressure drop would be 15 psi. If a leak occurred in the first flex hose in the line, the 15-psi additional pressure drop would occur with a leakage flowrate of approximately 0.2 lb/sec. Further downstream, the corresponding leak flow would be less. Because no increased pressure drop was detected, it is concluded that no leakage occurred in the fuel pressurization system.

As shown in Fig. 68 and 69, fuel pressurization module inlet temperature was higher than fuel injection temperature by about 10 degrees. The same phenomenon occurred on stage static firing. This indicates a temperature increase in the fuel pressurization line and, if true, comes as a result of a heat flux of 20 Btu/sec into the line. Analysis has proved that no such heat source is available, even with the fire in the engine area. Because this temperature increase occurred on AS-501 also, it is not believed associated with the failure.

Fuel injection temperature is not uniform around the periphery of the injection manifold. Temperature differences as great as 30 degrees have been measured on R&D thrust chambers. It is believed that these normal variations explain the differences between measurements on the flight.

Pressurization flow is calculated using compressible flow equations through the fixed orifices in the pressurization module. The module effective areas have been determined by McDonnell Douglas. The flow equation uses that effective area, the module inlet pressure, inlet temperature, and the gas properties of the fluid.

ENGINE START CONDITIONS

EVENT DESCRIPTION

The engine test conditions at liftoff, engine start command signal (ESC) for the first burn (T+577.2 seconds), and ESC for the restart (T+11,614 seconds) were within specified limits.

Table 14 summarizes the stage and engine propellant system parameters including helium tank conditions at liftoff, first burn, and restart. No anomalies were noted except for several minor discrepancies associated with instrumentation. Crossplots of oxidizer pump inlet pressure versus oxidizer pump inlet temperature, engine fuel inlet pressure versus engine fuel inlet temperature, and oxidizer pump discharge pressure versus discharge temperature are presented in Fig. 72 through 74. The data show that pump NPSH at start as well as the oxidizer propellant quality for both first burn and restart were adequate and well within the engine model specification limits.

Figure 74 presents the engine start bottle conditions at liftoff, first burn, and restart. All values were within the prescribed envelopes.

Table 15 presents the pertinent engine sequence data for both first burn and restart. All engine mechanical and electrical sequencing appeared normal.

Conclusions

It is concluded that:

1. All conditions at engine start signal (both first burn and restart) were proper.
2. All engine sequence functions were properly accomplished.

TABL[illegible]

STAGE AND ENGINE PROPELLANT SYSTEM PARAMETERS

Parameters	Liftoff		Engine Start		Engine Restart	
	Expected or Allowable	Actual	Expected or Allowable	Actual	Expected or Allowable	Actual
Fuel and Oxidizer Tank Conditions						
Fuel Pump Inlet Pressure (XD002), psia	DNA	44.4	28 to 46	44.5	28 to 46	37.0
Fuel Pump Inlet Temperature (XC0003), F	DNA	-420.5	Fig. 73	-421.4	Fig. 73	-420.2
Fuel Bleed Valve Temperature (C0012), F	--	-418	--	-421.0	--	-417.2
Fuel Pump Discharge Temperature (C0134), F	--	-415.6	--	-415.7	--	-417.7
Fuel Recirculation Return Pressure (D0062), psia	--	37.4	--	37.4	--	33.2
Fuel Recirculation Pump Outlet Temperature (C0157), F	--	-421.9	--	-421.6	--	-421.0
Fuel Recirculation Return Line Temperature (C0161), F	--	-417.2	--	-420.2	--	-418.1
Fuel Injection Temperature (C0200), F	--	-181	--	-89	--	-174
Fuel Tank Outlet Temperature (C0130), F	--	-422.3	--	-421.3	--	-420.9
Vuel Tank Ullage Pressure (VXD0177), psia	31 to 37	36.0	34	36.2	31 to 34	32.9
Fuel Tank Ullage Pressure (VD0178), psia	31 to 37	36.0	34	36.2	31 to 34	32.8

[redacted]

TABLE 14

(Continued)

Parameters	Liftoff		Engine Start		Engine Restart	
	Expected or Allowable	Actual	Expected or Allowable	Actual	Expected or Allowable	Actual
Fuel and Oxidizer Tank Conditions						
Fuel Recirculation Pump P (D0218), psid	--	8.0	--	8.4	--	0.2
Fuel Recirculation Pump Flow (VXF0005), gpm	--	131.0	--	132.0	--	
Fuel Pump Interstage Pressure (D0224), psia	--	42.2	--	40	--	*
Oxidizer Pump Inlet Pressure (XD0003), psia	DNA	44.0	33 to 48	40	33 to 48	41.0
Oxidizer Tank Ullage Temperature (C0135), F	--	-246	--	-276	--	-295.8
Oxidizer Pump Discharge Temperature (C0133), F	DNA	-292.2	Fig. 74	-294.5	Fig. 74	-293.6
Oxidizer Bleed Valve Temperature (C0013), F	--	-293	--	-294.7	--	-294.3
Oxidizer Recirculation Return Line Tank Inlet Temperature (C0159), F	--	-292.5	--	-295	--	-295.3
Oxidizer Recirculation Pump Outlet Temperature (C0163), F	--	-295.2	--	-295.2	--	-294.3
Oxidizer Tank Ullage Pressure (VSD0179), psia	--	41.7	40	39.8	40	41.2
Oxidizer Recirculation Pump P (D0219), psi	--	11.6	--	11.6	--	0.5

*Data questionable

[redacted]

TABLE 14
(Concluded)

Parameters	Liftoff		Engine Start		Engine Restart	
	Expected or Allowable	Actual	Expected or Allowable	Actual	Expected or Allowable	Actual
Fuel and Oxidizer Tank Conditions						
Oxidizer Recirculation Return Pressure (D061), psia	—	48.0	—	46.5	—	41.7
Oxidizer Tank Diffuser Inlet Helium Gas Temperature (C0229), F	—	-250	—	-270	—	-294
Oxidizer Pump Inlet Temperature (XC0004), F	-294	-295	Fig. 72	-295	Fig. 72	-294.6
Oxidizer Recirculation Pump Flow (VXF0004), gpm	—	42.7	—	42.8	—	49.5
Oxidizer Pump Bearing Cool Temperature (C202), F	—	-292.1	—	-295.4	—	-276.8
Helium Tank Conditions						
Helium Bottle Pressure (D0019), psia	2800 to 3280	2960	2800 to 3450	3000	—	1920
Helium Bottle Temperature (C0007), F	DNA	-170	DNA	-171	DNA	-213.9

[redacted]

[redacted]

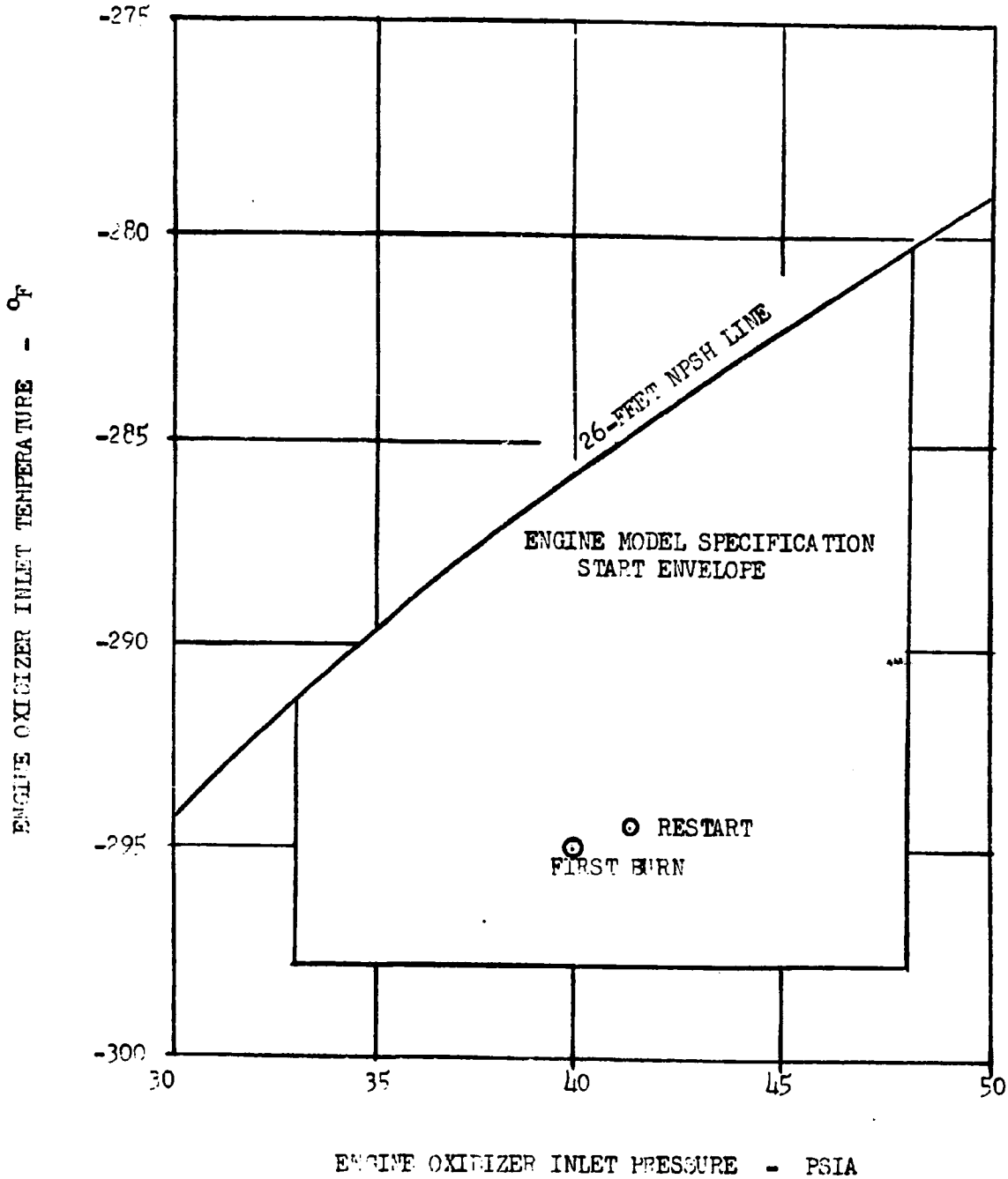

Figure 72. AS-502 Engine Oxidizer Inlet Pressure vs Engine Oxidizer Inlet Temperature

[redacted]

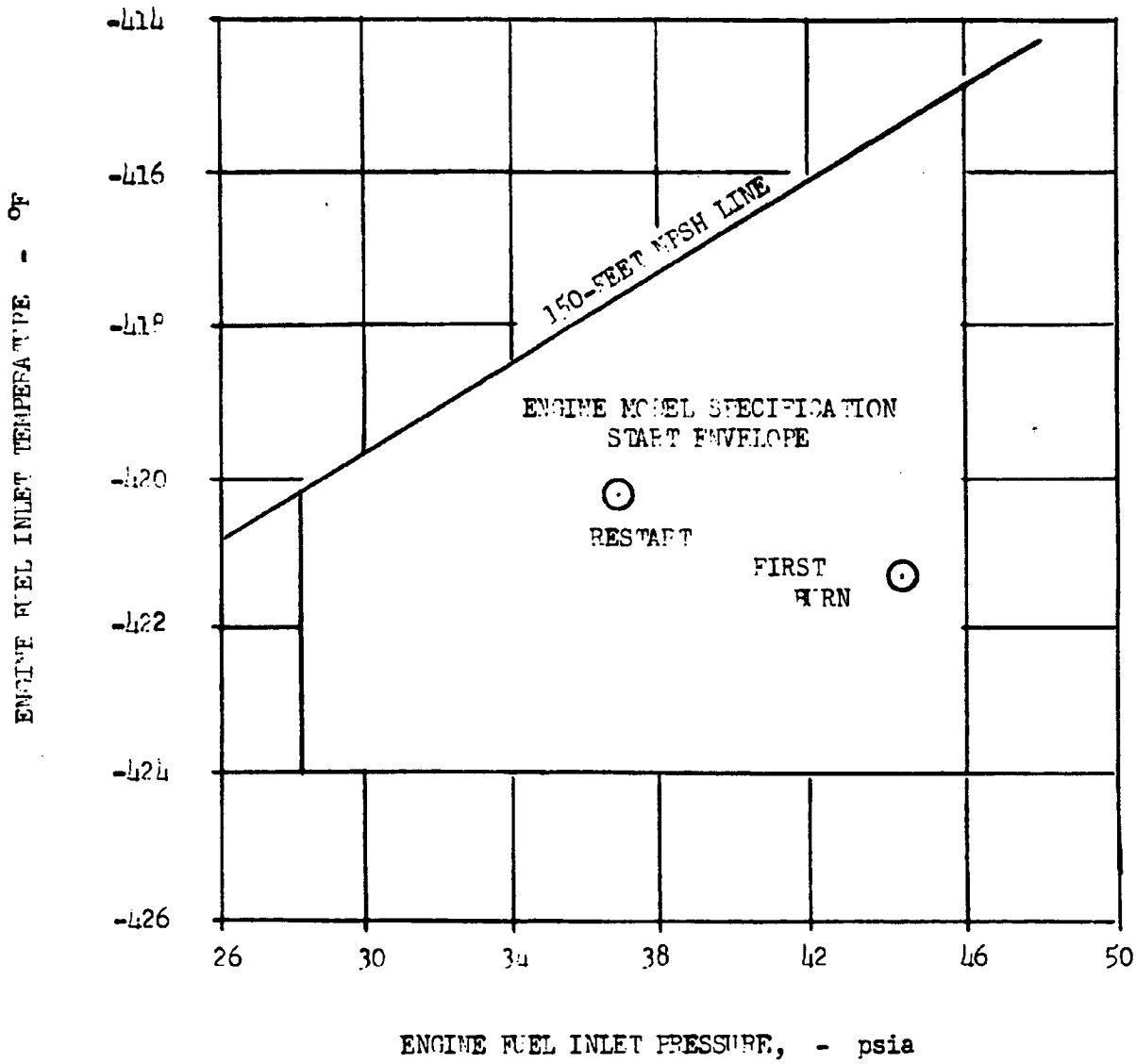

Figure 73. AS-502 S-IVB Fuel Inlet Pressure vs Fuel Inlet Temperature at Start

[redacted]

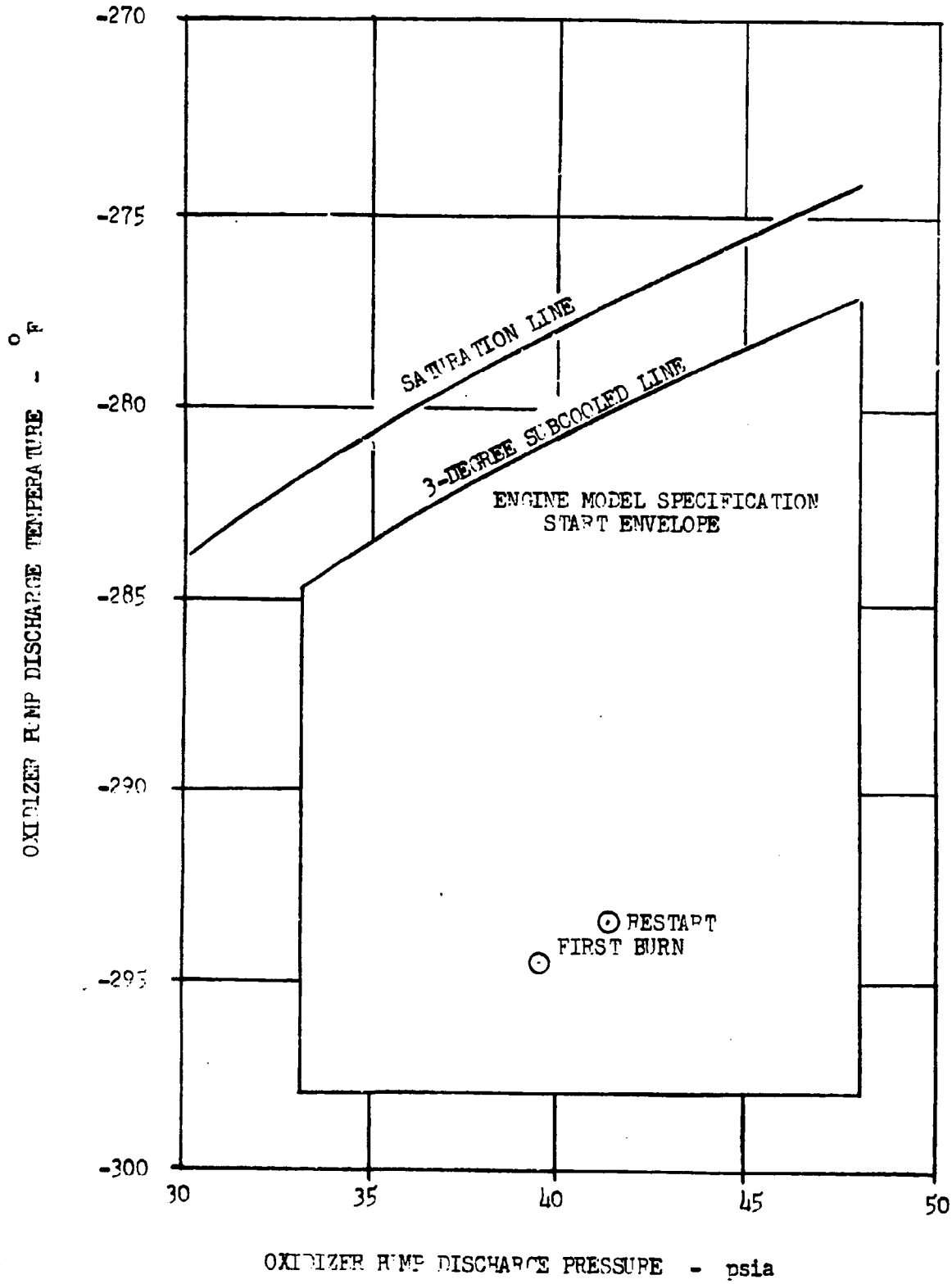

Figure 74. AS-502 S-IVB Oxidizer Pump Discharge Pressure vs Oxidizer Pump Discharge Temperature at Start

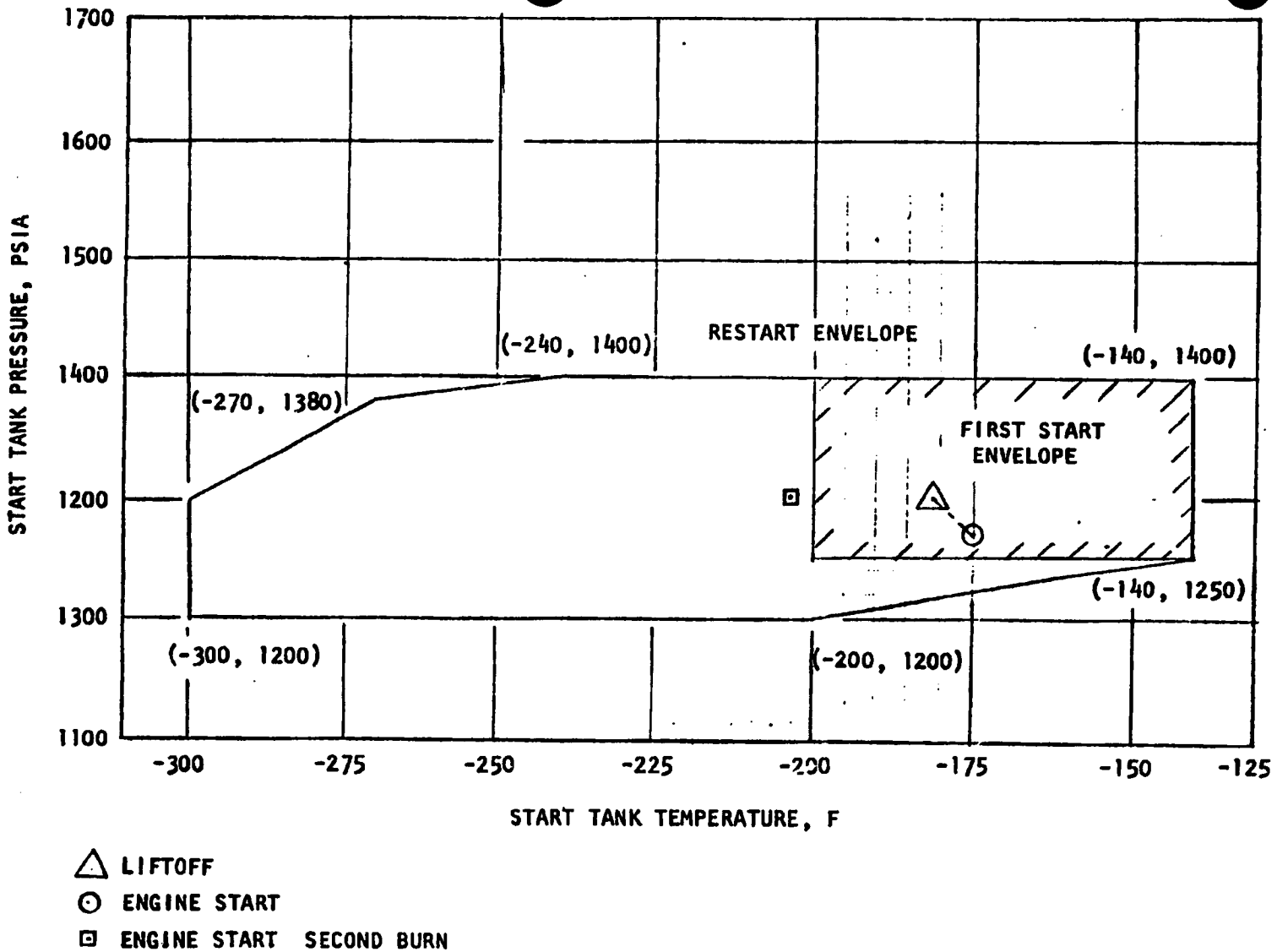

Figure 75. AS-502 Start Tank Temperature vs Start Pressure at Start

[redacted]

TABLE 15

AS-502-S-IVB FIRST-BURN AND RESTART ENGINE SEQUENCE DATA

Measure No. First Burn	Range Time, seconds	Event	State
K21	577.270	Engine Start - On	Yes
K7	577.270	Helium Control Solenoid Energize	Yes
K10	577.281	Thrust Chamber Spark System - On	Yes
K11	577.281	Gas Generator Spark System - On	Yes
K6	577.290	Ignition Phase Control Solenoid Energize	Yes
K126	577.338	Oxidizer Bleed Valve - Closed	Yes
K119	577.342	MFV - Closed	No
K118	577.365	MFV - Open	Yes
K20	577.382	ASI Oxidizer Valve - Open	Yes
K127	577.421	Fuel Bleed Valve - Closed	Yes
K96	580.289	Start Tank Discharge Control Energize	Yes
K123	580.432	Start Tank Discharge Valve - Closed	No
K122	580.515	Start Tank Discharge Valve - Open	Yes
K96	580.739	Start Tank Discharge Control Energize	No
K5	580.750	Mainstage Control Solenoid Energize	Yes
K121	580.840	MOV - Closed	No
K116	580.841	Gas Generator Valve - Closed	No
K122	580.882	STDV - Open	No
K117	580.968	Gas Generator Valve - Open	Yes
K124	580.990	OTBV - Open	No
K125	581.214	OTBV - Close	Yes
K157	582.031	Mainstage OK Pressure Switch No. 2	Yes
K159	582.031	Mainstage OK Pressure Switch No. 2 - Depress	No
K14	582.031	Mainstage OK Pressure Switch No. 1	Yes
K158	582.031	Mainstage OK Pressure Switch No. 1 - Depress	No
K120	582.930	MOV - Open	Yes

TABLE 15

(Continued)

Measure No. First Burn	Range Time, seconds	Event	State
K13	747.036	Engine Cutoff Signal	Yes
K12	747.037	Engine Ready Signal	No
K5	747.038	Mainstage Control Solenoid - Energize	No
K6	747.054	Ignition Phase Control Solenoid - Energize	No
K140	747.064	Engine Cutoff Command - On	Yes
K20	747.123	ASI Oxidizer Valve - Open	No
K120	747.145	MOV - Open	No
K117	747.195	Gas Generator Valve - Open	No
K118	747.203	MFV - Open	No
K116	747.253	Gas Generator Valve - Close	Yes
K14	747.269	Mainstage OK Pressure Switch No. 1	No
K157	747.269	Mainstage OK Pressure Switch No. 2	No
K158	747.269	Mainstage OK Pressure Switch No. 1 - Depress	Yes
K159	747.269	Mainstage OK Pressure Switch No. 2 - Depress	Yes
K121	747.271	MOV - Close	Yes
K119	747.455	MFV - Close	Yes
K124	747.919	OTBV - Open	Yes
K7	748.035	Helium Control Solenoid - Energize	No
K127	750.662	Fuel Bleed Valve - Close	No
K126	750.745	Oxidizer Bleed Valve - Close	No
Restart			
K140	11,613.308	Engine Cutoff Command - On	No
K21	11,614.617	Engine Start - On	Yes
K7	11,614.671	Helium Control Solenoid - Energize	Yes
K121	11,614.671	MOV - Close	Yes
K6	11,614.681	Ignition Phase Control Solenoid - Energize	Yes

TABLE 15

(Concluded)

Measure No. Restart	Range Time, seconds	Event	State
K10	11,614.681	Thrust Chamber Spark System - On	Yes
K11	11,614.681	Gas Generator Spark System - On	Yes
K119	11,614.733	MFV - Close	No
K118	11,614.756	MFV - Open	Yes
K20	11,614.783	ASI Oxidizer Valve - Open	Yes
K127	11,614.823	Fuel Bleed Valve - Close	Yes
K126	11,614.823	Oxidizer Bleed Valve - Close	Yes
K96	11,622.678	STDV Control Solenoid - Energize	Yes
K123	11,622.825	STDV - Close	No
K122	11,622.916	STDV - Open	Yes
K5	11,623.128	Mainstage Control Solenoid - Energize	Yes
K96	11,623.128	STDV Control Solenoid - Energize	No
K116	11,623.255	Gas Generator Valve - Close	No
K122	11,623.266	STDV - Open	No
K121	11,623.280	MOV - Close	No
K124	11,623.346	OTBV - Open	No
K123	11,623.466	STDV - Close	Yes
K125	11,623.571	OTBV - Close	Yes
K117	11,623.671	Gas Generator Valve - Open	Yes
K120	11,625.196	MOV - Open	Yes
K13	11,630.397	Engine Cutoff Signal	Yes
K5	11,630.403	Mainstage Control Solenoid - Energize	No
K12	11,630.447	Engine Ready Signal	No
K120	11,630.471	MOV - Open	No
K140	11,630.475	Engine Cutoff Command - On	Yes
K117	11,630.521	Gas Generator Valve - Open	No
K118	11,630.530	MFV - Open	No
K125	11,630.641	OTBV - Close	No
K119	11,630.757	MFV - Close	Yes
K127	11,633.989	Fuel Bleed Valve - Close	No
K126	11,633.989	Oxidizer Bleed Valve - Close	No

NOTE: Mainstage OK pressure switches did not pick up as a result of no thrust chamber pressure buildup.

VERIFICATION TESTING AT SSFL

Two J-2 R&D engines, J004-5 and J016-4, were tested at VTS-2 to investigate the hypothesized failure modes occurring on the S-II and S-IVB stages of AS-502. Engine J004-5 was tested to obtain engine performance gain factors with known quantities of propellant leakage. Gains from the simulated ASI fuel leak test (313-035) were used in the performance shift analysis (Engine Performance section). No gains were obtained from the oxidizer leak test because of a mechanical failure in the oxidizer system. One test was conducted on engine J005-4 in an attempt to simulate portions of the suspected S-II failure mode. This test (313-036) was not completely successful because the leak system was not sized properly. Engine J016-4 was set up specifically to simulate portions of the suspected S-IVB failure mode. It is this test (313-041) that is discussed in this section.

ENGINE J016-4 CONFIGURATION

J-2 R&D engine J016-4 was built up to a configuration similar to engine J2042, the S-IVB engine on AS-502. An ASI injector was installed that had a high oxidizer-side resistance and an average fuel-side resistance, and the ASI oxidizer orifice diameter was 0.125 inch.

The engine was calibrated to a thrust level of approximately 229K at an overall mixture ratio of 5.5 and a fuel turbine inlet temperature of 1250 F. These were the levels experienced during flight on engine J2042.

A servocontrolled throttle valve was installed in the ASI fuel line so that the ASI fuel flow could be regulated to the desired flowrate as a function of time. The system, including the servovalve, was flow calibrated in liquid hydrogen prior to installation on the engine. A tee was installed in the ASI fuel line immediately upstream of the ASI. The tee led to a low-resistance dump system which could essentially open the ASI fuel system to atmosphere, thus simulating an ASI line failure. These systems are depicted schematically in Fig. 76.

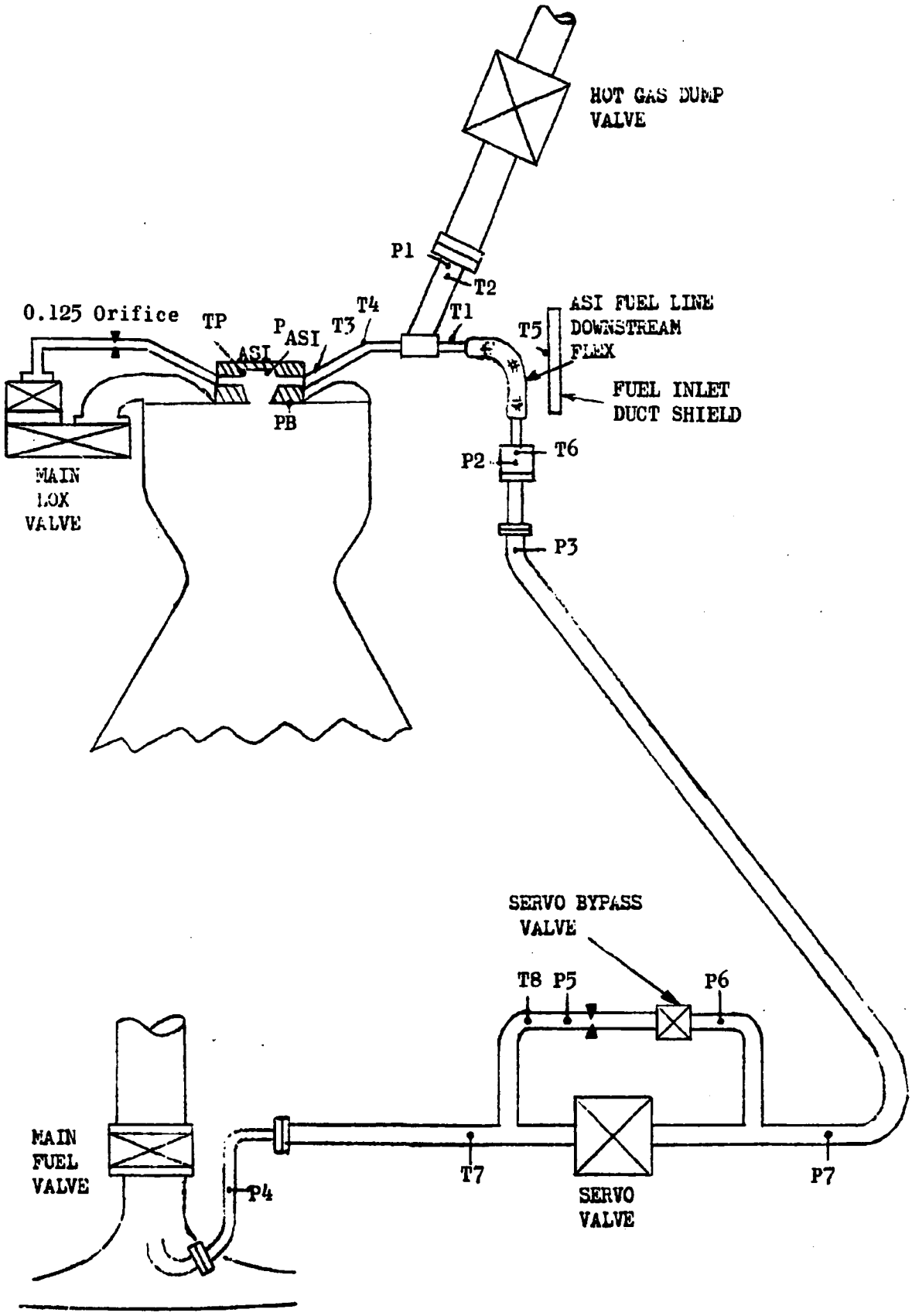

Figure 76. AS-502 S-IVB Failure Simulation Test, Engine J016-4, Test 313-041

Special instrumentation was installed so that the ASI fuel flow could be measured during the gradual flow decrease, and the temperature of the gas backflowing across the ASI fuel injector could be measured after the hot-gas dump valve was opened. Table 16 lists the special parameters measured, and Fig. 76 shows their locations. ASI fuel flow was measured using the pressure drop from P4 to P3, the density at T7, and the resistance versus valve position curve which had been generated during the ASI fuel system calibration. It was anticipated that the hot-gas temperature could be measured with the hot-gas dump fluid temperature (T2) and the skin temperatures T1, T3, T4, and T5. The ASI ignition detector probe was able to measure a temperature within the ASI chamber. A pressure measurement was installed in the ASI-to-injector seal bleed port to indicate when and if the primary seal burned through.

TEST OBJECTIVES

The primary objective of this test was to verify, if possible, the validity of the theory set forth on the cause of the chain of failure events occurring during AS-502 S-IVB first burn. These events have been discussed in detail in earlier sections of this report, and the proposed theory is summarized in Table 17 for the purpose of comparison with the failure simulation test on engine J016-4. The test was expected to determine whether significant ASI damage could occur when the ASI is forced to operate under the mixture ratio and backflow transients hypothesized during AS-502.

PROCEDURE

Test 041 events are shown in Fig. 77. After 20 seconds of mainstage, the PU valve was closed to bring engine performance to the level of engine J2042 on AS-502. At 65 seconds, the ASI fuel servovalve was closed to 42 percent, reducing ASI fuel from a nominal 0.9 lb/sec flowrate to 0.6 lb/sec. This results in ASI operation anticipated with an overboard leak of approximately 0.5 lb/sec from the downstream 1/2-inch flex hose in the ASI fuel line. The engine ran for 35 seconds in this situation, simulating

TABLE 16

SPECIAL INSTRUMENTATION FOR S-IVB FAILURE SIMULATION TEST
(Engine J016-4, Test 313-041)

Designation In Fig. 76	Parameter Name	Type of Measurement
P4	ASI Fuel Line Inlet Pressure	Fluid Static Pressure
T7	ASI Fuel Line Temperature	Fluid Temperature
T8	ASI Fuel Bypass Orifice Temperature	Fluid Temperature
P5	ASI Fuel Bypass Orifice Upstream Pressure	Fluid Static Pressure
P6	ASI Fuel Bypass Orifice Downstream Pressure	Fluid Static Pressure
P7	ASI Fuel Servovalve Outlet Pressure	Fluid Static Pressure
P3	ASI Fuel Line Pressure	Fluid Static Pressure
P2	Gas Generator Fuel Injection Pressure	Fluid Static Pressure
T6	ASI Fuel Injection Temperature	Fluid Temperature
T5	Fuel Duct Environment Temperature	Skin Temperature
T1	ASI Fuel Line Skin Temperature	Skin Temperature
T2	ASI Hot-Gas Dump Temperature	Fluid Temperature
P1	ASI Hot-Gas Dump Pressure	Fluid Static Pressure
T4	ASI Fuel Line Skin Temperature	Skin Temperature
T3	ASI Fuel Line Skin Temperature	Skin Temperature
P ASI	ASI Chamber Pressure	Fluid Pressure
P_B	ASI Seal Bleed Pressure	Fluid Pressure
T_P	Restart Probe Temperature	Fluid Temperature

[redacted]

TABLE 17

ENGINE J016-4 FAILURE SIMULATION TEST (313-041)

Suspected Problem on AS-502 S-IVB		Planned Simulation on Test 313-401	
Range Time, seconds	Event	Test Time, seconds	Event
645	Fuel leakage from ASI fuel line approximately 0.5 lb/sec causing external chilling and reducing ASI fuel flow from 0.93 to 0.6 lb/sec	65	Close servovalve from 80 to 42 percent to decrease ASI fuel flow from 0.9 to 0.6 lb/sec
684 to 696	Fuel leakage gradually increases to approximately 2 lb/sec causing performance shift and causing ASI fuel flow to drop gradually to 0 lb/sec	100 to 127	Close servovalve gradually from 42 to 0 percent to decrease ASI fuel flow from 0.6 to 0.03 lb/sec
696	ASI fuel injector backflow occurs and ASI fuel line is completely separated.	129	Open hot-gas dump valve to allow ASI fuel injector backflow. Close servo bypass valve to decrease external fire potential.
696 to 702	ASI injector erosion occurs because of backflow of hot gas through the fuel injector. Performance shifts because of increased amount of propellants lost overboard.	129 to 180	Allow engine to continue running with the ASI fuel injection manifold open to atmosphere to determine whether ASI injection damage occurs.

[redacted]

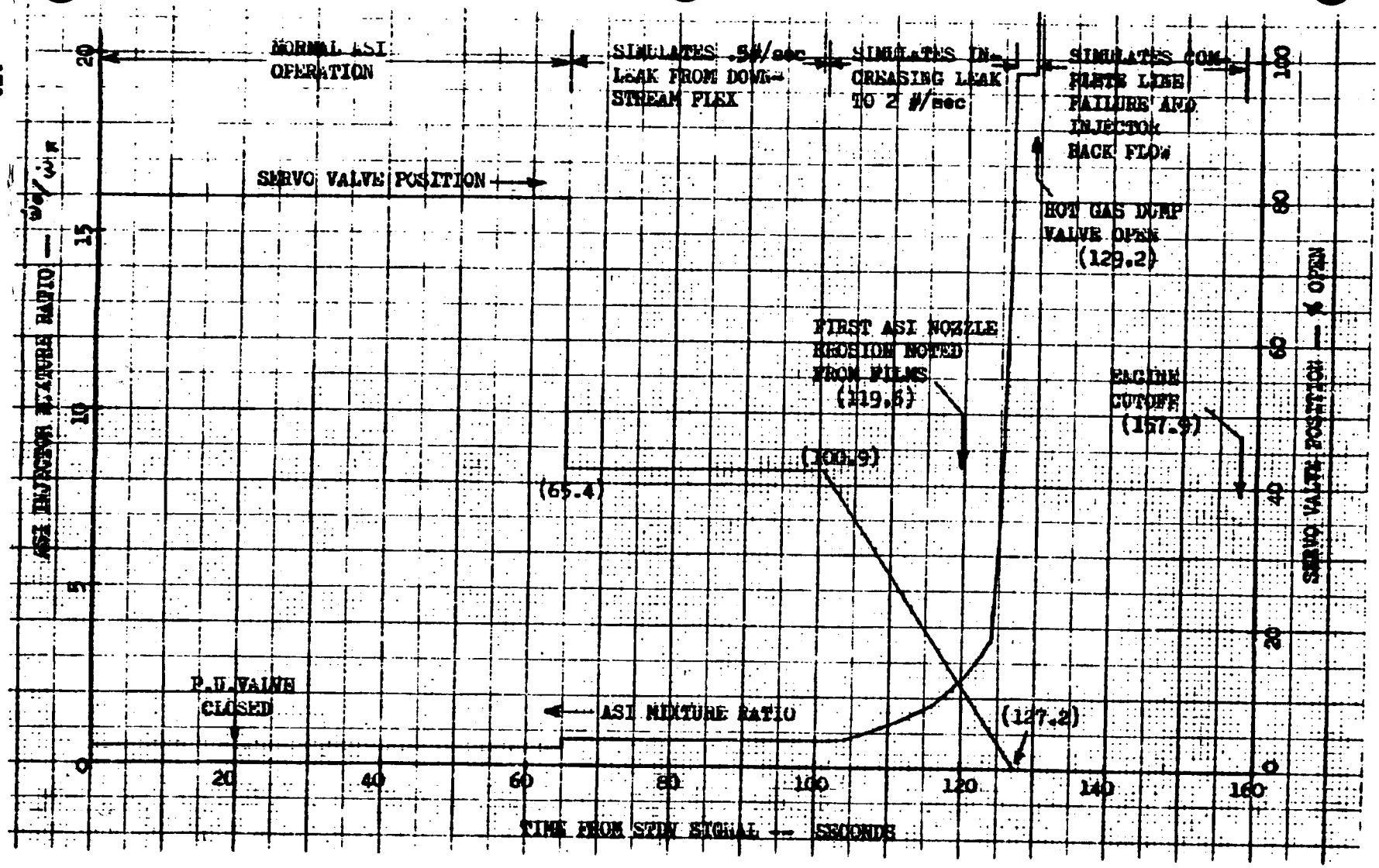

Figure 77. S-IVB Failure Simulation, Engine J016-4

the period between range time 645 and 680 seconds on AS-502 (where external chilling was noted but no performance change occurred).

Beginning at 100 seconds, the ASI fuel servovalve was ramped from 42-percent open to full-closed in 27 seconds. The servo bypass system was sized so that ASI fuel flow would be approximately 0.03 lb/sec when the servovalve was full closed. Gradually decreasing the ASI fuel flow simulated a gradually increasing leak in the ASI fuel line. This caused the ASI mixture ratio to increase from 0.9 to 20 over a period of 27 seconds. The ASI operated in an eroding region (above 2.5 mixture ratio) for 10 seconds, including 3 seconds at a mixture ratio of 20.

At this time, the hot-gas dump valve was opened, allowing the ASI fuel line to atmosphere. At the same time, the ASI fuel flow was completely shut off by closing the servovalve bypass. This allowed backflow through the ASI fuel injector and simulated a completely separated ASI fuel line. The engine was allowed to operate in this condition for 28 seconds, when an observer terminated the test because of excessive external fire.

TEST RESULTS

Test 313-041 proceeded as planned, with the exception of the premature shutdown because of excessive fire. The only abnormality noted when the ASI fuel servovalve was stepped to 42-percent open was that the restart probe temperature failed, possibly indicating a change in flame front location in the ASI at this time. As the servovalve was ramped from 42 percent to full closed, the ASI nozzle (main injector) eroded for approximately the last 10 seconds of the ramp. This was clearly seen in the films of the test.

Figure 77 illustrates the servovalve position and the resultant ASI mixture ratio during the entire test. The point of first ASI erosion, as determined from the films, was at an ASI mixture ratio of 2.5.

In Fig. 78 , the estimated ASI mixture ratio transient on AS-502, which was reconstructed based on the suspected location and magnitude of the ASI fuel system leak, is shown and compared with the results of the failure simulation test.

The resulting hardware damage clearly indicated that the S-IVB failure mode hypothesized is feasible. The ASI nozzle (main injector) was severely eroded, increasing the throat diameter from 0.7 to 0.9 inch (see Fig. 79). Erosion had progressed through the ASI nozzle wall into the main fuel injector for 360 degrees, and had invaded oxidizer elements 1 and 2. This damage is shown in Fig. 80 through 82. At 128 seconds after STDV (1.2 seconds prior to hot-gas dump valve open), the ASI-to-injector-to-primary seal failed. This was indicated by a sudden rise in the seal bleed port pressure at this time. All this damage occurred between 119.6 and 129.2 seconds after STDV while the ASI mixture ratio was increasing from 2.5 to 20.

After the hot-gas dump valve was opened, 129.2 seconds after STDV, damage occurred to the ASI itself and adjacent external engine components. The damage was a result of hot combustion products mixing with ASI oxidizer and flowing backward through the ASI fuel injector and out the ASI fuel inlet to atmosphere. Unfortunately, the skin temperature measurements, T1, T3, T4, and T5, and the hot-gas dump temperature, T2, all failed within seconds after the hot-gas dump valve was opened. T4 lasted about 2 seconds and indicated 1900 F when it failed. T5 lasted about 5 seconds, and was at 1500 F and rising when it failed.

Approximately 1/2 second after the hot-gas dump valve was opened, the ASI fuel line burned through, opening the ASI fuel injector manifold directly to atmosphere. From the films it appeared that the ASI fuel line burned through under the gimbal bearing and very close to the ASI body. Within seconds, the ASI fuel line had been burned back to the center of the downstream flex hose, and the hot-gas dump system had been burned back 1 foot from where it teed into the ASI fuel line. The first sign of green flame,

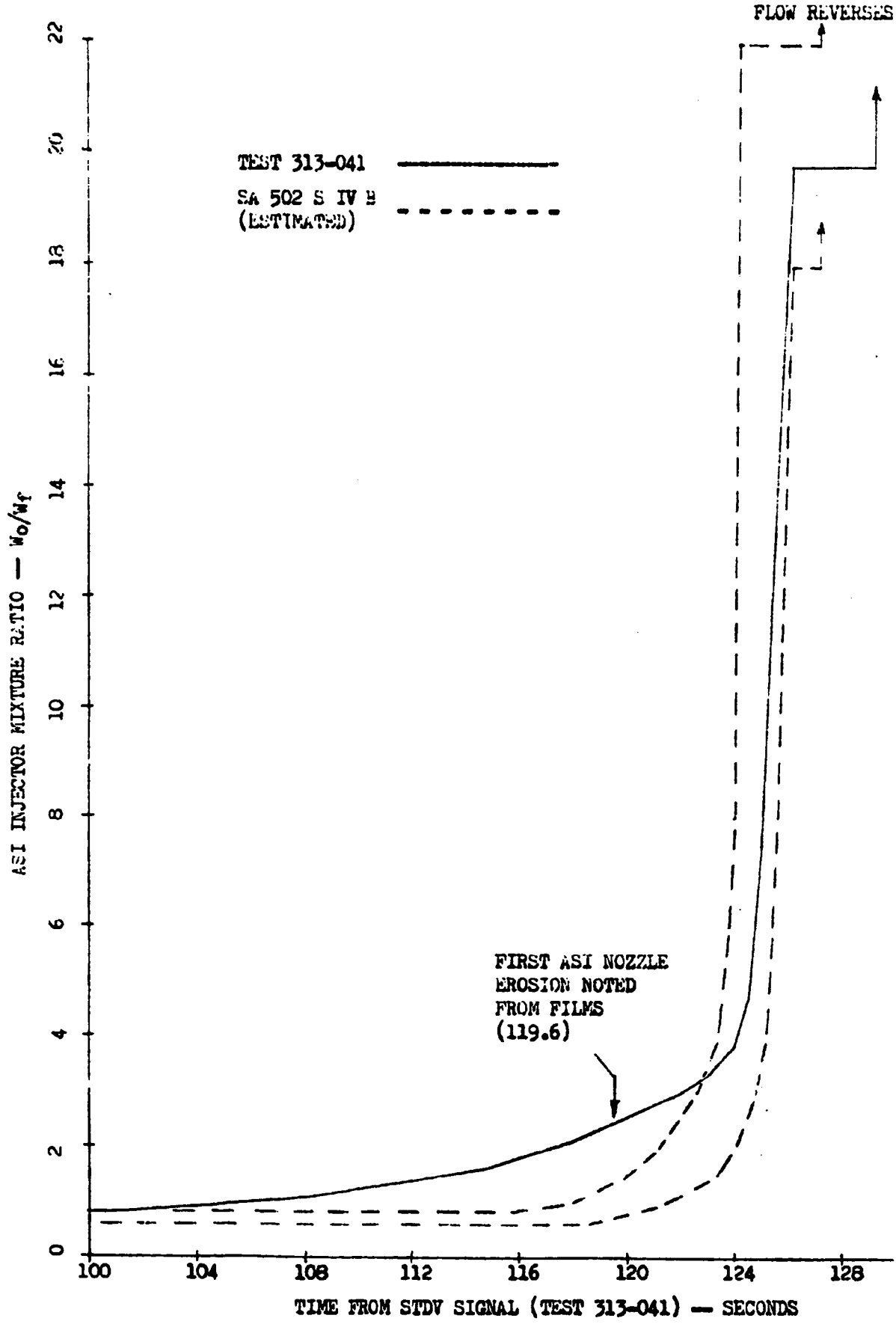

Figure 78. ASI Injector Mixture Ratio

[redacted]

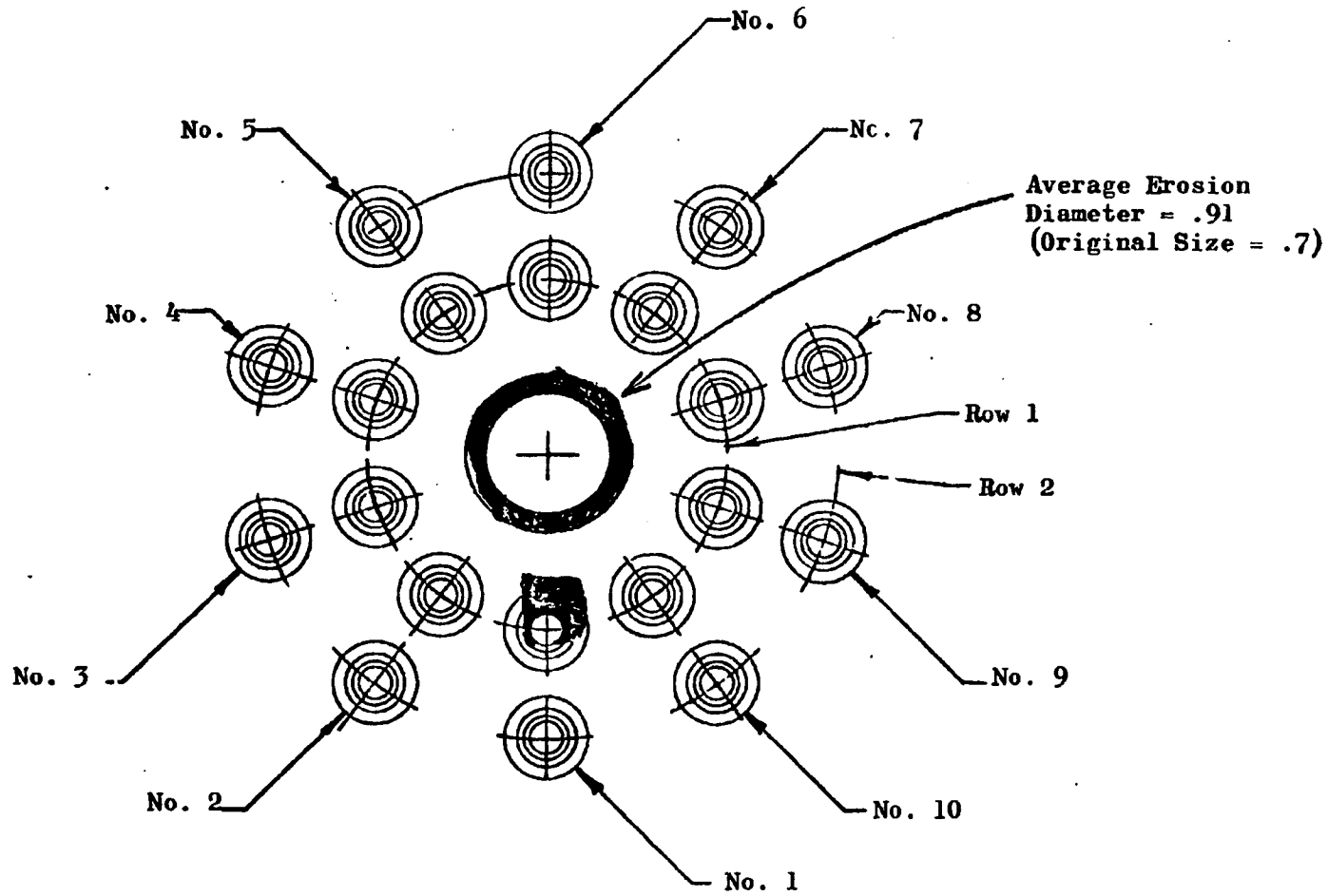

Figure 79. ASI Nozzle (Main Injector) Showing Erosion, Engine J016-4, Test 313-041, Posttest Injector Condition

[redacted]

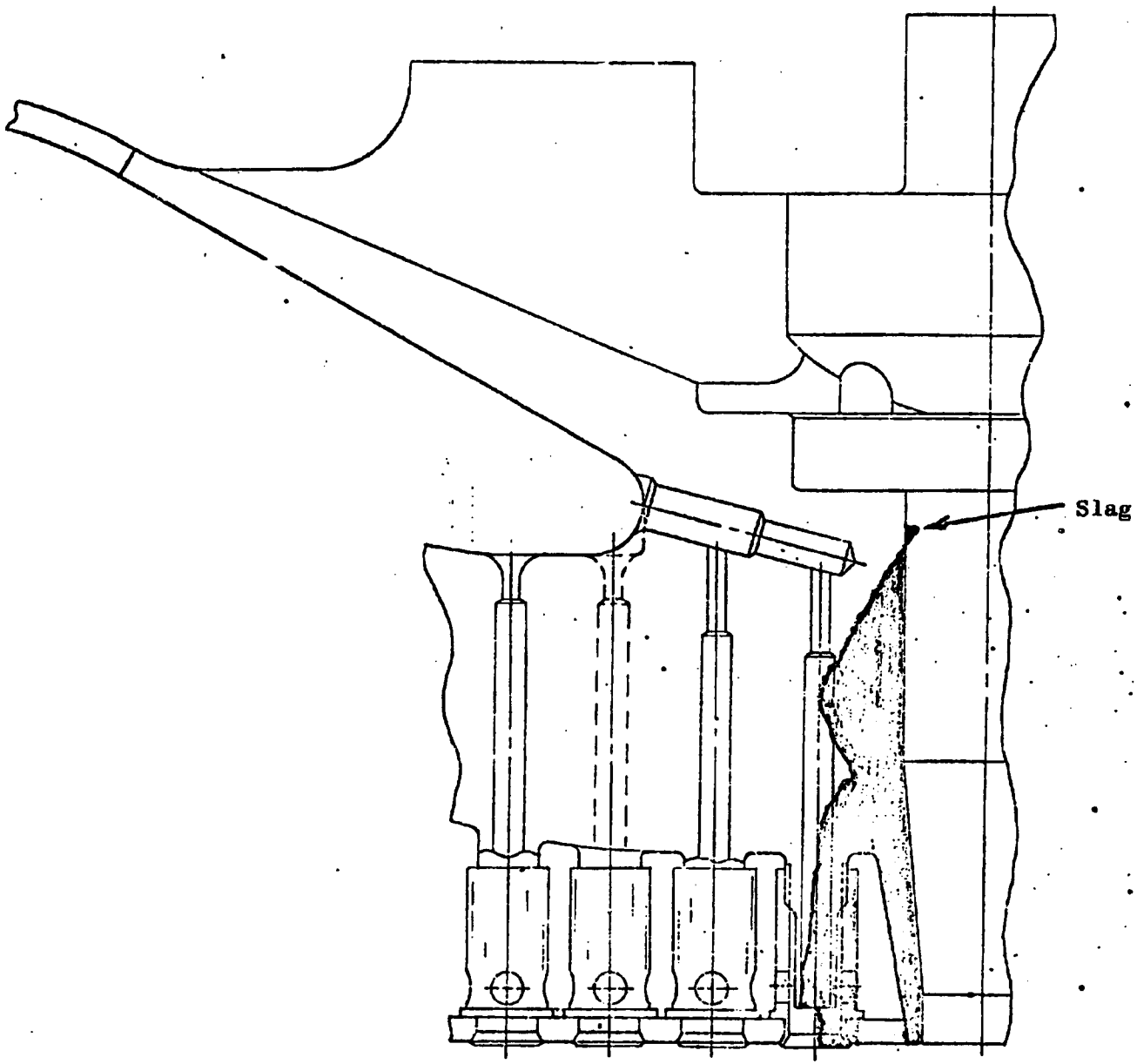

Figure 80. Engine J016-2, Test 313-041, Posttest Injector Condition (Section at Element 1)

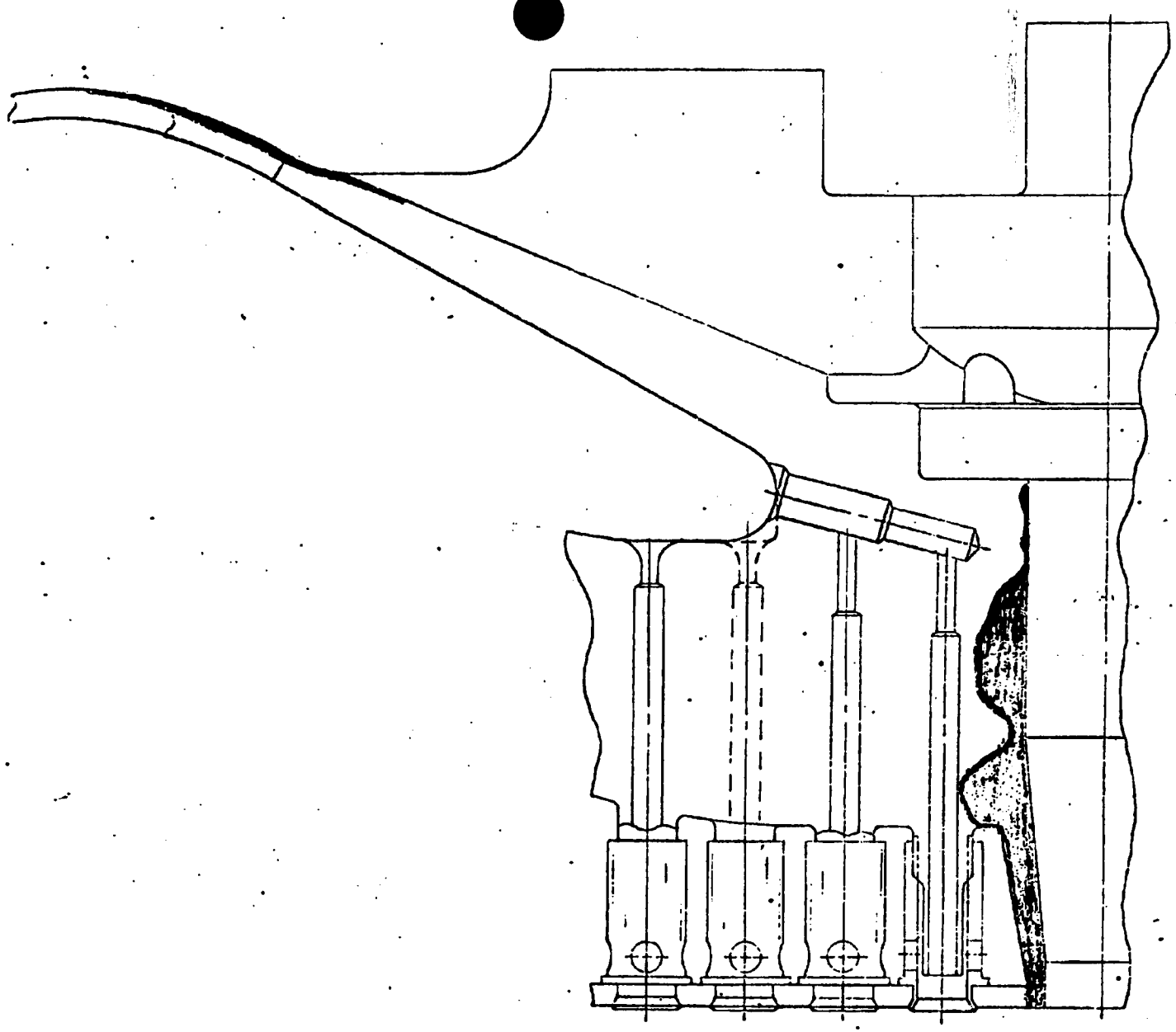

Figure 81. Engine J016-4, Test 313-041, Posttest Injector Condition (Section at Element 2)

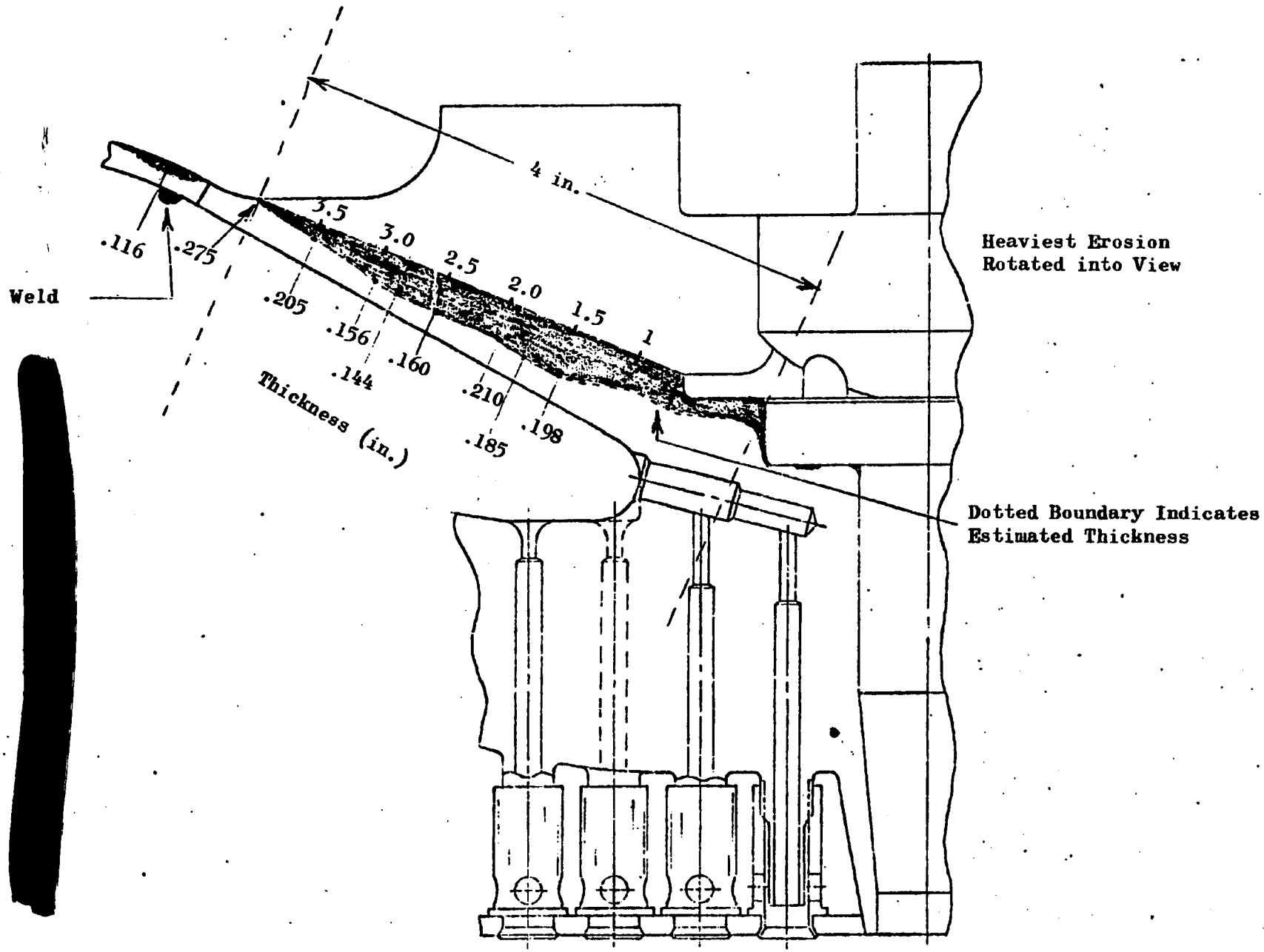

Figure 82. Engine J016-4, Test 313-041, Posttest Injector Condition

indicating burning copper, was noted (from the films) to occur 8 seconds after the external fire started, or about 8-1/2 seconds after injector backflow started.

Hot combustion products continued to spew from the ASI for the duration of the test, 28 seconds after the hot-gas dump valve opened. The ASI fuel injector was eroded so that over 180 degrees of the fuel injector manifold was exposed on the inside (only three of the eight fuel orifices were intact). Both spark plug tips, which are in the plane of the oxidizer fan, were severely eroded. A large hole (approximately 1/2 by 1 inch) was burned radially outward through the ASI body in the plane of the fuel inlet line. The spark plug cable on the fuel inlet side was burned off. Most of this damage is shown in Fig. 83. A portion of the hot gas and molten slag passed between the ASI body and the gimbal bearing and exited on the oxidizer side of the engine. Slag was deposited on the ASI oxidizer inlet line, the oxidizer-side spark plug, and the ASI ignition-detector probe housing, overheating these elements to some extent. This damage is illustrated in Fig. 84. The external surface of the main oxidizer dome and the gimbal bearing were eroded in the plane of the fuel inlet line. Figures 82 and 85 illustrate the damage to the oxidizer dome. The dome thickness had been reduced to 0.15 inch in this region, which is one-third its normal thickness.

A significant, but gradual, performance decay was noted during the first 12 seconds of hot-gas flow overboard through the ASI fuel injector. This performance decay is attributed to increasing overboard propellant flow as the opening through the ASI was aggravated by erosion. The performance decay is tabulated in the Engine Performance section and compared to the performance decay noted during S-IVB first burn of AS-502. Much of the instrumentation was erroneous after the hot gas began flowing overboard because of the external fire, but it does appear that the performance decay subsided after 12 seconds and that performance was stable for the remaining 16 seconds of the test. It is conjectured that the performance decay subsides when sufficient fuel is flowing from the main injector

1CT25-5/7/68-S1E

Figure 83. Engine J016-4 ASI Assembly Following Test 313-041

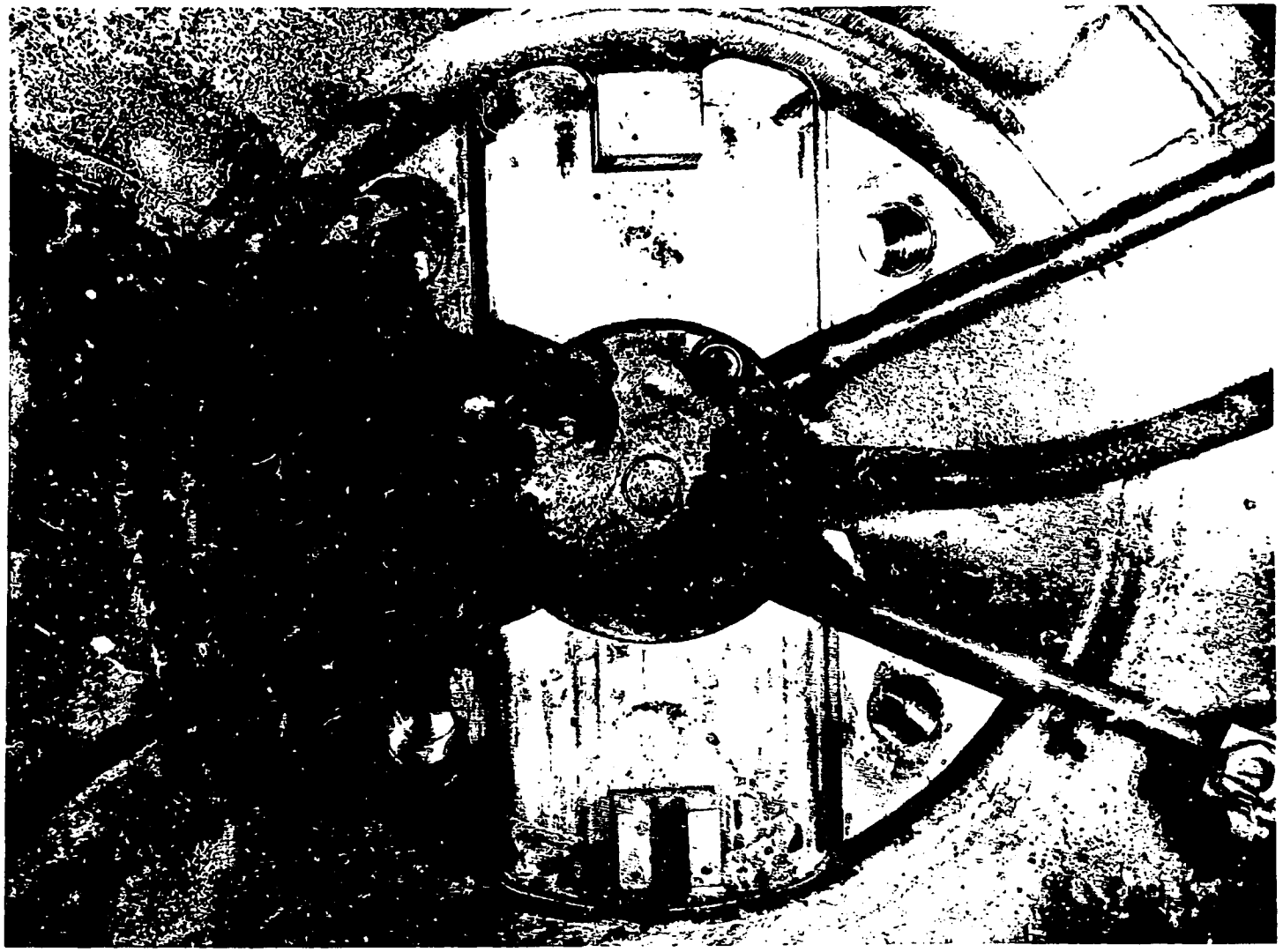

1CT25-5/7/68-S1L

Figure 84. Engine J016-4 ASI Assembly and Oxidizer Dome Following Test 313-041

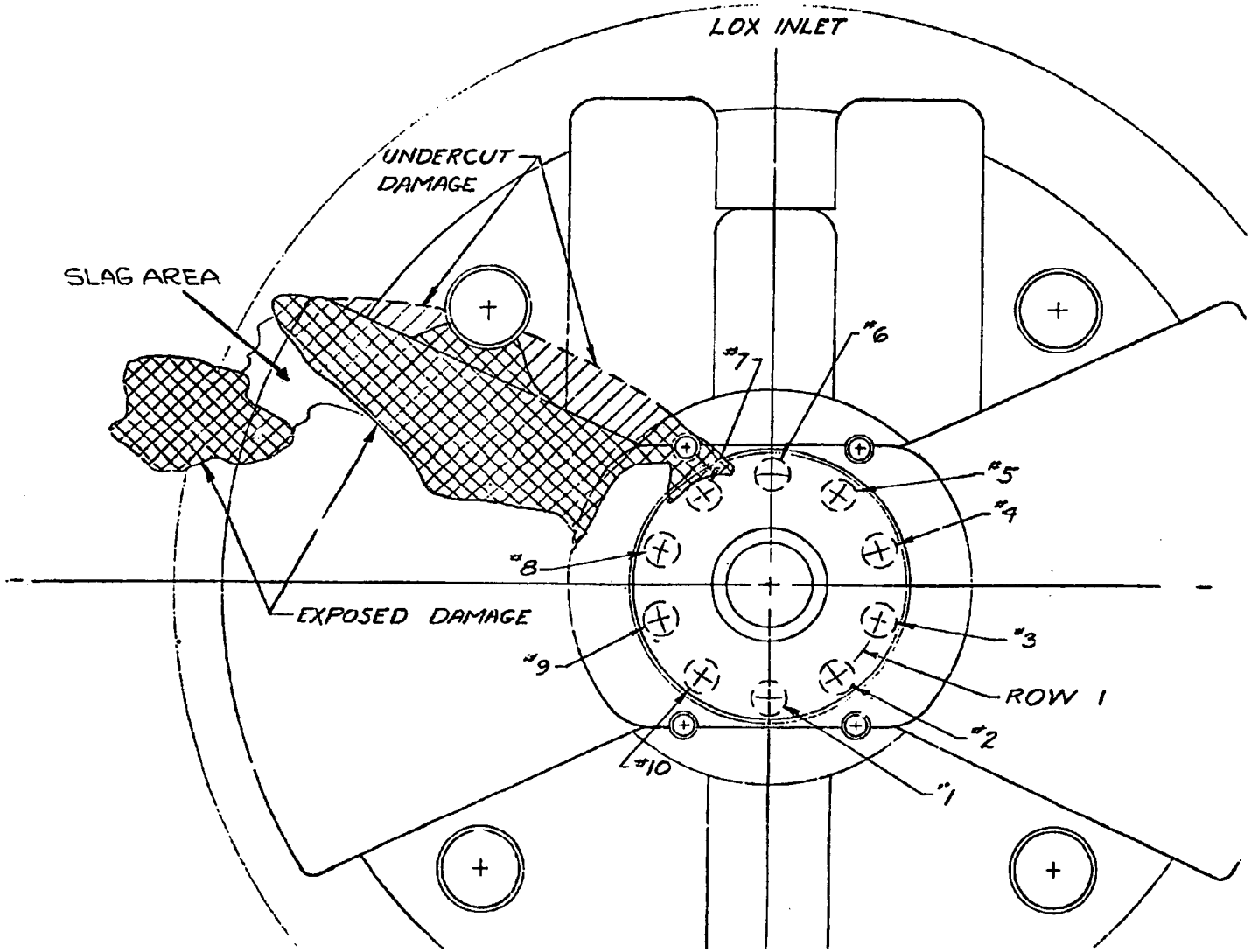

Figure 85. Engine J016-4, Test 313-041, Posttest Injector Condition Showing Oxidizer Dome Damage